The Oxidative Stress Defenses of *Campylobacter jejuni*

Annika Flint

A thesis submitted to the
Faculty of Graduate and Postdoctoral Studies
in partial fulfillment of the requirements
for the PhD degree in Biochemistry

Department of Biochemistry, Microbiology and Immunology
Faculty of Medicine
University of Ottawa

Abstract

Campylobacter jejuni infection is one of the leading causes of gastroenteritis in humans worldwide. During colonization of the gastrointestinal tract, *C. jejuni* will be unavoidably exposed to reactive oxygen species (ROS) produced by the host immune system and other intestinal microbiota. Identification of defenses against ROS is therefore important for understanding how *Campylobacter* survives this environmental stress during infection. Construction of isogenic deletion mutants into genes encoding potential oxidative stress defense systems followed by phenotypic screening revealed genes important for oxidant defense within *C. jejuni*. Surprisingly, genes involved in motility were found to play an indirect role in resistance to oxidative stress. Deletion of the flagellar motor apparatus genes, *motAB*, resulted in increased sensitivity towards superoxide which could be restored by fumarate supplementation or tandem deletion of *motAB* with *ccoQ* (cytochrome c oxidase). This finding suggested that disruption of the proton gradient across the inner membrane resulted in increased superoxide production in non-motile flagellar mutants. Phenotypic screening of the mutant library also identified a novel gene (*cj1386*) specifically involved in hydrogen peroxide defense within the cell. Hydrogen peroxide detoxification within living organisms is predominantly carried out by catalase enzymes. Interestingly, *cj1386* is located directly downstream from *katA* (catalase) in the *C. jejuni* genome and it was found that a Δ*cj1386* mutant had reduced catalase activity relative to wild-type *C. jejuni.* Immunoprecipitation of KatA from Δ*cj1386* revealed a significant reduction in hemin content associated with KatA suggesting a role for *cj1386* in hemin trafficking to KatA. Hemin binding experiments with purified Cj1386 demonstrated the ability of Cj1386 to bind hemin with a 1:1 hemin-to-protein binding ratio. Furthermore, co-immunoprecipitation experiments revealed an interaction between KatA and Cj1386. Mutagenesis of conserved amino acids in Cj1386 demonstrated that tyrosine 57 plays an important role in hemin affinity and is required for proper hemin content of KatA within the cell. Overall,

this work provides a global characterization of key oxidant defenses within *C. jejuni* and provides one of the first studies investigating hemin trafficking to KatA.

Acknowledgements

I would like to thank my supervisor Dr. Alain Stintzi for his guidance and support thoughout my PhD project. I would also like to thank Dr. Stintzi for providing me with the opportunity to conduct my PhD research project in his laboratory.

I thank all the members of the Stintzi lab, past and present, for their knowledge, insightful discussions, aid with experiments, and games nights. Dr. Yi-Qian Sun was instrumental in his instruction of laboratory techniques and James Butcher provided many insightful conversations about my project.

Table of Contents

List of Abbreviations

H_2O_2	Hydrogen peroxide
CHP	Cumene hydroperoxide
MND	Menadione sodium bisulphite
$O_2^{\bullet-}$	Superoxide radical
PerR	Peroxide stress regulator
MEMα	Minimal essential media alpha
LB	Luria-Bertani media
MH	Mueller-Hinton media
DMSO	Dimethylsulphoxide
HRP	Horseradish peroxidase
SDS PAGE	Sodium dodecyl sulphate polyacrylamide gel electrophoresis
PCR	Polymerase chain reaction
TEV	Tobacco etch virus
CFU	Colony forming unit
ETC	Electron transport chain
ROS	Reactive oxygen species
KatA	Catalase
qRT-PCR	Quantitative reverse transcriptase polymerase chain reaction

List of Figures

List of Tables

CHAPTER 1. GENERAL INTRODUCTION

1.1. *Campylobacter jejuni* infection and epidemiology

Campylobacter jejuni is a Gram-negative bacterium and belongs to the epsilon class of proteobacteria. *C. jejuni* is a curved, rod-shaped bacterium that grows optimally under microaerophilic conditions at temperatures ranging from 37-42°C (1). Birds, chicken, turkeys, swine, cattle, sheep and humans comprise the wide range of hosts that *C. jejuni* is able to colonize (1, 2). Following ingestion, *Campylobacter* must transit through the low pH of the stomach as well as survive bile exposure in the duodenum before colonizing the host's gastrointestinal tract. Typically, the colon and cecum intestinal segments display the highest level of colonization by *Campylobacter* (2). The colonization of the aforementioned hosts with *C. jejuni* is primarily commensal without onset of illness; however in humans, once colonization of the gastrointestinal tract is established, *Campylobacter* can adhere to and invade the intestinal epithelial cells leading to the onset of pathogenesis and campylobacteriosis (2). Campylobacteriosis is characterized by symptoms such as diarrhea, abdominal pain, fever, dizziness and vomiting and can result from ingestion of as few as 500 organisms (3, 4). In rare cases, *C. jejuni* infection can lead to Guillain-Barré syndrome, reactive arthritis and post-infectious inflammatory bowel syndrome (5-7). *C. jejuni* typically has a 2-5 day incubation period before the onset of symptoms with the illness usually being self-limiting and lasting from 2-10 days.

Campylobacter is one of the major causes of food-borne gastroenteritis causing up to 400-500 million cases of infection worldwide per year (8, 9). In the developing world, young children are typically affected by campylobacteriosis in contrast to developed countries where young adults show the greatest prevalence (10, 11). In Canada, there were 10,174 confirmed cases of *Campylobacter* infection reported in 2012 (12). However, many cases of *Campylobacter* infection go unreported and data from

2006 has estimated that *Campylobacter* could cause upwards of 145,000 infections in Canada annually (13). In the USA, there were 6,621 reported cases of *Campylobacter* infection in 2013 (14). Estimates from 2011 suggest that there could as many as 845,024 cases each year (15). Campylobacteriosis commonly occurs by ingestion of contaminated food such as poultry or from raw milk or water (16).

1.2. Sources, classes and defenses against reactive oxygen species

Campylobacter colonization of the gastrointestinal tract involves a multitude of key cellular mechanisms to facilitate growth and circumvent the host's innate and adaptive immune systems. Furthermore, successful colonization requires *Campylobacter* to survive the multitude of environmental challenges it is exposed to not just during transit from the external environment but also within the gastrointestinal tract. These stresses can include nutrient availability (17-19), low pH (20-22), bile exposure (23), osmolarity and temperature fluctuations (24-26), as well as nitrosative (27) and oxidative stresses (28-30). Reactive oxygen species (ROS) are particularly harmful to bacteria and can be produced as a consequence of the normal metabolic processes of *Campylobacter* (31, 32), as well as from the host microbiota (32, 33) and immune system (34). As a microaerophilic bacterium, *Campylobacter* requires molecular oxygen (O_2) for growth (35). However, this requirement for O_2 inevitably leads to generation of reactive oxygen species such as superoxide ($O_2^{\bullet-}$), hydrogen peroxide (H_2O_2), and the hydroxyl radical ($HO\cdot$) due to the reduction of molecular oxygen (equation 1).

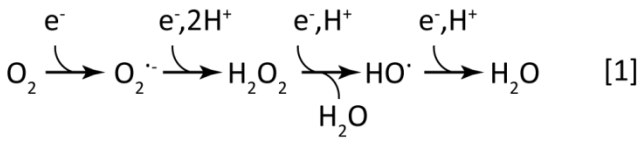

[1]

Molecular oxygen is small and uncharged allowing it to diffuse across cellular membranes. Given the ability of O_2 to diffuse easily across biological membranes, organisms have developed defense mechanisms to protect themselves from the harmful ROS that arise from oxygen exposure. O_2 has a low reduction potential of -0.16 V, which requires O_2 to accept an electron from strong electron donors such as metal centers, flavins or respiratory quinones (36). Respiratory dehydrogenases, which contain such cofactors, can be oxidized by O_2 leading to the production of $O_2^{\bullet-}$ (37). More recently, non-respiratory flavoproteins, such as glutathione reductase, lipoamide dehydrogenase, and glutamate reductase, have been identified as major sources of $O_2^{\bullet-}$ and H_2O_2 production within cells (36). The rate of *in vitro* $O_2^{\bullet-}$ production is estimated to be approximately 5 µM/s within *E. coli* cells (38). Consequently, this rate of $O_2^{\bullet-}$ production is sufficient to damage biological molecules (36) and thus detoxification enzymes such as superoxide dismutases (SODs) are required to convert $O_2^{\bullet-}$ into H_2O_2.

1.2.1. Superoxide dismutase

SOD enzymes dismutate $O_2^{\bullet-}$ into H_2O_2 according to equation 2.

$$2\,O_2^{\cdot-} + 2\,H^+ \longrightarrow H_2O_2 + O_2 \qquad [2]$$

$O_2^{\bullet-}$ is charged preventing diffusion back across bacterial membranes into the surrounding environment, which therefore requires compartmentalized antioxidant enzymes to detoxify $O_2^{\bullet-}$ produced within the cell. In *E. coli*, the presence of SOD enzymes help maintain the level of $O_2^{\bullet-}$ to approximately 0.1 nM (38). *E. coli* expresses multiple SOD enzymes: SodA, SodB, and SodC. SodA and SodB are cytoplasmic proteins, which contain manganese and iron cofactors respectively (39). SodC is a copper-zinc protein expressed within the periplasmic space of the bacteria (40). In contrast, *C. jejuni* only expresses a single, iron cofactored enzyme, SodB (41, 42).

Although SOD enzymes can facilitate the dismutation of harmful $O_2^{\bullet-}$ species, the reaction yields a second ROS, H_2O_2, which requires the expression of additional enzymes for its detoxification. H_2O_2 is a strong two-electron oxidant (with a reduction potential E^0 of + 1.32 V at pH 7.0) but a weak one-electron oxidant with a reduction potential of + 0.38 V (36). Importantly, one-electron reduction of H_2O_2 generates the powerful oxidizing species, the HO· radical (E^0 of + 2.33 V) (36). Like O_2, H_2O_2 is uncharged and can easily pass across biological membranes. H_2O_2 does not directly damage the majority of biological molecules, but in the presence of redox metals, Fenton chemistry can produce HO· radicals (37). The overall equation describing Fenton chemistry is presented in equation 3.

$$H_2O_2 + Fe^{2+} \longrightarrow Fe^{3+} + HO^{\cdot} + HO^{-} \qquad [3]$$

Transition metals such as iron or copper can directly interact with H_2O_2 to cleave the O-O bond to produce the HO· radicals (43). The ferrous ions required to drive Fenton chemistry can arise from low levels of free iron within the cell or those complexed to proteins (43). These radicals are thought to act at diffusion limiting rates and can directly damage most biological molecules resulting in the formation of protein carbonyls, peroxidation of membranes, and DNA lesions (31). Under physiological conditions, the rate constant for HO· formation is approximately 5-20 x 10^{-3} $M^{-1}s^{-1}$ (44, 45). It is estimated that in *E. coli*, H_2O_2 is produced at rates ranging from 10 µM-15 µM/s (46) with concentrations as low as 1 µM resulting in DNA damage (37). Consequently to prevent cellular damage and/or death due to the production of HO· radicals, cells express numerous H_2O_2 detoxification enzymes to reduce levels of H_2O_2 production and ultimately Fenton chemistry. Furthermore, cells express iron chelation proteins (ferritin, bacterioferritin) to reduce free iron levels (47, 48). Two of the major H_2O_2 detoxification enzymes present within cells are alkyl hydroperoxide reductases (Ahp) and catalases (Kat) (37). Ahp and Kat enzymes use different mechanisms to detoxify H_2O_2 as shown in equations 4 and 5 respectively.

$$H_2O_2 + NADH + H^+ \longrightarrow 2\,H_2O + NAD^+ \quad [4]$$

$$2\,H_2O_2 \longrightarrow 2\,H_2O + O_2 \quad [5]$$

1.2.2. Alkyl hydroperoxide reductase

Ahp is comprised of two subunits, AhpC and AhpF, which encode for a peroxidase and a NADH reducing flavoprotein respectively. H_2O_2 is reduced to H_2O (equation 4) by AhpCF by the transfer of electrons from NADH to H_2O_2 (36). In *C. jejuni*, AhpC has been identified and characterized (49), however, it remains unclear how AhpC is reduced as AhpF has yet to be identified (41, 49). It is thought that the thioredoxin reductase enzyme, TrxB, may function to regenerate AhpC as has been demonstrated in *H. pylori* (50, 51). AhpC is the primary scavenging enzyme of H_2O_2 within *E. coli* when extracellular H_2O_2 levels are below 20 µM. Indeed, AhpC is able to keep endogenous levels of H_2O_2 to approximately 20 nM (52) due to its high activity (k_{cat}/K_m of 4×10^{-7} $M^{-1}s^{-1}$ (53)) despite a H_2O_2 production rate of 10 µM-15 µM/s. However, if the extracellular concentration of H_2O_2 increases beyond 20 µM, AhpC activity becomes saturated due to an increased need for the cell to provide NADH as a reducing equivalent for AhpC (37). Consequently, catalase becomes the major detoxification enzyme of H_2O_2 as it does not rely on NADH to regenerate the catalase enzyme.

1.2.3. Catalase

Catalase dismutates H_2O_2 according to equation 5. There are 3 classes of catalase enzymes including monofunctional catalases, bifunctional catalase-peroxidases, and non-heme containing manganese catalases (54). KatA from *C. jejuni* belongs to the monofunctional class of catalase enzymes (41). The dismutation reaction that catalase enzymes catalyzed can be represented as a two steps reaction according to equations 6 and 7:

$$\text{KatA (Por-Fe}^{III}\text{)} + H_2O_2 \longrightarrow \text{KatA (Por}^{\cdot+}\text{-Fe}^{IV}\text{=O)} + H_2O \quad [6]$$

$$\text{KatA (Por}^{\cdot+}\text{-Fe}^{IV}\text{=O)} + H_2O_2 \longrightarrow \text{KatA (Por-Fe}^{III}\text{)} + H_2O + O_2 \quad [7]$$

The first step of the reaction involves the oxidation of the heme prosthetic group of catalase by one molecule of H_2O_2. This oxidation step generates a high valent, oxoferryl porphyrin cation radical intermediate (equation 6) and releases one water molecule. The oxoferryl porphyrin cation radical is then reduced by a second H_2O_2 molecule returning the enzyme back to its resting ferric state (equation 7) (55). This second step of the reaction releases one water and one oxygen molecule.

Numerous structures have been solved for monofunctional catalases including both large subunit (>75 kDa) and small subunit (>54 kDa) enzymes. Amongst the large subunit enzymes are those solved from *E. coli* (HPII) (56) and *Penicillium vitale* (PVC) (57), whereas the structures for small subunit enzymes consist of those solved from *Helicobacter pylori* (KatA) (58), *Enterococcus faecalis* (KatA) (59), *Pseudomonas syringae* (CatF) (60), bovine liver catalase (BLC) (61), and *Homo sapiens* erythrocyte catalase (HEC) (62). KatA from *C. jejuni* belongs to the small subunit class of enzymes with a subunit size of 54 kDa (41). Typically, monofunctional catalases are tetrameric proteins and consist of four identical subunits. The overall structure of the individual subunits consists of an N-terminal arm domain, an α-helical domain, a β-barrel domain, and a wrapping domain (Figure 1.2.1).

The N-terminal domain associates with other individual KatA subunits to help form higher quaternary structure (dimers) by forming 'knot-like' structures (63). The α-helical domain consists of four α-helices located near the surface of the β-barrel domain. The β-barrel domain is highly conserved across catalases from different species as it plays a highly important role for catalytic activity (64). This domain consists of an eight stranded anti-parallel β-barrel with six α-helices located within the turns of the β-strands (63). The β-barrel domain is important structurally in generating the quaternary structure

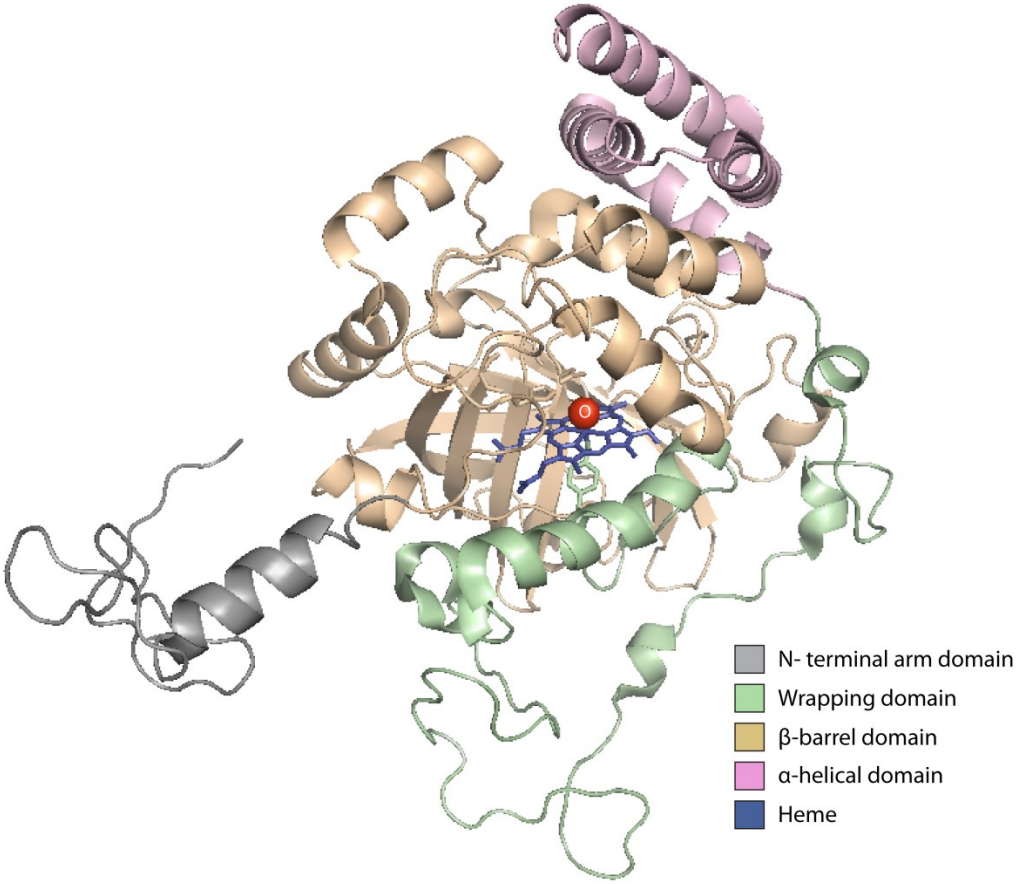

Fig 1.2.1. Crystal structure of the KatA subunit from *H. Pylori*. KatA subunits contain four domains: an N-terminal domain (gray), wrapping domain (green), β-barrel domain (brown), and α-helical domain (pink). Heme (blue) is located within the heme pocket of KatA. The axial ligand of the heme Fe^{3+} ion (tyrosine) is depicted within the wrapping domain. The histidine, serine, and asparagine residues of the β-barrel domain are located on the distal side of the heme prosthetic group (58). An oxygen atom acts as an axial ligand of the heme Fe^{3+} ion on the distal side. Visualization of the KatA subunit was performed using Pymol version 1.1 and Protein Data Base accession 1QWL.

of catalase by providing contact between two subunits due to location of the β-barrel domain near the surface of the subunit. Secondly, the β-barrel domain forms the distal heme cavity where the heme prosthetic group is located. The β-barrel contains three essential amino acids (histidine, serine and asparagine) located on the distal side of the heme group which form part of the heme pocket (Figure 1.2.2) (64). The histidine residue may also act as an acid-base catalyst in the first step of the catalase dismutation reaction (equation 6); however, the participation of this essential histidine residue in the catalase reaction mechanism has not yet been experimentally demonstrated (55). Regardless, it is clear from crystal structures of catalase enzymes that the imidazole ring of histidine is parallel to the pyrrole ring III of heme generating π-π interactions between the histidine and heme group. Thus histidine plays an important structural role in the heme cavity. The essential serine residue is also important for maintaining the structure of the heme pocket by stabilizing the positioning of the histidine residue (58, 64). Finally, the asparagine residue aids orienting the incoming H_2O_2 molecules within the heme pocket so that catalysis can occur (58). There are three channels that allow small uncharged molecules (i.e. H_2O_2) to access the heme prosthetic group buried within each catalase subunit. The major channel leading from the surface to the active center of the enzyme is perpendicular to the heme group and is the preferred channel that H_2O_2 uses to reach the active site (65). Finally, the wrapping domain of catalase enzymes contains an essential α-helix (α9), which is located within a major groove at the bottom of the β-barrel. A loop structure at the end of the helix also partially wraps itself halfway around the β-barrel domain (58, 64). A conserved tyrosine residue is located on the α-9 helix, which coordinates the heme Fe^{3+} ion on the heme proximal side, yielding a pentacoordinate heme coordination structure. This wrapping domain also participates in tetramer assembly (64, 66).

In *C. jejuni,* catalase is an important factor for colonization of an *in vivo* chick commensal model (29). Indeed, a *C. jejuni* isogenic deletion mutant strain of catalase, Δ*katA*, was completely attenuated

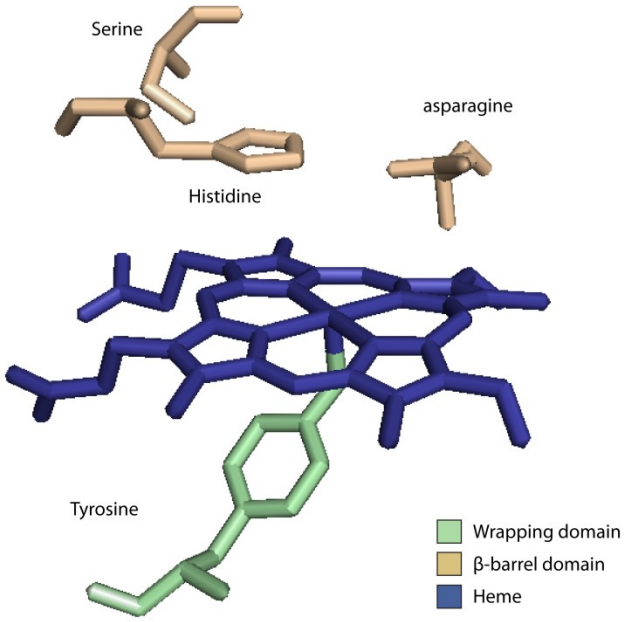

Fig 1.2.2. Heme pocket of *H. pylori* KatA. The heme Fe^{3+} ion is coordinated by a tyrosine residue located on the wrapping domain (green) on the proximal side of the heme prosthetic group (blue). A conserved histidine residue found within the β-barrel domain (brown) interacts with the pyrrole ring III of heme on the distal side of the heme pocket via π-π interactions. Conserved serine and asparagine residues within the β-barrel domain help maintain the structure of the heme pocket and orient incoming H_2O_2 molecules respectively (58). Visualization of the heme pocket was performed using Pymol version 1.1 and Protein Data Base accession 1QWL.

for colonization of chicks relative to the parental *C. jejuni* NCTC11168 strain (29). Thus, KatA expression is clearly essential for successful growth and survival of oxidative stress encountered within the gastrointestinal tract.

1.3. Biological molecules damaged by ROS

Exposure of living organisms to superoxide and hydrogen peroxide can lead to significant damage to biological molecules and impairment of key cellular processes. One of the major targets of oxidative damage is iron-sulphur $[4Fe\text{-}4S]^{2+}$ cluster containing proteins (67). $O_2^{\bullet-}$ is a strong univalent oxidant and is able to remove one electron from surface-exposed Fe-S clusters while generating H_2O_2 in the process. The resulting $[4Fe\text{-}4S]^{3+}$ cluster is unstable and results in the release of an Fe^{2+} ion which renders these enzymes catalytically inactive (68). In *E. coli*, several Fe-S cluster enzymes of the citric acid (TCA) cycle that are particularly liable to $O_2^{\bullet-}$ include aconitase B, and fumarase A and B (69-71). As these enzymes become damaged by $O_2^{\bullet-}$, the bacteria are unable to grow using TCA intermediates as carbon sources (68-70). H_2O_2 can also damage $[4Fe\text{-}4S]^{2+}$ clusters by two electron oxidation of the catalytic Fe ion. The resulting transient oxoferryl species pulls a second electron from the cluster releasing an Fe^{3+} ion and inactivating the enzyme (72). It is important to note that the catalytically inactive $[3Fe\text{-}4S]^{+}$ clusters of these damaged enzymes can be functionally reactivated by reduction and incorporation of Fe^{2+} ions by the cell (36).

Mononuclear iron proteins can also be damaged by $O_2^{\bullet-}$ and H_2O_2. Included among these proteins that can be damaged by ROS are epimerases (ribulose-5-phosphate 3-epimerase), dehydrogenases (threonine dehydrogenase), deformylases (peptide deformylase), and deaminases (cytosine deaminase) (73, 74). In the presence of H_2O_2, the Fe^{2+} ion of these proteins participates in the Fenton reaction, which results in the oxidation and release of a Fe^{3+} ion from the enzyme and the production of a $HO\cdot$

radical. Remetallation of these enzymes can restore enzymatic activity, however, the HO· radical can react with the polypeptide to induce irreversible damage to the enzyme which cannot be repaired (73). It has been observed in enzymes which coordinate the Fe^{2+} ion by a cysteine residue (threonine dehydrogenase, peptide deformylase) that the cysteine residue can be oxidized to quench the HO· radical that is produced during Fenton chemistry (75). This oxidation is beneficial for the enzyme as it protects the polypeptide from damage by HO· radicals and the cysteine residue can be subsequently reduced by cellular reductants (75). Superoxide damages mononuclear proteins by oxidizing the Fe^{2+} ion causing the release of Fe^{3+} and producing H_2O_2 in the process (74). Superoxide inactivation of the enzyme is not as detrimental as H_2O_2 as HO· radicals are not produced during the reaction. Enzyme inactivation by $O_2^{\bullet-}$ can be reversed by reinserting Fe^{2+} ions into the protein (74). However over time, this remetallation process can result in other transition metals such as Zn^{2+} being incorporated into the protein which results in a loss of enzyme activity (74).

DNA is another important biological molecule which can be damaged due to ROS exposure. One of the main types of DNA damage is mutagenesis of the nitrogenous bases and/or DNA backbone (45). Mutagenesis of the DNA arises indirectly from cell exposure to $O_2^{\bullet-}$ and H_2O_2 (8, 45). Specifically, H_2O_2 damages DNA via Fenton chemistry by reacting with free Fe^{2+} ions or Fe^{2+} ions that are bound to DNA (76). The HO· radicals can oxidize nitrogenous bases and/or the ribose moiety (77). One of the frequent occurrences of DNA mutagenesis is the oxidation of guanine to 8-hydroxyguanine (78). The generation of 8-hydroxyguanine on the DNA strand is particularly problematic for the cell as 8-hydroxyguanine is able to base pair with adenine resulting in a mis-match that is not easily detected and repaired by the cell (79). DNA lesions are created when ribose is oxidized by HO· radicals. These lesions halt polymerase activity and must subsequently be repaired by the cell.

Overall, the major pathways of oxidative damage by $O_2^{\bullet-}$ and H_2O_2 are iron mediated (Fe-S clusters, mononuclear Fe proteins, Fe^{2+} associated with DNA). Direct oxidation of amino acids by $O_2^{\bullet-}$ and H_2O_2 has yet to be experimentally demonstrated. Indeed, the generation of two types of irreversible protein damage (protein carbonyls and sulphonic acid formation) are the result of attack by HO· radicals (80). Clearly, cells must maintain an intricate balance between the iron acquisition needed to perform essential biological processes and uptake of excess iron which can lead to oxidative stress.

1.4. Heme uptake, heme synthesis and heme trafficking

1.4.1. Heme uptake systems

As mentioned in section 1.2.3, KatA dismutates H_2O_2 into H_2O and O_2 by an essential iron-coordinated heme prosthetic group. Therefore bacteria must be able to acquire sufficient heme for incorporation into catalase as well as other hemoproteins. Heme uptake and transport across the periplasmic space into the cytoplasm has been well characterized for numerous bacterial species (81-86). Gram-negative bacteria can use direct heme acquisition systems and/or secrete hemophores into the surrounding environment to acquire heme. This latter system of heme acquisition has been particularly well characterized for the hemophore HasA/receptor HasR in both *Serratia marcescens* (82, 83) and *Pseudomonas aeruginosa* (81). *C. jejuni* does not encode for an annotated HasAR hemophore secretion/acquisition system (41) and instead utilizes a direct heme uptake system (ChuABCD) to acquire heme from the surrounding environment (Figure 1.4.1) (87). This strategy for obtaining heme is analogous to the previously characterized Shu, Chu, and Phu heme acquisition systems of *Shigella dysenteriae, E. coli,* and *P. aeruginosa* (84-86). The *C. jejuni* heme uptake system encodes for the outer membrane heme receptor (ChuA), which transports heme across the outer bacterial membrane in a TonB-ExbB-ExbD energy dependent manner (41, 87). Heme is then transported across the periplasmic

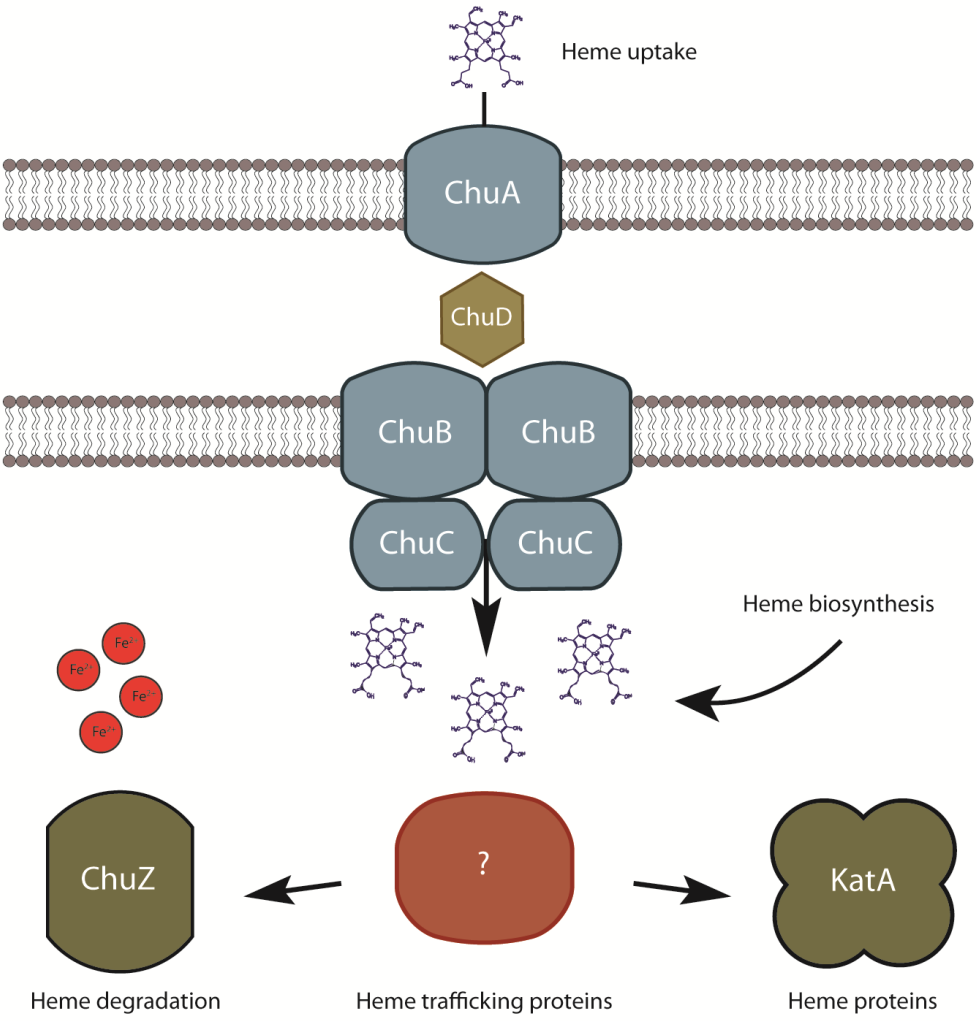

Fig 1.4.1. Heme uptake and trafficking within *C. jejuni*. Heme is transported from the external environment across the outer membrane, periplasmic space and inner membrane by the ChuABCD heme uptake system into the cytoplasm. Alternatively, heme can also be synthesized *de novo* within the cytoplasm if Fe^{2+} ions are readily available. Heme within the cytoplasm binds to unknown heme trafficking proteins and is either delivered to heme proteins or is degraded to release Fe^{2+} ions.

space by the periplasmic transport protein ChuD and finally across the inner membrane by the ABC transport complex, ChuBC (Figure 1.4.1) (87).

1.4.2. *De novo* synthesis of heme within *C. jejuni*

In addition to heme acquisition from the external environment, *Campylobacter* can also presumably synthesize heme *de novo* within the cytoplasmic space. *C. jejuni* encodes for *hemBCDENH* comprising an almost complete heme biosynthesis pathway. However, an annotated *hemG or hemY* gene*,* which convert protopyphorinogen IX into protopyphorin IX, are absent from the genome (88). *C. jejuni* is able to grow and express active KatA when grown in minimal media lacking heme as an iron source (89). It is thus likely that the enzyme responsible for this step of the pathway is present within *C. jejuni* but has yet to be identified.

1.4.3. The physiological requirement for heme trafficking proteins

Once heme is transported into the cytoplasm, it can either be trafficked to proteins that require a heme cofactor (KatA) or it can be degraded to release the ferrous ion to be used in other cellular processes (Figure 1.4.1). At neutral pH, ferrous heme carries no net charge allowing it to freely diffuse across lipid bilayers (90). The porphyrin ring of heme also imparts a hydrophobic character to the molecule (90). Consequently, heme is not easily dissolved in aqueous solutions, and thus the cell likely requires heme chaperone and/or trafficking proteins to bind heme. To enable stable heme binding to proteins, hemoproteins contain hydrophobic heme-pockets which typically consist of a high proportion of aromatic residues (tyrosine, phenylalanine, tryptophan) and hydrophobic residues (leucine, isoleucine, valine) (91, 92). The axial ligands of heme proteins typically consist of histidine, tyrosine, cysteine, methionine and lysine residues (91).

Importantly, levels of free heme are tightly regulated to decrease the amount of ROS that is generated within cells. Heme contains a Fe atom which is able to participate in chemical reactions leading to the production of radical species such as HO· radicals (93). Free heme levels have been estimated to be less than 0.1 µM in liver cells (94). Although the free heme concentration within any bacterial species has not been determined to date, it is speculated to be quite low due to the low solubility of heme in aqueous solutions and also to reduce harmful ROS production. Consequently, bacteria carefully control how much heme is transported into the cell, synthesized, inserted into hemoproteins, and degraded. Thus, to maintain heme solubility within cells and prevent ROS formation, cells require the expression of heme trafficking proteins to transfer heme to target proteins.

1.4.4. Heme trafficking proteins

To date, relatively few heme trafficking systems have been characterized within bacteria. In *P. aeruginosa*, a heme trafficking protein, PhuS, has been characterized which transports heme to its heme oxygenase (95). In *C. jejuni*, degradation of heme to obtain iron is accomplished by the heme oxygenase protein ChuZ (87). However, *C. jejuni* does not encode for a bacterial homolog of PhuS and thus the protein involved in trafficking heme to ChuZ remains unidentified (Figure 1.4.1). Other proteins that function in heme trafficking include those involved in the cytochrome c maturation (CCM) pathway, which has been well characterized in *E. coli* and *P. aeruginosa* (96, 97). The Ccm system transports heme from the cytoplasm and trafficks it to periplasmic cytochrome c enzymes. The Ccm system is comprised of CcmABCDEFGH which all encode for membrane proteins, with the exception of CcmA, which is a cytosolic soluble membrane associated protein. Heme is covalently attached to CcmE via CcmCD which form part of the ABC protein transport complex CmeABCD. Following heme attachment to CcmE, holo-CcmE is released from CcmCD by ATP hydrolysis via CcmA. Holo-CcmE trafficks heme to the CcmFH complex which transfers and covalently links heme from holo-CcmE to periplasmic apo-cytochrome C

(97, 98). Although the Ccm system has been well characterized and is important for trafficking heme to cytochrome c in other bacteria, *C. jejuni* does not appear to utilize the CcmE system. Instead *C. jejuni* likely uses a system similar to that observed in *Helicobacter* and other ε-proteobacteria species which consists of the proteins CcsAB, CcdA, and ResB (97). CcsAB are integral membrane proteins and it is thought that CcsA, which contains a heme binding site, is directly involved in covalently linking heme to apo-cytochrome c. Unlike the Ccm pathway, this cytochrome maturation system does not rely on the heme trafficking CmeE protein (97). Overall, the research on PhuS and CcmE represents the current knowledge on heme trafficking proteins within bacteria. Additionally, the absence of bacterial homologs of PhuS and CcmE in *C. jejuni* suggests significant diversity among bacterial species with regards to the proteins involved in heme transport, leading to increased difficulty in characterizing trafficking proteins across different bacterial species.

The importance of KatA for cellular survival of oxidative stress cannot be overstated. However, despite intense research into the structure and reaction mechanism of this enzyme over many decades, several fundamental questions about catalase biogenesis remain unanswered. Specifically, it is unknown how KatA acquires heme (Figure 1.4.1). Given the hydrophobic nature of heme and the detrimental consequences of having free heme within the cell, heme trafficking proteins likely play a highly important role in this process.

1.5. The oxidant stimulons of *Campylobacter*

Genes encoding proteins involved in oxidative stress defences are known to be induced in response to oxidant exposure within the cell. Therefore, to characterize the oxidant stimulons of *C. jejuni*, gene expression was monitored under iron-restriction in response to 10 min exposure to three classes of oxidants: cumene hydroperoxide (an organic hydroperoxide), hydrogen peroxide, and

menadione (a superoxide generator) (99). There were 57 genes found to be at least 1.5 fold differentially expressed upon exposure of *C. jejuni* to at least one of these three different oxidants (29). Notably, several genes were found to be only inducible by certain oxidants, suggesting specific inducible responses to particular classes of oxidative agent. Specifically, of the 57 differentially expressed genes, 26, 36 and 33 genes have their transcript abundance affected by the addition of hydrogen peroxide, cumene hydroperoxide and menadione, respectively. The hydrogen peroxide stimulon consists of 9 up- and 17 down-regulated genes; the cumene hydroperoxide stimulon consists of 18 up- and 18 down-regulated genes; and the menadione stimulon is composed of 15 up- and 18 down-regulated genes. While the differences in gene content between the three stimulons might indicate specific transcriptional responses to each oxidant, it is also possible that these differences result from distinct levels of oxidative stress induced by each oxidant. The majority of the oxidant-responsive genes grouped into five functional categories: oxidative stress defense, heat shock, heme transport, DNA replication, and surface structures.

1.5.1. Genes involved in oxidative stress defence

The analysis of the *C. jejuni* genome revealed the presence of enzymes and proteins that are thought or known to protect *Campylobacter* against the damaging effects of oxidative stress, including SodB (100), KatA (101), AhpC (49), Cft (47), FdxA (102), Dps (48), and Tpx (103). Previous reports have shown that AhpC and SodB are required for *C. jejuni* survival in aerobic conditions and that *C. jejuni* Δ*katA* and Δ*sodB* mutants are affected in their survival ability within macrophages and INT407 cells respectively (101, 104). Inactivation of *katA* resulted in severe sensitivity toward hydrogen peroxide demonstrating the importance of KatA for hydrogen peroxide detoxification (29). AhpC is the major enzyme in organic-hydroperoxide detoxification in *C. jejuni*, as demonstrated by an increased sensitivity of a *C. jejuni* NCTC 11168 Δ*ahpC* mutant toward cumene hydroperoxide. Interestingly, inactivation of

ahpC increased hydrogen peroxide resistance suggesting a compensatory effect, likely through the over-expression of genes that deal with this particular stress (such as *katA*, *tpx* or *bcp*)(29). Similarly, mutation of *ahpC* in *Staphylococcus aureus, Bacillus subtilis,* and *Xanthomonas campestris* was also shown to increase H_2O_2 resistance (105-107). Inactivation of *sodB* led to impaired resistance toward H_2O_2, cumene hydroperoxide and menadione (29). Menadione is known to be a superoxide generator. Consequently, the menadione sensitivity of the *sodB* mutant is in agreement with the function of SodB as an enzyme that dismutases superoxide to hydrogen peroxide. Interestingly, the *sodB* mutation also reduced the ability of *C. jejuni* to resist H_2O_2 and cumene hydroxyperoxide exposure (29); however these two oxidants are not directly detoxified by SodB. Based on this observation, it is tempting to speculate that the increase of endogenous superoxide anions produced during normal metabolism in the Δ*sodB* mutant will catalyze the release of ferrous iron from iron-sulfur clusters. In turn, a larger pool of labile iron will be available to catalyze the Fenton reaction in presence of hydrogen peroxide and produce hydroxyl radicals. In the presence of cumene hydroperoxide, this pool of iron might catalyze the generation of alkoxyl radicals which will initiate lipid peroxidation. As a consequence, the Δ*sodB* mutant might be sensitive to H_2O_2 and cumene hydroperoxide due to increased metal-catalyzed ROS production. Both *C. jejuni* Δ*cft* and Δ*dps* deletion mutants were found to be more sensitive to H_2O_2 than their parent strains (47, 48). The lack of Cft, which encodes for ferritin, may result in increased levels of labile iron in the cell, which would contribute to hydrogen peroxide toxicity by leading to increased hydroxyl radical formation. A similar mechanism of protection has also been proposed for Dps's role in protection against oxidative stress in *C. jejuni* (48). Although Dps proteins in other bacteria bind DNA and are believed to protect it from oxidative damage; *C. jejuni* Dps does not appear to have this ability and may solely confer resistance to H_2O_2 by sequestering iron (48). A *C. jejuni* Δ*fdxA* deletion mutant was significantly affected in its aerotolerance but not in its resistance to hydrogen peroxide and cumene hydroperoxide (102). The specific function of FdxA in oxidative stress defence remains to be elucidated.

It has been shown that a Δ*tpx*/Δ*bcp* double mutant is affected in aerotolerance and is hypersensitive to oxidant exposure (103). Given that the single mutants were not significantly affected, it has been proposed that Tpx and Bcp are partially redundant antioxidant enzymes (103). Finally, while the two cytochrome *c* peroxidases, Cj0020c and Cj0358, were expected to contribute to hydrogen peroxide resistance, they were not differentially expressed upon H_2O_2 exposure (29). Moreover, the peroxidase activities of these two proteins do not appear to contribute to resistance to hydrogen peroxide (108). Nevertheless, the transcript level of Cj0358 was increased upon menadione exposure suggesting a potential role in resistance to menadione-related stress.

1.5.2. Genes encoding proteins involved in heat shock

HrcA and *grpE* are two genes which are part of the cumene hydroperoxide stimulon and are involved in heat shock response in *C. jejuni* (109). The putative heat shock regulator HrcA, which is thought to repress the *groEL-groES* and *hrcA-grpE-dnaK* operons, was up-regulated in response to cumene hydroperoxide. GrpE is a nucleotide exchange factor involved in the exchange of ADP for ATP on DnaK, which along with DnaJ, helps prevent the formation of aggregates of denatured proteins within the cell (110). The induction of these genes in response to oxidative stress in *C. jejuni* may function to prevent harmful aggregations forming from damaged oxidized proteins.

1.5.3. Genes involved in heme transport

The transcript levels of the genes involved in heme transport, *chuABCD*, were down-regulated in response to oxidant exposure in *C. jejuni* (29). Inactivation of the outer-membrane receptor ChuA results in an inability to grow in the presence of heme or hemoglobin as an iron source (111). The genes *chuBCD* encode for a heme uptake system permease protein, ATP-binding protein and periplasmic heme-binding protein respectively (111). The down regulation of heme acquisition genes might

indirectly contribute to cell survival by preventing further production of reactive oxygen species catalyzed by the uptake of additional exogenous iron. In addition, the repression of these genes might also be an indirect consequence of iron released from protein iron-sulfur clusters (such as aconitase and fumarase) upon oxidative stress, which in turn would result in Fe^{2+}-Fur repression (112).

1.5.4. Genes encoding proteins involved in DNA replication

Several genes involved in DNA replication were down regulated in response to exposure to cumene hydroperoxide. These genes include *pyrE*, *pyrF*, *purD, dnaX*, *dnaA*, and *dnaG*. The genes *pyrE* and *pyrF* encode for a putative orotate phosphoribosyltransferase and an orotidine 5'-phosphate decarboxylase respectively. Both enzymes are involved in pyrimidine base biosynthesis whereas the gene *purD* encodes a phosphoribosylamine-glycine ligase involved in purine biosynthesis. *dnaX* encodes a putative DNA polymerase III gamma subunit, *dnaA* encodes a chromosomal replication initiator protein, and *dnaG* codes for DNA primase. The down-regulation of these genes in response to oxidative stress seems to indicate a growth arrest; possibly to allow for repair of damaged DNA, and thus avoiding the accumulation of mutations.

1.5.5. Genes encoding proteins involved in surface structures

The transcript levels of a number of genes encoding proteins involved in capsule and membrane biogenesis were found to be significantly decreased upon oxidant exposure suggesting a remodeling of the outer-membrane and cellular structure in response to oxidative stress. In particular, several genes involved in biogenesis of the lipids (*accA*, *accB, fabH*, and *plsX*), the peptidoglycan (*mraY*), the capsule (Cj1436c, Cj1432c, *glf*, Cj1423c, and Cj1437c), the O-linked glycosylated flagellum (Cj1305c, Cj1310c, *neuC2*, and *flhB*), and the N-linked glycosyl group (*pglH*) were found to be repressed. The extent and significance of this membrane structure remodelling remains to be investigated. Nevertheless, a similar

response was also observed in *Rhodobacter sphaeroides* cells exposed to hydrogen peroxide (113).

1.6. The oxidant stimulons of other bacteria

With respect to the specific genes belonging to the oxidant stimulons, there are some interesting similarities and differences present in *C. jejuni* when compared with other bacterial species, in particular with regard to the three main antioxidant enzymes KatA, AhpC and SodB. *C. jejuni* carries a single monofunctional catalase encoded by the *katA* gene (101). In contrast to this, *E. coli* contains two catalases: hydroperoxidase I (KatG) and hydroperoxidase II (KatE) (64). Interestingly, KatE is primarily expressed during stationary phase or during conditions which invoke slow growth in the bacteria, whereas KatG is part of the hydrogen peroxide stimulon and is induced upon exposure to this oxidant (114). These two different catalases are under the regulation of two different transcription factors. KatG is regulated by OxyR whereas KatE is regulated by the stationary phase sigma factor, σ^S. This accounts for KatG belonging to the hydrogen peroxide stimulon unlike KatE (65, 114). In *P. aeruginosa,* there are three monofunctional catalases present: KatA, KatB, and KatC (115). KatA is the major catalase present in *P. aeruginosa. KatA*'s expression is induced by both iron and quorum sensing, with its expression greatest during stationary growth (116). Both *katA* and *katB* are part of the hydrogen peroxide stimulon. However while *katB* is regulated by OxyR, *katA* is stimulated by an OxyR independant mechanism (115). The microaerophilic bacterium *H. pylori* contains a single monofunctional catalase, KatA, similar to *C. jejuni* (117). However, in contrast to *C. jejuni*, *H. pylori katA* appears to be activated by Fur in the presence of iron rather than repressed (118). It is not yet known whether KatA in *H. pylori* is part of the hydrogen peroxide stimulon. The *C. jejuni* genome contains a single iron containing superoxide dismutase encoded by the *sodB* gene, which is part of the hydrogen peroxide stimulon. Likewise, *H. pylori* contains a single *sodB* gene, which also contains an iron co-factor (117). In *H. pylori*, *sodB* is regulated by apo-Fur and its expression is repressed when iron levels are low (119, 120). This is

significantly different from the situation in *C. jejuni*, where the *sodB* gene is induced under iron restriction (121). This regulation of *sodB* expression in *C. jejuni* is paradoxical given that *sodB* requires iron as a cofactor and thus SodB would likely not be functional when iron is in short supply. Other bacteria have dealt with this problem by over-expressing a manganese-cofactored superoxide dismutase, SodA, under iron-limited conditions (39). The rationale behind *sodB* expression in *C. jejuni* is unclear.

1.7. Thesis hypothesis

Genes differentially expressed in response to oxidant exposure function in oxidative stress resistance in *Campylobacter jejuni*.

1.8. Objectives of this study

The characterization of the oxidative stress defence systems in Gram-negative bacteria, such as *E. coli* and *P. aeruginosa,* has provided insight into the defences present within *C. jejuni*; however, there are distinct differences between these bacteria and *C. jejuni* (as mentioned in section 1.6). Given these differences in the oxidative stress defences, it remains unclear exactly how *C. jejuni* survives oxidative stress. Microarray data (29) of the oxidant stimulons of *C. jejuni* revealed additional genes with potential roles in oxidative stress defense. Therefore based upon the thesis hypothesis, characterization of the complete set of ROS defence systems is necessary in order to gain a complete understanding of how *C. jejuni* is able to survive oxidative stress and cause infection in the host gastrointestinal tract.

The first major objective of this study was to globally identify and characterize the oxidative stress defenses of *C. jejuni*. Specifically, the genes identified from the transcriptomic analysis of the oxidant stimulons of *C. jejuni* were utilized to construct an isogenic deletion mutant library followed by

phenotypic screening of the mutants for oxidant sensitivity and *in vivo* colonization. Overall, these experiments would provide a general overview of the genes and processes that play an important role in oxidative stress defense in *C. jejuni*. The second major objective was to characterize a protein involved in heme trafficking to catalase. The characterization of a heme trafficking protein to catalase would provide important insight into understanding the fundamental biological processes involved in catalase biogenesis.

CHAPTER 2. MANUSCRIPTS

2.1. Phenotypic screening of a targeted mutant library reveals *Campylobacter jejuni* defenses against oxidative stress

Annika Flint[1,a], Yi-Qian Sun[1,a], James Butcher[1], Martin Stahl[1], Hongsheng Huang[2] and Alain Stintzi[1]

[1]Ottawa Institute of Systems Biology,

Department of Biochemistry, Microbiology and Immunology

Faculty of Medicine, University of Ottawa

451 Smyth Road, Ottawa, ON, K1H 8M5, Canada

[2]Canadian Food Inspection Agency, Ottawa Laboratory (Fallowfield)

3851 Fallowfield Road, Nepean, ON, K2J 1A1, Canada

Running title: *C. jejuni* defenses against oxidative stress

[a] Annika Flint and Yi-Qian Sun contributed equally to this work.

Published in the Journal Infection and Immunity (2014), 82(6), 2266-75**.**

2.1.1. STATEMENT OF MANUSCRIPT STATUS AND CONTRIBUTIONS

The manuscript “Phenotypic screening of a targeted mutant library reveals *Campylobacter jejuni* defenses against oxidative stress” has been published in the Journal of Infection and Immunity, 2014, 82(6), 2266-75.

Flint, A. constructed 21 isogenic deletion mutants and 5 complemented strains in *C. jejuni* and performed the phenotypic assays on these mutant strains. Flint A. designed, performed and analyzed the data generated from the chick colonization assays. Flint A. conducted the experiments elucidating the role of the flagellum mutants in oxidative stress defense including construction of double mutants and performing disc inhibition assays using the flagellum mutants in the presence of fumarate. Flint. A. wrote and revised the manuscript.

Sun, YQ. developed the high-throughput methodology for constructing deletion mutants in *C. jejuni*. Sun, YQ. constructed 88 isogenic deletion mutants and 14 complemented strains and performed the phenotypic analysis on these strains.

Butcher, J. aided in the inoculation and processing of the chicks used for the chick colonization assays. He constructed Figure 2.1.1 using the data generated from the phenotypic assays performed by Flint A. and Sun, YQ.

Stahl, M. aided in the inoculation and processing of the chicks used for the chick colonization assays. Stahl, M. constructed the Δ*acnB* mutant.

Huang, H. provided our lab with access to the temperature controlled incubators located at the CFIA (Fallowfield Facility). Huang, H. aided in the inoculation and sacrifice of the chicks used for the chick colonization assays.

Stintzi, A. was the project supervisor, conceived and designed the project, provided direction and feedback on the experiments. Stintzi, A. aided with the inoculation and necropsy of the chicks used in the colonization assays. Stintzi A. wrote and revised the manuscript.

2.1.2. ABSTRACT

During host colonization, *Campylobacter jejuni* is exposed to harmful reactive oxygen species (ROS) produced from the host immune system and from the gut microbiota. Consequently, identification and characterization of oxidative stress defenses is important for understanding how *C. jejuni* survives ROS stress during colonization of the gastrointestinal tract. Previous transcriptomic studies have defined the genes belonging to oxidant stimulons within *C. jejuni*. We have constructed isogenic deletion mutants into these identified genes to assess their role in oxidative stress survival. Phenotypic screening of 109 isogenic deletion mutants identified 22 genes which were either hypersensitive or hyposensitive to oxidants, demonstrating important roles for these genes in oxidant defense. The significance of these genes in host colonization was also assessed in an *in vivo* chick model of *C. jejuni* colonization. Overall, our findings identify an indirect role for motility in resistance to oxidative stress. We found that a non-motile flagellum mutant, Δ*motAB*, displayed increased sensitivity towards oxidants. Restoration of sensitivity towards superoxide in Δ*motAB* was achieved by fumarate supplementation or tandem deletion of *motAB* with *ccoQ,* suggesting that disruption of the proton gradient across the inner membrane resulted in increased superoxide production in this strain. Furthermore, we have identified genes involved in cation transport and binding, detoxification, and energy metabolism that are also important factors in oxidant defense. This report describes the first isogenic deletion mutant library construction for screening of relevant oxidative stress defense genes within *C. jejuni*, thus providing a comprehensive analysis of the total set of oxidative stress defenses.

2.1.3. INTRODUCTION

Campylobacter jejuni is a Gram-negative, microaerophilic, human pathogen (1) that is the second most reported cause of food-borne bacterial gastroenteritis in the United States (122) and results in 400-500 million cases of infection worldwide per year (9, 122). Illness caused by *C. jejuni* typically results in symptoms such as watery or bloody diarrhoea, fever, nausea and abdominal pain (2). Furthermore, *C. jejuni* infection has also been linked with the development of a rare but serious neuromuscular disorder known as Guillain Barré syndrome (123). As a microaerophilic bacterium, *C. jejuni* requires low levels of molecular oxygen for proper growth due to its dependence on an oxygen-dependent ribonucleotide reductase (35). However this dependence on the presence of oxygen for growth inevitably results in the exposure of important biological molecules, such as DNA, proteins and lipids, to reactive oxygen species (ROS).These ROS originate from several different sources; both within *C. jejuni* and from its environment. Superoxide radicals ($O_2^{\bullet-}$) and hydrogen peroxide (H_2O_2) are produced within *C. jejuni* during normal respiration as a consequence of molecular oxygen non-specifically oxidizing respiratory chain dehydrogenases (31). In addition, oxidation of cellular ferrous ions by H_2O_2 results in the production of the particularly powerful oxidizing species, hydroxyl radicals ($^{\bullet}OH$) (32). ROS are also produced by neutrophils, which are recruited to the gut in large numbers as part of the immune response, and which catalyze the formation of $O_2^{\bullet-}$ as a strategy for killing pathogenic bacteria (34). Finally the gut microbiota, in particular lactic acid bacteria, also produces exogenous H_2O_2 in an attempt to eliminate bacteria competing to colonize the same niche (32, 33). Consequently, *C. jejuni* contains numerous ROS detoxification pathways to survive both endogenously and exogenously produced ROS and colonize its host. The importance of these cellular defenses for *C. jejuni* survival against ROS has been demonstrated by characterizing ROS detoxification enzymes such as KatA, SodB, AhpC, Tpx, and Bcp (30, 124-126). In addition, these oxidative stress defense enzymes play an important role in host colonization and pathogenesis. Recent work has highlighted this role by demonstrating that

in the neonate piglet infectious model a Δ*katA* mutant was outcompeted by the wild type *C. jejuni* strain (89). Clearly, oxidative stress defenses play an important role in *C. jejuni* pathogenesis.

In order to identify unforeseen players in ROS defense in *C. jejuni,* our laboratory previously used genome-wide transcriptome analysis to characterize the oxidant stimulons of *C. jejuni*. Specifically, our work defined *C. jejuni*'s transcriptomic response to 1 mM H_2O_2, 1 mM cumene hydroperoxide, or 1 mM menadione sodium bisulphite exposure (99). Furthermore, we also characterized the transcriptomic responses in a Δ*perR* mutant background to identify potential novel oxidative stress defense genes regulated by the PerR peroxide-sensing regulator (99, 127). In this study, we describe the construction of an isogenic deletion mutant library into the genes identified by our microarray analysis, and their subsequent phenotypic characterization. A total of 109 isogenic deletion mutants were constructed followed by *in vitro* phenotypic analysis of oxidant sensitivity and *in vivo* characterization of selected mutants using chick colonization assays. We have identified 22 mutants that were either hypersensitive or hyposensitive to H_2O_2, cumene hydroperoxide, and/or menadione sodium bisulphite and thus have revealed important roles for these genes in oxidative stress defense in *C. jejuni*. The identified genes function in processes such as detoxification, cation transport and binding proteins, energy metabolism, and phosphate transport. We also identified an indirect role for bacterial motility in protecting *C. jejuni* against oxidative stress. The relevance of the oxidative stress defense mutants in chick colonization was also assessed and revealed important genes required for successful colonization of the chick ceca.

2.1.4. MATERIALS AND METHODS

I. Bacterial Strains, Plasmids and Growth Conditions

Escherichia coli DH5α and K12 strains were cultured aerobically at 37°C in Luria-Bertani (LB) broth or on LB agar plates. LB broth and plates were supplemented with 100 µg/mL ampicillin, 50 µg/mL kanamycin and/or 10 µg/mL chloramphenicol as required. *Campylobacter jejuni* NCTC11168 was grown under microaerophilic conditions (83% N2, 4%H2, 8% O2, and 5% CO2) at 37°C in a MACS-VA500 workstation (Don Whitley, West Yorkshire, England). *C. jejuni* was cultured in Mueller-Hinton (MH) broth in biphasic flasks or on MH agar plates. *Campylobacter* strains containing antibiotic resistance cassettes were grown on MH agar plates supplemented with 10 µg/mL kanamycin and/or 20 µg/mL chloramphenicol as required. The plasmids and bacterial strains used in this study are listed in Table S1.

II. Construction of Isogenic Deletion Mutants

Construction of isogenic deletion mutants was done using the In-fusion Dry-down PCR cloning kit (Clontech). Briefly, target genes plus flanking regions were amplified using *Taq* polymerase (Invitrogen) with the corresponding gene primers (Invitrogen) listed in Table S2. The In-fusion Dry-down cloning kit was used to directionally clone the amplified gene products into BamHI (Invitrogen) digested pUC19. Subsequently, inverse PCR was used to amplify pUC19 plus the flanking end regions of the target gene. A chloramphenicol or kanamycin antibiotic resistance cassette was directionally cloned into the inverse PCR product, disrupting the target gene. The final construct was sequenced to confirm the absence of point mutations and then naturally transformed into *C. jejuni* NCTC11168. Clones were selected for on chloramphenicol or kanamycin supplemented MH agar plates and positive colonies were confirmed by PCR.

Double deletion mutants were constructed by growing mutant strains on MH agar plates supplemented with the appropriate antibiotic for three days under microaerophilic conditions at 37°C. The mutant strains were then cultured overnight in biphasic flasks, spotted onto MH agar plates and allowed to grow overnight. DNA extracted from strains containing the desired secondary gene deletion was naturally transformed into the *C. jejuni* mutant strains grown on the MH agar plates. Clones were selected for on chloramphenicol and kanamycin MH agar plates and PCR was used to confirm the presence of both mutated genes.

III. Construction of Complemented Strains

Complemented *C. jejuni* NCTC11168 mutant strains were constructed as described previously (22). Target genes were amplified from extracted *C. jejuni* genomic DNA using the high fidelity polymerases *Pfx* (Invitrogen), *Pwo* (Roche) or Phusion (Finnzymes). The amplified gene products were subsequently directionally cloned into XhoI (Invitrogen) digested pRRK (22) using the In-fusion Dry-down cloning kit. The plasmids were sequenced to confirm the absence of mutations in the target genes. The corresponding *C. jejuni* mutant strains were then naturally transformed with the final construct and successful transformants were selected for on MH agar plates supplemented with chloramphenicol and kanamycin. Positive colonies were confirmed by PCR using the kanamycin cassette specific primer AR56 and ribosomal region specific primers ak233-ak235 (Table S2).

IV. Disc Inhibition and Motility Assays

C. jejuni NCTC11168 wild type, mutant and complemented strains were grown for three days under microaerophilic conditions on MH agar plates supplemented with chloramphenicol and/or kanamycin as required. Strains were then cultured in biphasic flasks overnight and subsequently diluted to an OD_{600} of 1 in MH broth. For each strain, 100 mL of MH agar (cooled to approximately 45°C and

supplemented with 20 mM sodium fumarate when required) was prepared followed by the addition of 4 mL of the OD_{600} 1.0 culture. The *C. jejuni*- MH agar mixture was then poured in equal volumes into three Petri dishes and allowed to solidify. Paper discs (6 mm diameter) were placed upon the surface of the agar followed by the addition of 10 µL 3% H_2O_2, 3% cumene hydroperoxide (CHP), and 90 mM menadione sodium bisulphite (MND) to each paper disc. Next, the MH agar plates were incubated under microaerophilic conditions and the diameter of growth inhibition (mm) was measured after 28 hours. Each mutant and complemented strain was tested in at least biological triplicate. The averages of the clear zones were used to determine if statistical significance existed between the mutant, complemented and wild type strains using Bayesian statistical analysis. *P* values < 0.001 were considered statistically significant.

The motility of all strains was assayed on 0.4 % MH agar plates. Plates were incubated for 28 hours under microaerophilic conditions at 37°C followed by measurement of the diameter of motility (mm). Motility assays were performed in at least biological triplicate and statistical significance was determined using Bayesian statistical analysis (*P* < 0.001 considered significant).

V. Chick Colonization Model

The chick colonization model for *C. jejuni* was employed as described previously (128). Briefly, one day old, specific pathogen-free layer chicks, raised at Ottawa Laboratory (Fallowfield) (OLF), Canadian Food Inspection Agency (CFIA), were housed in groups of 10 in temperature controlled isolators (32-34°C) and provided with clean water and a commercial, custom made chicken crumbles feed (Ritchie Feed and Seed, Ottawa, ON). *C. jejuni* strains were grown on MH agar plates for three days under microaerophilic conditions at 37°C. Several colonies from each plate were then selected and transferred to 0.4% MH agar motility plates and allowed to grow for an additional 48 hours. The most

motile *C. jejuni* from the motility plates were then sub-cultured in biphasic flasks and grown overnight. The cultures were then centrifuged, resuspended in fresh MH broth, and diluted to approximately 10^5 CFU/mL. Each chick was orally inoculated with 0.5 mL of the prepared culture. To confirm that the chicks received approximately the same number of viable *C. jejuni* for each strain tested, the inoculums were serially diluted and plated onto MH agar plates. The plates were incubated for 1-2 days under microaerophilic conditions before enumeration. The chicks were euthanized 7 days post inoculation, and the ceca were collected and individually weighed. The cecal contents were homogenized, serially diluted and plated onto selective Karmali agar (Oxoid) supplemented with chloramphenicol and/or kanamycin as required. The Karmali plates were incubated for two days under microaerophilic conditions at 42°C and the resulting colonies were counted. Colonization levels of wild-type, mutant and complemented strains are expressed as CFU/g cecal content and statistical significance was analyzed using a non-parametric Mann-Whitney rank sum test. Strains were considered significantly different from the wild type at P values < 0.05. Chicks were used in accordance with regulations outlined by the Canadian Council on Animal Care and experimental procedures were approved by the animal care committee at OLF, CFIA.

2.1.5. RESULTS

I. Selection of genes encoding proteins potentially involved in oxidative stress defense and production of a library of isogenic deletion mutants

The major objective of this study was to systemically identify genes encoding proteins involved in oxidative stress defense in *C. jejuni*. These genes are commonly induced by oxidants. Based on this premise we mined the transcriptome data of *C. jejuni* exposed to menadione (a superoxide generating agent), cumene hydroperoxide (an organic hydroperoxide) or H_2O_2 (an inorganic peroxide). This analysis led to the selection of 57 gene candidates responsive to one or more of the oxidants tested (Bayesian *P* value < 10^{-4}) (99). In *C. jejuni*, the transcriptional regulator PerR is known to repress genes involved in oxidative stress defense (127). In *B. subtilis*, PerR senses peroxide by Fe^{2+}-catalyzed oxidation of its regulatory binding site (consisting of 2 histidines) leading to gene derepression (129). We previously characterized the PerR regulon by microarray analysis and identified 104 PerR-regulated genes with 82 of them being PerR repressed (Bayesian *P* value < 10^{-4}) (99). Based on these transcriptomic analyses we selected a total of 127 genes as potential candidates of the oxidative stress defense system (Table S3). These genes were either up-regulated in response to at least one of the three oxidants tested and/or were PerR-repressed (fold change of > 1.5 with a P-value below 10^{-4}). To note, genes that were slightly below the cut-off Bayesian *P*-value of 10^{-4} but encoding proteins of functional interest were also included in the final selection (for a total of 145 targeted genes; Table S3).

Next, the selected genes were targeted for isogenic mutant construction to characterize their role in oxidative stress defense. The mutants were constructed by allelic exchange to introduce a chloramphenicol resistance cassette to disrupt the gene of interest (as described in the material and methods section). Using this approach we successfully constructed 109 isogenic deletion mutants (Table 2.1.1) from the total 145 gene candidates (Table S3). The construction of the remaining 36 mutants

TABLE 2.1.1. *C. jejuni* isogenic deletion mutant library gene names, functional categories and annotation.

Functional category and gene name	**Annotated gene function**
Detoxification	
cj0020c	cytochrome C551 peroxidase
cj0358	putative cytochrome C551 peroxidase
rrc	Non-haem iron protein
Cation Transport/Binding	
ceuB	enterobactin uptake permease
ceuE	enterobactin uptake periplasmic binding protein
cfbpA	putative iron-uptake ABC transport system, periplasmic iron-binding protein
cfbpB	putative iron-uptake ABC transport system permease
cfbpC	putative iron-uptake ABC transport system ATP-binding protein
cfrA	ferric enterobactin uptake receptor
chaN	putative iron transport protein
chuA	haemin uptake system outer membrane receptor
chuB	putative haemin uptake system permease protein
chuC	putative haemin uptake system ATP-binding protein
chuD	putative haemin uptake system periplasmic haemin-binding protein
chuZ	haem oxygenase
cj0045c	putative iron-binding protein
cj0178	putative TonB-dependent outer membrane receptor
cj1658	putative iron permease
cj1661	possible ABC transport system permease protein
cj1663	putative ABC transport system ATP-binding protein
exbB1	biopolymer transport protein
exbB2	putative exbB/tolQ family transport protein
exbD1	biopolymer transport protein
exbD2	putative exbD/tolR family transport protein
p19	periplasmic protein p19
p19 + cj1658	periplasmic protein p19/ putative iron permease
tonB1	possible tonB transport protein
tonB1+tonB2	possible tonB transport protein/ putative tonB transport protein
tonB2	putative tonB transport protein
tonB2+tonB3	putative tonB transport protein/ tonB transport protein
tonB3	tonB transport protein
Energy Metabolism	

acnB	bifunctional aconitate hydratase 2/2-methylisocitrate dehydratase
ald	putative aldehyde dehydrogenase
ccoQ	cb-type cytochrome C oxidase subunit IV
cj0073c	non-flavin iron–sulfur containing oxidoreductase complex
cj1207c	putative lipoprotein thioredoxin
cj1377c	putative ferredoxin
hypC	hydrogenase isoenzymes formation protein
Surface Structures	
flaG	flagellar protein
flgD	flagellar basal body rod modification protein
flgE	flagellar hook protein
flgE2	flagellar hook protein
flgG	flagellar basal body rod protein
flgG2	flagellar basal-body rod protein
flgH	flagellar basal body L-ring protein
flgI	flagellar basal body P-ring protein
flgK	flagellar hook-associated protein
flgL	flagellar hook-associated protein
flgM	anti FliA (sigma 28) factor
flgP	putative lipoprotein
flgR	sigma-54 associated transcriptional activator
flhB	flagellar biosynthesis protein
fliK	putative flagellar hook-length control protein
maf4	motility accessory factor
maf6	motility accessory factor
maf7	motility accessory factor
motAB	flagellar motor proteins
pseB	UDP-GlcNAc-specific C4,6 dehydratase/C5 epimerase
Drug Efflux	
cj0309c	putative efflux protein
cmeA	periplasmic fusion protein CmeA (multidrug efflux system CmeABC)
Membranes, Lipoproteins and Porins	
cj0385c	putative integral membrane protein
cj0587	putative integral membrane protein
cj0818	putative lipoprotein
cj1211	putative competence family protein
cj1356c	putative integral membrane protein

cj1484c	hypothetical protein
cj0062c	putative integral membrane protein
Miscellaneous	
acs	acetyl-CoA synthetase
cj0295	putative acetyltransferase
cj0494	putative exporting protein
cj0561c	putative periplasmic protein
cj0672	putative periplasmic protein
cj0947c	putative carbon-nitrogen hydrolase
cj0949c	putative peptidyl-arginine deiminase family protein
cj1036c	conserved hypothetical protein
cj1167	putative amino acid metabolism protein
cj1209	phosphodiesterase
cj1241	putative MFS (Major Facilitator Superfamily) transporter
cj1255	putative isomerase
cj1340c	conserved hypothetical protein (1318 family)
cj1388	putative endoribonuclease L-PSP
cj1406c	putative periplasmic protein
cj1623	hypothetical protein
dprA	DNA processing protein A
folP	dihydropteroate synthase
pstC	putative phosphate transport system permease protein
spoT	Putative guanosine-3',5'-bis(diphosphate) 3'-pyrophosphohydrolase
trpF	N-(5'-phosphoribosyl) anthranilate isomerase
truB	tRNA pseudouridine synthase B
Unknown Function	
cj0040	hypothetical protein
cj0044c	hypothetical protein
cj0148c	hypothetical protein
cj0171	merged with Cj0170
cj0202c	hypothetical protein
cj0253	hypothetical protein
cj0260c	small hydrophobic protein
cj0344	hypothetical protein
cj0416	hypothetical protein
cj0524	hypothetical protein
cj0554	hypothetical protein
cj0741	hypothetical protein
cj0786	small hydrophobic protein
cj0814	hypothetical protein

cj0819	hypothetical protein
cj0900c	hypothetical protein
cj0977	hypothetical protein
cj1159c	small hydrophobic protein
cj1242	hypothetical protein
cj1383c	hypothetical protein
mdaB	MdaB protein homolog

failed after multiple attempts suggesting an essential role of the targeted genes and/or poor recombinogenic potential. Indeed, of the 36 mutants that were not obtained, 7 have been identified as essential in *C. jejuni*, with an additional 10 located next to essential genes (130).

II. Phenotypic analysis of the mutant library identified C. jejuni protective mechanisms against oxidants

To identify protective mechanisms against oxidants, the entire mutant library was tested for hypersensitivity or resistance toward exposure to H_2O_2, cumene hydroperoxide and/or menadione bisulphite by disk inhibition assays (Fig 2.1.1 and Table S4). Of the 109 mutants tested, 22 were either hypersensitive or more resistant to one or more of the oxidants (Fig 2.1.1, Table 2.1.2) with values considered significant at $P < 0.001$ using Bayesian statistical analysis.

Of the 22 mutants that had a phenotype, 16 displayed increased sensitivity towards one or more of the oxidants. Nine mutants were specifically hypersensitive to H_2O_2 (Δ*flgP*, Δ*cj0062c*, Δ*cj0344*, Δ*flgI*, Δ*flgK, ΔflgL, Δcj1388*, Δ*acnB, ΔtonB2*), 4 were specifically hypersensitive to menadione sodium bisulphite (Δ*flgR*, Δ*flhB*, Δ*flgD*, Δ*pseB*), 2 were hypersensitive to both H_2O_2 and menadione sodium bisulphite (Δ*flgH,* Δ*cj0947c*), and 1 was hypersensitive to both H_2O_2 and cumene hydroperoxide (Δ*pstC*). The remaining 6 mutants displayed increased resistance towards the oxidants tested relative to the wild type *C. jejuni*. Of these 6 mutants, 2 were specifically more resistant to H_2O_2 (Δ*cj0358*, Δ*exbB1*), and 4 were specifically more resistant to cumene hydroperoxide (Δ*cj1623*, Δ*cj1159c*, Δ*chaN,* Δ*cj0260c*).

These 22 genes group into a wide range of functional categories with several that are not often identified as having an important role in oxidative stress defense. The categories include detoxification (Δ*cj0358*), cation transport/binding proteins (Δ*chaN*, Δ*exbB1,* Δ*tonB2*), energy metabolism (*ΔacnB*), surface structures (Δ*flhB,* Δ*flgD,* Δ*flgH,* Δ*flgI,* Δ*flgK, ΔflgL, ΔpseB)*, membranes, lipoproteins and porins

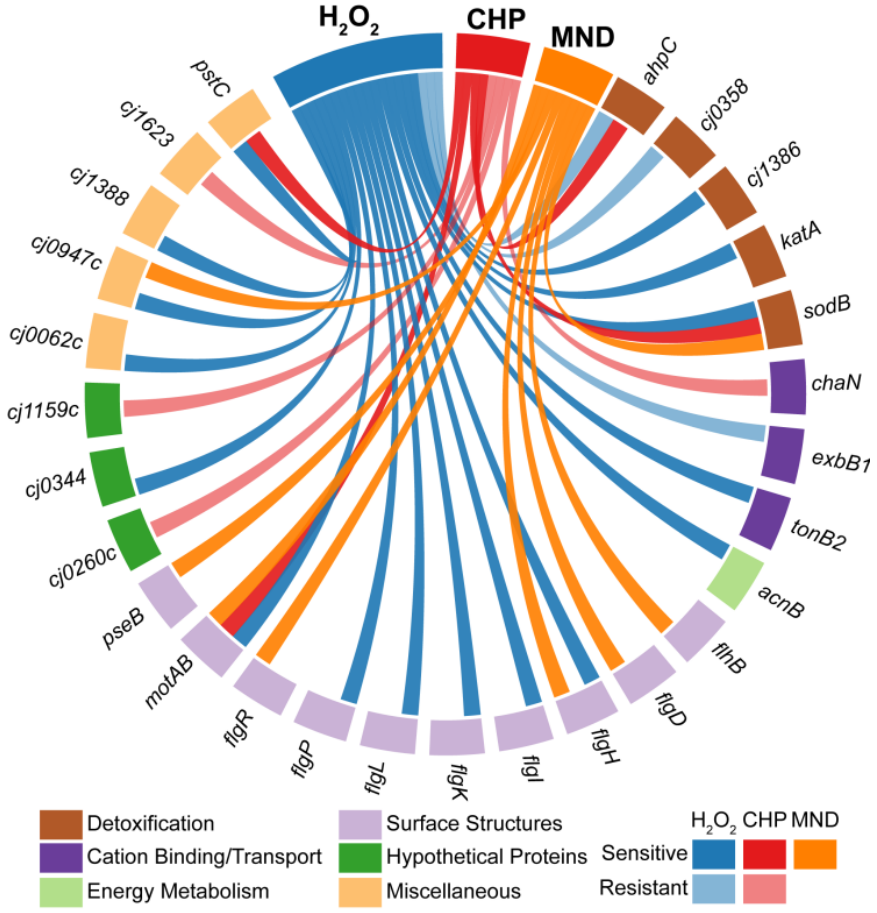

Fig 2.1.1. Sensitivity of isogenic deletion mutants and complemented strains to H_2O_2, cumene hydroperoxide or menadione sodium bisulphite. Mutant and complemented strains are represented along the circle. Lines connecting strains towards 3% H_2O_2, 3% cumene hydroperoxide (CHP), or 90 mM menadione bisulphite (MND) represent the sensitivity of each strain towards the three oxidants assayed relative to wild type *C. jejuni* as determined by disc inhibition analysis. Dark and light lines represent hypersensitivity or hyposensitivity towards the oxidants respectively. Each experiment was repeated in quadruplicate. Mutants were considered statistically significant compared to wild type *C. jejuni* at $P < 0.001$ using Bayesian statistical analysis. Strains are grouped according to functional category.

TABLE 2.1.2. Sensitivity of wild-type *C. jejuni*, isogenic deletion mutants, and corresponding complemented strains to H_2O_2, cumene hydroperoxide or menadione bisulphite.

Functional category and strain	Diam (mm) of zone of inhibition with oxidant[a]		
	H_2O_2	CHP	MND
C. jejuni NCTC11168	19.08 ± 0.19	24.50 ± 0.22	31.63 ± 0.36
Detoxification			
Δ*cj0358*	16.44 ± 0.72*	23.50 ± 0.53	29.63 ± 0.80
Δ*cj0358+cj0358*	17.40 ± 0.40	22.50 ± 0.52	31.93 ± 1.13
Δ*katA*[b]	28.85 ± 0.87*	26.43 ± 0.47	29.85 ± 1.39
Δ*katA+katA*[b]	10.83 ± 1.24*	23.83 ± 0.17	31.00 ± 1.20
Δ*ahpC*[b]	17.23 ± 0.50*	34.87 ± 0.79*	29.05 ± 1.81
Δ*ahpC+ahpC*[b]	18.45 ± 0.10	25.40 ± 0.34	28.38 ± 0.39
Δ*sodB*[b]	22.10 ± 0.35*	30.75 ± 3.53*	38.28 ± 1.96*
Δ*sodB+sodB*[b]	21.78 ± 0.33	25.40 ± 0.17	37.50 ± 2.62
Δ*cj1386*[c]	25.21 ± 0.28*	25.67 ± 0.76	35.04 ± 1.36
Δ*cj1386 + cj1386*[c]	19.90 ± 0.57	24.20 ± 0.51	37.30 ± 0.76
Cation Transport/Binding Proteins			
Δ*chaN*	17.37 ± 0.30	21.47 ± 0.17*	29.83 ± 0.61
Δ*chaN+chaN*	17.26 ± 0.75	22.82 ± 0.66	34.08 ± 1.97
Δ*exbB1*	16.90 ± 0.31*	23.13 ± 0.64	28.30 ± 0.58
Δ*exbB1+exbB1*	17.33 ± 0.60	22.63 ± 0.37	32.90 ± 1.16
Δ*tonB2*	21.10 ± 0.46*	26.47 ± 0.67	33.07 ± 1.39
Energy Metabolism			
Δ*acnB*	21.22 ± 0.45*	23.28 ± 0.24	36.28 ± 0.72
Δ*acnB+acnB*	20.27 ± 0.25	21.33 ± 0.44	33.44 ± 1.49
Surface Structures			
Δ*flhB*	19.80 ± 0.44	23.18 ± 0.32	36.53 ± 1.86*
Δ*flhB+flhB*	18.18 ± 0.76	20.86 ± 0.82	32.15 ± 0.99
Δ*flgD*	20.47 ± 0.47	26.27 ± 0.36	36.50 ± 0.31*
Δ*flgD+flgD*	18.40 ± 0.31	23.60 ± 0.80	31.70 ± 0.58
Δ*flgH*	21.00 ± 0.42*	26.55 ± 0.55	37.00 ± 1.30*
Δ*flgH+flgH*	19.07 ± 0.37	23.37 ± 0.23	32.33 ± 1.19
Δ*flgI*	21.35 ± 0.43*	26.00 ± 0.30	35.38 ± 1.89
Δ*flgI+flgI*	18.95 ± 0.34	23.95 ± 0.21	31.70 ± 1.13
Δ*flgK*	21.53 ± 0.13*	26.13 ± 0.46	34.90 ± 2.04
Δ*flgK+flgK*	19.67 ± 0.17	24.73 ± 0.15	31.10 ± 0.49
Δ*flgL*	21.00 ± 0.23*	25.08 ± 0.32	34.67 ± 1.73

Δ*flgL+flgL*	18.33 ± 1.17	21.25 ± 0.12	30.67 ± 0.10
Δ*pseB*	20.50 ± 0.32	25.92 ± 0.53	35.95 ± 1.40*
Δ*pseB+pseB*	18.95 ± 1.13	23.67 ± 1.20	26.94 ± 2.96
Δ*flgP*	21.63 ± 1.24*	26.25 ± 0.86	35.25 ± 2.21
Δ*flgP+flgP*	19.94 ± 0.59	25.74 ± 0.62	33.08 ± 1.26
Δ*flgR*	20.47 ± 0.75	25.63 ± 0.34	36.78 ± 1.35*
Δ*flgR+flgR*	17.90 ± 0.61	22.17 ± 0.35	32.83 ± 0.87
Hypothetical Unknown Proteins			
Δ*cj0260c*	17.42 ± 0.19	21.67 ± 0.44*	30.87 ± 0.75
Δ*cj0260c+cj0260c*	17.50 ± 0.35	22.83 ± 0.57	30.85 ± 0.35
Δ*cj0344*	20.92 ± 0.14*	23.92 ± 0.45	33.33 ± 1.01
Δ*cj0344+cj0344*	18.12 ± 0.73	21.25 ± 1.24	30.36 ± 1.33
Δ*cj1159c*	19.71 ± 0.90	22.25 ± 0.40*	30.42 ± 0.72
Miscellaneous			
Δ*cj0062c*	21.73 ± 0.21*	26.00 ± 0.39	35.67 ± 0.33
Δ*cj0062c+cj0062c*	19.44 ± 0.39	25.20 ± 0.50	33.63 ± 1.80
Δ*cj0947c*	23.94 ± 1.20*	26.44 ± 0.80	43.00 ± 3.76*
Δ*cj0947c+cj0947c*	20.66 ± 1.50	25.55 ± 0.50	32.33 ± 0.19
Δ*cj1388*	21.17 ± 0.41*	25.38 ± 0.61	35.33 ± 2.20
Δ*cj1623*	18.33 ± 0.50	21.95 ± 0.19*	34.78 ± 2.50
Δ*cj1623+cj1623*	17.44 ± 0.49	22.70 ± 0.39	32.63 ± 1.44
Δ*pstC*	20.75 ± 0.31*	27.25 ± 1.00*	32.33 ± 1.24
Δ*pstC+pstC*	20.60 ± 0.25	25.30 ± 0.41	36.84 ± 1.79

[a-] The diameter of the zone of inhibition is represented as the mean clear zone ± standard error for each strain (in mm) after exposure to 10 µl of 3% H_2O_2, 3% cumene hydroperoxide (CHP), or 90 mM menadione bisulphite (MND). Each experiment was repeated in quadruplicate. Values were considered significant (*) at $P < 0.001$ using Bayesian statistical analysis.

[b-] Data from reference (99).

[c-] Data from reference (89).

(Δ*cj1623*, Δ*flgP*), hypothetical proteins (Δ*cj0062c*, Δ*cj0260c*, Δ*cj0344*, Δ*cj1388*, Δ*cj1159c*), and miscellaneous functions (Δ*pstC,* Δ*flgR,* Δ*cj0947c*).

To confirm the observed phenotypes and rule out the possibility of secondary mutations or polar effects on neighboring genes, complemented strains were constructed for 19 of 22 of the mutant strains as described previously [(22) and materials and methods]. Complementation of the mutants either partially or completely restored the wild-type phenotype for oxidant resistance (Table 2.1.2), indicating that the specific genes mutated were responsible for the observed phenotypic differences. The partial but statistically significant restoration of the phenotype may be due to the differences in the level of gene expression between the complemented strain and wild type *C. jejuni* (as gene transcription is driven from the kanamycin resistance cassette promoter in the complemented strains). From the 109 mutant strains, 87 mutants showed no detectable phenotype toward oxidants (Table S4) suggesting that these genes are not functionally important for cell protection against oxidative stress under the assay conditions.

III. In vivo chick colonization assays of oxidant sensitive mutants reveal genes with important roles in colonization of chick ceca

To investigate the biological significance of important oxidative stress defense genes in an *in vivo* setting, chick colonization assays were performed using the constructed isogenic deletion mutants. Mutants that were identified as being hypersensitive or more resistant to oxidants using the disc inhibition assay were prioritized for testing in the chick colonization assay. Mutants were also selected based upon their functional category (flagellar mutants with sensitivity towards oxidants were not tested due to the motility defects associated with these strains). A total of 30 mutant and complemented strains were tested for their colonization ability. Of the 26 mutant strains, 19 (Δ*flgP*,

Δ*flgR*, Δ*pstC*, Δ*cj1036c*, Δ*acnB*, Δ*cj0344*, Δ*ald*, Δ*trpF*, Δ*cj0260c*, Δ*cj0202c*, Δ*cfbpB*, Δ*cj0062c*, Δ*cj0295*, Δ*cj0947c*, Δ*cj0073c*, Δ*hypC,* Δ*truB,* Δ*cj1207c*, Δ*cj0554*) had a significant reduction in their ability to colonize chick ceca relative to the wild type *C. jejuni* strain as shown in Fig 2.1.2. The remaining 7 strains (Δ*cj1383c*, Δ*chaN*, *Δrrc*, Δ*exbB1*, Δ*cj1209*, Δ*cj1377c*, Δ*cj0814*) were not significantly affected in their colonization levels relative to wild type *C. jejuni*. Four complemented strains were tested (Δ*flgP*+*flgP*, Δ*cj1036c*+*cj1036c*, Δ*cj0260c*+*cj0260c*, and Δ*cj0202c*+*cj0202c*) with the Δ*flgP*+*flgP,* Δ*cj1036c*+*cj1036c*, and Δ*cj0260c*+*cj0260c* complements showing statistically significant restoration of the phenotype compared to their respective mutants (Fig 2.1.2) confirming the observed *in vivo* phenotype. Importantly, the mutant strains assayed in the chicks did not display any *in vitro* growth defects except for *flgR* and *cj0947c* (Fig S1). Thus, it cannot be ruled out that the attenuated colonization observed in these strains is due to general growth defects in addition to increased susceptibility towards oxidants.

IV. Fumarate supplementation restores the menadione sensitivity of flagellar biogenesis mutants to wild type levels

Of the 22 oxidant sensitive mutants identified, 10 mutants constructed into genes encoding components of the flagellar apparatus (FlhB, FlgD, FlgI, FlgK, FlgL, FlgH and FlgP), proteins involved in flagellar modification (PseB and FlgP), and the flagellar regulatory protein FlgR exhibited significant hypersensitivity toward one or more of the three oxidants tested. Importantly, the complemented strains for these mutants displayed sensitivity towards oxidants to levels comparable to those of the wild-type parental *C. jejuni* strain (Table 2.1.2). Although several mutants into flagellum genes were not affected in oxidative stress resistance (*flgG*, *flgG2*, *flgE*, *flgE2*, *flaG*, *fliK*, *flgM*, *maf4*, *maf6*, and *maf7*), the present results indicate an important role for the flagella in oxidant sensitivity within *C. jejuni*. Interestingly, all the flagellum mutants that were sensitive toward oxidants also displayed reduced motility (Table 2.1.3). Conversely, the flagellum mutants that remained motile (*flgG*, *flgG2*, *flgE*, *flgE2*,

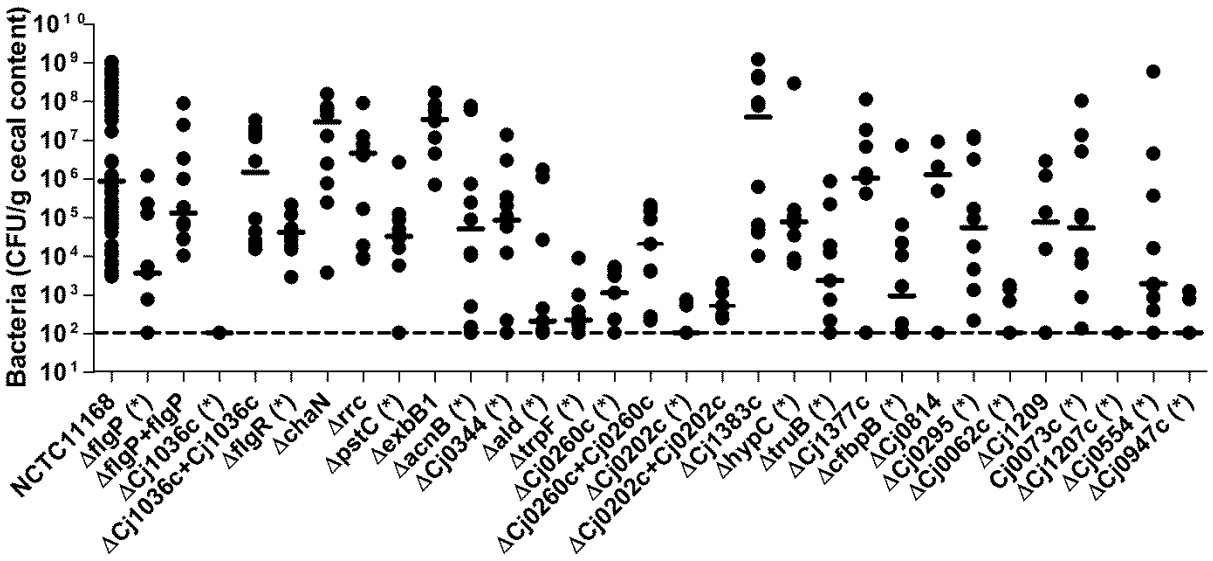

Fig 2.1.2. *C. jejuni* wild type, mutant and complemented strain colonization levels in the chick ceca. Each data point represents the CFU per gram of cecal content recovered for each strain tested. Bars represent the median colonization of each strain and the dashed line indicates the detection limit of the assay. An asterisk denotes statistical significance ($P < 0.05$) using a non-parametric Mann-Whitney rank sum test.

TABLE 2.1.3. Motilities of wild-type *C. jejuni*, flagellum gene mutants and corresponding complemented strains.

Strain	Motility (mm)[a]
NCTC11168	33.1 ± 0.4
Δ*flhB*	8.0 ± 1.2*
Δ*flhB+flhB*	31.3 ± 3.6
Δ*flgD*	8.0 ± 0.0*
Δ*flgD+flgD*	33.2 ± 1.2
Δ*flgE*	48.4 ± 3.9*
Δ*flgE+flgE*	43.5 ± 3.3
Δ*flgH*	18.3 ± 2.2*
Δ*flgH+flgH*	28.8 ± 1.5
Δ*flgI*	24.0 ± 3.4*
Δ*flgI+flgI*	38.3 ± 2.7
Δ*flgK*	11.2 ± 4.2*
Δ*flgK+flgK*	11.0 ± 0.6*
Δ*flgL*	10.5 ± 6.4*
Δ*pseB*	6.3 ± 0.4*
Δ*flgG*	34.8 ± 12.4
Δ*flgG2*	28.4 ± 7.5
Δ*flgP*	6.0 ± 0.0*
Δ*flgP+flgP*	10.0 ± 0.8
Δ*flgR*	17.1 ± 4.5*
Δ*flgR+flgR*	29.8 ± 0.2
Δ*flgM*	31.5 ± 0.5
Δ*flgM+flgM*	29.0 ± 0.8
Δ*fliK*	27.2 ± 1.2
Δ*fliK+fliK*	34.0 ± 2.8
Δ*flaG*	27.8 ± 7.4
Δ*flgE2*	50.3 ± 2.4*
Δ*maf4*	41.5 ± 3.5*
Δ*maf6*	29.3 ± 1.3
Δ*maf7*	33.5 ± 2.0
Δ*motAB*	6.0 ± 0.0*
Δ*motAB+motAB*	23.5 ± 2.6*

[a] Motility was assayed on 0.4% MH agar after 24 hr incubation under microaerophilic conditions. Experiments were performed in at least biological duplicate. Values (mean ± standard error) were considered significant (*) at $P < 0.001$ using Bayesian statistical analysis.

flaG, *fliK*, *flgM, maf4*, *maf6*, and *maf7*) showed no defect toward oxidant sensitivity (Table S4). Moreover, mutation of the *flgP* gene, which encodes a lipoprotein required for motility but not flagellum biogenesis (131), resulted in significant hypersensitivity toward oxidants. These observations suggest that it is bacterial motility as opposed to the flagellum apparatus itself that is key for oxidant resistance.

To further investigate this finding, we constructed a *ΔmotAB* double mutant. The *motA* and *motB* genes encode for the flagellar motor apparatus which utilizes the proton motive force across the inner membrane to drive flagellar rotation (132, 133). Previous studies using a *ΔmotAB* mutant have found that this mutant produces a full length flagellum but is non-motile (134). Consequently, we tested our Δ*motAB* mutant for sensitivity towards oxidants. Interestingly, the *ΔmotAB* mutant displayed significantly increased sensitivity towards all 3 oxidants (Fig 2.1.1, Fig 2.1.3), providing further evidence for a link between motility and oxidant sensitivity in *C. jejuni*. Complementation of Δ*motAB* restored the motility of the Δ*motAB* strain (Table 2.1.3), and sensitivity toward H_2O_2 and cumene hydroperoxide to that of wild type levels (Table S5). Restoration of the phenotype in the presence of menadione was, however, not found to be statistically significant (Fig 2.1.3).

The flagellar motor utilizes the proton potential of the inner cell membrane to generate torque for rotation (133). Consequently, flagellum mutants may conceivably exhibit a disturbed proton potential, which in turn, may perturb the activity of the electron transport chain (ETC). The ETC is known to be the main source of endogenous ROS production (32). Therefore, ETC disturbance may cause increased production of ROS through electron leakage leading to the observed hypersensitive phenotype of the flagellum mutants. It has been well documented that electron leakage at complexes I and III of the ETC lead to the endogenous production of superoxide (135). Disruption of proton/electron flow could also lead to the production of harmful oxy-intermediates and free radicals at complex IV

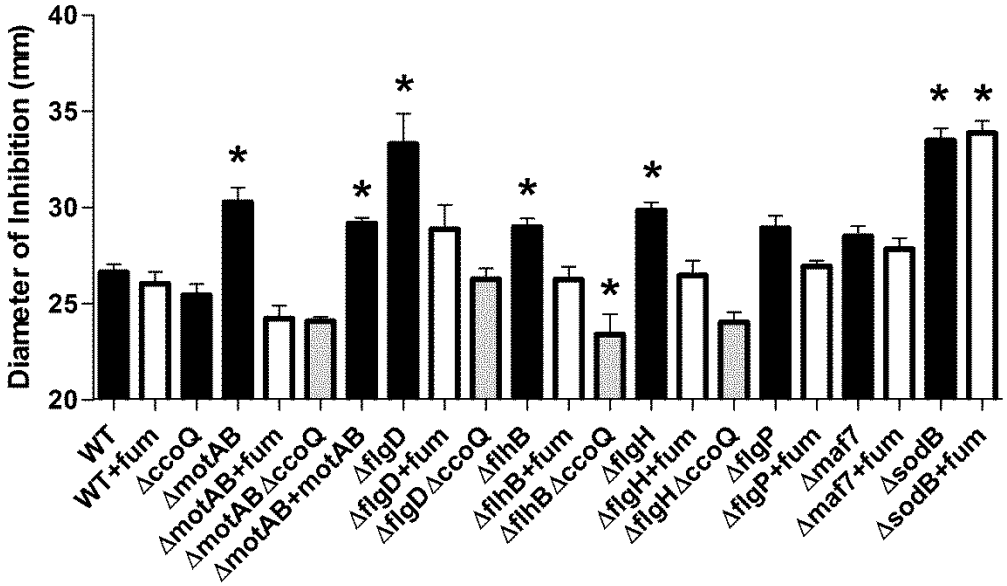

Fig 2.1.3. The use of an alternative electron acceptor or tandem deletion of ccoQ in flagellar mutants restores sensitivity towards menadione to parental *C. jejuni* levels. Wild type, isogenic single and double deletion mutants, and complemented *C. jejuni* strains were assessed for sensitivity to 90 mM menadione using disc inhibition analysis. When required, the MH agar was supplemented with 20 mM sodium fumarate (fum). The diameter of the zone of inhibition is represented as the mean clear zone ± standard error for each strain (in mm) after exposure to 10 µl of 90 mM menadione bisulphite. Each experiment was repeated in at least quadruplicate. Values were considered significant (*) at $P < 0.05$ using one way analysis of variance (ANOVA). Black bars, wild type and mutant *C. jejuni* strains; white bars, strains + fumarate; gray bars, double deletion mutant strains.

(cytochrome c oxidase) which is the only ETC complex that directly interacts with molecular oxygen (135). To test this hypothesis, we assessed the oxidant sensitivity of the flagellar mutants in the presence of an alternative terminal electron acceptor, fumarate. The use of fumarate allows for cellular respiration to occur without the involvement of complex IV (35). As shown in Fig 2.1.3, the Δ*motAB*, Δ*flgD*, Δ*flhB*, and Δ*flgH* strains all displayed increased resistance towards menadione when 20 mM fumarate was supplemented into the agar. Indeed, in the presence of fumarate, the Δ*motAB*, Δ*flgD*, Δ*flhB*, and Δ*flgH* mutants were no longer significantly sensitive towards menadione as compared to the parental *C. jejuni* strain. Importantly, the reduced susceptibility of the flagellar mutants to menadione is specific to the motility defects observed in these strains and not to any general antioxidant properties that fumarate supplementation may provide upon oxidant exposure. This observation is supported by the phenotypes obtained for the wild type, Δ*sodB*, and Δ*maf7* strains, which did not show a statistical difference in oxidant sensitivity in the presence of fumarate (Fig 2.1.3). Furthermore, the restoration of the phenotype was specific to menadione exposure. No significant decrease in sensitivity towards either H_2O_2 or cumene hydroperoxide was observed for the Δ*motAB*, Δ*flgD*, Δ*flhB*,and Δ*flgH* mutants (Table S5).

V. Complex IV of the ETC is the primary site of menadione induced oxidative stress in the non-motile flagellum mutants

The use of fumarate as an alternative terminal electron acceptor to oxygen alleviated the menadione sensitive phenotype of the Δ*motAB*, Δ*flgD*, Δ*flhB*,and Δ*flgH* mutants. This result suggested that complex IV of the ETC (which interacts directly with molecular oxygen) may be a major contributor in generating endogenous superoxide stress when oxygen is present in these mutants. This increased endogenous superoxide production may in turn make these mutants more susceptible to menadione induced stress. Given that we had successfully constructed a deletion mutant into the CcoQ subunit of

cytochrome c oxidase (132), we subsequently constructed double deletion mutants Δ*motABΔccoQ*, Δ*flgDΔccoQ*, Δ*flhBΔccoQ*, and Δ*flgHΔccoQ* to determine if complex IV plays an important role in generating oxidative stress. Deletion of *ccoQ* in tandem with the flagellum mutants significantly reduced the hypersensitivity phenotype of the individual flagellum mutants towards menadione (Fig 2.1.3). Thus, complex IV of the ETC contributes to the increased sensitivity towards menadione in the flagellum mutants. Similar to the results in the presence of fumarate, no significant restoration of phenotype towards either H_2O_2 or cumene hydroperoxide was observed for the double deletion mutants relative to their respective single deletion mutant (Table S5), showing that complex IV specifically contributes toward menadione sensitivity. Overall, these findings suggest that in non-motile flagellum mutants, superoxide stress is originating specifically at complex IV of the ETC leading to the hypersensitivity observed in these strains.

2.1.6. DISCUSSION

Bacterial pathogens that colonize the intestine are threatened by the host innate and adaptive immune responses, and face hostile conditions including the production of ROS. Under the auspice of the gut, oxygen can freely diffuse across cell membranes and be reduced to superoxide anions ($O_2^{\bullet-}$), which damage DNA, proteins and lipids. Moreover, the presence of pathogenic bacteria triggers activation of the NOX family of enzymes and yields potent $O_2^{\bullet-}$ (136). Pathogens have evolved mechanisms to detoxify and protect themselves from ROS in order to survive and colonize the gastrointestinal tract. To date and despite the physiological importance of oxidative stress defenses, only eight major detoxification enzymes/proteins have been identified and characterized within *C. jejuni*: AhpC (alkyl hydroxyperoxide reductase), SodB (superoxide dismutase), KatA (catalase), Tpx (thiol peroxidase), Bcp (thiol peroxidase), Dps (bacterioferritin), MsrA/B and Cj1386 (ankyrin-containing protein involved in heme trafficking to catalase) (42, 124-126, 137-139). To deepen our knowledge on genes and/or mechanisms involved in oxidative stress defense, we constructed a collection of 109 targeted mutants into genes that were previously shown to be induced by oxidant exposure and/or to be regulated by the peroxide stress regulator PerR. This collection constitutes a unique resource to comprehensively identify the measures employed by *C. jejuni* to cope with oxidative stress. All 109 mutants were screened for sensitivity or resistance towards H_2O_2, cumene hydroperoxide, and/or menadione sodium bisulphite using disc inhibition assays. Strikingly, only 20% of the constructed mutants had measurable phenotypes under the conditions tested. There are several reasons why phenotypes were not observed for all 109 mutants screened. Firstly, it is important to note that the microarray analysis of the oxidant stimulons and PerR regulon were conducted in iron-restricted MEMα media, whereas the oxidant inhibition assays were performed under iron-replete conditions in Mueller-Hinton (MH) agar. Changes in the growth media can significantly alter gene expression patterns. This is especially true for the three main oxidative defense genes in *C. jejuni; katA, ahpC* and *sodB.* The

expression of these three genes is iron responsive and both *katA* and *ahpC* are regulated by iron dependant transcriptional regulators (125, 127). In addition, both *katA* and *sodB* require iron or iron cofactors for their catalytic function (126). These changes in *C. jejuni's* antioxidant potential could influence the phenotypes observed. Secondly, many antioxidant proteins have overlapping and compensatory roles in detoxifying oxidants. This has already been reported in *C. jejuni* with the redundancy observed between the Tpx and Bcp proteins (124). While single mutants in these genes were not affected in oxidant sensitivity, the double mutant displayed significant sensitivity towards oxidants. Thus several mutants in genes identified using transcriptomic approaches may not exhibit a phenotype unless they are deleted in tandem with other genes. Indeed, we have demonstrated that tandem deletion of the flagellum mutants with *ccoQ* restored the oxidant sensitivity of these mutants. Thirdly, oxidant exposure likely induces genes not only involved in oxidative stress resistance but also in protection against other stresses. This last hypothesis would explain the unchanged phenotype of several mutants, including the mutants into drug efflux pumps (*cmeA*, *cj0309c*), stringent response (*spoT*), sulfonamide resistance (*folP*), and potential osmotic and/or temperature resistance (*truB*) with regards to oxidative stress defense. Finally, we also identified genes involved in *C. jejuni's* growth, energy metabolism, and biosynthesis that were not directly related to ROS detoxification and protection, and are likely a response of the bacteria to oxidant exposure and thus do not display a phenotype.

Despite these limitations however, a total of 22 mutants displayed a phenotype toward oxidant exposure. Importantly, to confirm the observed phenotypes and rule out possible polar effects or secondary mutations, the mutants were complemented which resulted in full or partial restoration of the wild-type phenotype in agreement with the role of these genes in oxidative stress defense. These genes encode two major groups of proteins, those directly involved in protective mechanisms and those contributing to metabolic rearrangements which indirectly affect the endogenous production of ROS.

Work from our lab and others has previously identified several genes involved in the direct detoxification of oxidants including the well characterized *katA, ahpC* and *sodB* genes (42, 99, 125, 126, 137). Despite our expectations, results from the mutant screening identified relatively few novel genes directly involved in detoxification. Indeed, with the exception of both *rrc* (*cj0012c*) and *cj0358* we did not identify any other genes with phenotypes towards oxidants that are directly involved in detoxification. Rrc, is a unique *C. jejuni* protein and appears to be a chimera of rubredoxin oxidoreductases (Rbo) and rubreythrins (Rbr) found in other bacteria (140). From our study, although just below our very stringent cut off for statistical significance (P<0.001), inactivation of *rrc* led to increased sensitivity towards menadione sodium bisulphite and H_2O_2 (P=0.00522 and 0.0052 respectively). Furthermore, *cj0358*, a putative cytochrome c peroxidase (132), displayed increased resistance towards H_2O_2. Although the *in vitro* results suggest important roles for Rrc and Cj0358 in cellular defense against oxidants, the *Δrrc* mutant and *Δcj0358* mutant (CJJ0382 in *C. jejuni* 81-176), were not significantly affected in their ability to colonize the ceca of chicks (our work and (141)). Thus, it appears that *C. jejuni* primarily relies on KatA and SodB to detoxify H_2O_2 and superoxide respectively during colonization despite deletion of Rrc or Cj0358.

In addition to *rrc* and *cj0358*, our screen identified 20 genes indirectly contributing to protection against oxidants exposure. These genes encode proteins involved in flagellum biogenesis, energy metabolism, cation transport, and general bacterial physiology. The larger number of genes involved in secondary or indirect protection mechanisms reflects the paucity of genuine oxidative defense pathways in *C. jejuni*. Indeed, it is now clear from our work that this organism primarily relies on KatA, AhpC and SodB to prevent cellular damage from ROS. As a result and compared to other bacteria, *C. jejuni* processes a relatively small number of genes involved in direct ROS detoxification suggesting a rudimentary oxidative stress defense system. This somewhat simple defense system is surprising given the continuous exposure of *C. jejuni* to ROS in the gastrointestinal tract and during inflammation. In

particular, the lack of enzyme isoforms present in other bacteria (e.g., multiple superoxide dismutase [SOD] enzymes) suggests that these multiple defense pathways might not be essential for *C. jejuni* gut colonization.

Among the genes indirectly contributing to oxidative defense pathways, the largest single functional category are those that encode proteins involved in flagellum biogenesis. More specifically, we found that defects in bacterial motility were indirectly responsible for the increased sensitivity towards the superoxide generator menadione. Mutants that displayed a reduced or non-motile phenotype likely experience a disrupted proton gradient, and consequently electron leakage along the ETC, contributing to increased endogenous $O_2^{\bullet-}$ production and thus increased oxidative stress in these strains. In support of this, fumarate supplementation or tandem deletion of *ccoQ* in non-motile flagellar mutants significantly reduced menadione induced cell death. From these results, complex IV of the ETC appears to be a particularly susceptible site for generating oxidative stress. Supplementation of the growth media with an alternative electron acceptor such as fumarate likely reduces the additional oxidative damage that occurs at complex IV by promoting fumarate respiration, which does not use an oxygen-dependent oxidase. Furthermore, deletion of *ccoQ* in the non-motile flagellum mutants restored the oxidant sensitivity towards menadione suggesting this complex plays an important role in the generation of oxidative stress. Although the precise mechanism by which complex IV generates stress in these strains is unknown, it is clear that bacterial motility and a functional ETC are required to minimize superoxide induced stress in the presence of menadione.

Mutants inactivated in the cation transport and/or binding proteins ChaN, ExbB1, and TonB2, also displayed significant differences in their resistance toward oxidants. The Δ*chaN* mutant exhibited increased resistance toward H_2O_2 (P= 0.002) and cumene hydroperoxide, whereas Δ*exbB1* was more resistant to specifically H_2O_2. The Δ*tonB2* mutant was more sensitive to H_2O_2 than the wild-type strain.

ChaN is an iron regulated lipoprotein that binds two heme groups per dimer and is thought to be involved in heme trafficking (142). Based on the phenotype of the Δ*chaN* mutant it is tempting to speculate that the heme sequestering capacity of ChaN might limit the amount of heme trafficking to the major H_2O_2 detoxifier in *C. jejuni*, KatA, explaining the observed resistance of the mutant toward H_2O_2. Likewise, the *exbB1* energy transduction protein was also found to have increased resistance to H_2O_2. The potential role of ExbB1 in oxidative stress defense is unclear, however it is interesting to note that *exbB1* is located downstream from *chaN* and also displays a similar phenotype. Moreover and in contrast to the Δ*exbB1* mutant, the Δ*tonB2* mutant displayed significant sensitivity towards H_2O_2, indicating that TonB2 plays an important role in hydrogen peroxide defense. Although the precise role that *tonB2* plays in oxidative stress defense is unknown, it is possible that deletion of this gene causes disruption in energy transduction for processes important to oxidant defense. While none of the other deletion mutants in iron acquisition genes were affected in oxidative stress resistance, phenotypic characterization under iron-limited growth conditions would be required to refute or validate their potential role in oxidant defense.

Our previous transcriptomic work pointed to a role for genes involved in energy metabolism in protection against oxidants. Among the 7 mutants constructed into energy metabolism genes, *ald*, *cj1377c*, *cj1207c*, *hypC*, *ccoQ*, *cj0073c* and *acnB,* only the Δ*acnB* (aconitase) mutant exhibited a phenotype. This mutant was hypersensitive towards H_2O_2 and menadione sodium bisulphite. In *E. coli*, the AcnA and AcnB proteins have been implicated in post-transcriptional regulation. Following oxidative damage to the iron-sulphur clusters of AcnA or AcnB, the apo-proteins specifically bind and stabilize the 3'UTR of their respective mRNA transcripts resulting in increased synthesis of their respective proteins (143). Moreover, the apo-aconitase proteins also post-transcriptionally regulate the synthesis of the SodA oxidative stress defense enzyme as well as many other proteins involved in oxidative stress defense (143). While our study shows a critical role for *acnB* in oxidative stress defense, whether AcnB

has a post-transcriptional regulatory role for its own transcript or other oxidative stress defense genes such as *sodB* remains to be experimentally investigated.

Our phenotypic screen revealed a link between numerous general biological processes and oxidative stress defenses. Mutation into *pstC*, a putative phosphate transport system permease protein, revealed increased sensitivity towards H_2O_2 and cumene hydroperoxide relative to the wild-type strain. Given the requirement for phosphorous for numerous biological processes, bacteria consequently must be able to acquire phosphorous from the surrounding environment. Phosphorous is taken up into the cell in the form of inorganic orthophosphate (P_i). An important feature of P_i is that it can be linked together by enzymes such as Ppk to form polyphosphates. Polyphosphates have important roles in pathogenesis as studied in several bacterial pathogens including *E. coli*, *P. aeruginosa*, *H. pylori*, *V. cholerea,* and *S. flexneri* (144-150). Polyphosphate has been reported within these bacteria to be involved in processes such as motility, biofilm formation, acid, heat and osmotic stress, stationary phase survival, and resistance to oxidative stress (144-150). The increased sensitivity towards oxidants in the Δ*pstC* mutant suggests a role for phosphate acquisition and polyphosphate synthesis in oxidative stress response in *C. jejuni* which requires further investigation.

The requirement of antioxidant enzymes for successful colonization of *C. jejuni in vivo* has been previously demonstrated for the major detoxification enzymes KatA, AhpC, and SodB. Indeed, the Δ*katA*, Δ*ahpC* and Δ*sodB* deletion mutants were all significantly attenuated in colonization of the chick ceca revealing the significant role that oxidative stress defenses play during colonization (99). Subsequently, we sought to assay key genes identified from our phenotypic screening to assess their biological relevance using the chick colonization model. Among the strains tested, the Δ*acnB* and Δ*pstC* mutants were found to be significantly attenuated for colonization of the chick ceca. Deletion mutants in the flagellum genes *flgR* and *flgP* were also affected in colonization; however, the attenuation observed for

these mutants may also be a result of the motility defects associated with these strains. Mutants into *cj0344, cj0947c and cj0062c* all displayed a significant decrease in colonization relative to the wild type strain. Given that the precise function these genes have in oxidant defense is unknown, it cannot be ruled out that mechanisms other than oxidative stress defense are contributing towards the observed *in vivo* phenotypes. Overall, the *in vivo* colonization experiments highlight the importance of these genes for chick colonization.

In this study we report the construction an isogenic deletion mutant library into potentially relevant oxidative stress defense genes as identified by microarray analysis. This genome-wide screening of a constructed mutant library into oxidant sensitive mutants is the first to be described in *C. jejuni*. Phenotypic characterization of the constructed mutants in both *in vitro* and *in vivo* assays revealed novel functions for genes important for oxidative stress defense within *C. jejuni*. We report a major role for genes involved in motility as an indirect contributor to oxidative stress through disruption of the ETC. These results have thus revealed an unexpected pathway used by oxidants to induce cell death in *C. jejuni*. We also identified important roles for *acnB*, cation transport and binding proteins as well as roles for previously uncharacterized genes in oxidative stress defense. Future characterization of these oxidant defense genes will provide insight into their function and the role they play in oxidant detoxification within the cell.

2.1.7. ACKNOWLEDGEMENTS

This work was supported by CIHR grant MOP84224 to A.S., a QEIIGSST scholarship to A.F., and a CIHR-Banting graduate scholarship to J.B. We thank J.E. Algire and the animal care staff for their professional and technical help during the *in vivo* chick colonization experiments at OLF, CFIA.

2.2. Cj1386 is an ankyrin-containing protein involved in heme trafficking to catalase in *Campylobacter jejuni*

Annika Flint[1], Yi-Qian Sun[1], and Alain Stintzi[1]

[1]Ottawa Institute of Systems Biology,

Department of Biochemistry, Microbiology and Immunology

Faculty of Medicine, University of Ottawa

451 Smyth Road, Ottawa, ON, K1H 8M5, Canada

Running title: Cj1386 is involved in heme trafficking

Published in the Journal of Bacteriology (2012), 194(2), 334-345.

2.2.1. STATEMENT OF MANUSCRIPT STATUS AND CONTRIBUTIONS

The manuscript "Cj1386 is an ankyrin-containing protein involved in heme trafficking to catalase in *Campylobacter jejuni*" has been published in the Journal of Bacteriology, 2012, 194(2), 334-345.

Flint, A. constructed the Δ*cj1386* deletion mutant in *C. jejuni* and performed all of the experiments. Flint, A. wrote and revised the manuscript.

Sun, YQ. constructed the Δ*katA*Δ*cj1386*, Δ*cj1386*+*cj1386*, and Δ*katA*Δ*cj1386* +*katAcj1386* strains. Sun, YQ. aided with the feeding and processing of the neonate piglet experiments.

Stintzi, A. was the project supervisor, provided direction and feedback on the experiments, and aided with the inoculation and necropsy of the neonate piglets and chicks used in the *in vivo* assays. Stintzi A. wrote and revised the manuscript.

2.2.2. ABSTRACT

Campylobacter jejuni, a microaerophilic bacterium, is the most frequent cause of human bacterial gastroenteritis. *C. jejuni* is exposed to harmful reactive oxygen species (ROS) produced during its own normal metabolic processes and during infection from the host immune system and from host intestinal microbiota. These ROS will damage DNA, proteins, and cause peroxidation of lipids. Consequently, identifying ROS defense mechanisms is important for understanding how *Campylobacter* survives this environmental stress during infection. Construction of a ΔCj1386 isogenic deletion mutant and phenotypic assays led to its discovery as a novel oxidative stress defense gene. The ΔCj1386 mutant has an increased sensitivity toward hydrogen peroxide. Cj1386 is located directly downstream from *katA* (catalase) in the *C. jejuni* genome. A double deletion mutant Δ*katA*ΔCj1386 was constructed and exhibited a similar sensitivity to hydrogen peroxide as was seen in the single deletion mutants ΔCj1386 and Δ*katA*. This observation suggests that Cj1386 may be involved in the same detoxification pathway as catalase. Despite identical KatA abundance, catalase activity assays showed that ΔCj1386 had a reduced catalase activity relative to wild-type *C. jejuni.* Heme quantification of KatA protein from ΔCj1386 revealed a significant decrease in heme concentration. This indicates an important role for Cj1386 in heme trafficking to KatA within *C. jejuni*. Interestingly, the ΔCj1386 mutant had a reduced ability to colonize the ceca of chicks and was out-competed by the wild-type strain for colonization of the gastrointestinal tract of neonate piglets. These results indicate an important role for Cj1386 in *Campylobacter* colonization and pathogenesis.

2.2.3. INTRODUCTION

Campylobacter jejuni is the most common cause of human food-borne bacterial gastroenteritis in both industrial and nonindustrial countries (151) . Morphologically, *C. jejuni* is a gram-negative, curved, rod-shaped bacteria that grows best under microaerophilic conditions at temperatures ranging from 37 to 42°C (1). Infection caused by *C. jejuni* can occur from the ingestion of quantities as little as 800 organisms (152), with colonization occurring in the jejunum, ileum and colon (153). Typically the symptoms of gastroenteritis include diarrhoea, abdominal pain, nausea, fever and fatigue which can last up to 10 days (2). In addition, *C. jejuni* infection has also been associated with the development of a rare neuromuscular disease, Guillain Barré syndrome, with approximately 1 in 1000 *C. jejuni* cases leading to the development of this disease (123).

While unable to grow at high concentrations of oxygen, *C. jejuni* still requires the presence of free oxygen for growth because of the use of an oxygen-dependent ribonucleotide reductase (35). Additionally, *C. jejuni* lacks an anaerobic-type ribonucleotide reductase (35, 132). Ribonucleotide reductase is essential for DNA synthesis, resulting in *C. jejuni's* dependence on oxygen for bacterial growth (35). *C. jejuni* also utilizes oxygen as a terminal electron acceptor in its respiratory chain (154), and a consequence of oxidative phosphorylation is the inadvertent production of reactive oxygen species (ROS); specifically, the superoxide radical, $O_2^{\bullet -}$, and hydrogen peroxide, H_2O_2 (31). These intracellular ROS are predominantly formed due to O_2 oxidizing the redox enzymes (dehydrogenases) of the respiratory chain, which generates ROS and prevents these enzymes from being oxidized by their intended substrates (31). Additionally, a third ROS, the hydroxyl radical ($^{\bullet}OH$), is produced within the cell via Fenton chemistry when endogenous ferrous ion is oxidized by H_2O_2 (32). In combination with the production of ROS from *C. jejuni's* normal metabolic processes, the host immune system and intestinal microflora also expose *C. jejuni* to ROS (33, 34). The three sources of ROS listed above are particularly detrimental to bacteria as they damage DNA, proteins and cause lipid peroxidation. Therefore bacteria

have evolved elaborate, inducible defense mechanisms to protect themselves from the harmful effects of these various sources of oxidative stress (155).

C. jejuni senses oxidative stresses through the peroxide-sensing regulator PerR (127). Recent transcriptome profiling experiments suggested that Cj1386 might be part of the PerR regulon (99). Cj1386 is located directly downstream from *katA* in the *C. jejuni* NCTC11168 genome (132). KatA, encoding catalase, is an enzyme responsible for the decomposition of H_2O_2 into O_2 and H_2O, and is an important enzyme in protecting *C. jejuni* against the oxidative damage induced by H_2O_2 (137). The genomic location of Cj1386 downstream from *katA,* in conjunction with its regulatory pattern, suggests that Cj1386 may have an important role in oxidative stress defense in *C. jejuni*. The aim of this study was to investigate the function of Cj1386 in response to oxidative stress and to characterize its role in the colonization and pathogenesis of animal models. Our work demonstrates that Cj1386 contributes to bacterial catalase activity by trafficking heme to the KatA enzyme, and that Cj1386 is required for the colonization of the gastrointestinal tract of chicks and piglets.

2.2.4. MATERIALS AND METHODS

I. Bacterial Strains, Plasmids and Growth Conditions

E. coli DH5α, K12 and BL21 strains were grown in Luria-Bertani (LB) broth or on LB agar plates at 37°C under aerobic conditions. LB plates and broth were supplemented with 100 µg/mL ampicillin, 50 µg/mL kanamycin and/or 10 µg/mL chloramphenicol as required. *Campylobacter jejuni* NCTC 11168 (WT) was cultured on Mueller-Hinton (MH) agar plates or in biphasic flasks under microaerophilic conditions (83% N2, 4%H2, 8% O2, and 5% CO2) at 37˚C in a MACS-VA500 workstation (Don Whitley, West Yorkshire, England). MH plates were supplemented with 10 µg/mL kanamycin and/or 20 µg/mL chloramphenicol as required for strains containing antibiotic resistance cassettes. Minimal essential medium MEMα (Invitrogen) was supplemented with 20 mM sodium pyruvate to enhance *Campylobacter growth*. The bacterial strains used in this study are listed in Table 2.2.1.

TABLE 2.2.1. Bacterial strains used in this study.

Strains or Plasmids	Genotype[a]	Source
E. coli		
K12	*endA1, hsdR17*(r_{K12}-, m_{K12+}), *supE44, thi-1, recA1, gyrA96, relA1, lacF'*[*proA*$^{+}$*B*$^{+}$, *lacI*^{q}*ZDM15*::tn10(tet^{R})]	Clontech
DH5α	*endA1 hsdR17* (r_K^- m_K^-) *supE44 thi-1 recA1 gyrA relA1 Δ(lacZYA-argF)U169 deoR [ϕ80dlac Δ(lacZ ΔM15)*]	Invitrogen
BL21(DE3)	F$^-$ *ompT gal dcm lon hsdS$_B$*(r_B^- m_B^-) λ(DE3)	Novagen
AS1082	*E. coli* BL21(DE3) + (pGST+KatA)amp^{R}	This study
C. jejuni		
AS144	*C. jejuni* NCTC 11168	National Collection of Type Cultures
AS433	AS144 Δ*katA*::cam^{R}	Stintzi (99)
AS942	AS144 ΔCj1386::cam^{R}	This study
AS1029	AS144 Δ*katA*ΔCj1386::cam^{R}	This study
AS978	AS433 +*katA*::cam^{R}kan^{R}	This study
AS1028	AS942 +Cj1386::cam^{R}kan^{R}	This study
AS1031	AS1029 +(*katA*+Cj1386)::cam^{R}kan^{R}	This study
Plasmids		
pRY111	Cam^{R} resistance gene	Yao (156)
pRRK	Cloning vector used for complementation of mutants, kan^{R}	Reid (22)
pUC19	Cloning vector, amp^{R}	Biolabs
pGST	Protein expression vector with GST tag and IPTG inducible promoter	Sheffield (157)

[a] cam^{R}, chloramphenicol resistance gene, kan^{R}, kanamycin resistance gene, amp^{R}, ampicillin resistance gene.

II. Construction of Isogenic Deletion Mutants

Construction of the ΔCj1386 and the Δ*kat*AΔCj1386 mutants was performed using the In-Fusion Dry-Down PCR Cloning kit (Clontech), which uses homologous recombination to clone gene products into the cloning vector in the correct orientation. The primers used in this study are listed in Table 2.2.2. Briefly, the gene of interest plus the flanking regions were amplified using Taq Polymerase (Invitrogen) and subsequently cloned into pUC19 using the cloning kit. Inverse PCR was performed using primers designed to introduce a deleted region into the gene of interest, yielding the amplification of pUC19 with the gene regions flanking the end of the vector. A chloramphenicol resistance cassette was subsequently cloned into the vector to disrupt the gene, and the constructed vectors were sequenced to confirm the absence of mutations. The final constructions were naturally transformed into *C. jejuni* NCTC11168 as previously described (158). MH-agar plates containing 20 µg/mL chloramphenicol were used to select for transformed mutants. The deletion mutants were confirmed by PCR amplification of the corresponding chromosomal regions followed by DNA sequencing.

TABLE 2.2.2. Primers used in this study.

Primer Name	Primer Sequence (5'- 3')[a]
Cj1386-sense	CGGTACCCGGGGATCCAAGGCGTAGCACAAAGATATGC
Cj1386-antisense	CGACTCTAGAGGATCCAAAAAGAAGAAATTGCTGAAAAGC
Cj1386-SE-inverse	GAACTAAAGGGCGCATTCTTATGAAAGCGCTAAAATGC
Cj1386-AS-inverse	GAACACCGCCGAGCAGCAAGCATAAGCAAGCTATCG
katA+Cj1386-SE	CGGTACCCGGGGATCCCGATTTTGGAAACATTATAGCTGA
katA+Cj1386-AS	CGACTCTAGAGGATCCTAAAAGGGGCGGTTCCTATC
katA+Cj1386-SE-inv	GAACTAAAGGGCGCAGGCGATAGCTTGCTTATGCT
katA+Cj1386-AS-inv	GAACACCGCCGAGCACGGATGAAGAATGTCGGAGT
Cj1386-SE-comp	GATTTAGATGTCTAGCGCTTCTATGGAAGGAGTTGA
Cj1386-AS-comp	GGGGAAGCTTTCTAGAAAAAGAAGAAATTGCTGAAAAGC
katA+Cj1386-SE-comp	GATTTAGATGTCTAGTTACGTGCATCCCAGTGTTC
katA+Cj1386-AS-comp	GGGGAAGCTTTCTAGTAAAAGGGGCGGTTCCTATC
Cat-SE	TGCTCGGCGGTGTTCCTTTCCAAG
Cat-AS	TGCGCCCTTTAGTTCCTAAAGGGT
AR56-AS	CATCCTCTTCGTCTTGGTAGC
ak233-SE	GCAAGAGTTTTGCTTATGTTAGCAG
ak234-SE	GAAATGGGCAGAGTGTATTCTCCG
ak235-SE	GTGCGGATAATGTTGTTTCTG
katA-RT-SE	AAGTGGAGCTTATGGCGAAA
katA-RT-AS	ACTTCGCTTTTTGCACGATT
katA-RTint-SE	AGCTGCCGAGCTTATAGCAA
Cj1386-RT-SE	GAGCTTTGCAAAATGGCTTT
Cj1386-RT-AS	CCACATCTTTGCGTCCAAAC
Cj1386-RTint-AS	TAATGGGGTTTGTCCACGAT
Cj1384c-RT-SE	TGGGATGCACGTAATGAAAA
Cj1387c-RT-AS	TTGATTTTCCAACAAGAGCCTTA
katA-SE-qPCR	GCGATGTGAGAGGTTTTGCT
katA-AS-qPCR	CAAAAATCCCAAGCAGCATT
Cj1386-SE-qPCR	GGCGATAGCTTGCTTATGCT
Cj1386-AS-qPCR	TAATGGGGTTTGTCCACGAT
metC_SE	CTAAACTTATTCATTGTGGCAGAGG
metC_AS	CTCTGTATTTTTCCAAGTTGCGTG
KatA_NcoI	**GCCATGGCT**ATGAAAAAATTGACTAACGA
KatA_NotI	**GCGGCCGC**TTAGTTTGCCACCAAAAGTGG

[a-] Restriction sites in bold.

III. Construction of Complemented Strains

Construction of the complemented mutant strains was performed as previously described (22). The *katA*, Cj1386, and *katA*+Cj1386 gene regions were amplified from the *C. jejuni* NCTC11168 genome using either Pfx (Invitrogen) or Pwo (Roche) high fidelity polymerase. The amplified PCR product was cloned into the pRRK vector (22) using the In-Fusion Dry-Down PCR Cloning kit (Clontech). The resulting construct was sequenced to confirm the absence of PCR-induced errors in the insert. The *C. jejuni* NCTC11168 deletion mutants were subsequently naturally transformed with the final construct as described above. Positive colonies were selected for on MH-agar plates supplemented with 20 µg/mL chloramphenicol and 10 µg/mL kanamycin. The insertion of the gene into the chromosomal rRNA locus was confirmed by PCR and DNA sequencing as previously described (22).

IV. Disc Inhibition Assay

Wild-type *C. jejuni,* ΔCj1386 mutant, and complemented strains were grown on MH agar plates for 3 days. Several colonies from each strain were sub-cultured in biphasic flasks and grown overnight to mid-log phase. Next, the bacteria were pelleted by centrifugation, and resuspended in MH broth to an optical density at 600 nm of 1.0. For each strain, 4 mL of this bacterial suspension was added to 100 mL of melted MH-agar (cooled to 45°C), and 25 mL was poured into Petri dishes. After solidification of the agar, three 6-mm disks were placed on the surface and 10 µL of 3% H_2O_2, 3% cumene hydroperoxide (CHP) in DMSO, or 90 mM menadione sodium bisulphite was added to the disks as previously described (99). Plates were incubated under microaerophillic conditions for 28 hours, and cleared zones of growth inhibition were measured in mm for each strain. All experiments were performed in quadruplicate for each strain. Averages for each zone of inhibition were calculated and the average of the average was statistically analysed with ANOVA. *P* values < 0.05 were considered as statistically significant.

V. Total Cell Extract and Cell Fractionation Preparation

Whole cell extracts of *C. jejuni* wild-type, ΔCj1386 mutant and complemented strains were prepared using the Peripreps Periplasting Kit (Epicenter Technologies, Madison, WI), which utilizes osmotic shock to disrupt the outer cell membrane followed by the use of lysozyme to digest the cell wall. Briefly, *C. jejuni* strains were grown to mid-log phase in MEMα medium followed by centrifugation and resuspension to an OD_{600} 2.0 in fresh MEMα. Subsequently, 1 mL of this culture was centrifuged and subsequently resuspended in 50 µL Peripreps Periplasting buffer and incubated for 5 min at room temperature. This was followed by addition of 50 µL Peripreps Lysis buffer with an additional 5 min incubation at room temperature. Cell debris was pelleted by centrifugation and the supernatant containing the total cellular protein fraction was transferred to a clean tube and stored at -20°C. As required, mid-log cultures of *C. jejuni* were exposed to 1 mM H_2O_2 for 15 minutes prior to protein extraction (described above). It has been previously shown that exposure of *C. jejuni* (grown in MEMα) to 1 mM H_2O_2 does not affect cell viability (99).

For cytoplasmic and periplasmic protein preparations, the same procedure was employed as described above with a slight modification to isolate the two different fractions. Bacterial cells were resuspended in 50 µL Peripreps Periplasting buffer followed by 5 min incubation at room temperature as described above. Next, 50 µl of chilled, purified water was added and this suspension was incubated on ice for 5 minutes. The culture was centrifuged and the supernatant, constituting the soluble periplasmic protein fraction, was transferred to a clean eppendorf tube. The remaining insoluble fraction (containing the spheroplasts) was resuspended in 100 µL of Peripreps Lysis buffer and incubated at room temperature for 5 min. Cell debris was pelleted by centrifugation and the supernatant containing the cytoplasmic cellular protein fraction was transferred to a clean tube and stored at -20°C.

VI. Catalase Activity Gel

The catalase activities of the wild-type *C. jejuni*, ΔCj1386 mutant, Δ*katA* mutant and complemented strain were assessed by the use of the negative gel staining protocol as described by Woodbury (159). Whole cell extracts were run on an 8% non-denaturing polyacrylamide gel at 25 mA, 4°C. The gel was washed 3 times in H_2O for 5 min followed by exposure to 0.003% hydrogen peroxide for 15 min. The gel was quickly rinsed in H_2O before staining with a solution of 2% w/v potassium ferricyanide (Sigma-Aldrich) and 2% w/v ferric chloride (Fisher Scientific) until bands became visible. The gel was washed 2 more times in H_2O for 10 min and photographed using a multi-image light cabinet (Alpha Innotech Corporation).

VII. Catalase Activity Assay

Catalase activities were quantified using the method developed by Beers and Sizer (160). Briefly, 30 µL of cytoplasmic or periplasmic protein preparation (130 ng/µL) was added to 220 µL KH_2PO_4 and 250 µL 20 mM hydrogen peroxide in a 500 µL volume quartz cuvette. The cuvette was quickly inverted several times to ensure uniform mixing and placed in a Beckman DU 640B spectrophotometer. Decomposition of the 10 mM hydrogen peroxide was measured at 240 nm with absorbance readings taken at 15 second time intervals for a total time of 3.5 min. The unit of activity of each sample is expressed as µmol hydrogen peroxide decomposed per min (U) and per mg of protein (µmol x min^{-1} x mg^{-1}). Each sample was tested in quadruplicate for each strain assayed. Statistical analysis was performed using the Students t test with p values < 0.05 considered statistically significant.

VIII. RNA Isolation

RNA extractions were performed as described previously (128). Briefly, strains were grown in 8 mL MH broth in biphasic flasks or in MEMα to mid-log phase (OD_{600} of 0.7 or 0.2) at 37^{o}C under microaerophilic conditions for the RT-PCR or qRT-PCR assays respectively. Cells were harvested following the addition of 800 µL of cold RNA degradation stop solution (10% buffer-saturated phenol pH 4.3 in ethanol) to prevent RNA turnover (161). The cultures were centrifuged, resuspended in TE buffer and total RNA was extracted using the hot phenol-chloroform method (162). The RNA was subsequently precipitated, resuspended in DEPC-treated water and treated with DNase-I (Invitrogen) to remove contaminating DNA. Finally, the RNA samples were further purified using the RNeasy kit (Qiagen). PCR was performed to ensure the absence of genomic DNA. RNA integrity and quantity were determined using the Experion RNA STDsens Analysis Kit (Bio-Rad Laboratories).

IX. RT-PCR Assay

Reverse transcription PCR experiments were performed using the Qiagen One Step RT-PCR Kit (Qiagen). All primers used in the RT-PCR experiments are listed in Table 2. Primers were designed to amplify transcripts specific for *katA*, Cj1386, and the intragenic region between *katA* and Cj1386. The reverse transcription was performed at 50°C for 30 min followed by an initial PCR activation step at 95°C for 15 min. The PCR cycling steps consisted of denaturing at 94°C for 1 min, annealing at 55°C for 1 min and extension at 72°C for 1 min for a total of 30 cycles and followed by a final extension step at 72°C for 10 min. A positive control using *C. jejuni* genomic DNA was included to confirm that the primers were able to anneal and amplify the intended target regions. Additionally, a negative control without reverse transcriptase was included to ensure the absence of contaminating genomic DNA.

X. Quantitative Reverse Transcriptase PCR (qRT-PCR)

The relative expression levels of the Cj1386 and *katA* transcripts in the Δ*perR* and ΔCj1386 mutants respectively, were determined using the QuantiTect Sybr green RT-PCR kit (Qiagen) and a 7300 real-time PCR system (Applied Biosystems) as described previously (128). The primers used for the qRT-PCR experiment are listed in Table 2. The relative expression levels of Cj1386 and *katA* were normalized to *metC* (putative cystathionine beta-lyase). *metC* expression levels remained unchanged in both the wild-type *C. jejuni, ΔperR* and ΔCj1386 strains, ensuring that *metC* was a suitable choice of gene to use as a reference for the quantification of the Cj1386 and *katA* transcripts (22). The $\Delta\Delta C_T$ method was used to calculate the relative fold change of the *katA* transcript and specific RT-PCR products were confirmed by dissociation curve analysis according to the manufacturer's recommendations (Applied Biosystems). Experiments were done in biological duplicate with technical triplicates for each gene.

XI. Purification of C. jejuni KatA and anti-KatA Antisera Production

Overexpression of KatA was performed in *E. coli* BL21 cells using the protein expression vector pGST as described previously (157). Briefly, the *C. jejuni katA* gene was PCR amplified using Pfx (Invitrogen) high fidelity polymerase and the KatA_NcoI and KatA_NotI primers listed in Table 2. The amplified gene was cloned into the protein overexpression vector pGST using *NcoI* and *NotI* restriction sites, followed by transformation of the final construct into *E. coli* BL21 cells. Sequencing was performed to confirm the absence of polymerase-introduced mutations in the *katA* gene. The strain containing the pGST+KatA construct was grown in 400 mL of LB broth supplemented with 100 μg/mL of ampicillin to an OD_{600} of 0.6 at 37°C with continual shaking. IPTG (500 μM) was added to the broth and the bacterial culture was incubated for an additional 3 hours at 37°C. The cells were then pelleted, resuspended in PBS containing protease inhibitor (Roche), and the cell membranes were disrupted by sonication. Cell

membranes and debris were removed by centrifugation at 13000 rpm for 15 min. The cell lysate containing the GST-KatA fusion protein was then affinity purified using glutathione sepharose 4B resin according to the manufacturer specifications (GE Healthcare). Cleavage of the GST tag from KatA was performed on the resin by addition of TEV protease (157) and gentle shaking overnight at 4°C. The KatA protein was washed from the resin the following day using 6 washes of 200 µL of PBS buffer. Purified protein was frozen and stored at -20°C until use.

Approximately 2.5 mg of KatA protein was used for antibody production by Immuno-Precise Antibodies Limited using 2 rabbits (Victoria, BC, Canada). For each rabbit, a pre-immune bleed was performed prior to the primary immunization with the KatA antigen (0.5 mg) using Complete Freund's Antigen. Over the course of the project, each rabbit received 3 additional boosts with KatA antigen (0.5 mg) using Incomplete Freund's Antigen followed by a terminal bleed and sera collection. Anti-KatA antisera was stored at -20°C until use.

XII. Western Blotting

Protein lysates from *C. jejuni* strains were separated by SDS-PAGE on a 12% denaturing gel and transferred to PVDF membrane (Millipore) using a wet-electroblotting transfer cell (Bio-Rad). Membranes were blocked overnight in 5% (w/v) skim milk, 0.1% Tween-20 in PBS followed by incubation with 0.1 µg/mL anti-KatA antisera in PBS for 1 hr at room temperature. The membranes were washed 6X with PBS followed by incubation with a 1:3000 dilution of anti-rabbit conjugated HRP antibody (Invitrogen) for 1 hr at room temperature. The immunoblot membrane was developed with a 1:1 mixture of luminol to peroxide solution (Thermo-Scientific) for 1 min, and chemiluminescence was detected by X-ray film (Thermo-Scientific). Densitometry of immunoblot results was performed with the use of Adobe Photoshop software (Version 10.0).

XIII. Immunoprecipitation of KatA

Immunoprecipitation experiments using wild-type *C. jejuni*, ΔCj1386, Δ*katA*, and ΔCj1386+Cj1386 strains were performed using Protein A-conjugated Dynabeads (Invitrogen). Strains were grown to mid-log phase (OD_{600} of 0.2) in MEMα under microaerophilic conditions at 37°C prior to harvesting total soluble proteins. Bacterial strains were spun at 6000 rpm for 10 min, resuspended in 1 mL PBS containing a bacterial protease inhibitior cocktail (Sigma) and 10 mg/mL lysozyme, and incubated on ice for 15 minutes. Cells were briefly sonicated on ice (5x5 second pulses) followed by centrifugation at 13000 rpm for 5 min at 4°C to remove membranes and cellular debris. 250 µg of anti-KatA antisera diluted in 200 µL PBS, 0.02% Tween-20 was incubated with 50 µL of Dynabeads for 1 hr with end-over-end rotation at room temperature. The anti-KatA bound dynabeads were washed once with 500 µL PBS, 0.02% Tween-20 before addition of 5 mg of protein lysate. The bead-lysate mixture was incubated overnight at 4°C with end-over-end rotation. The beads were washed 3 times with 200 µL of ice-chilled PBS and KatA was eluted from the beads twice in 100 µL soft elution buffer (50mM Tris pH 8.0, 0.2% SDS, 0.1% Tween-20 (163)) with end-over-end rotation for 7 minutes at room temperature. Immunoprecipitation of KatA from each strain was visualized by SDS PAGE run on a 10% denaturing gel followed by Coomassie Blue staining. KatA protein concentration was determined for each immunoprecipitated sample by densitometry of the SDS PAGE gel using Adobe Photoshop software (Version 10.0). KatA protein content was normalized and equal amounts of KatA (250 ng) from the wild-type NCTC11168, ΔCj1386, and ΔCj1386+Cj1386 strains were assayed for catalase activity using the method described above. Immunoprecipitate from the Δ*katA* strain was used as a negative control for the catalase activity assay. Catalase activity assays were performed in quadruplicate and statistical significance was determined using the Student's t test. *P* values < 0.05 were considered significant.

XIV. Hemin Quantification Assays

Heme content of KatA protein isolated from wild-type *C. jejuni* NCTC11168, ΔCj1386, Δ*katA* and ΔCj1386+Cj1386 strains was quantified using the Hemin Assay Kit (Biovision, Mountain View, Ca), which utilizes the peroxidase activity of hemin to produce a coloured substrate which can be assayed spectrophotometrically. Briefly, KatA was immunoprecipitated from wild-type *C. jejuni* NCTC11168, Δ*katA*, ΔCj1386, and ΔCj1386+Cj1386 strains using the same method as described above with slight modification to the elution step. Elution was carried out by addition of 20 µL of 50 mM glycine, pH 2.8 to the Dynabeads to release protein complexes and to extract heme from the KatA protein. Samples were incubated at room temperature for 2 minutes with end-over-end rotation and subsequently transferred to a clean tube. The samples were brought to neutral pH by the addition of 1M Tris, pH 7.4. Samples were visualized by SDS PAGE run on a 10% denaturing gel followed by Coomassie Blue staining. KatA protein content was normalized using densitometry (Adobe Photoshop software (Version 10.0)). Total hemin concentration was assayed from 40 ng of KatA protein prepared from each immunoprecipitated sample and the assay was performed according to the manufacturer's instructions (Hemin Assay Kit, Biovision, Mountain View, Ca). Background absorbance of IgG (determined from the Δ*katA* immunoprecipitated sample) was subtracted from each of the strains assayed. Experiments were performed in biological quadruplicate. Statistical significance was determined by the Student's t test with p values < 0.05 considered significant.

XV. Chick Colonization Model

The chick colonization model for *C. jejuni* was performed as described previously (128). One day old specific pathogen-free broiler chicks were checked upon arrival to ensure the absence of *Campylobacter* contamination by culturing the fecal contents on Karmali plates (Oxoid). Chicks were

provided with water and commercial chicken starter diet ad libitum. Wild-type *C. jejuni*, ΔCj1386 mutant, and ΔCj1386+Cj1386 strains were grown to mid-log phase in MH broth under microaerophilic conditions at 37°C. The strains were recovered by centrifugation, washed in PBS, and resuspended in fresh MH broth at a concentration of 2 x 10^4 cells per mL. Food and water were withheld from the chicks for 2 hours prior to inoculation. Each 3-day-old chick was inoculated with 0.5 mL of the bacterial suspension (containing approximately 10^4 viable *C. jejuni*). Each bacterial suspension was serially diluted and plated on MH-agar plates to confirm the inocula. Six days later the chicks were euthanized and necropsy was performed. The ceca were collected, weighed, and the cecal contents were extracted and homogenized in MH broth. Cecal contents were serially diluted and plated onto Karmali agar plates supplemented with either 20 μg/mL chloramphenicol or 10 μg/mL kanamycin for the mutant and complemented strains respectively. The plates were incubated for 48 hours at 42°C under microaerophilic conditions and the resulting colonies were counted and expressed as CFU per gram of ceca. Statistical analysis was done using the non-parametric Mann-Whitney rank sum test with *P* values < 0.05 being considered statistically significant.

XVI. Neonate Piglet Infectious Model

The procedure used for the neonate piglet infectious model has been previously described (164). Newborn piglets were housed in sterile conditions at room temperature provided with additional warmth from heat lamps. Newborn piglets were fed a milk replacer five times daily. On the first day of feeding, piglets were syringe fed 60-120 mL of the milk replacer. Wild-type, Δ*katA* and ΔCj1386 strains were grown up to mid-log phase overnight under microaerophilic conditions at 37°C in MH broth. Piglets were inoculated orally by the use of a syringe one day after they were received. Each piglet received approximately 10 mL of a 1:1 mixture of wildtype to ΔCj1386 or wild-type to Δ*katA* bacterial suspension (approximately 10^8 viable *C. jejuni*). Serial dilutions of the inoculum were spread onto MH-agar plates

and MH-agar plates supplemented with 20 µg/ml chloramphenicol to confirm the ratio of ΔCj1386 to wild-type and Δ*katA* to wild-type strain. The piglets were euthanized two days following inoculation and necropsy was performed immediately after. Two to three inch segments of the duodenum, jejunum, ileum, colon, and cecum were removed and weighed, and the mucus layer from each segment was collected and homogenized. Serial dilutions were made for each homogenate of intestine of which 100 µL was spread in triplicate onto Karmali agar plates (*Campylobacter* Selective Supplement, Oxoid) with choloramphenicol added to half the plates to select for the ΔCj1386 and Δ*katA* mutants. Karmali agar plates were placed in microaerophilic conditions at 37°C for 2 days. The resulting *Campylobacter* colonies were counted. The wild-type strain and mutant strains were tested in at least 3 piglets each. The colonization level of the mutant strains were directly obtained by counting the colonies present on the Karmali agar plates supplemented with chloramphenicol. The wild-type *C. jejuni* titre was obtained by subtracting the number of mutant colonies from the total number of colonies recovered on the Karmali agar plates. The competitive index was calculated by dividing the *in vivo* ratio of mutant to wild-type strain recovered (output ratio) by the *in vitro* ratio of the mutant to wild-type strain inoculated (input ratio). The data were analyzed for statistical significance using a non-parametric Mann-Whitney rank sum test. *P* values < 0.05 were considered statistically significant.

2.2.5. RESULTS

I. Cj1386 plays an important role in H_2O_2 detoxification

Analysis of the *katA* genetic region of *C. jejuni* NCTC 11168 revealed the presence of a downstream gene, Cj1386, encoding an ankyrin-repeat containing protein of unknown function. Transcriptome studies have demonstrated that Cj1386 transcript level increases in response to iron starvation (128, 165) and suggested that Cj1386 might be a member of the PerR regulon (99). Indeed, quantitative reverse-transcriptase PCR confirmed the regulation of Cj1386 expression by PerR with up to 72± 24 fold increase in Cj1386 transcript abundance in the Δ*perR* mutant strain compared to the wild-type. Interestingly, orthologues for Cj1386 are conserved among *Campylobacter* species and in *P. aeruginosa* a gene encoding an ankyrin-repeat containing protein (AnkB) has been also identified downstream of the *katB* gene and was found to enhance *Pseudomonas* catalase activity (166). To assess the potential role for Cj1386 in defense against ROS, an isogenic deletion mutant was constructed by allelic exchange as described in the Materials and Methods section. Additionally, a complemented strain was constructed by introducing Cj1386 into one of the three rRNA clusters in the ΔCj1386 mutant background. Next, the ΔCj1386 mutant was tested for its sensitivity towards three different oxidants: hydrogen peroxide (H_2O_2), cumene hydroperoxide (CHP) and menadione sodium bisulphite. As shown in Table 2.2.3, the ΔCj1386 mutant exhibited increased sensitivity towards 3% H_2O_2 relative to the wild-type *C. jejuni* ($P < 0.0005$), and the phenotype was fully restored by complementation with the Cj1386 gene (strain ΔC1386+Cj1386). The ΔCj1386 mutant was not, however, affected in its sensitivity towards either cumene hydroperoxide or menadione relative to the wild-type strain. These results indicate that Cj1386 plays an important function in resistance to hydrogen peroxide in *C. jejuni* and this function is oxidant specific.

TABLE 2.2.3. Sensitivity of wild-type *C. jejuni*, Δ*katA* and ΔCj1386 mutants, and corresponding complemented strains to three oxidants.

Strain	Oxidant[a]		
	H_2O_2	CHP	MND
C. jejuni NCTC11168	19.70 ± 0.38	22.90 ± 0.52	34.8 ± 0.79
Δ*katA*	25.30 ± 0.07*	24.58 ± 0.19	29.85 ±1.39
Δ*katA* + *katA*	10.83 ± 1.24	23.63 ± 0.47	31.00 ± 1.20
ΔCj1386	25.21 ± 0.28*	25.67 ± 0.76	35.04 ± 1.36
ΔCj1386 + Cj1386	19.90 ± 0.57	24.20 ± 0.51	37.30 ± 0.76
Δ*katA*ΔCj1386	25.80 ± 0.39*	22.90 ± 0.71	35.30 ± 1.12
Δ*katA*ΔCj1386 + (*katA* + Cj1386)	10.70 ± 0.85	23.90 ± 0.40	37.50 ± 0.60

[a] The diameter of the zone of inhibition is represented as the mean clear zone ± standard error for each strain (in mm) after exposure to 10 µl of 3% hydrogen peroxide (H_2O_2), 3% cumene hydroperoxide (CHP), or 90 mM menadione bisulphite (MND). Each experiment was repeated in quadruplicate. Values were considered significant (*) at $P < 0.05$ using ANOVA statistical analysis.

As indicated above, Cj1386 is located directly downstream from *katA* in the NCTC11168 genome (132). The gene *katA* encodes the only catalase of *C. jejuni*, which is the main enzyme responsible for the detoxification of hydrogen peroxide into oxygen and water. KatA has been previously demonstrated, both *in vitro* and *in vivo,* to have an important role in hydrogen peroxide defense in multiple strains of *C. jejuni* (30). Additionally a Δ*katA* mutant also displayed an increased sensitivity towards 3% H_2O_2 relative to the wild-type *C. jejuni* NCTC11168 ((99) and in Table 2.2.3). Because of the similar sensitivity of the Δ*katA* and ΔCj1386 mutants towards hydrogen peroxide, and the genomic location of Cj1386 directly downstream from *katA,* we postulated that Cj1386 may be involved in the same hydrogen peroxide detoxification pathway as KatA. To test this hypothesis a double *katA* and Cj1386 deletion mutant, Δ*katA*ΔCj1386, was constructed and assessed for H_2O_2 sensitivity. In the case of two independent H_2O_2 detoxification pathways encoded by *katA* and Cj1386, it would be expected that the loss of function of both KatA and Cj1386 would lead to an overall increase in sensitivity towards H_2O_2 relative to that of the single mutants. However, this phenotype was not observed (Table 2.2.3). Indeed, as shown in Table 3, the Δ*katA*, ΔCj1386 and Δ*katA*ΔCj1386 mutants exhibited equal susceptibility to H_2O_2 (with a growth

inhibition zone of approximately 25 mm compared to 19.7 mm for the wild-type strain). ANOVA statistical analysis confirmed that the three mutant strains were not significantly different from each other ($P > 0.05$). Complementation in *trans* of the Δ*katA*, ΔCj1386 and Δ*katA*ΔCj1386 mutants with the corresponding wild-type genes restored their sensitivity toward H_2O_2 at levels comparable to the parental strain. The increased resistance to H_2O_2 in the Δ*katA+katA* and Δ*katA*ΔCj1386+(*katA*+Cj1386) complemented strains relative to the wild-type is likely due to the loss of iron and H_2O_2 mediated regulation of the *katA* gene expression (99, 127) (as it is expressed from the kanamycin promoter in our construction). Altogether, these results indicate that Cj1386 is involved in the same detoxification pathway or mechanism as KatA.

II. The katA and Cj1386 genes are independently transcribed

The genetic proximity of *katA* and Cj1386 genes suggests that these two genes might be co-transcribed. Therefore, to determine if these two genes belong to the same operon, we mapped the potential transcripts by RT-PCR using primers that anneal within and across these two genes. As shown in Fig 2.2.1, amplicons of the expected sizes were obtained for the *katA* (Fig 2.2.1; lane 1) and Cj1386 (Fig 2.2.1; lane 2) transcripts. However, RT-PCR of the *katA*-Cj1386 region using one primer annealing within *katA* in conjunction with a Cj1386 specific primer failed to yield any product (Fig 2.2.1; lane 3). As expected, no products were obtained for Cj1384c-*katA* or Cj1386-Cj1387c specific transcripts (Fig 2.2.1; lanes 4, 5). To note, RT-PCR using the same primers but with genomic DNA as a template was successful (Fig 2.2.1; lane 6, 7). A negative control without the addition of reverse transcriptase was performed to confirm the absence of genomic DNA contamination in the extracted RNA (Fig 2.2.1; lane 8). Overall, these results indicate that *katA* and Cj1386 are not co-transcribed.

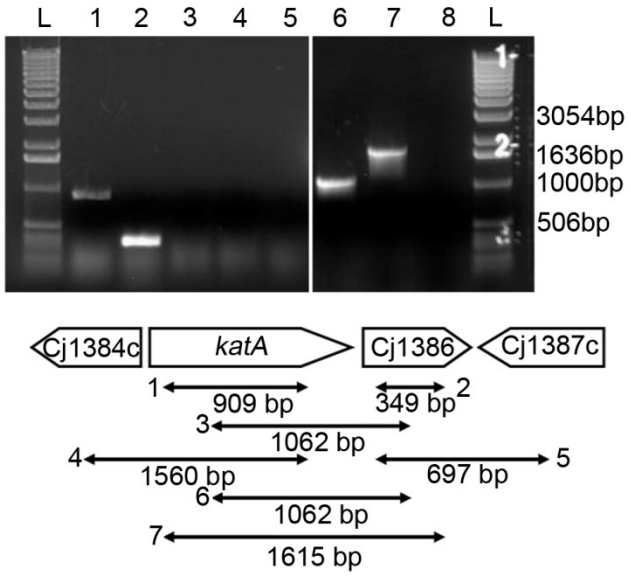

Fig 2.2.1. The *katA* and Cj1386 genes are independently transcribed. RT-PCR products from RNA extracted from *C. jejuni* NCTC11168 were analyzed by agarose gel electrophoresis for operon identification analysis. Lanes 1-5, RT-PCR from RNA extracted from *C. jejuni* NCTC11168; Lanes 6 and 7, RT-PCR from genomic DNA extracted from *C. jejuni* NCTC11168. Lanes: L, 1 kb ladder; 1, *katA*-RT-SE and *katA*-RT-AS (909 bp band visible demonstrating presence of *katA* transcript); 2, Cj1386-RT-SE and Cj1386-RT-AS (349 bp band visible demonstrating presence of Cj1386 transcript); 3, *katA*-RTint-SE and Cj1386-RTint-AS (absence of predicted 1062 bp band indicating *katA* and Cj1386 are not co-transcribed); 4, Cj1384c-RT-SE and *katA*-RT-AS (absence of predicted 1560 bp band indicating Cj1384c and *katA* are not co-transcribed); 5, Cj1386-RT-SE and Cj1387-RT-AS (absence of predicted 697 bp band indicating Cj1386 and Cj1387c are not co-transcribed); 6, positive control *katA*-RTint-SE and Cj1386-RTint-AS (1062 bp band present); 7, positive control *katA*-RT-SE and Cj1386-RT-AS (1615 bp band present); 8 negative control (no RT added to reaction mixture).

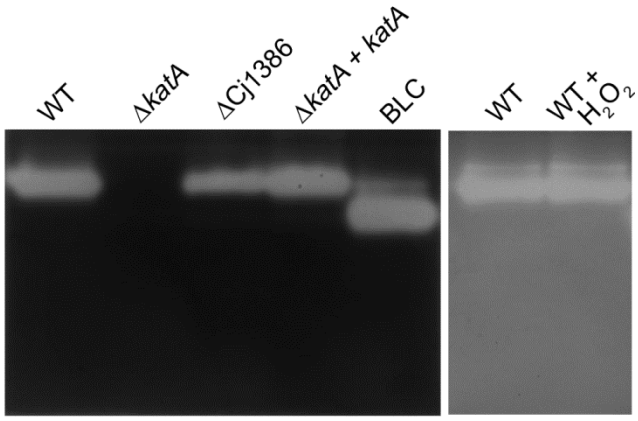

Fig 2.2.2. *C. jejuni* strain contains a single enzyme with catalase activity and ΔCj1386 exhibits a reduced catalase activity. All bacterial strains (*C. jejuni* NCTC11168, Δ*katA*, and ΔCj1386) were grown in MEMα to mid-log phase (OD_{600} of 0.2) under microaerophilic conditions at 37°C prior to cell extract preparation. When required, wild type *C. jejuni* was exposed to 1 mM H_2O_2 for 10 minutes prior to total protein isolation. Fifty micrograms of whole cell extract was loaded onto an 8% non-denaturing gel run at 25 mA at 4°C and assayed for catalase activity. BLC; bovine liver catalase (Sigma-Aldrich).

III. Zymographic analysis of C. jejuni catalase activity detected a single catalase

To further test the hypothesis that Cj1386 is involved in the same H_2O_2 detoxification pathway as KatA, we assessed the catalase activity of the wild-type strain and the Δ*katA* and ΔCj1386 mutants by zymographic analysis (Fig 2.2.2). The mutants and the wild-type strain were grown in iron limited MEMα medium in order to ensure high expression of *katA* and Cj1386 genes (128, 165). As shown in Fig 2.2.2, the wild-type *C. jejuni* strain contained a single enzyme with catalase activity, the Δ*katA* mutant did not produce detectable catalase activity, and the ΔCj1386 mutant showed catalase activity, yet at a reduced level relative to that of the wild-type strain. The catalase activity was fully restored in the Δ*katA*+*katA* complemented strain to levels of enzymatic activity comparable to the wild-type *C. jejuni*. Bovine liver catalase (Sigma) was used as a positive control for catalase activity. Finally, the addition of 1 mM H_2O_2 to wild-type *C. jejuni* did not induce expression of additional enzymes with detectable catalase activity. These results indicate that *C. jejuni* possesses a single enzyme with catalase activity (KatA). Furthermore, similar levels of catalase activity were observed in *C. jejuni* in the presence or absence of H_2O_2 exposure. This observation is in agreement with the relief of PerR repression under iron restricted conditions (used in this assay) enabling high levels of *katA* expression (99). Overall, the reduced catalase activity observed in the ΔCj1386 mutant suggests that Cj1386 contributes to KatA enzymatic function.

IV. Cj1386 plays a role in enhancing KatA catalase activity

According to our zymographic analysis, the absence of Cj1386 decreased catalase activity. To confirm this finding, the catalase activities of the wild-type strain, and the Δ*katA* and ΔCj1386 mutants were quantified and compared following the method developed by Beers and Sizer (160). Unlike many other bacteria which have two catalases, one cytoplasmic and one periplasmic, *C. jejuni* harbours a single catalase of as yet undefined location. A previous study by van Vliet *et al.* has shown KatA to be

present within the periplasmic space in *C. jejuni* (127). However, it remains unknown how KatA is transported into the periplasmic space as the translocation process appears to be TAT and Sec independent due to the absence of a TAT (167) or Sec leader sequence [SignalP(168)] in the KatA protein sequence. Therefore, to confirm the localization of *C. jejuni* catalase, the enzymatic activity was tested in both cytoplasmic and periplasmic protein preparations from *C. jejuni* grown to mid-log phase (OD_{600} of 0.2) in MEMα. Cytoplasmic and periplasmic protein fractions were prepared by using the Peripreps Periplasting Kit (Epicenter Technologies, Madison, WI), which utilizes a combination of osmotic shock and lysozyme treatment. We have previously used and validated this kit to isolate periplasmic fractions from *C. jejuni* (164). Nevertheless, we further confirmed the absence of significant contamination of our periplasmic protein fractions with cytoplasmic proteins by Western-blot analysis using antibodies against the transcriptional regulator PerR, which should be localized exclusively in the cytoplasm (Fig 2.2.3b). Fig 2.2.3 shows the catalase activities of the wild-type *C. jejuni*, the Δ*katA* and ΔCj1386 mutants, and their complemented strains for both cytoplasmic and periplasmic protein fractions. The ΔCj1386 mutant displayed an overall decrease in KatA activity in both the cytoplasm and periplasm. The ΔCj1386 mutant has significantly reduced catalase activity ($1.1x10^4 \pm 2.0x10^3$ U/mg protein) relative to the wild-type *C. jejuni* ($2.0x10^4 \pm 2.3x10^3$ U/mg protein) in the cytoplasmic preparation ($P<0.05$). The ΔCj1386 mutant also had reduced catalase activity as compared to the wild type strain in the periplasmic fraction but this reduction was not statistically significant. The complemented ΔCj1386 strain exhibited catalase activity equal to that of the wild-type in both the periplasmic and cytoplasmic fractions. As expected, no appreciable catalase activity could be detected in the Δ*katA* mutant in either the cytoplasm or periplasmic fractions; while catalase activity was restored in the Δ*katA+katA* complemented strain. Altogether, these results indicate that that Cj1386 is important in promoting proper catalase activity in *C. jejuni* and that *C. jejuni* catalase is located in both the periplasmic and cytoplasmic fractions. Catalase enzymes have also been shown to be present within both the cytoplasmic and periplasmic spaces of

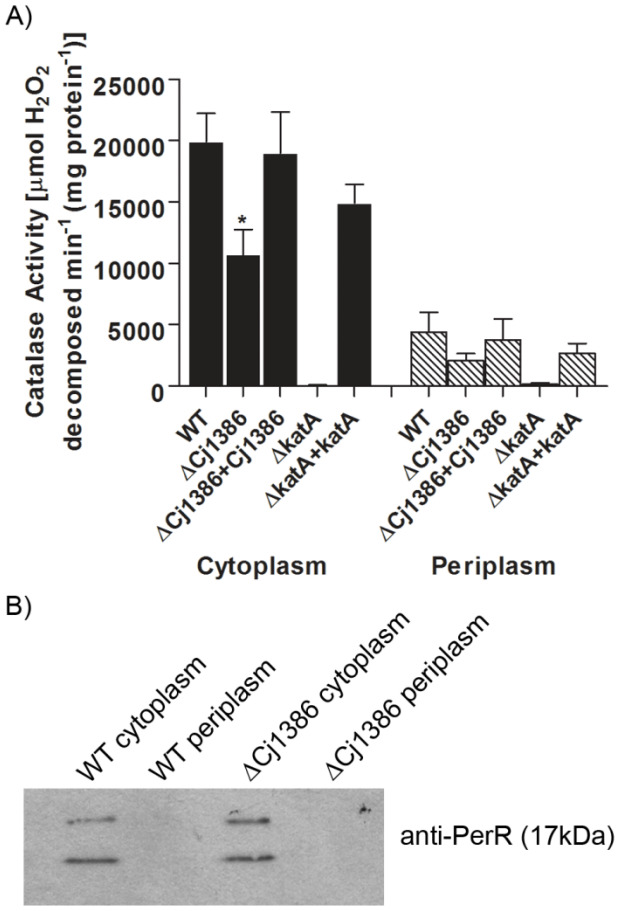

Fig 2.2.3. Cj1386 enhances KatA catalase activity. (A) Catalase activities of cytoplasmic and periplasmic cellular protein fractions for wild-type *C. jejuni*, ΔCj1386, ΔCj1386+Cj1386, Δ*katA* and Δ*katA*+*katA* are expressed as μmol of hydrogen peroxide decomposed per minute per mg of protein. Error bars indicate standard error of the mean (n=4). An asterisk (*) indicates a $P < 0.05$ using the Student *t* test. (B) Cell fractionation control assay using Western blot analysis. Five micrograms of wild-type *C. jejuni* and ΔCj1386 cytoplasmic and periplasmic protein extracts were loaded into each well and subsequently assessed for cytoplasmic protein contamination by immunoblotting using an anti-PerR antibody.

bacterial species including KatA in *Helicobacter pylori* (169), *Vibrio rumoiensis* (170), *Pseudomonas aeruginosa* (171), CatF *in Pseudomonas syringae* (172), and a catalase/peroxidase in *Caulobacter crescentus* (173).

The observed decrease in catalase activity in the ΔCj1386 mutant could be explained either by a direct role for Cj1386 in KatA function or by an effect of Cj1386 on KatA expression. To determine whether the reduction in catalase activity seen in the ΔCj1386 mutant was the result of a decrease in KatA expression, quantitative real-time PCR (qRT-PCR) and Western blot analysis were performed. No significant difference in *katA* transcript abundance could be detected in the ΔCj1386 mutant strain compared to the wild-type *C. jejuni* by qRT-PCR analysis (data not shown). Additionally, Western blot analysis using anti-KatA antisera to compare the relative KatA protein levels in whole cell extracts from wild-type *C. jejuni*, ΔCj1386, Δ*katA,* and the complemented strains indicated no significant decrease in the amount of KatA in the ΔCj1386 mutant strain as compared to the wild-type strain (Fig 2.2.4). The lack of a band in the *ΔkatA* mutant confirmed the specificity of the anti-KatA antibody (Fig 2.2.4a, lane 3). Equal loading of each protein lysate sample was confirmed using an anti-Fur antibody (Fig 2.2.4a, lower panel). Quantification of the results is seen in Fig 2.2.4b. These results demonstrate that the decrease in catalase activity seen in the ΔCj1386 mutant strain is not due to a decrease in either *katA* transcript or KatA protein level.

V. Cj1386 is involved in heme trafficking to KatA

The catalase activity and KatA expression quantification results for the ΔCj1386 strain suggest that Cj1386 is playing a direct role on KatA function. To date, the reaction catalyzed by catalase has been well documented and involves a two-step oxidation and reduction reaction to detoxify hydrogen peroxide. Central to this reaction is a heme prosthetic group, which plays an important role in electron

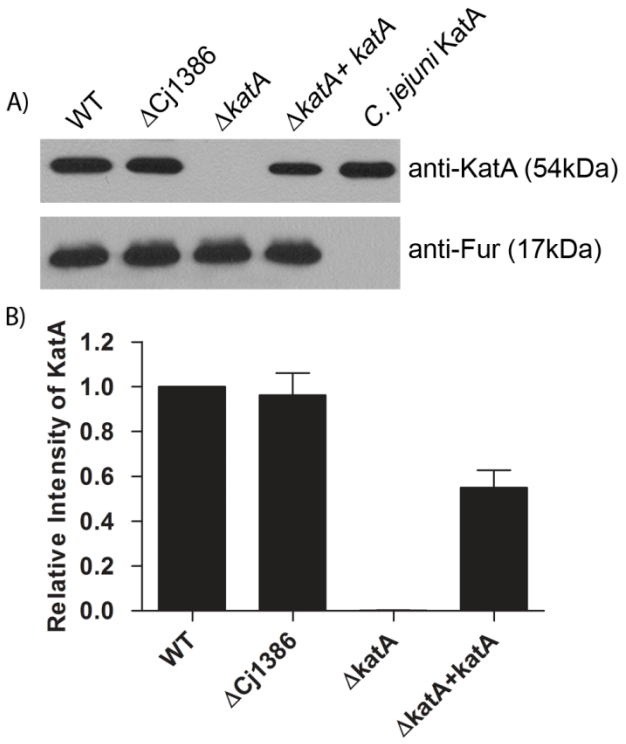

Fig 2.2.4. KatA expression is not affected in ΔCj1386 as shown by Western blot analysis of KatA protein content in wild-type *C. jejuni*; ΔCj1386, Δ*katA*, Δ*katA+katA* mutants; and affinity-purified *C. jejuni* KatA. (A) Five micrograms of protein lysate or 100 ng of purified protein was loaded into each lane followed by immunoblotting using anti-KatA or anti-Fur antisera. (Top) KatA protein level as detected by anti-KatA antisera. (Bottom) loading control of total protein content detected by anti-Fur antisera. (B) Quantification of KatA protein level in wild-type *C. jejuni*, ΔCj1386, Δ*katA*, and Δ*katA*+*katA* strains. Relative intensity of KatA was determined by quantifying each band from the immunoblot and standardized against WT KatA. Error bars represent the standard error of 3 biological replicates.

transfer to facilitate the redox reactions that decompose the hydrogen peroxide molecules (66). Given that there was a significant decrease in catalase activity, but no decrease in KatA expression in the ΔCj1386 strain, we hypothesized that the decrease in KatA activity might be due to a decrease in the heme cofactor in the expressed KatA protein. To test this hypothesis, the KatA from the wild-type other *C. jejuni* NCTC1168, Δ*katA*, ΔCj1386, and ΔCj1386+Cj1386 strains was immunoprecipitated, assayed for catalase activity, and the heme content of the protein was quantified. Fig 2.2.5a shows typical results of the immunoprecipitation experiments eluted in 50 mM glycine, pH 2.8. The specificity of the immunoprecipitated KatA can be seen in the Δ*katA* mutant strain in which the band corresponding to 54 kDa KatA is absent. Catalase activity assays were performed on the immunoprecipitated samples that were eluted in soft-elution buffer (the soft elution buffer did not decrease the activity of wild-type KatA, data not shown). Interestingly, the catalase activity of the immunoprecipitated strains revealed that the ΔCj1386 mutant KatA had a severe reduction in catalase activity (625 U/mg protein) relative to the wild-type *C. jejuni* KatA ($5.2x10^4$ U/mg protein)(Fig 2.2.5b). The catalase activity was restored in the complemented ΔCj1386+Cj1386 KatA protein ($4.9x10^4$ U/mg protein).

Next, we quantified the heme content of the immunoprecipitated KatA samples from each strain. To do this, the heme was extracted from the immunoprecipitated KatA protein samples under acidic conditions by suspending the KatA-conjugated beads in 50mM glycine solution at pH 2.8. Exposing heme-containing proteins to low pH conditions allows for extraction of heme from proteins (174, 175) and also elutes the proteins bound to the beads. Following elution from the beads, the immunoprecipitated samples were brought to neutral pH by addition of 1M Tris, pH 7.4. No detectable catalase activity was observed in the immunoprecipitated samples (data not shown).

Quantification of the heme content from the immunoprecipitated KatA samples (Table 2.2.4) revealed a significant reduction in the concentration of heme present in the ΔCj1386 mutant strain (0.19

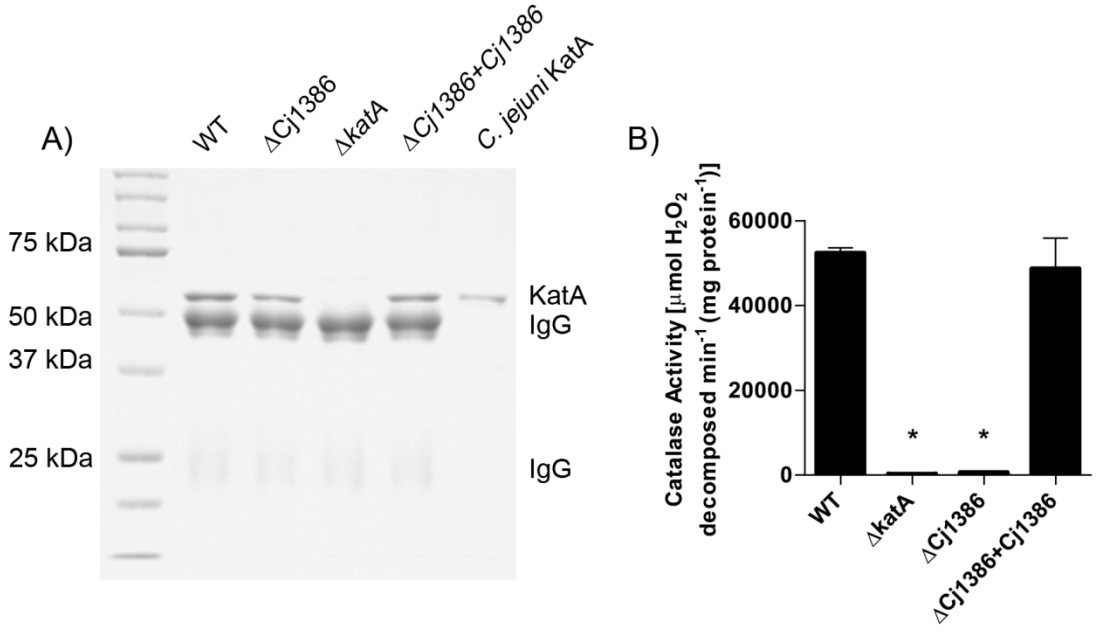

Fig 2.2.5. KatA immunoprecipitated from ΔCj1386 has decreased catalase activity relative to wild type *C. jejuni*. (A) Immunoprecipitated KatA from wild-type *C. jejuni*, ΔCj1386, Δ*katA* and ΔCj1386+Cj1386 eluted in 50mM glycine, pH 2.8. Five microliters of each immunoprecipitated sample and 0.5 μg of purified *C. jejuni* KatA was loaded into each lane and separated on a 10% denaturing, SDS PAGE gel. (B) Catalase activity of KatA immunoprecipitated samples eluted in soft elution buffer from wild-type *C. jejuni*, ΔCj1386, Δ*katA* and ΔCj1386+Cj1386. KatA protein concentrations were determined by densitometry from SDS PAGE gel (not shown) and 250 μg of KatA was assayed for activity. Catalase activity is expressed as μmol of hydrogen peroxide decomposed per minute per mg of protein. Error bars indicate standard error of the mean (n=4). An asterisk (*) indicates a $P < 0.05$ using the Student *t* test.

TABLE 2.2.4. Quantification of heme content from KatA protein immunoprecipitated from wild type *C. jejuni* NCTC11168, ΔCj1386, and ΔCj1386+Cj1386 strains[a].

	Concn (nM) of:		
Source of immunoprecipitated KatA	KatA (subunits)	Heme	Ratio (heme/KatA)
C. jejuni NCTC11168	7.4	6.99 ± 0.19	0.94
ΔCj1386	7.4	0.19 ± 0.10*	0.03
ΔCj1386 + Cj1386	7.4	6.41 ± 0.54	0.87

[a] The amount of heme is represented as the mean concentration of heme detected ± the standard error (nM) for equal starting concentrations of KatA protein for each strain tested. Experiments were repeated in biological quadruplicate. The Student *t* test was used to determine statistical significance with *P* values of < 0.05 (*) considered significant.

± 0.1 nM) relative to the wild-type *C. jejuni* (6.99 ± 0.19 nM). The concentration of heme was restored to wild-type levels in the complemented ΔCj1386+Cj1386 strain (6.41 ± 0.54 nM). Furthermore, the ratio of heme per KatA subunit (54 kDa) was close to a 1:1 ratio (0.94, Table 2.2.4) as would be expected for tetrameric, monofunctional, heme-containing catalases (66). The ΔCj1386 immunoprecipitated KatA-heme ratio was significantly reduced at approximately 0.03 heme groups per KatA subunit. This result suggests that 97% of the immunoprecipitated KatA from the ΔCj1386 mutant strain is lacking the heme prosthetic group providing an explanation for the significant reduction in enzymatic activity of this protein as assayed in Fig 2.2.5b. These results suggest an important role for Cj1386 in heme trafficking to KatA.

VI. Chick Colonization Model

To determine whether Cj1386 is important in the colonization of chick ceca, one day old specific pathogen-free broiler chicks were inoculated with wild-type *C. jejuni* NCTC11168, ΔCj1386 mutant, and the ΔCj1386+Cj1386 strains. As shown in Fig 2.2.6, the wild-type *C. jejuni* colonized the ceca at a level of approximately 10^6 CFU per gram. The ΔCj1386 mutant was significantly affected in its ability to colonize the ceca relative to the wild-type strain and colonized at a level of approximately 2.5 x 10^3 CFU per gram

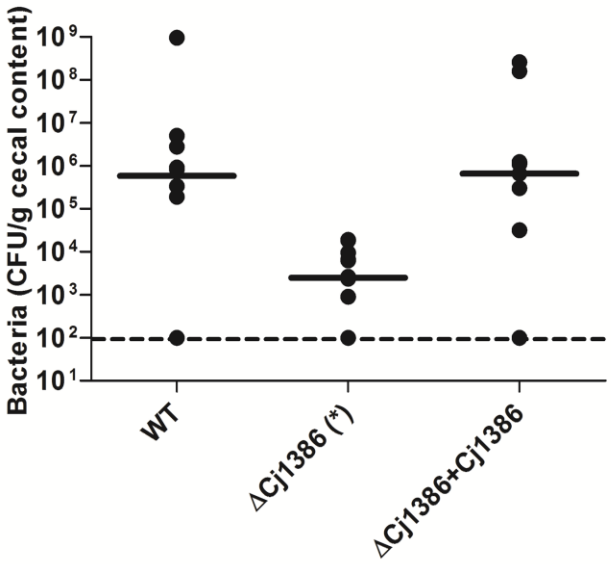

Fig 2.2.6. ΔCj1386 is defective in for cecal colonization of chicks. Chicks were grouped into two sets of 10 (WT and ΔCj1386 + Cj1386) and one set of 12 (ΔCj1386). Data points correspond to the level of colonization of the ceca per chick. The dashed line represents the limit of detection for the assay. Solid bars indicate the median colonization level of bacteria for each strain. The asterisk indicates a *P* value of <0.05 using a nonparametric Mann-Whitney rank sum test.

(P < 0.05). Complementation *in trans* of ΔCj1386 with Cj1386 restored the colonization ability of the mutant strain to levels comparable to that of the wild-type. These results indicate an important role for Cj1386 in chick colonization.

VII. Neonate Piglet Infectious Model

It has been previously shown that upon infection with *C. jejuni,* piglets become ill and display symptoms which are similar to those observed in humans affected by Campylobacteriosis (176). Therefore, neonate piglets were used as an infectious model to assess the importance of Cj1386 and KatA in pathogenesis and colonization of piglet intestines. Colostrum deprived piglets were inoculated with a suspension containing a 1:1 ratio of wild-type *C. jejuni* to ΔCj1386 or Δ*katA* (approximately 10^8 viable *C. jejuni*). The piglets were euthanized two days after infection and the competitive index was calculated (as described in the materials and methods section) for each intestinal segment. A competitive index of less than 1 indicates that the ΔCj1386 mutant was outcompeted by the wild-type *C. jejuni.* As shown in Fig 2.2.7a, the median for the competitive index corresponding to the five different intestinal segments from the ΔCj1386-wild type competition was less than 1 (p < 0.0013), indicating that Cj1386 was significantly outcompeted by the wild-type *C. jejuni* in the colonization of piglet intestines. Fig 2.2.7b shows that the Δ*katA* mutant was significantly outcompeted by the wild-type *C. jejuni*, in colonization of all five intestinal segments (p< 0.0001). Importantly, *in vitro* competitive growth assays of wild-type *C. jejuni* and ΔCj1386 mutant and *C. jejuni* and Δ*katA* mutant found that the ΔCj1386 and Δ*katA* mutants were not outcompeted by the wild-type strain (data not shown). These results indicate that the out competition of ΔCj1386 and Δ*katA* by the wild-type strain (Fig 2.2.7) *in vivo* is not due to an *in vitro* growth difference between the mutants and the wild-type strain. The data from the neonate competitive piglet assay suggests that Cj1386 and KatA play important roles in colonization of the piglet intestine.

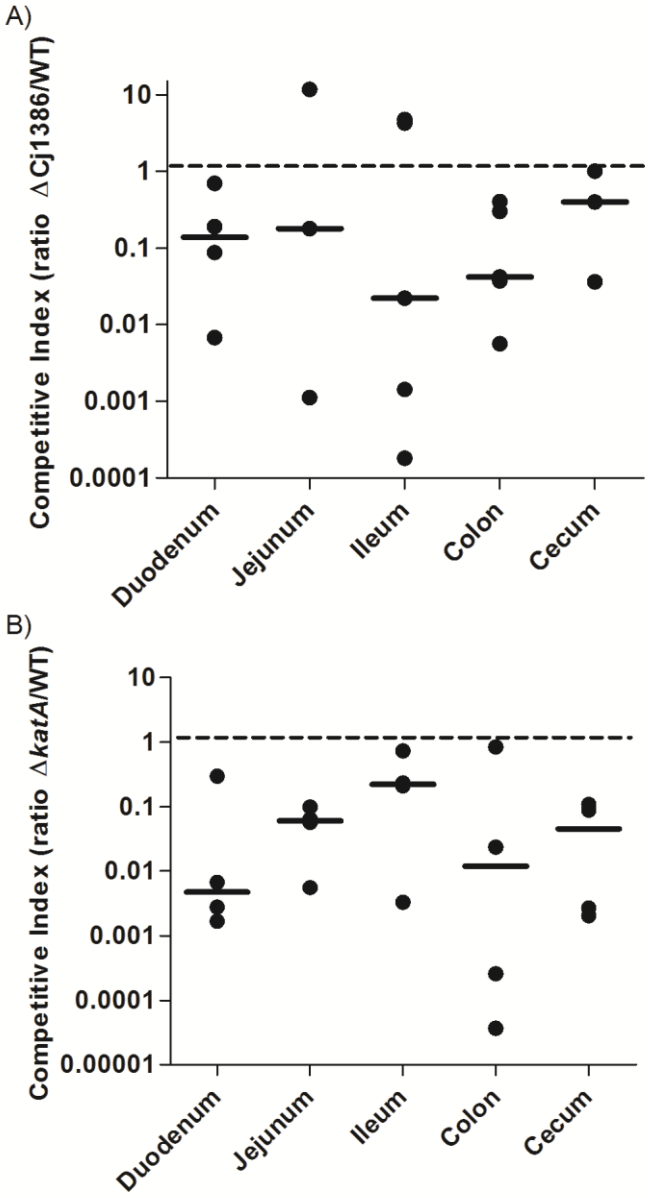

Fig 2.2.7. ΔCj1386 and Δ*katA* are affected for intestinal colonization of piglets. Competitive index in neonate piglets. Each data point represents the competitive index for *C. jejuni* NCTC11168 and the ΔCj1386 (A) or *ΔkatA* (B) mutant in five intestinal segments from one piglet. The dashed line represents the ratio at which wild-type *C. jejuni* and the ΔCj1386 (A) or *ΔkatA* (B) mutant are colonizing the intestinal segment at similar levels (one is not outcompeting the other). Solid bars represent the medians for each segment.

2.2.6. DISCUSSION

Hydrogen peroxide is a harmful by-product of metabolic bacterial activities, mainly from the electron transfer chains (31). In presence of iron, the Fenton reaction process converts H_2O_2 to hydroxyl radicals, the most powerful oxidizing species in the biosphere (31). Efficient and rapid removal of H_2O_2 is therefore vital for all living organisms. Hydrogen peroxide is primarily detoxified by catalases, which degrade H_2O_2 to water and oxygen (52). Alternatively, cytochrome c peroxidases and peroxiredoxins could also catalyze the reduction of H_2O_2 to water using cytochrome c or reduced pyridine dinucleotides as the electron donor. *C. jejuni* NCTC 11168 contains one catalase (KatA), two cytochrome c peroxidases (Cj0358 and Cj0020c), and three peroxiredoxins (AhpC, Tpx and Bcp) (132). KatA, Tpx, and Bcp have been shown to contribute, at least to some extent, to H_2O_2 detoxification in *C. jejuni* (30, 124), and Cj0358 and Cj0020c have been demonstrated to have peroxidase activity (141). AhpC has also been demonstrated to scavenge H_2O_2 in *E. coli* (52) and likely performs a similar function in *C. jejuni*. In this study, we identified and characterized one additional member of *C. jejuni* anti-H_2O_2 defense, Cj1386, and demonstrated that KatA is localized in both the cytoplasmic and periplasmic fractions. A ΔCj1386 mutant exhibited increased sensitivity towards H_2O_2. Complementation *in trans* of ΔCj1386 with Cj1386 restored the wild-type levels of sensitivity, confirming that the observed phenotype was due to deletion of Cj1386 and not due to polar effects in surrounding genes (in particular, *katA*). These observations indicate that Cj1386 functions to protect the cell from exposure to H_2O_2. Cj1386 is an ankyrin-repeat containing protein of 156 amino-acids (132). An ankyrin repeat is comprised of a series of 33 amino acids and these repeats mediate protein-protein interactions (177). Cj1386 is located directly downstream from *katA* within the *C. jejuni* NCTC11168 genome (132). Although *katA* and Cj1386 are not co-transcribed, the Δ*katA*, ΔCj1386, and Δ*katA*ΔCj1386 mutants all displayed a similar sensitivity towards H_2O_2, indicating that KatA and Cj1386 are involved in the same H_2O_2 defense pathway within the cell. Another important finding is the presence of KatA-mediated catalase activity in both the

periplasmic and cytoplasmic fractions. Periplasmic catalase activity might confer *C. jejuni* with enhanced resistance toward aggressive H_2O_2 production during host inflammation by detoxifying H_2O_2 before it reaches and damages essential cytoplasmic proteins. The ΔCj1386 mutant has reduced catalase activity in both compartments (the reduction in periplasmic fraction, however, was not statistically significant) suggesting that Cj1386 is required for proper KatA function and not for KatA localization. Furthermore, the KatA enzyme in the ΔCj1386 mutant strain was found to have a significant decrease in heme content. This finding indicates that Cj1386 is involved in heme trafficking within *C. jejuni*. Although to date there is little known about heme incorporation and folding of catalase enzymes in bacteria, we favour this explanation over a role for Cj1386 in KatA protein folding as experiments performed with purified, denatured bovine-liver catalase have demonstrated complete protein refolding and restoration of activity without the aid of chaperone or additional factors (178). In addition, preliminary data carried out on the large (90 kDa) catalase in the fungus *Aspergillus terreus,* suggest that apo-catalase enzymes can be partially reconstituted with heme under *in vitro* conditions to regain catalase activity (175). These observations suggest that catalase enzymes are able to fold without the aid of chaperones and that heme may play an important role in the folding process. Given that Cj1386 contains ankyrin repeats, it is tempting to hypothesize that KatA and Cj1386 may interact and that this interaction is required for heme transfer to the KatA protein. However, the precise function that Cj1386 plays in heme trafficking remains to be investigated.

Cj1386 homologs are found within several species of *Campylobacter* including *C. coli*, *C. lari*, *C. fetus*, and C. showae. The genomic orientation of these Cj1386 homologs downstream from *katA* is also conserved. Additionally, homologs of Cj1386 are also present in many pathogenic bacteria, including *Streptomyces avermitilis*, *Pseudomonas putida*, *Vibrio cholera* and *Helicobacter hepaticus*, and are similarly located downstream of their respective catalase. The conservation of Cj1386 and its genetic organization among diverse microorganisms underscore its importance in bacterial physiology. Studies

involving genes that affect catalase activity have been carried out in other bacterial species such as *Helicobacter pylori* (169) and *Pseudomonas aeruginosa* (166), however, our findings demonstrate a novel role for Cj1386 compared to these previous studies.

Helicobacter pylori encodes for a gene named *kapA* which is located directly downstream from its *katA* gene. KapA, like Cj1386, is important in defense against hydrogen peroxide and its gene genomic orientation is similar to what is observed in *C. jejuni* (with respect to *katA* and Cj1386) (118). A Δ*kapA* deficient mutant has decreased catalase activity in the periplasmic fraction relative to the wild-type *H. pylori* strain while no differences were observed in the cytosolic fraction (169). Although there is no significant amino acid identity between KapA and Cj1386, mutants into both of these genes disrupt the normal catalase activity levels within the cell. However, KapA is only required for the periplasmic catalase activity (169), and has a distinctly different function from Cj1386. Interestingly, the N-terminal sequence of KapA contains a twin-arginine translocate (TAT) like signal sequence and was proposed to function as a transport accessory protein involved in the translocation of KatA via the TAT secretion system (169). This TAT-like motif is absent from Cj1386. Moreover Cj1386 was not identified as a potential substrate of *C. jejuni* TAT secretion machinery (167, 179). However, the absence of secretion motifs in both Cj1386 and KatA questions how KatA and possibly Cj1386 are translocated into the periplasmic space.

Cj1386 shares 31% identity at the amino-acid level with AnkB from *Pseudomonas aeruginosa* which is also critical for optimal H_2O_2 resistance (166). *AnkB* is located directly downstream from its catalase enzyme, KatB, and codes for an ankyrin-like protein. A Δ*ankB* deficient mutant was shown to exhibit an increased sensitivity towards hydrogen peroxide and a decrease in KatB-mediated catalase activity (determined using whole cell extracts) (166). Interestingly, Howell *et al.* reported that AnkB is found primarily within the periplasmic space of *P. aeruginosa*. AnkB contains a single membrane

spanning domain with a small 3 amino acid C-terminus located within the cytoplasmic space, while the remaining N-terminus of the protein is hydrophilic and predicted to be located in the periplasmic space (166). The specific catalase activity of the Δ*ankB* mutant in the cytoplasmic and periplasmic spaces was not reported; however, KatB activity was found in both of these two cellular compartments. It is therefore not known whether the catalase activity is affected in both the cytoplasmic and periplasmic compartments of *P. aeruginosa* (as is observed in the ΔCj1386 mutant) or whether the reduction in catalase activity primarily occurs in the periplasmic space as is reported in *H. pylori*. Howell *et al.* suggested that AnkB may be interacting with KatB to either localize KatB to the inner membrane surface (to protect H_2O_2 sensitive biological proteins or molecules) or to stabilize or enhance KatB activity (166). Use of the same transmembrane spanning domain prediction programs (TopPred 2.0,(180)) did not indicate the presence of any putative transmembrane domains in Cj1386. Further experiments will be required to determine the localization of Cj1386 within the cell as well as any interaction of Cj1386 with KatA.

We have previously shown that the ability of *C. jejuni* to cope with oxidative stress is fundamental for its colonization of the chick gastrointestinal tract. A Δ*katA* deficient mutant was significantly altered in its ability to colonize the chick cecum compared to the wild-type strain (99). It is therefore not surprising that our ΔCj1386 mutant exhibited a similar colonization defect. We further confirmed the importance of oxidative stress defence in host colonization by testing our Δ*katA* mutant in the neonate piglet infectious model, revealing that the Δ*katA* mutant was significantly out-competed by the wild-type *C. jejuni* strain. Additionally, the ΔCj1386 mutant was out-competed by the wild-type strain in the neonate piglet infectious model; further highlighting the importance of Cj1386 function for gut colonization. An analogous result was reported in *H. pylori* where KapA was found to be essential to sustain a long term colonization in the murine model of *H. pylori* infection (181). It is likely that the lower catalase activity in the ΔCj1386 mutant is the cause of the reduced colonization in both animal

models, as the mutant is more susceptible to the damaging effects of exogenously produced hydrogen peroxide (either from the host or host intestinal flora). In the absence of Cj1386, H_2O_2 will be detoxified at slower rates allowing the oxidant to damage DNA, protein and lipids.

In summary, we demonstrated that Cj1386 is important in defense against hydrogen peroxide within the cell by promoting optimal levels of catalase activity and by contributing to heme trafficking to KatA. Cj1386 also plays an important role in the colonization of the gastrointestinal tract in the chick colonization model and in the piglet pathogenesis model. Future experiments will determine the heme binding ability of Cj1386 and the proteins involved in this process.

2.2.7. ACKNOWLEDGEMENTS

This work was supported by the Canadian Institute of Health Research (to A.S.) and the Ontario Graduate Scholarship of Science and Technology (to A.F.).

We also thank J.-F. Couture (Ottawa Institute of Systems Biology, University of Ottawa) for providing the pGST vector and TEV protease.

2.3. Cj1386, an atypical hemin-binding protein, mediates hemin trafficking to KatA in *Campylobacter jejuni*

Annika Flint[1] and Alain Stintzi[1]

[1]Ottawa Institute of Systems Biology,

Department of Biochemistry, Microbiology and Immunology

Faculty of Medicine, University of Ottawa

451 Smyth Road, Ottawa, ON, K1H 8M5, Canada

Running title: Cj1386 is a heme protein

Submitted to the Journal of Bacteriology (2014).

2.3.1. STATEMENT OF MANUSCRIPT STATUS AND CONTRIBUTIONS

The manuscript "Cj1386, an atypical hemin-binding protein, mediates hemin trafficking to KatA in *Campylobacter jejuni*" has been submitted to the Journal of Bacteriology.

Flint, A. performed all of the experiments. Flint, A. wrote and revised the manuscript.

Stintzi, A. was the project supervisor, provided direction and feedback on the experiments, and revised the manuscript.

2.3.2. ABSTRACT

Catalase enzymes detoxify H_2O_2 by the dismutation of H_2O_2 into O_2 and H_2O through the use of hemin cofactors. While the structure and biochemical properties of catalase enzymes have been well characterized over many decades of research, it remained unclear how catalases acquire hemin. We have previously reported that Cj1386 is essential for ensuring proper hemin content in *Campylobacter jejuni* catalase (KatA). In this report, in-depth molecular characterization of Cj1386 was performed to elucidate the mechanistic details of this association. Co-immunoprecipitation assays revealed that KatA-Cj1386 transiently interact *in vivo* and UV-vis spectroscopy demonstrated that purified Cj1386 protein binds hemin. Furthermore, hemin titration experiments determined that hemin binds to Cj1386 in a 1:1 ratio with hexa-coordinate hemin binding. Mutagenesis of potential hemin coordinating residues in Cj1386 showed that tyrosine 57 was essential for hemin coordination when Cj1386 was overexpressed in *Escherichia coli*. Introducing the *cj1386*^{Y57A} allele into a *C. jejuni* Δ*cj1386* background failed to restore its sensitivity towards H_2O_2 back to wild type levels suggesting that KatA was not functional in this strain. In support of this, KatA immunoprecipitated from the Δ*cj1386+cj1386*^{Y57A} mutant had significantly reduced hemin content as compared to the *cj1386*^{WT} background. Overall, these findings indicate that Cj1386 is involved in directly trafficking hemin to KatA and that tyrosine 57 plays a key role in this function.

2.3.3. INTRODUCTION

Hydrogen peroxide is a reactive oxygen species (ROS) that damages biological molecules such as DNA, protein and lipids. H_2O_2 is inadvertently produced during cellular processes, such as aerobic metabolism, due to oxidation of respiratory dehydrogenases by molecular oxygen (31). Furthermore, Fenton chemistry results in the production of hydroxyl radicals from the reaction of H_2O_2 with ferrous ions (37). Detoxification of H_2O_2 by antioxidant enzymes is therefore highly important in preventing cellular damage and/or death in living organisms.

Catalase is one of the major H_2O_2 detoxification enzymes present within cells and it is found in almost all aerobically respiring organisms (54). Catalase functions by dismutating H_2O_2 into molecular oxygen and water (182). Although multiple crystal structures have been solved (66) and the biochemical properties of catalase have been extensively studied (182), the biogenesis of the enzyme has not yet been elucidated. The steps of catalase folding and hemin (defined as protoporphyrin IX containing a ferric ion) insertion, as well as potential chaperone proteins involved in this process, remain unknown. A recent report investigating genes important for catalase biogenesis was carried out in *Enterococcus faecalis* (183). By screening for catalase activity using a transposon mutant library, seven genes important for catalase activity were identified which code for the catalase itself (*katA*), RNA turnover global regulators (*rnjA, srmB*), NADH peroxidase (*npr*), stress response regulator (*etaR*), and membrane transport proteins (*oppBC*) (183). Excluding *katA*, the precise function of these genes for catalase activity requires further investigation; however, Baureder and Hederstedt speculate that these genes have an indirect role on catalase activity within the cell (183). Furthermore, despite in-depth characterization of heme transport into the cytoplasmic space of bacteria, very little is known about the potential proteins involved in trafficking heme to heme-proteins within the cytoplasmic space.

Recently, our lab has identified a novel protein, Cj1386, that plays an important role in catalase biogenesis and the hemin content of *C. jejuni* KatA (89). We demonstrated that Cj1386 is required for optimal H_2O_2 detoxification within the cell and the presence of hemin within KatA. Specifically, KatA immunoprecipitated from a Δ*cj1386* mutant had a significant reduction in the hemin content associated with its KatA relative to KatA isolated from the wild type strain. In turn, the decreased hemin content of KatA in the Δ*cj1386* mutant resulted in reduced catalase activity within the cell and consequently sensitivity to H_2O_2 (89).

In this report, we further characterize Cj1386 function to demonstrate its direct role in hemin trafficking within *C. jejuni*. Specifically, we investigated the biochemical and spectroscopic properties of the Cj1386 protein and also identified interacting proteins. We found that Cj1386 binds hemin at a 1:1 hemin-to-Cj1386 ratio and that tyrosine 57 is required for hemin-coordination to Cj1386. Furthermore, co-immunoprecipitation experiments revealed that the KatA and Cj1386 proteins transiently interact. Overall our results contribute to a greater fundamental understanding of hemin trafficking and catalase biogenesis within *C. jejuni* and establish that Cj1386 binds and trafficks hemin to KatA.

2.3.4. MATERIALS AND METHODS

I. Bacterial Strains, Plasmids and Growth Conditions

E. coli DH5α, BL21 and Rosetta strains were grown at 37°C under aerobic conditions in Luria-Bertani (LB) broth or on LB agar plates supplemented with 100 μg/mL ampicillin, 50 μg/mL kanamycin and/or 50 μg/mL chloramphenicol as required. *Campylobacter jejuni* NCTC 11168 was cultured under microaerophilic conditions (83% N_2, 4%H_2, 8% O_2, and 5% CO_2) at 37˚C in a MACS-VA500 workstation (Don Whitley, West Yorkshire, England). *C. jejuni* strains were grown on Mueller-Hinton (MH) agar plates supplemented with 10 μg/mL kanamycin and/or 20 μg/mL chloramphenicol as required, in biphasic flasks, or in minimal essential medium MEMα (Invitrogen) supplemented with 20 mM sodium pyruvate. The bacterial strains and plasmids used in this study are listed in Table 2.3.1.

II. Purification of C. jejuni Cj1386 and anti-Cj1386 antisera production

Overexpression of Cj1386 was performed in *E. coli* Rosetta cells using the protein expression vector pGST as described previously (157). Briefly, the *C. jejuni cj1386* gene was PCR amplified using Pfx high fidelity polymerase (Invitrogen) and the cj1386_NcoI and cj1386_NotI primers listed in Table 2.3.2. The amplified gene was cloned into digested pGST vector using NcoI and NotI restriction sites, followed by transformation of the construct into *E. coli* DH5α cells. Sequencing was performed to confirm the absence of polymerase-introduced mutations in the *cj1386* gene. The pGST+*cj1386*^{WT} construct was subsequently transformed into *E. coli* Rosetta cells for Cj1386 overexpression. The *E. coli* Rosetta pGST+*cj1386*^{WT} strain was grown in 1 L of LB broth supplemented with 100 μg/mL of ampicillin and 50 μg/mL chloramphenicol to an OD_{600} of 0.6 at 37°C with continual shaking. Induction of protein expression was performed by addition of IPTG (500 μM) and overnight incubation with continual shaking at 18°C. The cells were then pelleted, resuspended in phosphate buffered saline (PBS, 137 mM NaCl, 2.7

TABLE 2.3.1. Bacterial strains used in this study.

Strains or Plasmids	Genotype[a]	Source
E. coli		
DH5α	*endA1 hsdR17* (r_K^- m_K^-) *supE44 thi-1 recA1 gyrA relA1 Δ(lacZYA-argF)U169 deoR [ϕ80dlac Δ(lacZ ΔM15)*]	Invitrogen
BL21(DE3)	F^- *ompT gal dcm lon hsdS*$_B$(r_B^- m_B^-) λ(DE3)	Novagen
Rosetta	F^- *ompT hsdS*$_B$(r_B^- m_B^-) *gal dcm* pRARE cam^R	Novagen
AS1082	*E. coli* BL21(DE3) + (pGST+*katA*)amp^R	Flint (89)
AS1091	*E. coli* Rosetta + (pGST+*cj1386*)$amp^R cam^R$	This study
AS1138	*E. coli* Rosetta + (pGST+*cj1386*^{Y57A}) $amp^R cam^R$	This study
AS1142	*E. coli* Rosetta + (pGST+*cj1386*^{H46A}) $amp^R cam^R$	This study
AS1150	*E. coli* Rosetta + (pGST+*cj1386*^{C89A}) $amp^R cam^R$	This study
C. jejuni		
AS144	*C. jejuni* NCTC 11168	National Collection of Type Cultures
AS216	AS144 Δ*perR*::cam^R	Palyada (29)
AS433	AS144 Δ*katA*::cam^R	Palyada (29)
AS942	AS144 Δ*cj1386*::cam^R	Flint (89)
AS1028	AS942+*cj1386*::$cam^R kan^R$	Flint (89)
AS1139	AS942+*cj1386*^{Y57A}	This study
AS1144	AS942+*cj1386*^{H46A}	This study
AS1149	AS942+*cj1386*^{C89A}	This study
Plasmids		
pRY111	Cam^R resistance gene	Yao (156)
pRRK	Cloning vector used for complementation of mutants, kan^R	Reid (22)
pUC19	Cloning vector, amp^R	Biolabs
pGST	Protein expression vector with GST tag and IPTG inducible promoter	Sheffield (157)

[a] cam^R, chloramphenicol resistance gene, kan^R, kanamycin resistance gene, amp^R, ampicillin resistance gene.

TABLE 2.3.2. Primers used in this study.

Primer Name	Primer Sequence (5'- 3')[a]
Cj1386_NcoI	**GCCATGGCT**ATGACAACTCTTAGTTTAGA
Cj1386_NotI	**GCGGCCGC**TAAAAGGGGCGGTTCCTATC
Cat-SE	TGCTCGGCGGTGTTCCTTTCCAAG
Cat-AS	TGCGCCCTTTAGTTCCTAAAGGGT
AR56-AS	CATCCTCTTCGTCTTGGTAGC
ak233-SE	GCAAGAGTTTTGCTTATGTTAGCAG
ak234-SE	GAAATGGGCAGAGTGTATTCTCCG
ak235-SE	GTGCGGATAATGTTGTTTCTG
Y57A-SE	GCTTGCAGCTGCTAATAATTCT
Y57A-AS	ATAAGCAAGCTATCGCCTTTATGA
H46A-SE	TTTAAAAACTGCTAAAGGCGATAG
H46A-AS	TTTACATTTAAACCTGCTTCTATCATG
C89A-SE	AGCGGGAGTTGCTTTTAAAGGAT
C89A-AS	AATGGGGTTTGTCCACGATCGTTTT

[a-] Restriction sites in bold.

mM KCl, 10 mM Na_2HPO_4, 2 mM KH_2PO_4, pH 7.4) containing protease inhibitor (Roche), and lysed by sonication. Cell membranes and debris were removed by centrifugation at 16,060 x g for 15 min. The cell lysate containing the GST-Cj1386 fusion protein was then affinity purified using glutathione sepharose 4B resin according to the manufacturer instructions (GE Healthcare). Cleavage of the GST tag from Cj1386 was performed on the resin by addition of TEV protease (157) and gentle shaking overnight at 4°C. The Cj1386 protein was washed from the resin the following day using 6 washes of 500 µl of PBS buffer and concentrated using a 10 kDa cut-off centrifugal filter unit (Millipore). Concentrated Cj1386 protein was further purified by size exclusion chromatography using the AKTA fast protein liquid chromatography (FPLC) system equipped with a Superdex-75 column (GE Healthcare) using PBS used as the filtration buffer. Purified protein was frozen and stored at -20°C until use.

Cj1386 antibody production was performed by Immuno-Precise Antibodies Limited (Victoria, BC, Canada). For each rabbit, a pre-immune bleed was performed prior to the primary immunization with the Cj1386 antigen (0.5 mg) using Complete Freund's Antigen. Over the course of the project, each rabbit received 4 additional boosts with Cj1386 antigen (0.25 mg) using Incomplete Freund's Antigen followed by a terminal bleed and sera collection. Anti-Cj1386 antiserum was stored at -20°C until use.

III. Preparation of apo-Cj1386

Hemin was extracted from purified Cj1386 using the acid-acetone method as described previously (174, 184). HCl-acetone solution was prepared by adding 0.34 volumes of 12 M HCl to 30 volumes of acetone. One millilitre of 50 µM purified Cj1386 was slowly added to 10 volumes of cold HCl-acetone and the precipitated protein was pelleted by centrifugation at 16,060 x g for 15 min. The heme extraction step was repeated once more and the precipitated Cj1386 protein was resuspended in 4 M urea. Buffer exchange with 100 mM NaCl, 20 mM Tris, pH 7.4 was performed using a 10 kDa cut-off

centrifugal filter unit (Millipore). UV-vis spectra of 10 µM of prepared apo-Cj1386 protein (see below) was used to confirm successful hemin removal by the absence of a Soret peak. Apo-Cj1386 was stored at -20°C until use.

IV. UV-vis spectroscopy and hemin titration

All spectroscopy measurements were recorded at room temperature using a sealed quartz cuvette with a 1 cm path length on a SpectraMax Plus 384 spectrophotometer (Molecular Devices). Hemin stock solutions (2.5 mM hemin in 20 mM NaOH) were prepared fresh, diluted to 500 µM in 100 mM NaCl, 20 mM Tris, pH 7.4 buffer, and added in 1 µM increments to 500 µl of 10 µM apo-Cj1386 or 500 µl of 100 mM NaCl, 20 mM Tris, pH 7.4 buffer. Spectral readings were taken 5 min after addition of hemin to the protein and reference solutions. Hemin-Cj1386 binding spectra from 260 nm to 700 nm were determined by subtracting the non-bound background hemin at each concentration titrated. The hemin stoichiometric binding ratio was determined by the absorbance value of the Soret peak at each concentration. Dissociation constants, K_d, were calculated with GraphPad Prism v.6 using non-linear regression assuming one site, specific ligand binding. Statistical differences between K_d values were calculated using a paired *t* test with *P* values < 0.05 considered significant.

V. Site-Directed Mutagenesis of Cj1386

The *cj1386*^{H46A}, *cj1386*^{Y57A}, and *cj1386*^{C89A} mutant alleles were constructed by PCR amplification of both pGST-Cj1386^{WT} and pRRK-Cj1386^{WT} using Phusion Hot Start II High-Fidelity DNA polymerase with primers H46A-SE, H46A-AS, Y57A-SE, Y57A-AS, C89A-SE, and C89A-AS (cartridge filtered, Invitrogen). PCR products were purified with the PureLink PCR Purification Kit (Invitrogen) followed by 5' phosphorylation of 25 ng of PCR product using T4 Polynucleotide Kinase (New England Biolabs) for 30 mins at 37°C. Phosphorylated products were ligated using Quick T4 DNA Ligase (New England Biolabs)

for 5 min at room temperature and subsequently transformed into *E. coli* DH5α. Mutation of the *cj1386* gene in each of the pGST-*cj1386* and pRRK-*cj1386* constructs was confirmed by sequencing. The resulting pGST-*cj1386* and pRRK-*cj1386* H46A/Y57A/C89A mutant plasmids were then transformed into *E. coli* Rosetta and *C. jejuni* Δ*cj1386* mutant strains respectively. Confirmation of chromosomal insertion of the *C. jejuni* Δ*cj1386* mutant strain with the H46A/Y57A/C89A plasmids was performed by PCR using the AR56 and AK233-235 primers.

VI. Sequence Analysis

Homologs of Cj1386 were identified by protein BLAST analysis using the non-redundant protein sequences database and standard protein blast parameters (protein-protein blast algorithm) (185). Cj1386 homologs from different Gram-negative bacteria were selected and aligned using Clustal Omega (186) on EBI (187). The multiple sequence alignment was constructed using Jalview (188) and Adobe Illustrator 3.

VII. Disc Inhibition Assay

C. jejuni NCTC11168 wild type, mutant and complemented strains were grown on MH agar plates supplemented with chloramphenicol and/or kanamycin as required for three days under microaerophilic conditions at 37°C. Strains were then cultured in MH broth in biphasic flasks overnight. The overnight cultures were diluted in MH broth to an OD_{600} of 1 and 4 mL was added to 100 mL molten MH agar (cooled to 50°C). The agar was subsequently poured in equal volumes into Petri dishes, and allowed to solidify before the placement of 6 mm paper discs to the agar surface. Ten microlitres of 3% H_2O_2 was added to each disc and the plates were incubated for 28 h under microaerophilic conditions at 37°C followed by measurement of the diameter of inhibition (mm). Each mutant and complemented strain was tested in at least biological triplicate. The averages of the clear zones were used to determine

if statistical significance existed between the mutant, complemented and wild type strains using ANOVA. *P* values < 0.05 were considered statistically significant.

VIII. Co-Immunoprecipitation of Cj1386 and KatA

Co-immunoprecipitation of Cj1386 or KatA from the Δ*perR* mutant strain was performed using protein-A conjugated Dynabeads (Invitrogen). Briefly, the *C. jejuni* Δ*perR* mutant strain was grown under microaerophilic conditions in MEMα to mid-log phase (OD_{600} 0.2) at 37°C and cross-linked in 0.75% formaldehyde for 2 minutes. Tris-HCl pH 8.0 was subsequently added to the cultures at a final concentration of 250 mM to quench remaining formaldehyde and the cells were incubated for a further 10 min. Cultures were centrifuged at 6000 x g for 10 minutes to pellet the cells and the pellets were resuspended in RIPA buffer (50 mM Tris-HCl pH 7.4, 140 mM NaCl, 1 mM EDTA, 1% Triton-X100, 0.1% sodium deoxycholate, 0.1% SDS) containing a bacterial protease inhibitor cocktail (Sigma). Cells were lysed by sonication on ice and cellular debris was removed by centrifugation at 16,060 x g for 5 min. Dynabeads were prepared by addition of 250 µg of anti-KatA or anti-Cj1386 sera, or 25 µg affinity purified anti-Fur antibody (189) (diluted in 0.02% Tween-PBS) to 50 µl beads and rotated end-over-end for 1 hour at room temperature. Antibodies were covalently conjugated to the beads using Bis (sulfosuccinimidyl) suberate, BS^3 (Invitrogen) according to the manufacturer's instructions. Two milligrams of cross-linked Δ*perR* lysate was added to the beads and incubated for 1 hour at room temperature with end-over-end rotation. Beads were washed 3 times with 200 µl RIPA buffer, transferred to a clean tube, resuspended in 20 µl 2X Laemmli buffer and heated at 70°C for 10 min to dissociate the protein complexes from the antibody conjugated beads. Immunoprecipitated protein was separated from the magnetic beads and transferred to a clean tube. Eluted protein samples were further heated at 99°C for 25 min to reverse formaldehyde cross-links. Protein samples were separated by SDS PAGE on a 12% polyacrylamide gel. Immunoprecipitated proteins were visualized using Western

blot analysis as described previously (89) using anti-Cj1386 (0.5 µg/mL) or anti-KatA (0.1 µg/mL) polyclonal antibodies. Use of a high sensitivity chemiluminescent detection substrate (SuperSignal West Femto, Pierce) was utilized to visualize target proteins. Experiments were performed in at least biological triplicate.

IX. Hemin Quantification Assays

Hemin content of KatA protein isolated from wild-type *C. jejuni* NCTC11168 and Δ*cj1386+cj1386*^{Y57A}, strains was quantified using the Hemin Assay Kit (Biovision, Mountain View, Ca) as described previously (89). KatA was immunoprecipitated from wild-type *C. jejuni* NCTC11168 and Δ*cj1386+cj1386*^{Y57A} strains according to the same method as described above with slight modifications to the cell lysis, bead preparation and elution steps. Briefly, cells were harvested without formaldehyde cross-linking and resuspended in PBS containing a bacterial protease inhibitor cocktail (Sigma). Anti-KatA antibody was added to the Dynabeads without covalently linking the antibody to the beads. Elution of KatA protein was carried out by addition of 20 µl of 50 mM glycine, pH 2.8 to the Dynabeads. Samples were incubated at room temperature for 2 minutes with end-over-end rotation and subsequently transferred to a clean tube. The samples were brought to neutral pH by the addition of 1M Tris, pH 7.4. Samples were visualized by SDS PAGE run on a 10% denaturing gel followed by Coomassie Blue staining. Total hemin concentration was assayed from 40 ng of KatA protein prepared from each immunoprecipitated sample and the assay was performed according to the manufacturer's instructions (Hemin Assay Kit, Biovision, Mountain View, Ca). Experiments were performed in biological triplicate. Statistical significance was determined by the Student's t test with p values < 0.05 considered significant.

2.3.5. RESULTS

I. Cj1386 is a hemin binding protein

To date, the structure, biochemical properties and biological importance of catalase enzymes have been well studied in both prokaryotic and eukaryotic organisms. However, the order of events and potential chaperones involved in the biogenesis of catalase has not been clearly elucidated. Recently, our laboratory identified a key role for Cj1386 in promoting proper hemin content in catalase within *Campylobacter jejuni* (89). Characterization of an isogenic deletion mutant into *cj1386* revealed a significant reduction in catalase activity relative to wild type *C. jejuni*. Western blot analysis of the KatA protein from the Δ*cj1386* mutant demonstrated that the decrease in catalase activity in the Δ*cj1386* mutant strain was not due to a decrease in KatA expression. Furthermore, quantification of the hemin content of immunoprecipitated KatA from the Δ*cj1386* strain showed a reduction in the number of hemin prosthetic groups per subunit of KatA, suggesting that Cj1386 might be involved in hemin trafficking to catalase within the cell (89).

To demonstrate and investigate the molecular mechanism of Cj1386 in hemin trafficking and KatA biogenesis, Cj1386 was purified and assessed for hemin binding by absorption spectroscopy (Figure 2.3.1). Purification of Cj1386 yielded a solution with a yellowish hue suggesting that Cj1386 is a hemin-binding protein (Figure 2.3.1a). UV-vis spectroscopy further supported that Cj1386 binds hemin by presence of a Soret peak, which is a characteristic of hemin binding proteins (Figure 2.3.1c) (190). Quantification of the hemin content from purified Cj1386 revealed that a significant proportion of the purified protein was bound to hemin (Figure 2.3.1c). Therefore to determine the hemin binding stoichiometry of Cj1386 and dissociation constant, hemin was removed from purified Cj1386 using an acid-acetone method to prepare apo-Cj1386 protein (see Materials and Methods). Complete hemin

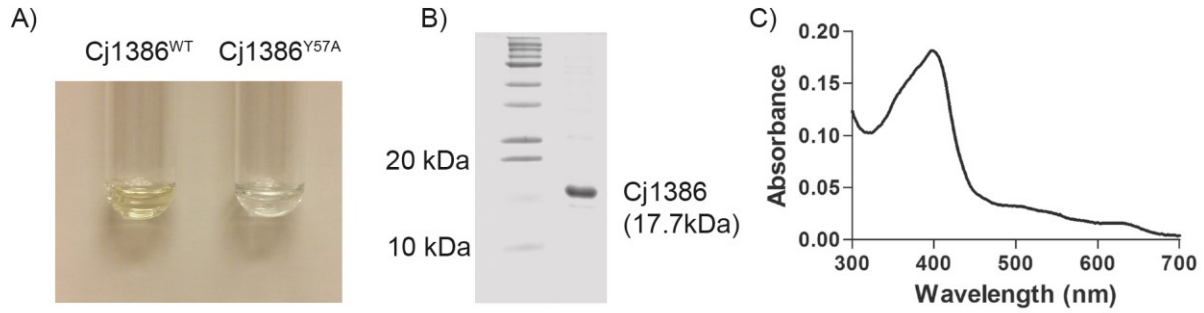

Fig 2.3.1. Cj1386 is a hemin binding protein. (A) Purified Cj1386^{WT} and Cj1386^{Y57A} protein solutions at 50 µM. Cj1386^{WT} has a yellowish hue in contrast to Cj1386^{Y57A} which is colorless. (B) Cj1386 purification after size exclusion chromatography. Five microliters of purified protein was loaded and separated on a 14% denaturing SDS PAGE gel. (C) Absorption spectrum of 10 µM purified Cj1386 in 100 mM NaCl, 20 mM Tris, pH 7.4 at 22 °C.

removal from Cj1386 was confirmed by the absence of a Soret peak when 10 µM of apo-Cj1386 was analyzed by absorbance spectroscopy (Figure 2.3.2a). Reconstitution of apo-Cj1386 with increasing concentrations of hemin showed one prominent Soret peak at 412 nm with shoulder bands at 550 nm, and 640 nm (Figure 2.3.2a). The presence of a Soret band at 412 nm suggests low spin, hexacoordinate hemin binding to Cj1386 (191, 192). Reduction of holo-Cj1386 with 1 mM DTT shifted the Soret peak at 412 nm to 422 nm and the α/β bands from 550 nm and 640 nm to 554 nm and 630 nm in accordance with the proposed hemin coordination (Figure 2.3.2b). Titration of 10 µM apo-Cj1386 with hemin revealed a 1:1 molar binding ratio demonstrating that one hemin molecule binds to one Cj1386 subunit (Figure 2.3.2c). The hemin binding constant, K_d, for Cj1386 is 4.3 ± 0.3 x 10^{-6} M for the 412 nm peak. The K_d value for Cj1386 indicates that it has a weaker affinity for hemin as compared to the K_d values for heme binding proteins, such as BSA and myoglobin (6.4 x 10^{-9} and 1.3 x 10^{-14} M respectively, Table 2.3.3). Furthermore, Cj1386 has a similar hemin affinity to that observed for the *Pseudomonas aeruginosa* heme trafficking protein, PhuS, (K_d of 0.2 x 10^{-6} M) (193). Overall, the hemin binding affinities for Cj1386 support a role for this protein in hemin trafficking.

II. Tyrosine 57 is important for hemin affinity to Cj1386 and hemin trafficking in C. jejuni

Hemin titration of apo-Cj1386 determined that one hemin prosthetic group binds per Cj1386 subunit. Inspection of the Cj1386 protein sequence did not reveal any known hemin binding motif such as those characterized for cytochrome (97) and catalase enzymes (59). Therefore to determine residues involved in hemin binding, the Cj1386 protein sequence was aligned against Cj1386 homologs from different bacterial species to identify conserved residues potentially important for hemin binding. Heme coordination with proteins commonly occurs through histidine, tyrosine, methionine, or cysteine residues (194). A multiple sequence alignment of Cj1386 against homologs of *Campylobacter coli* CCO11496, *Helicobacter hepaticus* YahD*, Arcobacter butzleri* Abu0197, and *Pseudomonas putida* Pp1834

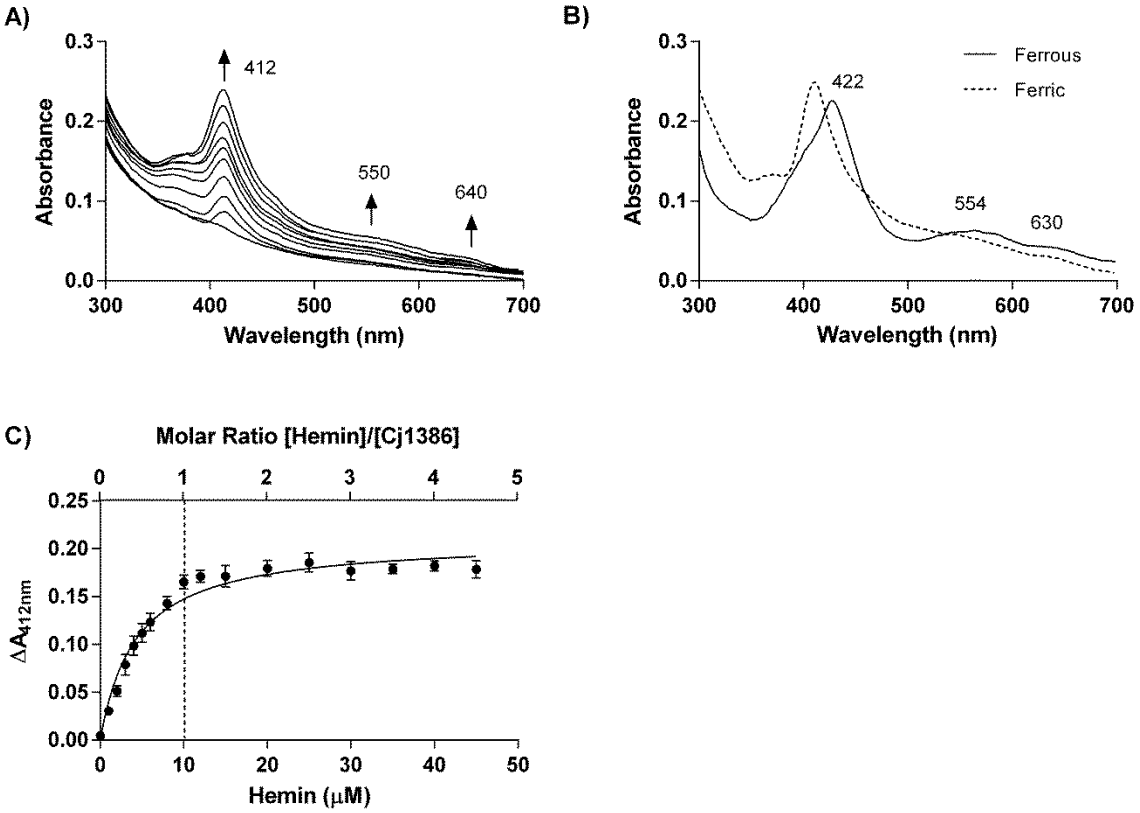

Fig 2.3.2. Cj1386 displays hexacoordinate hemin binding with 1:1 binding stoichiometry. (A) Absorption spectra of 10 μM apo-Cj1386 in the presence of increasing concentrations of hemin. Hemin was extracted from purified Cj1386 using acid acetone to produce apo-Cj1386. Hemin titration was performed in 1 μM increments against 10 μM apo-Cj1386 in 100 mM NaCl, 20 mM Tris, pH 7.4. Arrows represent the direction of increased absorbance readings upon hemin addition (B) Absorption spectrum of 10 μM ferrous holo-Cj1386 after reduction of 10 μM ferric holo-Cj1386 using 1 mM sodium dithionite in 100 mM NaCl, 20 mM Tris, pH 7.4. (C) Hemin:Cj1386 binding stoichiometry determined by difference absorbance values at 412 nm. The dashed line represents the concentration of Cj1386 and hemin that yield a 1:1 hemin-to-Cj1386 binding ratio. Error bars represent the standard error as determined from hemin titration from 2 independent protein purifications.

TABLE 2.3.3. Binding affinities of heme-proteins.

Heme-protein	K_d (M)	Source
BSA	5×10^{-9}	(195)
PhuS	0.2×10^{-6}	(193)
Myoglobin	1.3×10^{-14}	(196)
$Cj1386^{WT}$		
412 nm	4.3×10^{-6}	This study
$Cj1386^{Y57A}$		
372 nm	7.7×10^{-6}	This study
412 nm	6.9×10^{-6}	This study

is shown in Figure 2.3.3. From the sequence alignments, histidine 46, tyrosine 57 and cysteine 89 were found to be highly conserved and were consequently targeted for site-directed mutagenesis and assessed for hemin occupancy.

Overexpression and purification of the $Cj1386^{Y57A}$ mutant did not yield a solution with a yellow hue in contrast to purified $Cj1386^{WT}$, suggesting that hemin was no longer bound to the purified $Cj1386^{Y57A}$ mutant (Figure 2.3.1a). Indeed, absorption spectroscopy of 10 µM purified $Cj1386^{WT}$ and 10 µM $Cj1386^{Y57A}$ revealed that the $Cj1386^{Y57A}$ mutant no longer purified with a fraction of the protein coordinated to hemin as illustrated by the absence of a Soret peak (Figure 2.3.4a). Although the Y57A mutant did not purify with hemin bound to the protein, the mutation did not prevent hemin coordination *in vitro*. The $Cj1386^{Y57A}$ mutant displayed a different absorption spectra to that observed for reconstituted $Cj1386^{WT}$ but still bound hemin at a 1:1 stoichiometry (Figure 2.3.4b, 2.3.5). Reconstitution of apo-$Cj1386^{Y57A}$ with increasing concentrations of hemin showed two prominent Soret peaks at 372 nm and 412 nm with shoulder bands at 550 nm and 640 nm (Figure 2.3.4b, 2.3.5a). The presence of the Soret band at 412 nm suggests low spin, hexacoordinate hemin binding to Cj1386 (191, 192), whereas a peak at 372 nm indicates high spin, pentacoordinate hemin binding. Interestingly, the presence of two Soret peaks suggests two configurations of hemin binding upon titration, with possible equilibrium between the pentacoordinate and hexacoordinate hemin binding modes. The K_d value for

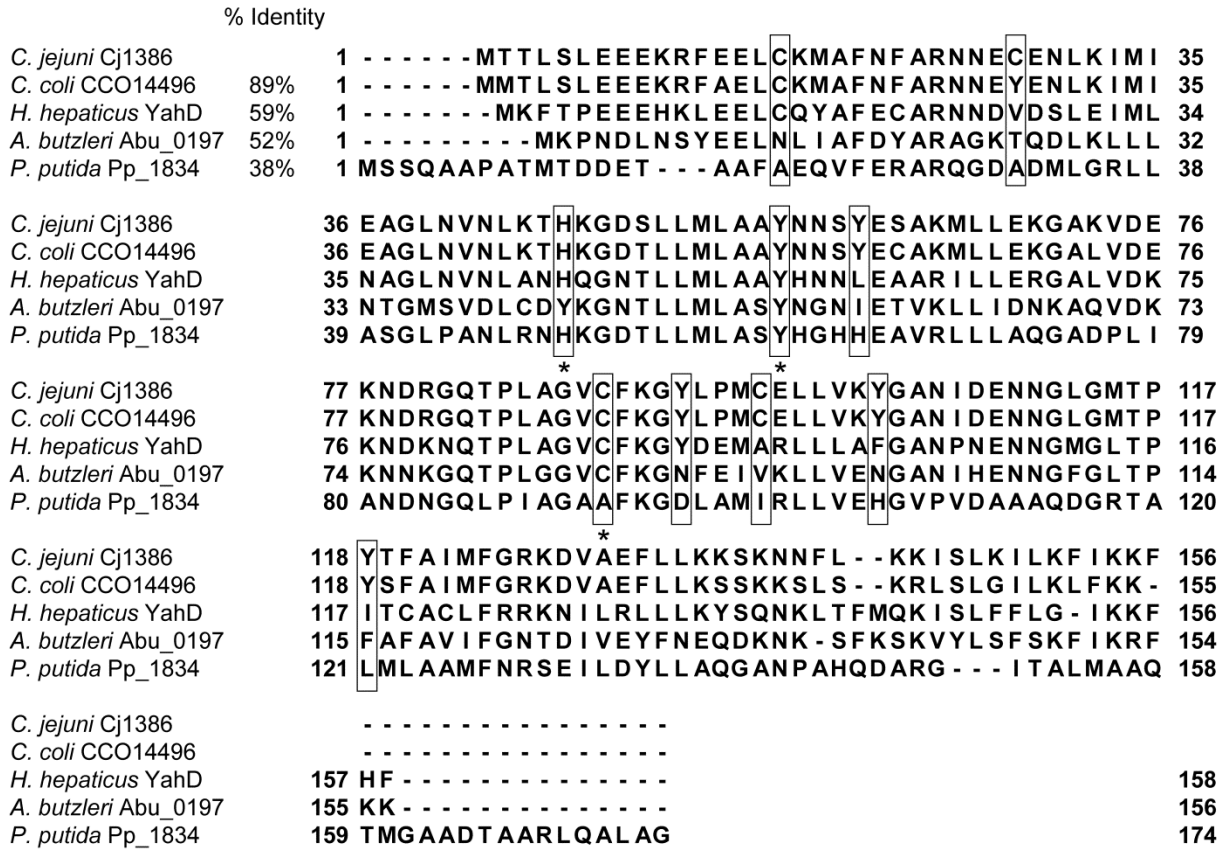

Fig 2.3.3. Multiple sequence alignment of ankyrin-repeat Cj1386 homologs. Tyrosine, cysteine and histidine residues present in the Cj1386 sequence are boxed. Asterisks represent highly conserved residues potentially involved in hemin coordination. Percent sequence identity for each protein sequence relative to Cj1386 is reported. Protein name and bacterial species are listed: *C. jejuni*, *Campylobacter jejuni*; *C. coli*, *Campylobacter coli*; *H. hepaticus*, *Helicobacter hepaticus*; *A. butzleri*, *Arcobacter butzleri*; *P. putida*, *Pseudomonas putida*.

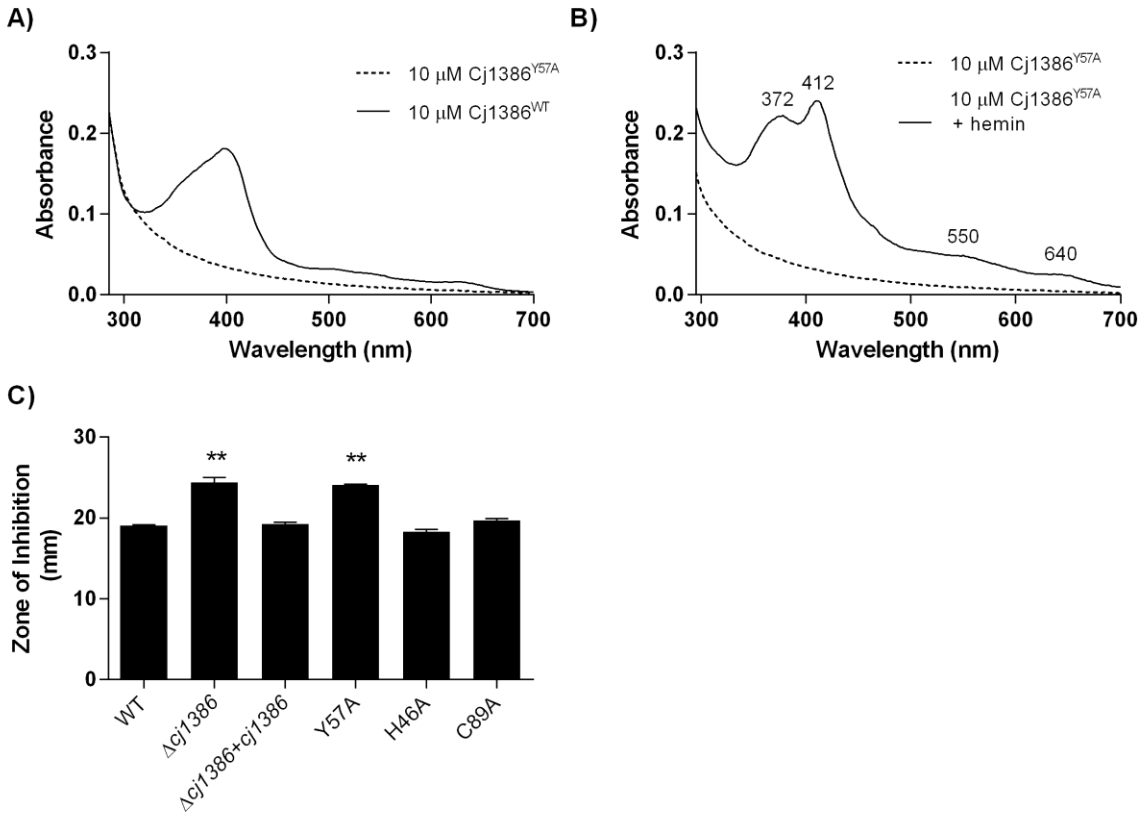

Fig 2.3.4. Tyrosine 57 is important for hemin affinity to Cj1386. (A) Absorption spectra of 10 μM Cj1386^{WT} and 10 μM Cj1386^{Y57A} in 100 mM NaCl, 20 mM Tris, pH 7.4. (B) Absorption spectra of 10 μM Cj1386 ^{Y57A} and 10 μM Cj1386 ^{Y57A} + 10 μM hemin in 100 mM NaCl, 20 mM Tris, pH 7.4. (C) Growth inhibition analysis of wild type *C. jejuni*, Δ*cj1386*, Δ*cj1386+cj1386*^{WT}, and Δ*cj1386+cj1386*^{Y57A}. Strains were exposed to 10 μL of H_2O_2 and incubated under microaerophilic conditions at 37°C for 28 hours followed by measurement of the diameter of growth inhibition. Experiments were repeated in biological triplicate. Statistical significance was determined by ANOVA with *p* values < 0.05 considered significant.

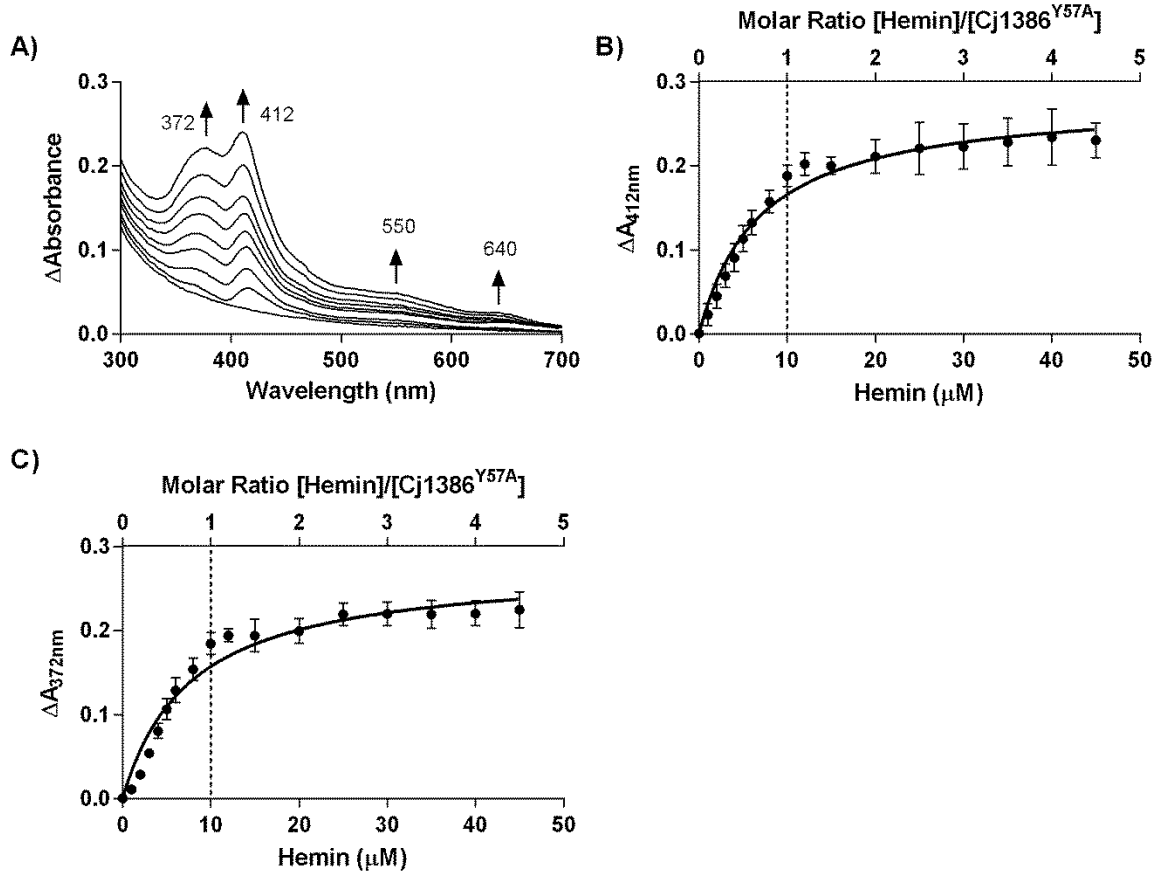

Fig 2.3.5. Cj1386^{Y57A} can be reconstituted with hemin and displays 1:1 hemin binding stoichiometry. (A) Absorption spectra of Cj1386^{Y57A} when titrated with hemin at 1 μM increments against 10 μM apo-Cj1386^{Y57A} in 100 mM NaCl, 20 mM Tris, pH 7.4. Arrows represent the direction of increased absorbance readings upon hemin addition. (B) and (C) Differential absorption spectra of Cj1386^{Y57A} at Soret peaks at 372 nm and 412 nm. The dashed line represents the concentration of Cj1386^{Y57A} and hemin that yield a 1:1 heme-to-Cj1386^{Y57A} binding ratio. Error bars represent the standard error as determined from hemin titration from 2 independent protein purifications.

the 412 nm peak displayed a significantly weaker affinity for hemin (p = 0.0025) at 6.9 ± 1.1 x 10^{-6} M for Cj1386^{Y57A} compared to 4.3 ± 0.3 x 10^{-6} M for Cj1386^{WT} (Table 2.3.3). The hemin affinity at the 372 nm peak for Cj1386^{Y57A} was 7.7 ± 1.0 x 10^{-6} M (Table 2.3.3). Overall, these results suggests that the tyrosine 57 residue plays an important role in the affinity of hemin to Cj1386 when competing for hemin inside bacterial cells as observed by the absence of a Soret peak from *E. coli* purified Cj1386^{Y57A} protein.However, Cj1386^{Y57A} is still able to coordinate hemin when titrated with hemin in a non-competitive assay, albeit with weaker hemin binding at the hexacoordinate 412 nm position.

To assess the biological significance of the Y57A mutant phenotype, a *C. jejuni* strain expressing a Cj1386^{Y57A} allele in a Δ*cj1386* mutant background was constructed and tested for hydrogen peroxide sensitivity using growth inhibition assays. As shown in Figure 2.3.4c, the Δ*cj1386+cj1386*^{Y57A} mutant strain had an increased sensitivity towards H_2O_2 of 24.11 mm relative to 19.06 mm for the wild type *C. jejuni* (p<0.001). Furthermore, the increased sensitivity towards H_2O_2 of 24.11 mm in the Δ*cj1386+cj1386*^{Y57A} strain was not significantly different from the Δ*cj1386* diameter of inhibition of 24.39 mm, demonstrating that expression of *cj1386*^{Y57A} was not sufficient to restore the phenotype of the Δ*cj1386* mutant to that of wild type sensitivity (Figure 2.3.4c). Importantly, sensitivity of the Δ*cj1386* mutant towards H_2O_2 was restored in the Δ*cj1386+cj1386*^{WT} strain. To verify that the Δ*cj1386+cj1386*^{Y57A} H_2O_2 phenotype is due to the change of amino acid at the tyrosine 57 residue and not due to the absence of protein expression, Western blot analysis was performed and confirmed the presence of Cj1386^{Y57A} expression in the Δ*cj1386+cj1386*^{Y57A} strain at levels comparable to the wild type (SFig 2).

The inability of the *cj1386*^{Y57A} allele to restore the H_2O_2 sensitive phenotype of the Δ*cj1386* mutant to wild type levels indicates that tyrosine 57 is key for Cj1386 function within *C. jejuni*. The absorption spectra of Cj1386^{Y57A} expressed and purified from *E. coli* cells revealed that Y57 plays an important role for hemin affinity to Cj1386; specifically, the Cj1386^{Y57A} protein was purified without

coordinated hemin. It is thus probable that the Cj1386^{Y57A} within the Δ*cj1386+cj1386*^{Y57A} mutant is either unable to bind or is outcompeted for hemin binding within *C. jejuni*. Consequently the Cj1386^{Y57A} protein would not be able to traffick hemin to KatA resulting in decreased H_2O_2 detoxification within the cell. Indeed, when KatA was immunoprecipitated from the Δ*cj1386+cj1386*^{Y57A} strain (SFig 3) and the hemin content was quantified, a significant reduction in the hemin-KatA ratio was observed (Table 2.3.4). KatA is a tetrameric protein consisting of four identical subunits with each subunit coordinating one hemin prosthetic group. The hemin content of the Δ*cj1386+cj1386*^{Y57A} strain was found to have a hemin-KatA ratio of 0.4 per KatA subunit as compared to 0.94 for the wild-type strain. Furthermore, the hemin-KatA ratio for the Δ*cj1386+cj1386*^{Y57A} strain was similar to that previously obtained for the Δ*cj1386* mutant (0.3) highlighting the importance for Y57 for optimal function within *C. jejuni*.

Purification of the Cj1386^{H46A} and Cj1386^{C89A} proteins both yielded a yellow-hued solution suggesting that hemin is bound to the Cj1386^{H46A} and Cj1386^{C89A} proteins. Absorbance spectroscopy of the Cj1386^{H46A} and Cj1386^{C89A} proteins confirmed this result with both Cj1386^{H46A} and Cj1386^{C89A} proteins displaying a broad Soret peak (data not shown). Although the histidine 46 and cysteine 89 appear to be highly conserved (Figure 2.3.3), mutation of these residues did not affect the ability of the protein to coordinate hemin following purification. Furthermore, the Δ*cj1386+cj1386*^{H46A} and Δ*cj1386+cj1386*^{C89A} mutants were not affected in their sensitivity towards H_2O_2 relative to the wild type using disc inhibition assays (Figure 2.3.4). Thus, in contrast to the Δ*cj1386+cj1386*^{Y57A} mutant, mutation of these amino acids did not significantly affect the function of Cj1386 in *C. jejuni*.

III. Cj1386 and KatA interact

To further assess the role of Cj1386 in hemin trafficking to KatA, co-immunoprecipitation experiments were performed to probe for a KatA-Cj1386 interaction. Initial experiments using non

TABLE 2.3.4. Hemin quantification of KatA immunoprecipitated from *C. jejuni* NCTC11168 and Δ*cj1386+cj1386*^{Y57A}. The amount of hemin is represented as the mean concentration of hemin detected ± the standard error (in nM) for equal starting concentrations of KatA protein for each strain tested. Experiments were repeated in biological triplicate. The student's t test was used to determine statistical significance with *p* values < 0.05 (*) considered significant.

Source of immunoprecipitated KatA	Concentration of KatA (subunits, nM)	Concentration of hemin (nM)	Ratio (hemin:KatA)	Source
C. jejuni NCTC11168	7.4	6.99 ± 0.19	0.94	(89)
Δ*cj1386*	7.4	0.19 ± 0.10*	0.03	(89)
Δ*cj1386* + *cj1386*^{WT}	7.4	6.41 ± 0.54	0.87	(89)
Δ*cj1386* + *cj1386*^{Y57A}	7.4	0.29 ± 0.18*	0.04	This study

cross-linked whole cell lysates to pull down KatA or Cj1386 followed by Western blot analysis did not identify any interaction between KatA and Cj1386. Given the role of Cj1386 in hemin trafficking to KatA, we hypothesized that any direct interaction between the two proteins is likely to be transient. Thus, it is probable that the absence of any detectable interaction between KatA and Cj1386 was due to the lack of formation of a stable protein complex. Consequently, co-immunoprecipitation of KatA and Cj1386 was performed after the cells were fixed by formaldehyde cross-linking to capture any transient interactions between the proteins. Furthermore, due to the low expression levels of Cj1386 in wild type *C. jejuni* (SFig 4), we subsequently probed for a KatA-Cj1386 interaction in a Δ*perR* mutant background in which *cj1386* is derepressed (89). Detection of a KatA-Cj1386 protein-protein interaction was observed by co-immunoprecipitation of KatA from cross-linked proteins isolated from the Δ*perR* mutant strain and subsequent probing for Cj1386 using Western blot analysis (Figure 2.3.6). As seen in Figure 2.3.6, a band corresponding to Cj1386 was detected when KatA was pulled down from the Δ*perR* mutant lysate. Immunoprecipitation using an anti-Fur antibody was performed using the Δ*perR* cross-linked lysate as a

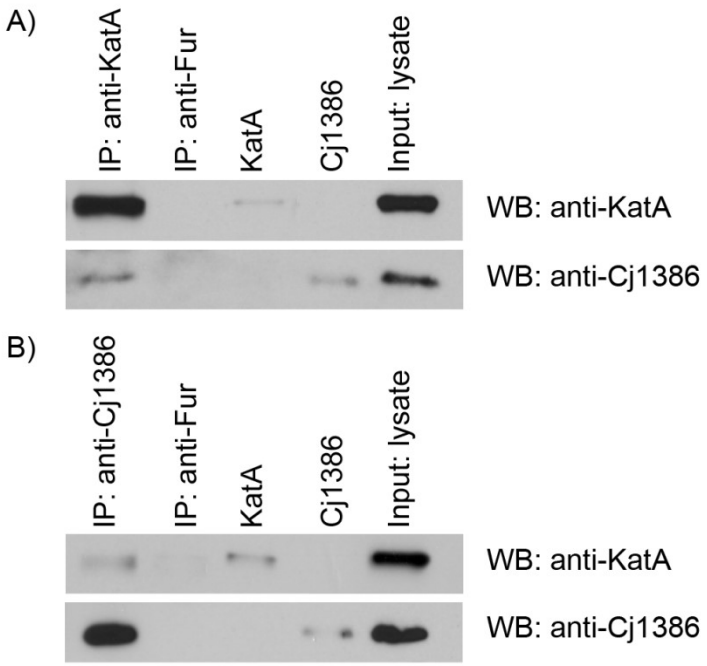

Fig 2.3.6. The Cj1386 and KatA proteins interact. (A) Immunoprecipitation of KatA from cross-linked Δ*perR* protein lysate using an anti-KatA antibody. (B) Immunoprecipitation of Cj1386 from cross-linked *ΔperR* protein lysate using an anti-Cj1386 antibody. (A) and (B) Immunopreciptated protein samples were separated by SDS PAGE followed by immunoblotting with either anti-KatA or anti-Cj1386 antibodies to visualize protein interactions. Immunoprecipitation using an anti-Fur antibody was performed as a negative control. Purified Cj1386 and KatA proteins were run as positive controls. IP: immunoprecipitation; WB: Western blot; Input: whole cell lysate from Δ*perR* mutant.

negative control. Importantly, Cj1386 and KatA were not detectable when the pull-down was performed using the anti-Fur antibody. Next we performed the reciprocal experiment where Cj1386 was co-immunoprecipitated from cross-linked Δ*perR* mutant lysate using an anti-Cj1386 antibody. KatA protein was detected in the Cj1386 pull-down when probed with an anti-KatA antibody (Figure 2.3.6). Furthermore, Cj1386 and KatA were not detected in the anti-Fur immunoprecipitated sample (Figure 2.3.6). Overall, these results demonstrate an interaction between the KatA and Cj1386 proteins.

2.3.6. DISCUSSION

Catalase enzymes are one of the major H_2O_2 detoxification enzymes found within almost all respiring organisms (54). There are three distinct evolutionary classes of catalases which include monofunctional hemin-containing catalases (including large and small subunit enzymes), bifunctional hemin-containing catalase-peroxidases, and non-hemin manganese containing catalases (54). *C. jejuni* encodes for only one catalase enzyme, *katA*, which belongs to the small subunit, hemin-containing monofunctional class of catalases (41). Although the structure of KatA from *C. jejuni* has not been solved to date, several other catalase proteins with structural similarity to *C. jejuni* KatA have been crystalized and their structures resolved. Included among these crystal structures are KatA from *Helicobacter pylori* (56% identity) (58), and *Enterococcus faecalis* (55% identity) (59). Thus, based upon structural similarity and bioinformatic analysis, the KatA enzyme from *C. jejuni* is thought to be a tetrameric protein consisting of four identical subunits. Each subunit contains a hemin prosthetic group which is essential for facilitating the dismutation of H_2O_2 into O_2 and H_2O. The *C. jejuni* KatA protein sequence contains the conserved distal-hemin ligand motif (RERIPERVVHAKG) and the proximal-hemin ligand motif (RLFSYGD) (41, 197). The distal histidine residue and the proximal tyrosine residue are important for the catalytic function and coordination of hemin in catalase respectively (197). Furthermore, expression of *katA* within *C. jejuni* is primarily regulated by Fur (189), and PerR (127). However more recently, additional transcriptional regulators of *katA* expression have been identified including Cj1000 (198) and CosR (199) which add additional layers of complexity to *katA* regulation. In this report, we further contribute to the wealth of knowledge on *C. jejuni* KatA by providing important insight into a key protein required for trafficking hemin to KatA.

This work identifies Cj1386 as a hemin binding and trafficking protein to catalase and thus contributes to a greater understanding of the fundamental biological processes involved in hemin trafficking within the cytoplasm and catalase biogenesis. The Cj1386 protein was found to coordinate

hemin at a 1:1 heme-to-Cj1386 ratio as determined by hemin titration assays. Bioinformatic analysis of Cj1386 reveals that it is a 17 kDa protein which contains three ankyrin repeats (41). Each ankyrin repeat consists of a series of 33 amino acids that are thought to play a role in protein-protein interactions (177). Currently, there is no structural homology model available for the Cj1386 protein. However, Cj1386 appears to represent a unique type of hemin-protein as it does not contain any previously characterized hemin binding motif. Canonical heme/hemin motifs include those characterized for catalase as well as cytochrome proteins. Catalase coordinates hemin at the ferric ion via a tyrosine residue contained in the proximal hemin binding motif RLFSYGD (59). Cytochrome c proteins typically contain a CXXCH heme binding motif where the heme prosthetic group is covalently attached to the cytochrome at the cysteine residues (97). The heme trafficking protein CcmE from *E. coli,* which trafficks heme to periplasmic cytochrome enzymes, is covalently linked to heme at His130 (200). Heme is coordinated to the PhuS protein at the conserved His209 residue or the non-conserved His212 residue (201). Therefore, given the absence of a crystal structure or a clear hemin binding motif, the conserved tyrosine (Y57), cysteine (C89), and histidine (H46) residues in Cj1386 were mutated to identify residues important for hemin ligand binding in Cj1386. Mutagenesis experiments revealed that Y57 is important for coordinating hemin as the Cj1386^{Y57A} protein purified in its apo form. Expression of Cj1386^{Y57A} in the *C. jejuni* Δ*cj1386+ cj1386*^{Y57A} strain did not restore the sensitivity of the strain to H_2O_2 to levels observed in the parental wild-type strain. Additionally, the hemin-KatA ratio in the Δ*cj1386+cj1386*^{Y57A} strain was significantly reduced relative to the wild type strain. These results suggest that without the efficient hemin coordination seen in Cj1386^{WT}, the Cj1386^{Y57A} protein is unable to transfer hemin to KatA. Thus, KatA is unable to catalyze the dismutation of H_2O_2 into H_2O and O_2, resulting in the observed increased H_2O_2 sensitivity in the Δ*cj1386+ cj1386*^{Y57A} strain. Mutation of the conserved histidine (H46A) or the conserved cysteine (C89A) residues did not prevent hemin binding to the Cj1386 protein during purification nor did the *C. jejuni* Δ*cj1386+ cj1386*^{H46A} or Δ*cj1386+ cj1386*^{C89A} strains display an increased

sensitivity to H_2O_2, indicating that H46 and C89 are not essential for hemin binding and trafficking to KatA. In the absence of Y57, the Cj1386 protein can still coordinate hemin *in vitro*. The presence of the Soret peak at 412 nm for the Cj1386^{Y57A} mutant suggests that hemin is still bound in a hexa-coordinate configuration. It may be possible that additional amino acids may compensate for hemin binding in the absence of Y57 to produce the 6-coordinate peak. Indeed, heme coordination to PhuS in *P. aeruginosa*, can still be achieved in a His209 mutant by compensation by an alternative heme coordinating residue, His212 (201). From the multiple sequence alignment of Cj1386, a less conserved tyrosine residue (Y61), which is in close proximity to Y57, could potentially play a role as an alternative hemin coordinating residue. However, the UV-vis spectra also revealed the presence of an additional Soret peak at 372 nm for Cj1386^{Y57A} suggesting penta-coordinate hemin binding. It may be possible that the reduced hemin affinity at 412 nm for Cj1386^{Y57A} is insufficient to maintain the hemin in a hexa-coordinate configuration, which results in a mixed population with an equilibrium of penta and hexa-coordinate binding. It is also important to note that although Y57 has been identified as important for hemin binding, the identity of the second residue involved in the hexa-coordinate binding to Cj1386 has not been identified. Importantly, we found that Cj1386 has a weaker affinity towards hemin than other characterized heme-proteins such as BSA and myoglobin. A weaker affinity towards hemin would help facilitate hemin transfer from Cj1386 to a protein with a greater hemin affinity such as KatA. Future structural studies will be required to determine the residues interacting directly with the ferric ion of hemin as well as the structure of the hemin binding pocket.

In addition to identifying Cj1386 as a heme-protein, Cj1386 was also found to transiently interact with KatA. Formaldehyde cross-linking of bacterial cultures was required to be able to detect an interaction between Cj1386 and KatA suggesting that after transfer of hemin, Cj1386 no longer remains associated with KatA. This finding provides strong evidence that the Cj1386 protein is trafficking hemin to KatA. Furthermore to our knowledge, this is the first report identifying a protein which directly

interacts with KatA and is important for catalase biogenesis. Cj1386 homologs are found in the *C. jejuni* strains doylei, 81-176, 81116, S3, as well as the *Campylobacter* strains *C. coli, C. fetus, C. lari,* and *C. showae.* Interestingly, catalase negative strains of *Campylobacter* (*C. concisus*, *C. mucosalis*, *C. sputorum*, *C. helveticus*, *C. curvus*, *C. rectus, C. upsaliensis, C. hominis* (202, 203)) lack a homolog of Cj1386. The absence of a Cj1386 homolog in these strains may suggest that Cj1386 is only required specifically for catalase biogenesis and does not play a role in trafficking hemin to other heme-proteins within the cell. However, co-immunoprecipitation experiments of Cj1386 followed by mass spec analysis would be required to determine any additional protein interaction partners. Cj1386 homologs are also present in other bacterial genus including *Helicobacter*, *Arcobacter*, *Pseudomonas, Sulfurospirillum,* and *Acetobacter.* Cj1386 homologs are absent from bacterial species such as *E. coli, Salmonella,* and *Enterococcus* suggesting that hemin trafficking to catalase may occur by other proteins or mechanisms specific to those bacterial species that have yet to be identified.

Heme uptake and transport across the periplasmic space into the cytoplasm has been well characterized for numerous bacterial species. *C. jejuni* utilizes a direct heme uptake system (ChuABCD) to acquire heme from the surrounding environment (87). This strategy for obtaining heme is analogous to the previously characterized Shu, Chu, and Phu heme acquisition systems of *Shigella dysenteriae, E. coli ,* and *P. aeruginosa* (84-86). The *C. jejuni* heme uptake system encodes for the outer membrane heme receptor (ChuA), which transports heme across the outer bacterial membrane in a TonB-ExbB-ExbD energy dependent manner (41, 87). Heme is then transported across the periplasmic space by the periplasmic transport protein ChuD and finally across the inner membrane by the ABC transport complex, ChuBC (87). The proteins and mechanism for which Cj1386 obtains hemin within the cytoplasm is currently uncharacterized, however the ChuBC complex may play a role in this process.

In summary, we have identified Cj1386 as a hemin binding protein which displays a weaker affinity towards hemin than other heme-proteins. This characteristic is likely essential for facilitating hemin transfer to KatA. Additionally we have identified tyrosine 57 as a critical residue required for optimal Cj1386 function within *C. jejuni*. Future structural studies of Cj1386 should provide key insight into the hemin coordination sites and hemin binding pocket of this unique hemin trafficking protein.

2.3.7. ACKNOWLEDGEMENTS

This work was supported by CIHR (MOP#84224) to A.S. and a QEIIGSST scholarship to A.F.

CHAPTER 3. DISCUSSION

In this study, we have performed global characterization of the oxidative stress responsive genes of *C. jejuni* to gain a more in-depth understanding of the direct and indirect oxidant defenses required for successful colonization of the host. The construction and phenotypic characterization of a targeted isogenic deletion mutant library represents the first and largest of this type of library to be constructed within *C. jejuni*. As such, it proved to be a valuable tool in identifying novel genes important for oxidant defense as well as identifying functional categories of genes that have crucial functions that indirectly affect the fitness of the bacteria when exposed to oxidants. Additionally, using both biochemical and molecular biological techniques, Cj1386 was identified from the phenotypic screening of the library and further characterized as a novel hemin trafficking protein. This work provides the first experimental evidence of a protein involved in catalase biogenesis. Overall, several major conclusions can be drawn from my PhD project that help advance the scientific knowledge on *C. jejuni* and oxidative stress defense.

3.1. *Campylobacter jejuni* contains a rudimentary antioxidant defense system

Compared to other bacteria, *C. jejuni* encodes for a very small subset of enzymes directly involved in detoxifying oxidants within the cell. From growth inhibition assays involving the isogenic deletion mutant library, we identified 22 mutants that had clear phenotypes towards oxidants (28). However with the exception of Rrc, we did not identify any additional genes that had direct enzymatic activity against the oxidants tested. Indeed, the majority of enzymes responsible for antioxidant defense are genes that have been characterized previously. The major antioxidant enzymes of *C. jejuni* are SodB, KatA, AhpC, Tpx, and Bcp (30, 42, 124-126, 137). It is important to note that there are genes that we identified from the growth inhibition assays that still require characterization to determine if they

perform enzymatic functions directly involved in detoxifying oxidants. Included in this list are the potential candidate genes *cj0344*, *cj0260c*, and *cj1159c,* which are all categorized as hypothetical proteins and do not have any annotated function. Of these three genes only *cj0344* displayed sensitivity towards H_2O_2, which may suggest a direct role in oxidant detoxification. *Cj0260c* and *cj1159c* have increased resistance towards cumene hydroperoxide. It may be possible that deletion of these genes results in up-regulation of additional genes (i.e. AhpC) to compensate for the loss of these enzymes. Alternatively, these proteins may be targets of cumene hydroperoxide damage and lead to increased oxidative stress within the cell. Consequently upon their deletion, the level of oxidative stress within these strains is reduced compared to wild type cell.

It is evident that *C. jejuni* relies on relatively few antioxidant enzymes to survive oxidative stress but these enzymes are highly critical for bacterial survival. Deletion of SodB, KatA or AhpC results in hypersensitivity towards ROS and significant decreased fitness during colonization of a chick commensal model compared to wild type *C. jejuni* (99). This situation is markedly different from other Gram-negative bacteria that contain multiple Sod and KatA enzymes that are under control of different transcriptional regulators and/or expressed during different phases of bacterial growth. *E. coli* expresses two Sod enzymes (SodA and SodB) and two catalase enzymes (KatG and KatE). Consequently, double deletion mutants *ΔsodAΔsodB* or *ΔkatGΔkatE* need to be constructed to observe maximal sensitivity towards superoxide and hydrogen peroxide respectively. Expression of one of the enzymes is able to compensate for deletion of the other (204). Regardless, it is clear that despite a rudimentary oxidative stress defense system, *C. jejuni* is a highly successful food-borne pathogen able to survive oxidative stress by reliance on only a few key antioxidant enzymes.

3.2. The majority of mutants with oxidant sensitivities indirectly contribute to oxidative stress defense within *C. jejuni*

The vast majority of the genes with phenotypes towards oxidants were found to be involved in oxidative stress defense by indirect mechanisms (28). In particular, we found that loss of bacterial motility was found to have highly detrimental effects on the cell by an inadvertent increase in endogenous superoxide production (Figure 3.1). Loss of bacterial motility likely results in perturbation of the electron transport chain due to disruption of proton movement across the inner membrane by the flagellar motor complex (MotAB) or due to loss of key flagellar components (FlgDHIKPR, FlgP). In turn, this disruption to the ETC causes electron leakage at the complexes along the ETC, which can be advantageously oxidized by O_2 to produce ROS (Figure 3.1). Furthermore, Complex IV of the ETC was found to be the major contributor to the oxidant sensitivity phenotype within these non-motile flagellar biogenesis mutants. Deletion of Complex IV or use of an alternative electron acceptor (fumarate), which would not require complex IV to generate ATP, completely alleviated the oxidant sensitivity of these strains. Thus, screening of the mutant library also provides insight into biological molecules and processes that are indirect targets of oxidative damage.

Overall, this work highlights the strength of using a transcriptomic/isogenic deletion mutant library approach for the identification of novel genes which may be important for oxidative stress defense (both directly and indirectly).

3.3. Cj1386 plays an important role in hydrogen peroxide defense by functioning in hemin trafficking to KatA

From screening the isogenic mutant library against oxidants, we identified a novel gene involved in H_2O_2 defense. The work on Cj1386 has provided key insight into two poorly investigated areas of

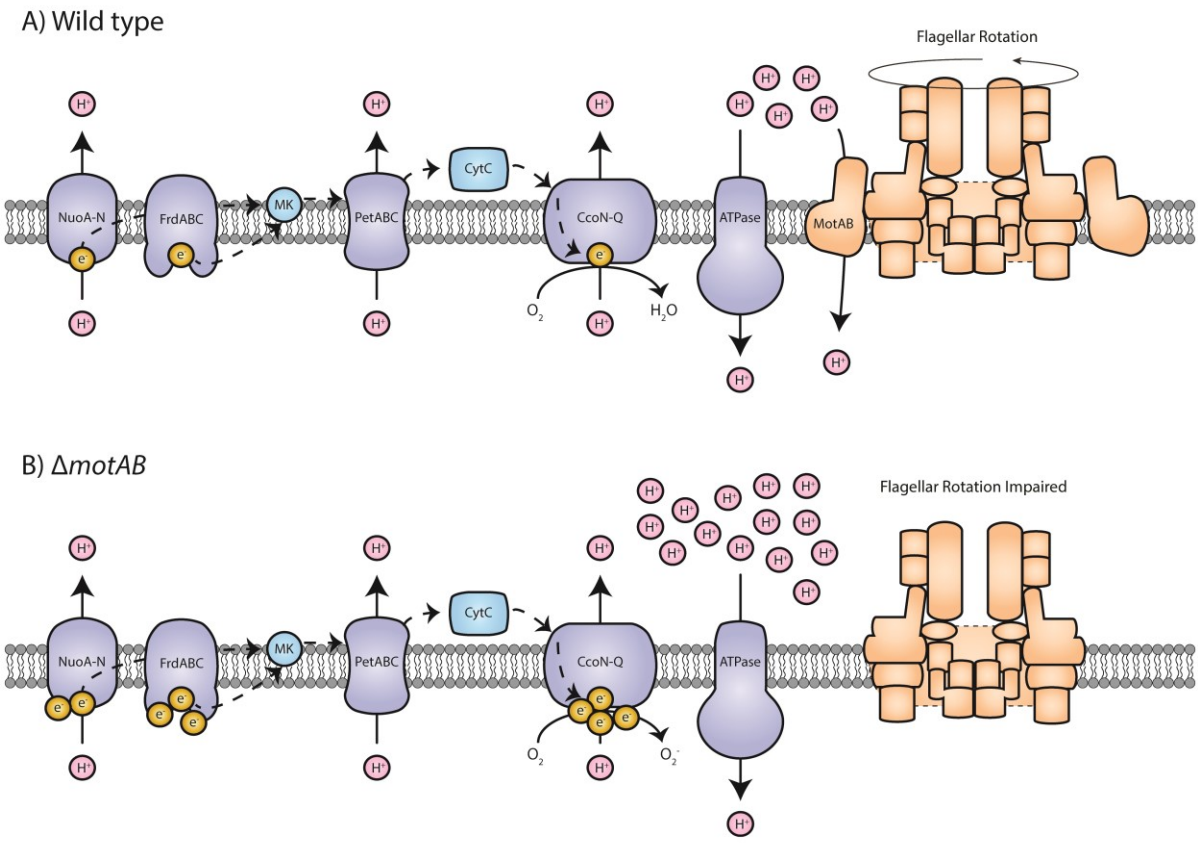

Fig 3.1. Disruption of bacterial motility indirectly leads to increased oxidant sensitivity in non-motile flagellar mutant strains. (A) The electron transport chain of wild-type *C. jejuni* transfers electrons across the complexes of the ETC. Electron transfer is coupled to proton transport into the periplasmic space generating a proton gradient. The proton gradient drives ATP synthesis via ATP synthase. MotAB also utilizes the proton gradient to drive bacterial motility. (B) Disruption of bacterial motility in a Δ*motAB* mutant perturbs the proton gradient along the inner membrane due to the loss of proton movement at the MotAB complex. Disturbance of the proton gradient leads to electron leakage at complexes along the ETC and increases $O_2^{\bullet-}$ production by inadvertent reduction of O_2.

research – heme trafficking and catalase biogenesis. Indeed, identifying Cj1386 as a hemin protein involved in transferring hemin to KatA provides the first experimentally demonstrated example of a protein important for KatA biogenesis. In addition to characterizing the role this gene plays in hemin trafficking to KatA within *C. jejuni*, it is also clear from this work that it plays a key important role in *in vivo* colonization under both commensal and pathogenic colonization conditions (89). The attenuated colonization levels within an *in vivo* setting make Cj1386 a potential target for drug development to help reduce *C. jejuni* numbers with the host.

The current proposed model for Cj1386 and its role in hemin trafficking in *C. jejuni* is shown in Figure 3.2. Heme is taken up from the external environment into the cell by the ChuABCD heme acquisition system. Alternatively, heme can also likely be synthesized within the cell via the heme biosynthesis pathway (HemBCDENH). Within the cytoplasm of the cell, Cj1386 is able to bind hemin and interact with KatA. From the characterization of Cj1386, it was observed that Cj1386 displays hexacoordinate hemin binding and that mutation of tyrosine 57 to alanine results in decreased hemin affinity. Tyrosine 57 likely represents one of the axial hemin ligands. Furthermore, mutation of tyrosine 57 significantly impaired hemin trafficking to KatA. The decreased hemin trafficking to KatA within *C. jejuni* results in increased sensitivity towards H_2O_2.

3.4. Future directions

One of the novel findings of this work has been the elucidation of the function of Cj1386 and its importance for hemin trafficking within *C. jejuni*. Preliminary co-immunoprecipitation experiments identified additional proteins that co-eluted with Cj1386 (SFig 5) suggesting Cj1386 may traffick heme to proteins other than KatA. Future studies focusing on identifying these additional Cj1386 protein-protein

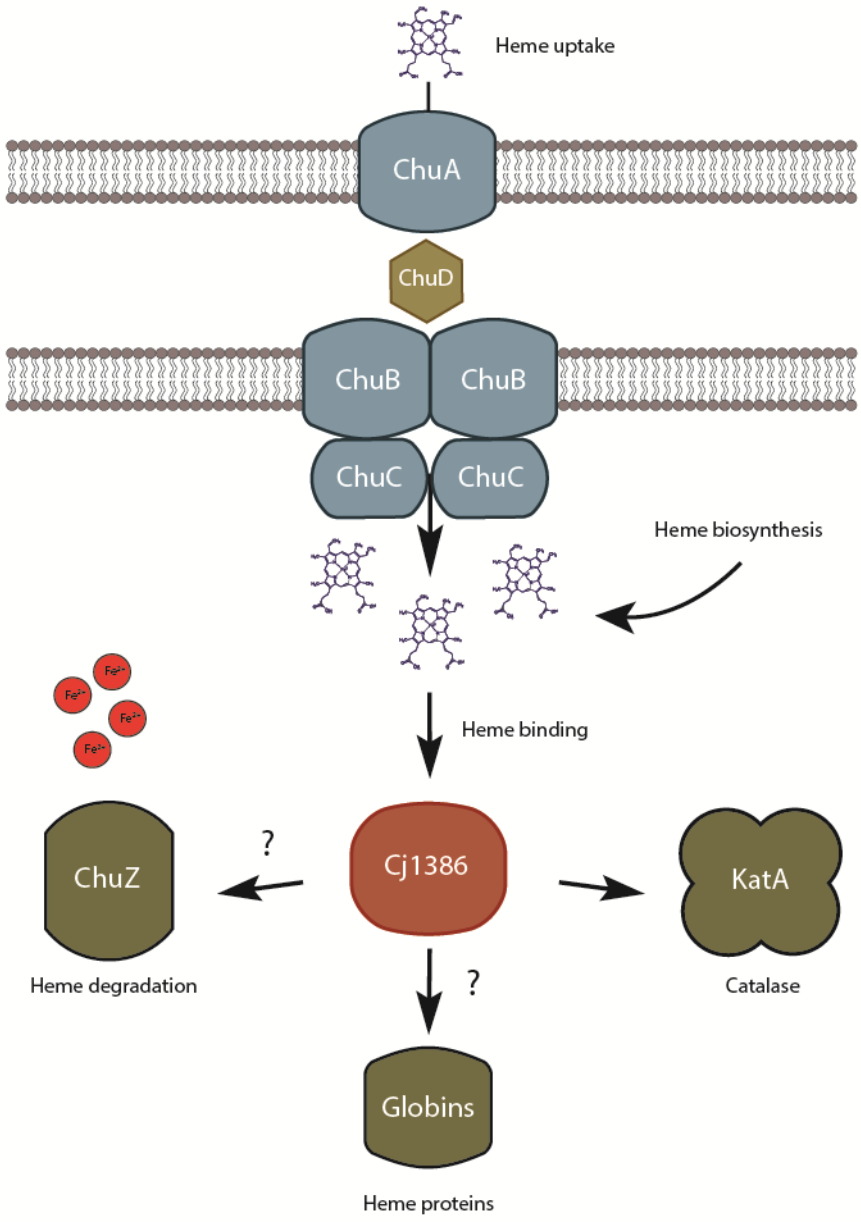

Fig 3.2. Cj1386 is a hemin trafficking protein to KatA in *C. jejuni*. Heme is transported into the cytoplasm from the external environment by ChuABCD or is synthesized in the cytoplasm. Within the cytoplasm, Cj1386 binds hemin and interacts with KatA to transfer hemin to KatA. It is currently unknown if Cj1386 trafficks heme to other proteins within the cell.

interactions would answer several key questions on Cj1386 and heme trafficking within the cell. First, identification of these Cj1386 interaction partners would determine if Cj1386 is a specific hemin trafficking protein to KatA or if Cj1386 trafficks hemin to additional heme-proteins (Figure 3.2). *C. jejuni* contains two additional, characterized heme containing proteins (that are not cytochrome proteins), Ctb and Ctg (88). These proteins encode for a truncated hemoglobin and a single domain hemoglobin respectively (205). How these proteins obtain heme is currently unknown. However, by identifying the additional protein interaction partners of Cj1386, it may be possible to gain deeper insight as to whether Cj1386 is also trafficking heme to these proteins too. Secondly, protein-protein interaction data for Cj1386 may help to determine which proteins Cj1386 obtains heme from within the cell. Given the toxicity of heme and its hydrophobicity in aqueous solutions, it is likely that Cj1386 obtains heme from specific proteins instead of trying to scavenge the low levels of free heme available within the cell. It is tempting to speculate that Cj1386 may interact with ChuC to directly acquire the heme being transported into the cell. Alternatively, Cj1386 may also obtain heme from the terminal protein of the heme biosynthesis pathway, ferrochelatase (HemH) (88). Finally, identification of these Cj1386 interacting proteins has the potential to detect novel proteins that are involved in the heme trafficking process and/or form complexes with Cj1386 that may be important during hemin transfer to KatA.

From UV-vis spectral analysis of holo-Cj1386, the presence of the 412 nm Soret peak suggests hexacoordinate hemin binding. Furthermore, the UV-vis spectra of Cj1386^{Y57A} suggested Y57 to be one of the hemin axial ligands. However, structural characterization of Cj1386 is needed to provide definitive evidence as to whether hemin is bound to the protein in a hexacoordinate configuration and to also determine the identity of the two axial heme ligands. Crystallization of Cj1386 or resonance Raman spectroscopy are two commonly used techniques that could be utilized to provide more insight into hemin binding to Cj1386. To date, no protein structures have been solved that have structural homology to Cj1386. Thus, crystallization of Cj1386 would provide the first structural analysis of this unique

protein fold that functions in hemin trafficking. Additionally, a crystal structure of Cj1386 will elucidate the overall fold of the hemin pocket and can identify additional residues that may be interacting with the hemin prosthetic group.

Our co-immunoprecipitation experiments also demonstrated a transient interaction between Cj1386 and KatA. However, it cannot be conclusively determined if this is a direct protein-protein interaction between KatA and Cj1386 or if additional proteins may form part of a complex. Experiments investigating hemin transfer from Cj1386 to KatA using purified holo-Cj1386 and apo-KatA proteins would provide insight as to whether these proteins directly interact and would also help to conclusively demonstrate hemin transfer from Cj1386 to KatA. Stopped flow spectroscopy or Surface Plasmon Resonance (SPR) could be utilized to answer these questions and these experiments would also be able to determine the hemin binding kinetics of KatA. It is important to note that although Cj1386 is important for hemin trafficking to KatA, it is unknown if the KatA polypeptide receives hemin during protein folding or if it occurs post-translation. Thus, success using stopped-flow spectroscopy or SPR to measure hemin transfer using purified (and folded) KatA may be limited. Experiments using *in vitro* translation systems (rabbit reticulocyte protein expression system) could prove useful in addressing this issue. KatA could be expressed in this system without hemin addition and followed by post-translational addition of hemin (+/- Cj1386) and subsequent catalase activity assays. Alternatively, KatA could be expressed with hemin addition (+/- Cj1386) during protein translation followed by catalase activity assays to measure KatA enzyme activity. Thus, direct hemin trafficking to KatA could be investigated as well as determining if hemin transfer occurs during translation or post-translation during KatA biogenesis.

Overall, the work presented in this thesis contributes to the field of *Campylobacter* biology by discovering and characterizing one of the important mechanisms for catalase biogenesis – hemin

acquisition. Additionally, the work on the isogenic mutant library has provided further detailed insight into the major and important antioxidant systems within *C. jejuni*.

CHAPTER 4. REFERENCES

1. **Altekruse SF, Stern NJ, Fields PI, Swerdlow DL.** 1999. *Campylobacter jejuni*--an emerging foodborne pathogen. Emerging infectious diseases **5:**28-35.
2. **Humphrey T, O'Brien S, Madsen M.** 2007. *Campylobacters* as zoonotic pathogens: a food production perspective. Int J Food Microbiol **117:**237-257.
3. **Black RE, Levine MM, Clements ML, Hughes TP, Blaser MJ.** 1988. Experimental *Campylobacter jejuni* infection in humans. J. Infect. Dis. **157:**472-479.
4. **Robinson DA.** 1981. *Campylobacter* infection. R. Soc. Health J. **101:**138-140.
5. **Blaser MJ, Engberg J.** 2008. Clinical aspects of *Campylobacter jejuni* and *Campylobacter coli*, p. 99-121. *In* Nachamkin I, Szymanski C, Blaser MJ (ed.), *Campylobacter*. ASM Press, Washington.
6. **Boyanova L, Gergova G, Spassova Z, Koumanova R, Yaneva P, Mitov I, Derejian S, Krastev Z.** 2004. *Campylobacter* infection in 682 bulgarian patients with acute enterocolitis, inflammatory bowel disease, and other chronic intestinal diseases. Diagn. Microbiol. Infect. Dis. **49:**71-74.
7. **Moore JE, Corcoran D, Dooley JS, Fanning S, Lucey B, Matsuda M, McDowell DA, Megraud F, Millar BC, O'Mahony R, O'Riordan L, O'Rourke M, Rao JR, Rooney PJ, Sails A, Whyte P.** 2005. *Campylobacter*. Vet. Res. **36:**351-382.
8. **Farr SB, D'Ari R, Touati D.** 1986. Oxygen-dependent mutagenesis in *Escherichia coli* lacking superoxide dismutase. Proceedings of the National Academy of Sciences of the United States of America **83:**8268-8272.
9. **Ruiz-Palacios GM.** 2007. The health burden of *Campylobacter* infection and the impact of antimicrobial resistance: playing chicken. Clin Infect Dis **44:**701-703.
10. **Coker AO, Isokpehi RD, Thomas BN, Amisu KO, Obi CL.** 2002. Human campylobacteriosis in developing countries. Emerging infectious diseases **8:**237-244.
11. **Masanta WO, Heimesaat MM, Bereswill S, Tareen AM, Lugert R, Gross U, Zautner AE.** 2013. Modification of intestinal microbiota and its consequences for innate immune response in the pathogenesis of campylobacteriosis. Clinical & developmental immunology **2013:**526860.
12. **PHAC** 2014, posting date. Notifiable diseases on-line. Public Health Agency of Canada. [Online.]
13. **Thomas MK, Murray R, Flockhart L, Pintar K, Pollari F, Fazil A, Nesbitt A, Marshall B.** 2013. Estimates of the burden of foodborne illness in Canada for 30 specified pathogens and unspecified agents, circa 2006. Foodborne pathogens and disease **10:**639-648.
14. **CDC** 2014, posting date. Incidence and Trends of Infection with Pathogens Transmitted Commonly Through Food — Foodborne Diseases Active Surveillance Network, 10 U.S. Sites, 2006–2013. Centers for Disease Control and Prevention. [Online.]
15. **CDC** 2014, posting date. CDC Estimates of Foodborne Illness in the United States. Centers for Disease Control and Prevention. [Online.]
16. **Young KT, Davis LM, Dirita VJ.** 2007. *Campylobacter jejuni*: molecular biology and pathogenesis. Nat Rev Microbiol **5:**665-679.
17. **Hooper LV, Bry L, Falk PG, Gordon JI.** 1998. Host-microbial symbiosis in the mammalian intestine: exploring an internal ecosystem. BioEssays : news and reviews in molecular, cellular and developmental biology **20:**336-343.
18. **Stahl M, Butcher J, Stintzi A.** 2012. Nutrient acquisition and metabolism by *Campylobacter jejuni*. Frontiers in cellular and infection microbiology **2:**5.

19. **Stahl M, Friis LM, Nothaft H, Liu X, Li J, Szymanski CM, Stintzi A.** 2011. L-fucose utilization provides *Campylobacter jejuni* with a competitive advantage. Proceedings of the National Academy of Sciences of the United States of America **108:**7194-7199.
20. **Kumar-Phillips GS, Hanning I, Slavik M.** 2013. Influence of acid-adaptation of *Campylobacter jejuni* on adhesion and invasion of INT 407 cells. Foodborne pathogens and disease **10:**1037-1043.
21. **Birk T, Wik MT, Lametsch R, Knochel S.** 2012. Acid stress response and protein induction in *Campylobacter jejuni* isolates with different acid tolerance. BMC microbiology **12:**174.
22. **Reid AN, Pandey R, Palyada K, Naikare H, Stintzi A.** 2008. Identification of *Campylobacter jejuni* genes involved in the response to acidic pH and stomach transit. Appl Environ Microbiol **74:**1583-1597.
23. **Fox EM, Raftery M, Goodchild A, Mendz GL.** 2007. *Campylobacter jejuni* response to ox-bile stress. FEMS immunology and medical microbiology **49:**165-172.
24. **Chan KF, Le Tran H, Kanenaka RY, Kathariou S.** 2001. Survival of clinical and poultry-derived isolates of *Campylobacter jejuni* at a low temperature (4 degrees C). Appl Environ Microbiol **67:**4186-4191.
25. **Cameron A, Frirdich E, Huynh S, Parker CT, Gaynor EC.** 2012. Hyperosmotic stress response of *Campylobacter jejuni*. Journal of bacteriology **194:**6116-6130.
26. **Konkel ME, Kim BJ, Klena JD, Young CR, Ziprin R.** 1998. Characterization of the thermal stress response of *Campylobacter jejuni*. Infection and immunity **66:**3666-3672.
27. **Elvers KT, Turner SM, Wainwright LM, Marsden G, Hinds J, Cole JA, Poole RK, Penn CW, Park SF.** 2005. NssR, a member of the Crp-Fnr superfamily from *Campylobacter jejuni*, regulates a nitrosative stress-responsive regulon that includes both a single-domain and a truncated haemoglobin. Molecular microbiology **57:**735-750.
28. **Flint A, Sun YQ, Butcher J, Stahl M, Huang H, Stintzi A.** 2014. Phenotypic screening of a targeted mutant library reveals *Campylobacter jejuni* defenses against oxidative stress. Infection and immunity **82:**2266-2275.
29. **Palyada K, Sun YQ, Flint A, Butcher J, Naikare H, Stintzi A.** 2009. Characterization of the oxidative stress stimulon and PerR regulon of *Campylobacter jejuni*. BMC Genomics **10:**481.
30. **Day WA, Jr., Sajecki JL, Pitts TM, Joens LA.** 2000. Role of catalase in *Campylobacter jejuni* intracellular survival. Infection and immunity **68:**6337-6345.
31. **Imlay JA.** 2003. Pathways of oxidative damage. Annu Rev Microbiol **57:**395-418.
32. **Imlay JA.** 2008. Cellular Defenses against Superoxide and Hydrogen Peroxide. Annu. Rev. Biochem **77:**755–776.
33. **Annuk H, Shchepetova J, Kullisaar T, Songisepp E, Zilmer M, Mikelsaar M.** 2003. Characterization of intestinal *lactobacilli* as putative probiotic candidates. J Appl Microbiol **94:**403-412.
34. **Segal AW.** 2005. How neutrophils kill microbes. Annu Rev Immunol **23:**197-223.
35. **Sellars MJ, Hall SJ, Kelly DJ.** 2002. Growth of *Campylobacter jejuni* supported by respiration of fumarate, nitrate, nitrite, trimethylamine-N-oxide, or dimethyl sulfoxide requires oxygen. J Bacteriol **184:**4187-4196.
36. **Imlay JA.** 2013. The molecular mechanisms and physiological consequences of oxidative stress: lessons from a model bacterium. Nat Rev Microbiol **11:**443-454.
37. **Imlay JA.** 2008. Cellular defenses against superoxide and hydrogen peroxide. Annu Rev Biochem **77:**755-776.
38. **Imlay JA, Fridovich I.** 1991. Assay of metabolic superoxide production in *Escherichia coli*. The Journal of biological chemistry **266:**6957-6965.

39. **Carlioz A, Touati D.** 1986. Isolation of superoxide dismutase mutants in *Escherichia coli*: is superoxide dismutase necessary for aerobic life? EMBO J **5:**623-630.
40. **Gort AS, Ferber DM, Imlay JA.** 1999. The regulation and role of the periplasmic copper, zinc superoxide dismutase of *Escherichia coli*. Molecular microbiology **32:**179-191.
41. **Parkhill J, Wren BW, Mungall K, Ketley JM, Churcher C, Basham D, Chillingworth T, Davies RM, Feltwell T, Holroyd S, Jagels K, Karlyshev AV, Moule S, Pallen MJ, Penn CW, Quail MA, Rajandream M-A, Rutherford KM, Vliet AHMV, Whitehead S, Barell BG.** 2000. The genome sequence of the food-borne pathogen *Campylobacter jejuni* reveals hypervariable sequences. Nature **403:**665-668.
42. **Purdy D, Park SF.** 1994. Cloning, nucleotide sequence and characterization of a gene encoding superoxide dismutase from *Campylobacter jejuni* and *Campylobacter coli*. Microbiology **140 (Pt 5):**1203-1208.
43. **Winterbourn CC.** 2013. The biological chemistry of hydrogen peroxide. Methods in enzymology **528:**3-25.
44. **Rush JD, Koppenol WH.** 1990. Reactions of Fe(II)-ATP and Fe(II)-citrate complexes with t-butyl hydroperoxide and cumyl hydroperoxide. FEBS letters **275:**114-116.
45. **Park S, You X, Imlay JA.** 2005. Substantial DNA damage from submicromolar intracellular hydrogen peroxide detected in Hpx- mutants of *Escherichia coli*. Proceedings of the National Academy of Sciences of the United States of America **102:**9317-9322.
46. **Seaver LC, Imlay JA.** 2004. Are respiratory enzymes the primary sources of intracellular hydrogen peroxide? The Journal of biological chemistry **279:**48742-48750.
47. **Wai SN, Nakayama K, Umene K, Moriya T, Amako K.** 1996. Construction of a ferritin-deficient mutant of *Campylobacter jejuni*: contribution of ferritin to iron storage and protection against oxidative stress. Mol. Microbiol. **20:**1127-1134.
48. **Ishikawa T, Mizunoe Y, Kawabata S, Takade A, Harada M, Wai SN, Yoshida S.** 2003. The iron-binding protein Dps confers hydrogen peroxide stress resistance to *Campylobacter jejuni*. J. Bacteriol. **185:**1010-1017.
49. **Baillon ML, van Vliet AH, Ketley JM, Constantinidou C, Penn CW.** 1999. An iron-regulated alkyl hydroperoxide reductase (AhpC) confers aerotolerance and oxidative stress resistance to the microaerophilic pathogen *Campylobacter jejuni*. J. Bacteriol. **181:**4798-4804.
50. **Baker LM, Raudonikiene A, Hoffman PS, Poole LB.** 2001. Essential thioredoxin-dependent peroxiredoxin system from *Helicobacter pylori*: genetic and kinetic characterization. Journal of bacteriology **183:**1961-1973.
51. **van Vliet AH, Ketley JM, Park SF, Penn CW.** 2002. The role of iron in *Campylobacter* gene regulation, metabolism and oxidative stress defense. FEMS microbiology reviews **26:**173-186.
52. **Seaver LC, Imlay JA.** 2001. Alkyl hydroperoxide reductase is the primary scavenger of endogenous hydrogen peroxide in *Escherichia coli*. Journal of bacteriology **183:**7173-7181.
53. **Parsonage D, Youngblood DS, Sarma GN, Wood ZA, Karplus PA, Poole LB.** 2005. Analysis of the link between enzymatic activity and oligomeric state in AhpC, a bacterial peroxiredoxin. Biochemistry **44:**10583-10592.
54. **Zamocky M, Gasselhuber B, Furtmuller PG, Obinger C.** 2012. Molecular evolution of hydrogen peroxide degrading enzymes. Archives of biochemistry and biophysics **525:**131-144.
55. **Alfonso-Prieto M, Biarnes X, Vidossich P, Rovira C.** 2009. The molecular mechanism of the catalase reaction. Journal of the American Chemical Society **131:**11751-11761.
56. **Bravo J, Verdaguer N, Tormo J, Betzel C, Switala J, Loewen PC, Fita I.** 1995. Crystal structure of catalase HPII from *Escherichia coli*. Structure **3:**491-502.

57. **Vainshtein BK, Melik-Adamyan WR, Barynin VV, Vagin AA, Grebenko AI, Borisov VV, Bartels KS, Fita I, Rossmann MG.** 1986. Three-dimensional structure of catalase from *Penicillium vitale* at 2.0 A resolution. Journal of molecular biology **188:**49-61.
58. **Loewen PC, Carpena X, Rovira C, Ivancich A, Perez-Luque R, Haas R, Odenbreit S, Nicholls P, Fita I.** 2004. Structure of *Helicobacter pylori* catalase, with and without formic acid bound, at 1.6 A resolution. Biochemistry **43:**3089-3103.
59. **Hakansson KO, Brugna M, Tasse L.** 2004. The three-dimensional structure of catalase from *Enterococcus faecalis*. Acta crystallographica. Section D, Biological crystallography **60:**1374-1380.
60. **Carpena X, Soriano M, Klotz MG, Duckworth HW, Donald LJ, Melik-Adamyan W, Fita I, Loewen PC.** 2003. Structure of the Clade 1 catalase, CatF of *Pseudomonas syringae*, at 1.8 A resolution. Proteins **50:**423-436.
61. **Longley W.** 1967. The crystal structure of bovine liver catalase: a combined study by x-ray diffraction and electron microscopy. Journal of molecular biology **30:**323-327.
62. **Ko TP, Safo MK, Musayev FN, Di Salvo ML, Wang C, Wu SH, Abraham DJ.** 2000. Structure of human erythrocyte catalase. Acta crystallographica. Section D, Biological crystallography **56:**241-245.
63. **Melik-Adamyan WR, Barynin VV, Vagin AA, Borisov VV, Vainshtein BK, Fita I, Murthy MR, Rossmann MG.** 1986. Comparison of beef liver and *Penicillium vitale* catalases. Journal of molecular biology **188:**63-72.
64. **Zamocky M, Koller F.** 1999. Understanding the structure and function of catalases: clues from molecular evolution and in vitro mutagenesis. Prog. Biophys. Mol. Biol. **72:**19-66.
65. **Zamocky M, Furtmuller PG, Obinger C.** 2008. Evolution of catalases from bacteria to humans. Antioxid. Redox. Signal. **10:**1527-1548.
66. **Chelikani P, Fita I, Loewen PC.** 2004. Diversity of structures and properties among catalases. Cell Mol Life Sci **61:**192-208.
67. **Flint DH, Smyk-Randall E, Tuminello JF, Draczynska-Lusiak B, Brown OR.** 1993. The inactivation of dihydroxy-acid dehydratase in *Escherichia coli* treated with hyperbaric oxygen occurs because of the destruction of its Fe-S cluster, but the enzyme remains in the cell in a form that can be reactivated. The Journal of biological chemistry **268:**25547-25552.
68. **Flint DH, Tuminello JF, Emptage MH.** 1993. The inactivation of Fe-S cluster containing hydro-lyases by superoxide. The Journal of biological chemistry **268:**22369-22376.
69. **Gardner PR, Fridovich I.** 1991. Superoxide sensitivity of the *Escherichia coli* aconitase. The Journal of biological chemistry **266:**19328-19333.
70. **Liochev SI, Fridovich I.** 1992. Fumarase C, the stable fumarase of *Escherichia coli*, is controlled by the soxRS regulon. Proceedings of the National Academy of Sciences of the United States of America **89:**5892-5896.
71. **Varghese S, Tang Y, Imlay JA.** 2003. Contrasting sensitivities of *Escherichia coli* aconitases A and B to oxidation and iron depletion. Journal of bacteriology **185:**221-230.
72. **Jang S, Imlay JA.** 2007. Micromolar intracellular hydrogen peroxide disrupts metabolism by damaging iron-sulfur enzymes. The Journal of biological chemistry **282:**929-937.
73. **Sobota JM, Imlay JA.** 2011. Iron enzyme ribulose-5-phosphate 3-epimerase in *Escherichia coli* is rapidly damaged by hydrogen peroxide but can be protected by manganese. Proceedings of the National Academy of Sciences of the United States of America **108:**5402-5407.
74. **Gu M, Imlay JA.** 2013. Superoxide poisons mononuclear iron enzymes by causing mismetallation. Molecular microbiology **89:**123-134.
75. **Anjem A, Imlay JA.** 2012. Mononuclear iron enzymes are primary targets of hydrogen peroxide stress. The Journal of biological chemistry **287:**15544-15556.

76. **Henle ES, Han Z, Tang N, Rai P, Luo Y, Linn S.** 1999. Sequence-specific DNA cleavage by Fe2+-mediated fenton reactions has possible biological implications. The Journal of biological chemistry **274:**962-971.
77. **Dizdaroglu M, Rao G, Halliwell B, Gajewski E.** 1991. Damage to the DNA bases in mammalian chromatin by hydrogen peroxide in the presence of ferric and cupric ions. Archives of biochemistry and biophysics **285:**317-324.
78. **Wolf P, Jones GD, Candeias LP, O'Neill P.** 1993. Induction of strand breaks in polyribonucleotides and DNA by the sulphate radical anion: role of electron loss centres as precursors of strand breakage. International journal of radiation biology **64:**7-18.
79. **Hogg M, Wallace SS, Doublie S.** 2005. Bumps in the road: how replicative DNA polymerases see DNA damage. Current opinion in structural biology **15:**86-93.
80. **Costa V, Quintanilha A, Moradas-Ferreira P.** 2007. Protein oxidation, repair mechanisms and proteolysis in *Saccharomyces cerevisiae*. IUBMB life **59:**293-298.
81. **Letoffe S, Redeker V, Wandersman C.** 1998. Isolation and characterization of an extracellular haem-binding protein from *Pseudomonas aeruginosa* that shares function and sequence similarities with the Serratia marcescens HasA haemophore. Molecular microbiology **28:**1223-1234.
82. **Ghigo JM, Letoffe S, Wandersman C.** 1997. A new type of hemophore-dependent heme acquisition system of *Serratia marcescens* reconstituted in *Escherichia coli*. Journal of bacteriology **179:**3572-3579.
83. **Letoffe S, Ghigo JM, Wandersman C.** 1994. Secretion of the *Serratia marcescens* HasA protein by an ABC transporter. Journal of bacteriology **176:**5372-5377.
84. **Wyckoff EE, Duncan D, Torres AG, Mills M, Maase K, Payne SM.** 1998. Structure of the *Shigella dysenteriae* haem transport locus and its phylogenetic distribution in enteric bacteria. Molecular microbiology **28:**1139-1152.
85. **Ochsner UA, Johnson Z, Vasil ML.** 2000. Genetics and regulation of two distinct haem-uptake systems, phu and has, in *Pseudomonas aeruginosa*. Microbiology **146 (Pt 1):**185-198.
86. **Tong Y, Guo M.** 2009. Bacterial heme-transport proteins and their heme-coordination modes. Archives of biochemistry and biophysics **481:**1-15.
87. **Ridley KA, Rock JD, Li Y, Ketley JM.** 2006. Heme utilization in *Campylobacter jejuni*. Journal of bacteriology **188:**7862-7875.
88. **Parkhill J, Wren BW, Mungall K, Ketley JM, Churcher C, Basham D, Chillingworth T, Davies RM, Feltwell T, Holroyd S, Jagels K, Karlyshev AV, Moule S, Pallen MJ, Penn CW, Quail MA, Rajandream MA, Rutherford KM, van Vliet AH, Whitehead S, Barrell BG.** 2000. The genome sequence of the food-borne pathogen *Campylobacter jejuni* reveals hypervariable sequences. Nature **403:**665-668.
89. **Flint A, Sun YQ, Stintzi A.** 2012. Cj1386 is an ankyrin-containing protein involved in heme trafficking to catalase in *Campylobacter jejuni*. Journal of bacteriology **194:**334-345.
90. **Kumar S, Bandyopadhyay U.** 2005. Free heme toxicity and its detoxification systems in human. Toxicology letters **157:**175-188.
91. **Li T, Bonkovsky HL, Guo JT.** 2011. Structural analysis of heme proteins: implications for design and prediction. BMC structural biology **11:**13.
92. **Schneider S, Marles-Wright J, Sharp KH, Paoli M.** 2007. Diversity and conservation of interactions for binding heme in b-type heme proteins. Natural product reports **24:**621-630.
93. **Balla J, Jacob HS, Balla G, Nath K, Eaton JW, Vercellotti GM.** 1993. Endothelial-cell heme uptake from heme proteins: induction of sensitization and desensitization to oxidant damage. Proceedings of the National Academy of Sciences of the United States of America **90:**9285-9289.

94. **Granick S, Sinclair P, Sassa S, Grieninger G.** 1975. Effects by heme, insulin, and serum albumin on heme and protein synthesis in chick embryo liver cells cultured in a chemically defined medium, and a spectrofluorometric assay for porphyrin composition. The Journal of biological chemistry **250:**9215-9225.
95. **Lansky IB, Lukat-Rodgers GS, Block D, Rodgers KR, Ratliff M, Wilks A.** 2006. The cytoplasmic heme-binding protein (PhuS) from the heme uptake system of *Pseudomonas aeruginosa* is an intracellular heme-trafficking protein to the delta-regioselective heme oxygenase. The Journal of biological chemistry **281:**13652-13662.
96. **Sanders C, Turkarslan S, Lee DW, Daldal F.** 2010. Cytochrome c biogenesis: the Ccm system. Trends in microbiology **18:**266-274.
97. **Travaglini-Allocatelli C.** 2013. Protein Machineries Involved in the Attachment of Heme to Cytochrome c: Protein Structures and Molecular Mechanisms. Scientifica **2013:**505714.
98. **San Francisco B, Kranz RG.** 2014. Interaction of holoCcmE with CcmF in heme trafficking and cytochrome c biosynthesis. Journal of molecular biology **426:**570-585.
99. **Palyada K, Sun YQ, Flint A, Butcher J, Naikare H, Stintzi A.** 2009. Characterization of the oxidative stress stimulon and PerR regulon of *Campylobacter jejuni*. BMC genomics **10:**481.
100. **Pesci EC, Cottle DL, Pickett CL.** 1994. Genetic, enzymatic, and pathogenic studies of the iron superoxide dismutase of *Campylobacter jejuni*. Infect. Immun. **62:**2687-2694.
101. **Day WA, Jr., Sajecki JL, Pitts TM, Joens LA.** 2000. Role of catalase in *Campylobacter jejuni* intracellular survival. Infect. Immun. **68:**6337-6345.
102. **van Vliet AH, Baillon MA, Penn CW, Ketley JM.** 2001. The iron-induced ferredoxin FdxA of *Campylobacter jejuni* is involved in aerotolerance. FEMS Microbiol. Lett. **196:**189-193.
103. **Atack JM, Harvey P, Jones MA, Kelly DJ.** 2008. The *Campylobacter jejuni* thiol peroxidases Tpx and Bcp both contribute to aerotolerance and peroxide-mediated stress resistance but have distinct substrate specificities. J. Bacteriol. **190:**5279-5290.
104. **Purdy D, Cawthraw S, Dickinson JH, Newell DG, Park SF.** 1999. Generation of a superoxide dismutase (SOD)-deficient mutant of *Campylobacter coli*: evidence for the significance of SOD in *Campylobacter* survival and colonization. Appl. Environ. Microbiol. **65:**2540-2546.
105. **Cosgrove K, Coutts G, Jonsson IM, Tarkowski A, Kokai-Kun JF, Mond JJ, Foster SJ.** 2007. Catalase (KatA) and alkyl hydroperoxide reductase (AhpC) have compensatory roles in peroxide stress resistance and are required for survival, persistence, and nasal colonization in *Staphylococcus aureus*. J. Bacteriol. **189:**1025-1035.
106. **Bsat N, Chen L, Helmann JD.** 1996. Mutation of the *Bacillus subtilis* alkyl hydroperoxide reductase (*ahpCF*) operon reveals compensatory interactions among hydrogen peroxide stress genes. J. Bacteriol. **178:**6579-6586.
107. **Charoenlap N, Eiamphungporn W, Chauvatcharin N, Utamapongchai S, Vattanaviboon P, Mongkolsuk S.** 2005. OxyR mediated compensatory expression between *ahpC* and *katA* and the significance of *ahpC* in protection from hydrogen peroxide in *Xanthomonas campestris*. FEMS Microbiol. Lett. **249:**73-78.
108. **Bingham-Ramos LK, Hendrixson DR.** 2008. Characterization of two putative cytochrome c peroxidases of *Campylobacter jejuni* involved in promoting commensal colonization of poultry. Infect. Immun. **76:**1105-1114.
109. **Stintzi A.** 2003. Gene expression profile of *Campylobacter jejuni* in response to growth temperature variation. J. Bacteriol. **185:**2009-2016.
110. **Harrison C.** 2003. GrpE, a nucleotide exchange factor for DnaK. Cell Stress Chaperones **8:**218–224.
111. **Ridley KA, Rock JD, Li Y, Ketley JM.** 2006. Heme utilization in *Campylobacter jejuni*. J. Bacteriol. **188:**7862-7875.

112. **Imlay JA.** 2008. Cellular defenses against superoxide and hydrogen peroxide. Annu. Rev. Biochem. **77:**755-776.
113. **Zeller T, Moskvin OV, Li K, Klug G, Gomelsky M.** 2005. Transcriptome and physiological responses to hydrogen peroxide of the facultatively phototrophic bacterium Rhodobacter sphaeroides. J. Bacteriol. **187:**7232-7242.
114. **Zheng M, Wang X, Templeton LJ, Smulski DR, LaRossa RA, Storz G.** 2001. DNA microarray-mediated transcriptional profiling of the *Escherichia coli* response to hydrogen peroxide. J. Bacteriol. **183:**4562-4570.
115. **Ochsner UA, Vasil ML, Alsabbagh E, Parvatiyar K, Hassett DJ.** 2000. Role of the *Pseudomonas aeruginosa* oxyR-recG operon in oxidative stress defense and DNA repair: OxyR-dependent regulation of katB-ankB, ahpB, and ahpC-ahpF. J. Bacteriol. **182:**4533-4544.
116. **Hassett DJ, Ma JF, Elkins JG, McDermott TR, Ochsner UA, West SE, Huang CT, Fredericks J, Burnett S, Stewart PS, McFeters G, Passador L, Iglewski BH.** 1999. Quorum sensing in *Pseudomonas aeruginosa* controls expression of catalase and superoxide dismutase genes and mediates biofilm susceptibility to hydrogen peroxide. Mol. Microbiol. **34:**1082-1093.
117. **Wang G, Alamuri P, Maier RJ.** 2006. The diverse antioxidant systems of *Helicobacter pylori*. Mol. Microbiol. **61:**847-860.
118. **Harris AG, Hinds FE, Beckhouse AG, Kolesnikow T, Hazell SL.** 2002. Resistance to hydrogen peroxide in *Helicobacter pylori*: role of catalase (KatA) and Fur, and functional analysis of a novel gene product designated 'KatA-associated protein', KapA (HP0874). Microbiology **148:**3813-3825.
119. **Ernst FD, Bereswill S, Waidner B, Stoof J, Mader U, Kusters JG, Kuipers EJ, Kist M, van Vliet AH, Homuth G.** 2005. Transcriptional profiling of *Helicobacter pylori* Fur- and iron-regulated gene expression. Microbiology **151:**533-546.
120. **Ernst FD, Homuth G, Stoof J, Mader U, Waidner B, Kuipers EJ, Kist M, Kusters JG, Bereswill S, van Vliet AH.** 2005. Iron-responsive regulation of the *Helicobacter pylori* iron-cofactored superoxide dismutase SodB is mediated by Fur. J. Bacteriol. **187:**3687-3692.
121. **Palyada K, Threadgill D, Stintzi A.** 2004. Iron acquisition and regulation in *Campylobacter jejuni*. J. Bacteriol. **186:**4714-4729.
122. 2011. Vital signs: incidence and trends of infection with pathogens transmitted commonly through food--foodborne diseases active surveillance network, 10 U.S. sites, 1996-2010. MMWR Morb Mortal Wkly Rep **60:**749-755.
123. **Nachamkin I.** 2002. Chronic effects of *Campylobacter* infection. Microbes Infect **4:**399-403.
124. **Atack JM, Harvey P, Jones MA, Kelly DJ.** 2008. The *Campylobacter jejuni* thiol peroxidases Tpx and Bcp both contribute to aerotolerance and peroxide-mediated stress resistance but have distinct substrate specificities. Journal of bacteriology **190:**5279-5290.
125. **Baillon ML, van Vliet AH, Ketley JM, Constantinidou C, Penn CW.** 1999. An iron-regulated alkyl hydroperoxide reductase (AhpC) confers aerotolerance and oxidative stress resistance to the microaerophilic pathogen *Campylobacter jejuni*. Journal of bacteriology **181:**4798-4804.
126. **Pesci EC, Cottle DL, Pickett CL.** 1994. Genetic, enzymatic, and pathogenic studies of the iron superoxide dismutase of *Campylobacter jejuni*. Infection and immunity **62:**2687-2694.
127. **van Vliet AH, Baillon ML, Penn CW, Ketley JM.** 1999. *Campylobacter jejuni* contains two fur homologs: characterization of iron-responsive regulation of peroxide stress defense genes by the PerR repressor. Journal of bacteriology **181:**6371-6376.
128. **Palyada K, Threadgill D, Stintzi A.** 2004. Iron acquisition and regulation in *Campylobacter jejuni*. J Bacteriol **186:**4714-4729.
129. **Lee JW, Helmann JD.** 2006. The PerR transcription factor senses H_2O_2 by metal-catalysed histidine oxidation. Nature **440:**363-367.

130. **Stahl M, Stintzi A.** 2011. Identification of essential genes in *C. jejuni* genome highlights hyper-variable plasticity regions. Functional & integrative genomics **11:**241-257.
131. **Sommerlad SM, Hendrixson DR.** 2007. Analysis of the roles of FlgP and FlgQ in flagellar motility of *Campylobacter jejuni*. J Bacteriol **189:**179-186.
132. **Parkhill J, Wren BW, Mungall K, Ketley JM, Churcher C, Basham D, Chillingworth T, Davies RM, Feltwell T, Holroyd S, Jagels K, Karlyshev AV, Moule S, Pallen MJ, Penn CW, Quail MA, Rajandream M-A, Rutherford KM, Vliet AHMv, Whitehead S, Barrell BG.** 2000. The genome sequence of the food-borne pathogen *Campylobacter jejuni* reveals hypervariable sequences. Nature **403:**665-668.
133. **Terashima H, Kojima S, Homma M.** 2008. Flagellar motility in bacteria structure and function of flagellar motor. International review of cell and molecular biology **270:**39-85.
134. **Mertins S, Allan BJ, Townsend HG, Koster W, Potter AA.** 2013. Role of *motAB* in adherence and internalization in polarized Caco-2 cells and in cecal colonization of *Campylobacter jejuni*. Avian Dis **57:**116-122.
135. **Musatov A, Robinson NC.** 2012. Susceptibility of mitochondrial electron-transport complexes to oxidative damage. Focus on cytochrome c oxidase. Free radical research **46:**1313-1326.
136. **Lambeth JD.** 2007. Nox enzymes, ROS, and chronic disease: an example of antagonistic pleiotropy. Free radical biology & medicine **43:**332-347.
137. **Grant KA, Park SF.** 1995. Molecular characterization of *katA* from *Campylobacter jejuni* and generation of a catalase-deficient mutant of *Campylobacter coli* by interspecific allelic exchange. Microbiology **141 (Pt 6):**1369-1376.
138. **Atack JM, Kelly DJ.** 2008. Contribution of the stereospecific methionine sulphoxide reductases MsrA and MsrB to oxidative and nitrosative stress resistance in the food-borne pathogen *Campylobacter jejuni*. Microbiology **154:**2219-2230.
139. **Ishikawa T, Mizunoe Y, Kawabata S, Takade A, Harada M, Wai SN, Yoshida S.** 2003. The iron-binding protein Dps confers hydrogen peroxide stress resistance to *Campylobacter jejuni*. J Bacteriol **185:**1010-1017.
140. **Yamasaki M, Igimi S, Katayama Y, Yamamoto S, Amano F.** 2004. Identification of an oxidative stress-sensitive protein from *Campylobacter jejuni*, homologous to rubredoxin oxidoreductase/rubrerythrin. FEMS Microbiol Lett **235:**57-63.
141. **Bingham-Ramos LK, Hendrixson DR.** 2008. Characterization of two putative cytochrome c peroxidases of *Campylobacter jejuni* involved in promoting commensal colonization of poultry. Infect Immun **76:**1105-1114.
142. **Chan AC, Lelj-Garolla B, F IR, Pedersen KA, Mauk AG, Murphy ME.** 2006. Cofacial heme binding is linked to dimerization by a bacterial heme transport protein. Journal of molecular biology **362:**1108-1119.
143. **Tang Y, Quail MA, Artymiuk PJ, Guest JR, Green J.** 2002. *Escherichia coli* aconitases and oxidative stress: post-transcriptional regulation of *sodA* expression. Microbiology **148:**1027-1037.
144. **Price-Carter M, Fazzio TG, Vallbona EI, Roth JR.** 2005. Polyphosphate kinase protects *Salmonella enterica* from weak organic acid stress. J Bacteriol **187:**3088-3099.
145. **Rao NN, Kornberg A.** 1996. Inorganic polyphosphate supports resistance and survival of stationary-phase *Escherichia coli*. J Bacteriol **178:**1394-1400.
146. **Rashid MH, Rao NN, Kornberg A.** 2000. Inorganic polyphosphate is required for motility of bacterial pathogens. J Bacteriol **182:**225-227.
147. **Rashid MH, Rumbaugh K, Passador L, Davies DG, Hamood AN, Iglewski BH, Kornberg A.** 2000. Polyphosphate kinase is essential for biofilm development, quorum sensing, and virulence of *Pseudomonas aeruginosa*. Proc Natl Acad Sci U S A **97:**9636-9641.

148. **Tan S, Fraley CD, Zhang M, Dailidiene D, Kornberg A, Berg DE.** 2005. Diverse phenotypes resulting from polyphosphate kinase gene (ppk1) inactivation in different strains of *Helicobacter pylori*. J Bacteriol **187:**7687-7695.
149. **Jahid IK, Silva AJ, Benitez JA.** 2006. Polyphosphate stores enhance the ability of *Vibrio cholerae* to overcome environmental stresses in a low-phosphate environment. Appl Environ Microbiol **72:**7043-7049.
150. **Kim KS, Rao NN, Fraley CD, Kornberg A.** 2002. Inorganic polyphosphate is essential for long-term survival and virulence factors in *Shigella* and *Salmonella* spp. Proc Natl Acad Sci U S A **99:**7675-7680.
151. **Blaser MJ.** 1997. Epidemiologic and clinical features of *Campylobacter jejuni* infections. J Infect Dis **176 Suppl 2:**S103-105.
152. **Black RE, Levine MM, Clements ML, Hughes TP, Blaser MJ.** 1988. Experimental *Campylobacter jejuni* infection in humans. J Infect Dis **157:**472-479.
153. **Dasti JI, Tareen AM, Lugert R, Zautner AE, Gross U.** *Campylobacter jejuni*: a brief overview on pathogenicity-associated factors and disease-mediating mechanisms. Int J Med Microbiol **300:**205-211.
154. **Smith MA, Finel M, Korolik V, Mendz GL.** 2000. Characteristics of the aerobic respiratory chains of the microaerophiles *Campylobacter jejuni* and *Helicobacter pylori*. Arch Microbiol **174:**1-10.
155. **Farr SB, Kogoma T.** 1991. Oxidative stress responses in *Escherichia coli* and *Salmonella typhimurium*. Microbiol Rev **55:**561-585.
156. **Yao R, Alm RA, Trust TJ, Guerry P.** 1993. Construction of new *Campylobacter* cloning vectors and a new mutational *cat* cassette. Gene **130:**127-130.
157. **Sheffield P, Garrard S, Derewenda Z.** 1999. Overcoming expression and purification problems of RhoGDI using a family of "parallel" expression vectors. Protein Expr Purif **15:**34-39.
158. **Wang Y, Taylor DE.** 1990. Natural transformation in *Campylobacter* species. J Bacteriol **172:**949-955.
159. **Woodbury W, Spencer AK, Stahman MA.** 1971. An improved procedure using ferricyanide for detecting catalase isozymes. Anal Biochem **44:**301-305.
160. **Beers RF, Jr., Sizer IW.** 1952. A spectrophotometric method for measuring the breakdown of hydrogen peroxide by catalase. J Biol Chem **195:**133-140.
161. **Bernstein JA, Khodursky AB, Lin PH, Lin-Chao S, Cohen SN.** 2002. Global analysis of mRNA decay and abundance in *Escherichia coli* at single-gene resolution using two-color fluorescent DNA microarrays. Proc Natl Acad Sci U S A **99:**9697-9702.
162. **Tao H, Bausch C, Richmond C, Blattner FR, Conway T.** 1999. Functional genomics: expression analysis of *Escherichia coli* growing on minimal and rich media. J Bacteriol **181:**6425-6440.
163. **Antrobus R, Borner GH.** Improved elution conditions for native co-immunoprecipitation. PLoS One **6:**e18218.
164. **Naikare H, Palyada K, Panciera R, Marlow D, Stintzi A.** 2006. Major role for FeoB in *Campylobacter jejuni* ferrous iron acquisition, gut colonization, and intracellular survival. Infect Immun **74:**5433-5444.
165. **Holmes K, Mulholland F, Pearson BM, Pin C, McNicholl-Kennedy J, Ketley JM, Wells JM.** 2005. *Campylobacter jejuni* gene expression in response to iron limitation and the role of Fur. Microbiology **151:**243-257.
166. **Howell ML, Alsabbagh E, Ma JF, Ochsner UA, Klotz MG, Beveridge TJ, Blumenthal KM, Niederhoffer EC, Morris RE, Needham D, Dean GE, Wani MA, Hassett DJ.** 2000. AnkB, a periplasmic ankyrin-like protein in *Pseudomonas aeruginosa*, is required for optimal catalase B (KatB) activity and resistance to hydrogen peroxide. J Bacteriol **182:**4545-4556.

167. **Rajashekara G, Drozd M, Gangaiah D, Jeon B, Liu Z, Zhang Q.** 2009. Functional characterization of the twin-arginine translocation system in *Campylobacter jejuni*. Foodborne Pathog Dis **6:**935-945.
168. **Bendtsen JD, Nielsen H, von Heijne G, Brunak S.** 2004. Improved prediction of signal peptides: SignalP 3.0. J Mol Biol **340:**783-795.
169. **Harris AG, Hazell SL.** 2003. Localisation of *Helicobacter pylori* catalase in both the periplasm and cytoplasm, and its dependence on the twin-arginine target protein, KapA, for activity. FEMS Microbiol Lett **229:**283-289.
170. **Yumoto I, Ichihashi D, Iwata H, Istokovics A, Ichise N, Matsuyama H, Okuyama H, Kawasaki K.** 2000. Purification and characterization of a catalase from the facultatively psychrophilic bacterium *Vibrio rumoiensis* S-1(T) exhibiting high catalase activity. J Bacteriol **182:**1903-1909.
171. **Brown SM, Howell ML, Vasil ML, Anderson AJ, Hassett DJ.** 1995. Cloning and characterization of the katB gene of *Pseudomonas aeruginosa* encoding a hydrogen peroxide-inducible catalase: purification of KatB, cellular localization, and demonstration that it is essential for optimal resistance to hydrogen peroxide. J Bacteriol **177:**6536-6544.
172. **Klotz MG, Kim YC, Katsuwon J, Anderson AJ.** 1995. Cloning, characterization and phenotypic expression in *Escherichia coli* of *catF*, which encodes the catalytic subunit of catalase isozyme CatF of *Pseudomonas syringae*. Appl Microbiol Biotechnol **43:**656-666.
173. **Schnell S, Steinman HM.** 1995. Function and stationary-phase induction of periplasmic copper-zinc superoxide dismutase and catalase/peroxidase in *Caulobacter crescentus*. J Bacteriol **177:**5924-5929.
174. **Ascoli F, Fanelli MR, Antonini E.** 1981. Preparation and properties of apohemoglobin and reconstituted hemoglobins. Methods Enzymol **76:**72-87.
175. **Vatsyayan P, Goswami P.** Acidic pH conditions induce dissociation of the haem from the protein and destabilise the catalase isolated from *Aspergillus terreus*. Biotechnol Lett **33:**347-351.
176. **Babakhani FK, Bradley GA, Joens LA.** 1993. Newborn piglet model for campylobacteriosis. Infect Immun **61:**3466-3475.
177. **Bennett V.** 1992. Ankyrins. Adaptors between diverse plasma membrane proteins and the cytoplasm. J Biol Chem **267:**8703-8706.
178. **Prakash K, Prajapati S, Ahmad A, Jain SK, Bhakuni V.** 2002. Unique oligomeric intermediates of bovine liver catalase. Protein Sci **11:**46-57.
179. **Hitchcock A, Hall SJ, Myers JD, Mulholland F, Jones MA, Kelly DJ.** Roles of the twin-arginine translocase and associated chaperones in the biogenesis of the electron transport chains of the human pathogen *Campylobacter jejuni*. Microbiology **156:**2994-3010.
180. **von Heijne G.** 1992. Membrane protein structure prediction. Hydrophobicity analysis and the positive-inside rule. J Mol Biol **225:**487-494.
181. **Harris AG, Wilson JE, Danon SJ, Dixon MF, Donegan K, Hazell SL.** 2003. Catalase (KatA) and KatA-associated protein (KapA) are essential to persistent colonization in the *Helicobacter pylori* SS1 mouse model. Microbiology **149:**665-672.
182. **Zamocky M, Furtmuller PG, Obinger C.** 2008. Evolution of catalases from bacteria to humans. Antioxid Redox Signal **10:**1527-1548.
183. **Baureder M, Hederstedt L.** 2012. Genes important for catalase activity in *Enterococcus faecalis*. PloS one **7:**e36725.
184. **Kobayashi C, Suga Y, Yamamoto K, Yomo T, Ogasahara K, Yutani K, Urabe I.** 1997. Thermal conversion from low- to high-activity forms of catalase I from *Bacillus stearothermophilus*. J Biol Chem **272:**23011-23016.

185. **Altschul SF, Madden TL, Schaffer AA, Zhang J, Zhang Z, Miller W, Lipman DJ.** 1997. Gapped BLAST and PSI-BLAST: a new generation of protein database search programs. Nucleic Acids Res **25:**3389-3402.
186. **Sievers F, Wilm A, Dineen D, Gibson TJ, Karplus K, Li W, Lopez R, McWilliam H, Remmert M, Soding J, Thompson JD, Higgins DG.** 2011. Fast, scalable generation of high-quality protein multiple sequence alignments using Clustal Omega. Molecular systems biology **7:**539.
187. **Goujon M, McWilliam H, Li W, Valentin F, Squizzato S, Paern J, Lopez R.** 2010. A new bioinformatics analysis tools framework at EMBL-EBI. Nucleic Acids Res **38:**W695-699.
188. **Waterhouse AM, Procter JB, Martin DM, Clamp M, Barton GJ.** 2009. Jalview Version 2--a multiple sequence alignment editor and analysis workbench. Bioinformatics **25:**1189-1191.
189. **Butcher J, Sarvan S, Brunzelle JS, Couture JF, Stintzi A.** 2012. Structure and regulon of *Campylobacter jejuni* ferric uptake regulator Fur define apo-Fur regulation. Proceedings of the National Academy of Sciences of the United States of America **109:**10047-10052.
190. **Lykkegaard MK, Ehlerding A, Hvelplund P, Kadhane U, Kirketerp MB, Nielsen SB, Panja S, Wyer JA, Zettergren H.** 2008. A Soret marker band for four-coordinate ferric heme proteins from absorption spectra of isolated Fe(III)-Heme+ and Fe(III)-Heme+(His) ions in vacuo. Journal of the American Chemical Society **130:**11856-11857.
191. **Rao F, Ji Q, Soehano I, Liang ZX.** 2011. Unusual heme-binding PAS domain from YybT family proteins. Journal of bacteriology **193:**1543-1551.
192. **Smulevich G, Neri F, Marzocchi MP, Welinder KG.** 1996. Versatility of heme coordination demonstrated in a fungal peroxidase. Absorption and resonance Raman studies of *Coprinus cinereus* peroxidase and the Asp245-->Asn mutant at various pH values. Biochemistry **35:**10576-10585.
193. **Bhakta MN, Wilks A.** 2006. The mechanism of heme transfer from the cytoplasmic heme binding protein PhuS to the delta-regioselective heme oxygenase of *Pseudomonas aeruginosa*. Biochemistry **45:**11642-11649.
194. **Pellicer S, Gonzalez A, Peleato ML, Martinez JI, Fillat MF, Bes MT.** 2012. Site-directed mutagenesis and spectral studies suggest a putative role of FurA from *Anabaena* sp. PCC 7120 as a heme sensor protein. The FEBS journal **279:**2231-2246.
195. **Gattoni M, Boffi A, Sarti P, Chiancone E.** 1996. Stability of the heme-globin linkage in alphabeta dimers and isolated chains of human hemoglobin. A study of the heme transfer reaction from the immobilized proteins to albumin. J Biol Chem **271:**10130-10136.
196. **Hargrove MS, Barrick D, Olson JS.** 1996. The association rate constant for heme binding to globin is independent of protein structure. Biochemistry **35:**11293-11299.
197. **Alyamani EJ, Brandt P, Pena JA, Major AM, Fox JG, Suerbaum S, Versalovic J.** 2007. *Helicobacter hepaticus* catalase shares surface-predicted epitopes with mammalian catalases. Microbiology **153:**1006-1016.
198. **Dufour V, Li J, Flint A, Rosenfeld E, Rivoal K, Georgeault S, Alazzam B, Ermel G, Stintzi A, Bonnaure-Mallet M, Baysse C.** 2013. Inactivation of the LysR regulator Cj1000 of *Campylobacter jejuni* affects host colonization and respiration. Microbiology **159:**1165-1178.
199. **Hwang S, Zhang Q, Ryu S, Jeon B.** 2012. Transcriptional regulation of the CmeABC multidrug efflux pump and the KatA catalase by CosR in *Campylobacter jejuni*. Journal of bacteriology **194:**6883-6891.
200. **Harvat EM, Redfield C, Stevens JM, Ferguson SJ.** 2009. Probing the heme-binding site of the cytochrome c maturation protein CcmE. Biochemistry **48:**1820-1828.
201. **Block DR, Lukat-Rodgers GS, Rodgers KR, Wilks A, Bhakta MN, Lansky IB.** 2007. Identification of two heme-binding sites in the cytoplasmic heme-trafficking protein PhuS from *Pseudomonas aeruginosa* and their relevance to function. Biochemistry **46:**14391-14402.

202. **Bourke B, Chan VL, Sherman P.** 1998. *Campylobacter* upsaliensis: waiting in the wings. Clinical microbiology reviews **11:**440-449.
203. **Lawson AJ, On SL, Logan JM, Stanley J.** 2001. *Campylobacter hominis* sp. nov., from the human gastrointestinal tract. International journal of systematic and evolutionary microbiology **51:**651-660.
204. **Papp-Szabo E, Sutherland CL, Josephy PD.** 1993. Superoxide dismutase and the resistance of *Escherichia coli* to phagocytic killing by human neutrophils. Infection and immunity **61:**1442-1446.
205. **Tinajero-Trejo M, Shepherd M.** 2013. The globins of *Campylobacter jejuni*. Advances in microbial physiology **63:**97-145.
206. **Naikare H, Butcher J, Flint A, Xu J, Raymond K, Stintzi A.** 2013. *C. jejuni* ferric-enterobactin receptor CfrA is TonB3 dependent and mediates iron acquisition from structurally diverse catechol siderophores. Metallomics **Submitted**.
207. **Stintzi A, Marlow D, Palyada K, Naikare H, Panciera R, Whitworth L, Clarke C.** 2005. Use of genome-wide expression profiling and mutagenesis to study the intestinal lifestyle of *Campylobacter jejuni*. Infect Immun **73:**1797-1810.

CHAPTER 5. SUPPLEMENTARY MATERIALS

5.1. SUPPLEMENTARY FIGURES

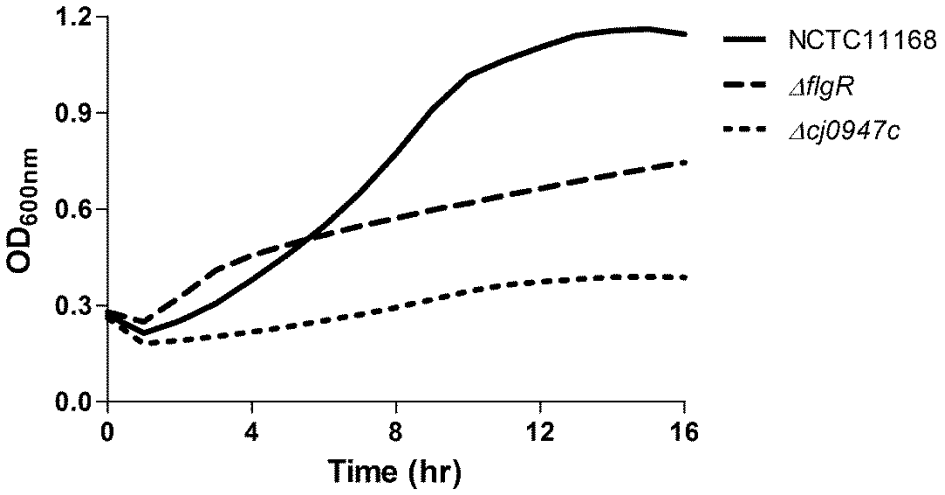

Fig S1. Growth of *C. jejuni* NCTC11168, Δ*flgR*, and Δ*cj0947c* in MH media over 16 hours. OD_{600nm} readings were taken every 15 min using a 96 well plate reader with continual shaking at 37 °C.

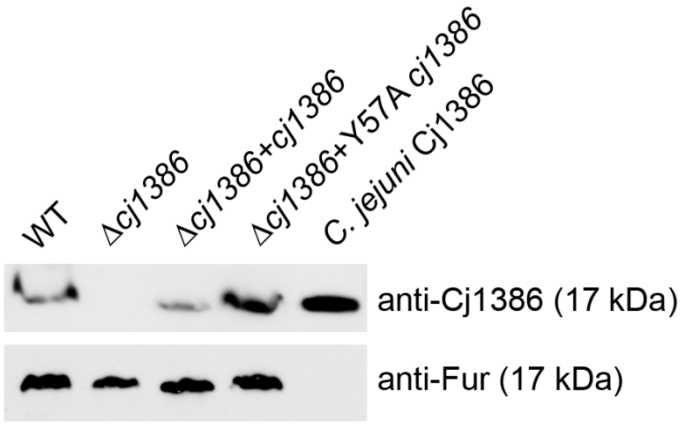

Fig S2. Y57A Cj1386 protein is expressed in the Δ*cj1386+cj1386*^{Y57A} *C. jejuni* mutant construct at levels comparable to Cj1386^{WT} expression. Bacterial cultures were grown in MEMα media at 37°C under microaerophilic conditions. Bacterial cultures were pelleted, resuspended in PBS + protease inhibitor and soluble proteins were extracted following sonication. Two hundred and forty micrograms of lysates or 100 ng of purified Cj1386 were separated by SDS PAGE on a 14% polyacrylamide gel followed by immunoblotting. (Upper) Wild-type (WT), Δ*cj1386,* Δ*cj1386+cj1386*^{WT} and Δ*cj1386+cj1386*^{Y57A} lysates and Cj1386 protein was detected using an anti-Cj1386 antiserum. (Bottom) Loading control of total protein contents as detected by an anti-Fur antiserum.

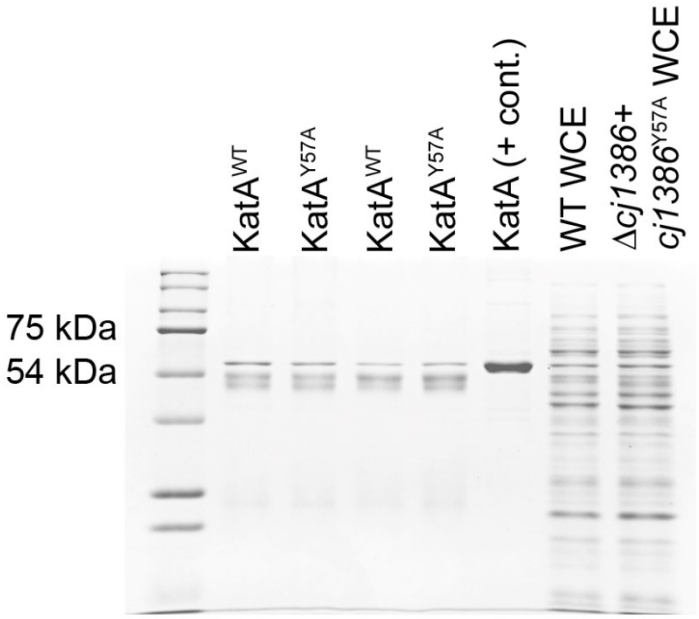

Fig S3. Immunoprecipitation of KatA from wild type and Δ*cj1386+cj1386*^{Y57A} *C. jejuni* strains. KatA was immunoprecipitated from prepared wild type and Δ*cj1386+cj1386*^{Y57A} whole cell extracts and eluted in 50 mM glycine, pH 2.8. Four microlitres of each immunoprecipitated sample, 1 µg of purified KatA, and 5 µg of whole cell extract were separated on a 10% SDS-PAGE gel and visualized by coomassie staining.

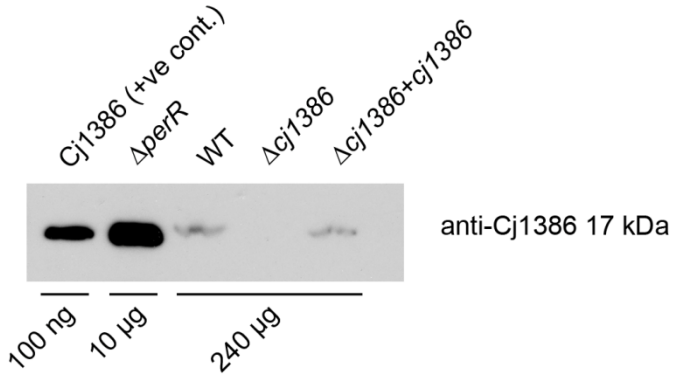

Fig S4. Cj1386 is expressed at low levels in wild-type *C.jejuni*. Bacterial cultures were grown in MEMα media at 37°C under microaerophilic conditions. Bacterial cultures were pelleted, resuspended in PBS + protease inhibitor and soluble proteins were extracted following sonication. Two hundred and forty micrograms of wild-type, Δ*cj1386*, and Δ*cj1386*+*cj1386* lysate, 10 µg of Δ*perR* lysate, and 100 ng of purified Cj1386 protein were separated by SDS PAGE on a 14% polyacrylamide gel. Proteins were visualized by Western blotting using an anti-Cj1386 antibody.

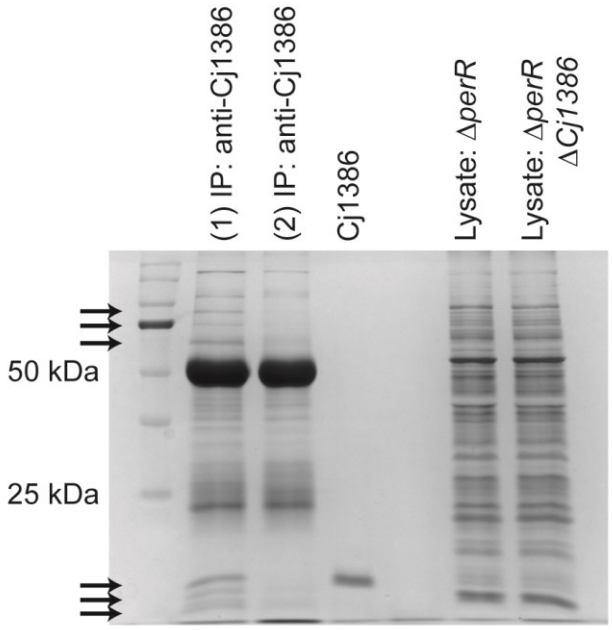

Fig S5. Co-immunoprecipitation of Cj1386 reveals additional interacting proteins. Co-immunoprecipitation of Cj1386 from cross-linked *ΔperR* protein lysate was performed using an anti-Cj1386 antibody (lane 1). Co-immunoprecipitation of Cj1386 from cross-linked *ΔperRΔcj1386* protein lysates was performed using an anti-Cj1386 antibody as a negative control (lane 2). Immunopreciptated protein samples were separated by SDS PAGE followed Coomassie straining. Purified Cj1386 protein was run as positive control. Ten micrograms of *Δper* and *ΔperRΔcj1386* protein lysate were used to demonstrate equal amounts of input lysate for the Co-IP. Arrows represent proteins uniquely immunoprecipitated from the *ΔperR* strain but absent in the negative control. IP: immunoprecipitation.

5.2. SUPPLEMENTARY TABLES

TABLE S1. Bacterial strains and plasmids used in this study.

Strains or Plasmids	Genotype[a]	Source
E.coli		
K12	*endA1, hsdR17*(r_{K12}-, m_{K12+}), *supE44, thi-1, recA1, gyrA96, relA1, lacF'*[*proA*$^+$*B*$^+$, *lacI*^{q}*ZDM15*::tn10(tet^R)]	Clontech
DH5α	*endA1 hsdR17* (r_K^- m_K^-) *supE44 thi-1 recA1 gyrA relA1 Δ(lacZYA-argF)U169 deoR [ϕ80dlac Δ(lacZ ΔM15)*]	Invitrogen
C. jejuni		
AS144	*C. jejuni* NCTC 11168	National Collection of Type Cultures
AS27	AS144 Δ*tonB1*::cam^R	(206)
AS211	AS144 ΔCj0178::cam^R	(128)
AS240	AS144 Δ*tonB2*::cam^R	(206)
AS241	AS144 Δ*tonB1+tonB2*::cam^{R}kan^R	(206)
AS242	AS144 Δ*tonB2+tonB3*::cam^{R}kan^R	(206)
AS256	AS144 Δ*p19*::cam^R	This study
AS260	AS144 ΔCj1658::cam^R	This study
AS265	AS144 Δ*ceuE*::cam^R	(128)
AS269	AS144 Δ*cfrA*::cam^R	(128)
AS287	AS144 Δ*spoT*::cam^R	(207)
AS335	AS144 Δ*chuA*::cam^R	(87)
AS450	AS144 Δ*p19+Δ*Cj1658::cam^R	This study
AS498	AS144 Δ*acs*::cam^R	This study
AS735	AS144 Δ*truB*::cam^R	This study
AS736	AS144 ΔCj1340c::cam^R	This study
AS737	AS144 Δ*ald*::cam^R	This study
AS738	AS144 ΔCj1341c::cam^R	This study
AS739	AS144 ΔCj0020c::cam^R	This study
AS740	AS144 ΔCj0358::cam^R	This study
AS741	AS144 Δ*mdaB*::cam^R	This study
AS742	AS144 ΔCj1026c::cam^R	This study
AS743	AS144 Δ*ccoQ*::cam^R	This study
AS745	AS144 ΔCj1167::cam^R	This study
AS746	AS144 Δ*pstC*::cam^R	This study
AS747	AS144 ΔCj0073c::cam^R	This study
AS748	AS144 ΔCj0818::cam^R	This study
AS749	AS144 ΔCj1613c::cam^R	This study
AS750	AS144 ΔCj1663::cam^R	This study
AS751	AS144 Δ*flgR*::cam^R	This study
AS752	AS144 ΔCj1377c::cam^R	This study
AS753	AS144 Δ*exbD1*::cam^R	This study
AS754	AS144 ΔCj0045c::cam^R	This study

AS755	AS144 ΔCj0202c::cam^R	This study
AS756	AS144 ΔCj0385c::cam^R	This study
AS757	AS144 Δ*flgH*::cam^R	This study
AS758	AS144 Δ*cfbpB*::cam^R	This study
AS759	AS144 ΔCj1335::cam^R	This study
AS760	AS144 ΔCj1036c::cam^R	This study
AS761	AS144 Δ*flhB*::cam^R	This study
AS762	AS144 Δ*cfbpA*::cam^R	This study
AS763	AS144 ΔCj0040::cam^R	This study
AS764	AS144 Δ*flgD*::cam^R	This study
AS765	AS144 Δ*flgK*::cam^R	This study
AS766	AS144 ΔCj0041::cam^R	This study
AS767	AS144 ΔCj0416::cam^R	This study
AS768	AS144 Δ*flgE*::cam^R	This study
AS769	AS144 ΔCj1342c::cam^R	This study
AS772	AS144 Δ*ceuB*::cam^R	This study
AS773	AS144 ΔCj0494::cam^R	This study
AS774	AS144 Δ*trpF*::cam^R	This study
AS775	AS144 ΔCj1241::cam^R	This study
AS776	AS144 ΔCj0295::cam^R	This study
AS777	AS144 ΔCj0524::cam^R	This study
AS778	AS144 Δ*chuB*::cam^R	This study
AS778	AS144 ΔCj0741::cam^R	This study
AS779	AS144 ΔCj1661::cam^R	This study
AS780	AS144 ΔCj0148c::cam^R	This study
AS781	AS144 ΔCj0554::cam^R	This study
AS782	AS144 ΔCj0561::cam^R	This study
AS783	AS144 ΔCj1406c::cam^R	This study
AS784	AS144 ΔCj0587::cam^R	This study
AS785	AS144 ΔCj0819::cam^R	This study
AS786	AS144 Δ*flgM*::cam^R	This study
AS787	AS144 ΔCj0672::cam^R	This study
AS789	AS144 ΔCj1209::cam^R	This study
AS790	AS144 ΔCj1356c::cam^R	This study
AS791	AS144 ΔCj0786::cam^R	This study
AS792	AS144 ΔCj0949c::cam^R	This study
AS793	AS144 ΔCj1211::cam^R	This study
AS794	AS144 ΔCj0814::cam^R	This study
AS795	AS144 ΔCj1242::cam^R	This study
AS796	AS144 ΔCj1623::cam^R	This study
AS797	AS144 Δ*flgG*::cam^R	This study
AS798	AS144 Δ*exbB2*::cam^R	This study
AS799	AS144 ΔCj0634::cam^R	This study
AS800	AS144 Δ*cfbpC*::cam^R	This study
AS801	AS144 Δ*hypC*::cam^R	This study
AS802	AS144 ΔCj0260c::cam^R	This study
AS803	AS144 Δ*flgI*::cam^R	This study
AS804	AS144 Δ*chuD*::cam^R	This study

AS805	AS144 Δ*exbB1*::cam^R	This study
AS806	AS144 ΔCj1207c::cam^R	This study
AS807	AS144 Δ*flgE2*::cam^R	This study
AS808	AS144 ΔCj0062c::cam^R	This study
AS809	AS144 Δ*chaN*::cam^R	This study
AS830	AS144 Δ*flaG*::cam^R	This study
AS831	AS144 Δ*flgG2*::cam^R	This study
AS832	AS144 ΔCj0309c::cam^R	This study
AS833	AS144 ΔCj1388::cam^R	This study
AS940	AS144 Δ*cmeA*::cam^R	This study
AS941	AS144 ΔCj1255::cam^R	This study
AS943	AS144 ΔCj0253::cam^R	This study
AS959	AS144 Δ*chuC*::cam^R	This study
AS961	AS786 + *flgM*::cam^{R}kan^R	This study
AS962	AS808 + Cj0062c::cam^{R}kan^R	This study
AS963	AS809 + c*haN*::cam^{R}kan^R	This study
AS964	AS747 + Cj0073c::cam^{R}kan^R	This study
AS965	AS794 + Cj0814::cam^{R}kan^R	This study
AS966	AS796 + Cj1623::cam^{R}kan^R	This study
AS967	AS742 + Cj1026c::cam^{R}kan^R	This study
AS968	AS774 + *trpF*::cam^{R}kan^R	This study
AS970	AS803 + *flgI*::cam^{R}kan^R	This study
AS971	AS802 + Cj0260c::cam^{R}kan^R	This study
AS972	AS760 + Cj1036c::cam^{R}kan^R	This study
AS973	AS757 + *flgH*::cam^{R}kan^R	This study
AS974	AS144 ΔCj0171::cam^R	This study
AS975	AS746 + *pstC*::cam^{R}kan^R	This study
AS976	AS805 + *exbB1*::cam^{R}kan^R	This study
AS977	AS766 + Cj0041::cam^{R}kan^R	This study
AS979	AS764 + *flgE*::cam^{R}kan^R	This study
AS980	AS765 + Δ*flgK*::cam^{R}kan^R	This study
AS981	AS752 + Cj1377c::cam^{R}kan^R	This study
AS982	AS751 + *flgR*::cam^{R}kan^R	This study
AS983	AS761 + *flhB*::cam^{R}kan^R	This study
AS984	AS740 + Cj0358::cam^{R}kan^R	This study
AS991	AS755 + Cj0202c::cam^{R}kan^R	This study
AS992	AS764 + *flgD*::cam^{R}kan^R	This study
AS993	AS798 + *exbB2*::cam^{R}kan^R	This study
AS1014	AS498 + *acs*::cam^{R}kan^R	This study
AS1030	AS144 ΔCj0977::cam^R	This study
AS1060	AS144 ΔCj1383c::cam^R	This study
AS1061	AS144 ΔCj0344::cam^R	This study
AS1062	AS144 Δ*flgL*::cam^R	This study
AS1063	AS144 ΔCj1159c::cam^R	This study
AS1064	AS144 Δ*folP*::cam^R	This study
AS1065	AS144 Δ*exbD2*::cam^R	This study
AS1066	AS144 ΔCj0947c::cam^R	This study
AS1067	AS144 *ΔpseB*::cam^R	This study

AS1068	AS144 ΔCj0900c::cam^R	This study
AS1071	AS144 *Δrrc*::cam^R	This study
AS1123	AS1060 + Cj1383c::cam^{R}kan^R	This study
AS1124	AS1061 + Cj0344::cam^{R}kan^R	This study
AS1125	AS1066 + Cj0947c::cam^{R}kan^R	This study
AS1126	AS1071 + *rrc*::cam^{R}kan^R	This study
AS1127	AS1131 + *acnB*::cam^{R}kan^R	This study
AS1128	AS1062 + *flgL*::cam^{R}kan^R	This study
AS1129	AS1067 + *pseB*::cam^{R}kan^R	This study
AS1131	AS144 Δ*acnB*::cam^R	This study
AS1132	AS144 Δ*tonB3*::cam^R	(206)
AS1133	AS1132 + *tonB3*::cam^{R}kan^R	(206)
Plasmids		
pRY111	Cam^R resistance gene	Yao (156)
pRRK	Cloning vector used for complementation of mutants, kan^R	Reid (22)
pUC19	Cloning vector, amp^R	Biolabs

[a-] cam^R, chloamphenicol resistance gene, kan^R, kanamycin resistance gene, amp^R, ampicillin resistance gene.

TABLE S2. Primers used in this study.

Primer Name	Primer Sequence (5'- 3')[a]
acs_AS	CGACTCTAGAGGATCCTCCACGCCCTGTGACAAATCC
acs_AS_inverse	GAACACCGCCGAGCAGCTCATTAGGTGCATCAGCA
acs_SE	CGGTACCCGGGGATCCAACGGCTGATGGTGCTTTTCG
acs_SE_inverse	GAACTAAAGGGCGCAGGCGAGTCATTGTTTGCTTT
ald_AS	CGACTCTAGAGGATCCCCATCAGCTCCGCCTATGC
ald_AS_inverse	GAACACCGCCGAGCATAAAGCAGGTGCCATCTTCC
ald_SE	CGGTACCCGGGGATCCATGGCAAGAGATGAAAGCACAC
ald_SE_inverse	GAACTAAAGGGCGCAAGTGTGCAAAGATGCGGATA
ccoQ_AS	CGACTCTAGAGGATCCCATGACAAGCCGAACACTGAAC
ccoQ_AS_inverse	GAACACCGCCGAGCACAAAAACATCACGAGTGCAAA
ccoQ_SE	CGGTACCCGGGGATCCGGACCTGATCTTGCTCGTGTAG
ccoQ_SE_inverse	GAACTAAAGGGCGCATGCAAACCTTGCCTTAAAAGA
ceuB_AS	CGACTCTAGAGGATCCATTAGCCGCACCAAAAGAAA
ceuB_AS_inverse	GAACACCGCCGAGCACTTCACCCATGCCAACTATG
ceuB_SE	CGGTACCCGGGGATCCATGCAACAACTCACGCAAAA
ceuB_SE_inverse	GAACTAAAGGGCGCATGATTGTAAGCGTTGGGATT
cfbpA_AS	CGACTCTAGAGGATCCAGCAGAACTCACACCCAAAATC
cfbpA_AS_inverse	GAACACCGCCGAGCATCGCAAACCATTCTTTATCCTT
cfbpA_SE	CGGTACCCGGGGATCCCTATGCGTTGGCTTTGCTTTTG
cfbpA_SE_inverse	GAACTAAAGGGCGCAAAGTGGGGAATTCTTTGGGTA
cfbpB_AS	CGACTCTAGAGGATCCATCCTCTTGCCATAGCTCTAGC
cfbpB_AS_inverse	GAACACCGCCGAGCACCAAATAAGCACTTGCACCA
cfbpB_SE	CGGTACCCGGGGATCCTGATTTTGGGTGTGAGTTCTGC
cfbpB_SE_inverse	GAACTAAAGGGCGCACAGCTTTGCCTTCCTTGTTT
cfbpC_AS	CGACTCTAGAGGATCCACAGTAGCCACACGACTTACCC
cfbpC_AS_inverse	GAACACCGCCGAGCACACTCTTTGCGCTTGTCCTC
cfbpC_SE	CGGTACCCGGGGATCCTGATGCAGCTTTGCCTTCCTTG
cfbpC_SE_inverse	GAACTAAAGGGCGCAAAAATCAAGGCATTACGGCTA
chuB_AS	CGACTCTAGAGGATCCTGCTTTTGCCTGAGCCATTTGG
chuB_AS_inverse	GAACACCGCCGAGCATCGCCATTATAATCCGTGGT
chuB_SE	CGGTACCCGGGGATCCGCTGGGCTTGAATACGCTTGG
chuB_SE_inverse	GAACTAAAGGGCGCATGGTTTCGTGTGGGAATTTT
chuC_AS	CGACTCTAGAGGATCCGGTGATTTGGCCTAAGGTTGTG
chuC_AS_inverse	GAACACCGCCGAGCATGAGGCACAAAGCCACAAAT
chuC_SE	CGGTACCCGGGGATCCGCGGACTTATAGGCTTTGTTGG
chuC_SE_inverse	GAACTAAAGGGCGCAAGCCGTTGTTGCTATCTTGC
chuD_AS	CGACTCTAGAGGATCCTGGTGCCTTGCTGTTTGGATAC
chuD_AS_inverse	GAACACCGCCGAGCATGAAAAAGTGCCTACGCTTG
chuD_SE	CGGTACCCGGGGATCCGATGAACCCACTTCAGCCCTTG
chuD_SE_inverse	GAACTAAAGGGCGCATTAAGCCCGCAAAGTCAAAT
Cj0012c_AS	CGACTCTAGAGGATCCATCGCTTTAGCTTTAGCTTCGC
Cj0012c_AS_comp	GGGGAAGCTTTCTAGCACCAAAGAGAAAAGCCGTTA
Cj0012c_AS_inverse	GAACACCGCCGAGCATTTCATTTTCAGCCGCTTCT
Cj0012c_SE	CGGTACCCGGGGATCCTCGCATCGCTTCTCATTGTAAC

Cj0012c_SE_comp	GATTTAGATGTCTAGAGCAAAGCTTAATTTTTGTGAAA
Cj0012c_SE_inverse	GAACTAAAGGGCGCATGCAAAAATCGCTGAAGATG
Cj0020c_AS	CGACTCTAGAGGATCCCGCTTGAACACTTGGATCGTAG
Cj0020c_AS_inverse	GAACACCGCCGAGCAGCCGTGTTGATCAAGCCTAT
Cj0020c_SE	CGGTACCCGGGGATCCAGAAGAACTTAGCGCAGGCATG
Cj0020c_SE_inverse	GAACTAAAGGGCGCAGCATCTCTTGCCATCAAGGT
Cj0040_AS	CGACTCTAGAGGATCCCGCTCTCATCAAAAGCTCCT
Cj0040_AS_inverse	GAACACCGCCGAGCAAAAAGCTCTAAAACTTGAAGCAAAA
Cj0040_SE	CGGTACCCGGGGATCCCGTTCTACTTCTCCGCCAAA
Cj0040_SE_inverse	GAACTAAAGGGCGCATGGCAAGAATTTCAAGTGAGC
Cj0041_AS	CGACTCTAGAGGATCCTGCGTTTTTGTTTGCTCTTG
Cj0041_AS_comp	GGGGAAGCTTTCTAGGGTAGCATTTGGATTGCTCA
Cj0041_AS_inverse	GAACACCGCCGAGCATCGTGTTTGCTTTCTTTGGA
Cj0041_SE	CGGTACCCGGGGATCCGAAGCGATGAGCAGACTTCA
Cj0041_SE_comp	GATTTAGATGTCTAGTGAAAGAAAAATTTCCTAATGTAATGG
Cj0041_SE_inverse	GAACTAAAGGGCGCAGAAGAAGATACCACAGATGCTAAAAA
Cj0044c_AS	CGACTCTAGAGGATCCCAACGGCAAATAGCGGTGATG
Cj0044c_AS_inverse	GAACACCGCCGAGCAAAATCCATAATTGGCGCTAAAA
Cj0044c_SE	CGGTACCCGGGGATCCTCCAACTCCAACCTAACCCATC
Cj0044c_SE_inverse	GAACTAAAGGGCGCAAGCCGAAAATATCGGAGAGG
Cj0045c_AS	CGACTCTAGAGGATCCAGATGGGTTAGGTTGGAGTTGG
Cj0045c_AS_inverse	GAACACCGCCGAGCATCAATCAAAGGAAAATCAATGC
Cj0045c_SE	CGGTACCCGGGGATCCAAACCCTTCCCCAGATAACTGC
Cj0045c_SE_inverse	GAACTAAAGGGCGCATTCTTTGCGTATCCATGCAG
Cj0062c_AS	CGACTCTAGAGGATCCTTTATCGTAACGGCGTGAAAGC
Cj0062c_AS_comp	GGGGAAGCTTTCTAGTTGAAGGCAAGCGTTCTTTT
Cj0062c_AS_inverse	GAACACCGCCGAGCATCCACAAACAGTGAAAAATGC
Cj0062c_SE	CGGTACCCGGGGATCCGCAGCAATCACTGATGCGTATG
Cj0062c_SE_comp	GATTTAGATGTCTAGGCCCTAGCTTCCAAGCTTTT
Cj0062c_SE_inverse	GAACTAAAGGGCGCATGAAGCCTTTGATATACTGATTTTT
Cj0073c_AS	CGACTCTAGAGGATCCCCTTGCTTGCAAGTTCACAA
Cj0073c_AS_comp	GGGGAAGCTTTCTAGTTGGAATTAGTTTATCTAAAAGCACCT
Cj0073c_AS_inverse	GAACACCGCCGAGCATTTTGCGACAATTTCATTGATT
Cj0073c_SE	CGGTACCCGGGGATCCGCCCTAGAAGCCTTTGCTTT
Cj0073c_SE_comp	GATTTAGATGTCTAGCGGTACAAAATTTCGCAAGC
Cj0073c_SE_inverse	GAACTAAAGGGCGCAGCCTTGCACCTAAACTTTGC
Cj0148c_AS	CGACTCTAGAGGATCCGCGTAGGAATAGAGCGAACACC
Cj0148c_AS_inverse	GAACACCGCCGAGCACAAGCCTTATCTTCCCCTAAAA
Cj0148c_SE	CGGTACCCGGGGATCCAGCAGGAGCAGGAGGAGAGG
Cj0148c_SE_inverse	GAACTAAAGGGCGCACCGAGCGTTTGGATAGAAAA
Cj0171_AS	CGACTCTAGAGGATCCTCGCTAAAGGAATTTGGCAAGG
Cj0171_AS_inverse	GAACACCGCCGAGCAGCAAGGATCTTTTTCCCAAA
Cj0171_SE	CGGTACCCGGGGATCCAATGCACGCCCTGCTTATTTAG
Cj0171_SE_inverse	GAACTAAAGGGCGCAGCTTTTAAAGAAGCTGTGCAAGA
Cj0177_AS	CGACTCTAGAGGATCCCACGCCCAAAACCACTCATACC
Cj0177_AS_comp	GGGGAAGCTTTCTAGTTTTTCATTCCTCCCCCTTA
Cj0177_AS_inverse	GAACACCGCCGAGCATCGCCAAGCAGTATCACATC
Cj0177_SE	CGGTACCCGGGGATCCAGCAAGCAAAAGCAAAGCCAAC

Cj0177_SE_comp	GATTTAGATGTCTAGAAGCAAAGCCAACGCATAGT
Cj0177_SE_inverse	GAACTAAAGGGCGCAACAGGCGTATGGCTGATGTA
Cj0202c_AS	CGACTCTAGAGGATCCTTTTCTGCCTAAATGTTCCAAA
Cj0202c_AS_comp	GGGGAAGCTTTCTAGTTCCTGCACGAAAGACAAGA
Cj0202c_AS_inverse	GAACACCGCCGAGCAGCTGCATTTTCAGCAACAAC
Cj0202c_SE	CGGTACCCGGGGATCCAAAACCAAGCCGTTCAAGAAT
Cj0202c_SE_comp	GATTTAGATGTCTAGAAAACCAAGCCGTTCAAGAAT
Cj0202c_SE_inverse	GAACTAAAGGGCGCAAGCAAAAAGAATGGGTGGTG
Cj0253_AS	CGACTCTAGAGGATCCGCACTTTCAGCGGTTTCTTT
Cj0253_AS_inverse	GAACACCGCCGAGCACGCACTTGAATTCGAATGTTT
Cj0253_SE	CGGTACCCGGGGATCCCGGCTATAATGGGGGTTAAAA
Cj0253_SE_inverse	GAACTAAAGGGCGCAAAAAAGATCGTTTGGATATATTTGA
Cj0260c_AS	CGACTCTAGAGGATCCTTGTGCCGCAGGTGTATTTA
Cj0260c_AS_comp	GGGGAAGCTTTCTAGCGTGCCTTATATGGCTGGAG
Cj0260c_AS_inverse	GAACACCGCCGAGCACATCAAGAATCAAGCGTCCA
Cj0260c_SE	CGGTACCCGGGGATCCAAATTTATCTTGGTTGGGCTGA
Cj0260c_SE_comp	GATTTAGATGTCTAGTGGCATTTAAGTATGAACAAAATCA
Cj0260c_SE_inverse	GAACTAAAGGGCGCAGCATTGGATTTTTAGCTGGTTT
Cj0295_AS	CGACTCTAGAGGATCCACCATAGCCACGCAAGAAGAAG
Cj0295_AS_inverse	GAACACCGCCGAGCAGCAAATCAAGCAATTTCTGC
Cj0295_SE	CGGTACCCGGGGATCCTCAACAGGTGGAGCTAGAAAGC
Cj0295_SE_inverse	GAACTAAAGGGCGCATGAAATTTACACTTTCGCATCC
Cj0309c_AS	CGACTCTAGAGGATCCTTTGCTACCAAAATCGTAGGG
Cj0309c_AS_inverse	GAACACCGCCGAGCAGCAACGCTCATAGCGATATTT
Cj0309c_SE	CGGTACCCGGGGATCCGGCTTCATGTGAATGAAAAATTC
Cj0309c_SE_inverse	GAACTAAAGGGCGCATATGGACAGGAGCTGGAACC
Cj0344_AS	CGACTCTAGAGGATCCAATCCAGCAAAGTCGCAAAT
Cj0344_AS_comp	GGGGAAGCTTTCTAGAATCCAGCAAAGTCGCAAAT
Cj0344_AS_inverse	GAACACCGCCGAGCATTATATTTTATAATATTTTGAAACAT
Cj0344_SE	CGGTACCCGGGGATCCCATTCCGCTAAAGCTTGCTC
Cj0344_SE_comp	GATTTAGATGTCTAGACCAATGCCAAAAAGTCCAG
Cj0344_SE_inverse	GAACTAAAGGGCGCAATTTTCATAAAAGTCTTAATTTTTGA
Cj0358_AS	CGACTCTAGAGGATCCAATCGCAGGAGTTGGCATAGG
Cj0358_AS_comp	GGGGAAGCTTTCTAGCAGCCATTGCTAAACGCATA
Cj0358_AS_inverse	GAACACCGCCGAGCAAGCAGGAGTTGCCATTTCAG
Cj0358_SE	CGGTACCCGGGGATCCTGCTAATCGCATCCTTAGTTGC
Cj0358_SE_comp	GATTTAGATGTCTAGTTAGCCCAAAAGGGATTGAA
Cj0358_SE_inverse	GAACTAAAGGGCGCATGTTGCTGAAACTGCTCCAT
Cj0385c_AS	CGACTCTAGAGGATCCTGCTGCGGCTACAAGTAAATCG
Cj0385c_AS_inverse	GAACACCGCCGAGCAAGCCAAAAATATCCCCCTTC
Cj0385c_SE	CGGTACCCGGGGATCCTCACTTTCATCAAGCCCTCCAC
Cj0385c_SE_inverse	GAACTAAAGGGCGCAAAACAAGCAGGAGTGGTTGC
Cj0416_AS	CGACTCTAGAGGATCCGCTGATCCTAGCCCACAAGA
Cj0416_AS_inverse	GAACACCGCCGAGCATGTCTGCAGAGGATTATTTCCA
Cj0416_SE	CGGTACCCGGGGATCCTGGGCGCAGATAGAGAAACT
Cj0416_SE_inverse	GAACTAAAGGGCGCAGAGATGAAAGTATTGAAAATGCAAA
Cj0494_AS	CGACTCTAGAGGATCCTGCAAGGGTAAAAATTCCTGA
Cj0494_AS_inverse	GAACACCGCCGAGCAAATTTACTGGGCTTTGTGCTG

Cj0494_SE	CGGTACCCGGGGATCCTTGCTGCTTCTATGGGCTTT
Cj0494_SE_inverse	GAACTAAAGGGCGCAAAAGAACAGCTTCCAAAACG
Cj0524_AS	CGACTCTAGAGGATCCCGAAGCCGCTAAAACGATGC
Cj0524_AS_inverse	GAACACCGCCGAGCACGACTAAAACCTATAGCATGAGCA
Cj0524_SE	CGGTACCCGGGGATCCAGTGTTGGAGGAGTTGTAACGG
Cj0524_SE_inverse	GAACTAAAGGGCGCACACAACAGCTGAAGGAATTTCA
Cj0554_AS	CGACTCTAGAGGATCCCGCTCCTATCACTCACACTCAC
Cj0554_AS_inverse	GAACACCGCCGAGCATTCACCAAAAGCCAGTGAGA
Cj0554_SE	CGGTACCCGGGGATCCTTACTGCTGCTATTGCTTTGCC
Cj0554_SE_inverse	GAACTAAAGGGCGCATTCAAAACCCTGCACACAAA
Cj0561c_AS	CGACTCTAGAGGATCCAGCTTTTCCGTCTGCATCATTG
Cj0561c_AS_inverse	GAACACCGCCGAGCAAGCCGTAGCTGATTGGGTTA
Cj0561c_SE	CGGTACCCGGGGATCCAAGGAGTGGCAAGAATTTCTGC
Cj0561c_SE_inverse	GAACTAAAGGGCGCATTCAACCTTGGCAAACAGTG
Cj0587_AS	CGACTCTAGAGGATCCTGAACAAAACCGCCCGTACTAG
Cj0587_AS_inverse	GAACACCGCCGAGCAAAAAAGCCCATAAAATGCATAAA
Cj0587_SE	CGGTACCCGGGGATCCGGAGAAGAGGCAGGTTCTAAGC
Cj0587_SE_inverse	GAACTAAAGGGCGCATGCCTTAAAATCCGAACAAGA
Cj0634_AS	CGACTCTAGAGGATCCTGATCCACCCTTAGGAATGC
Cj0634_AS_inverse	GAACACCGCCGAGCATTGATCTAAACCATTGGCAAAA
Cj0634_SE	CGGTACCCGGGGATCCCGCAGTAAAACTCGCACAAA
Cj0634_SE_inverse	GAACTAAAGGGCGCATAAGGCTGTTGTGGTTGCAC
Cj0672_AS	CGACTCTAGAGGATCCTGCCTGTATTTTGCGAAAGC
Cj0672_AS_inverse	GAACACCGCCGAGCAGAAGCAAAGCAAAGATAATATCCA
Cj0672_SE	CGGTACCCGGGGATCCCGGCTGCTTGTTATGGGTAT
Cj0672_SE_inverse	GAACTAAAGGGCGCACGCGGATGATATTTTTACTAGTTTT
Cj0741_AS	CGACTCTAGAGGATCCTGTGGTTCATTTGCTTCAGGAG
Cj0741_AS_inverse	GAACACCGCCGAGCACAGCATCTGTTGCCTTGGTA
Cj0741_SE	CGGTACCCGGGGATCCGTGGGTGGCATAGGCAGAC
Cj0741_SE_inverse	GAACTAAAGGGCGCAGAAAAGCAGTTTGCGGATCT
Cj0786_AS	CGACTCTAGAGGATCCTGTCTTCTTTGCTCTTCCATGA
Cj0786_AS_inverse	GAACACCGCCGAGCATCAATTCCAAAAATAACACCAA
Cj0786_SE	CGGTACCCGGGGATCCATCGTTTCAGGCTTTGGTGA
Cj0786_SE_inverse	GAACTAAAGGGCGCAAAAAATCAAGATTTAAAAGTGCAAG
Cj0814_AS	CGACTCTAGAGGATCCATCACCTTCTATGCCACTCTGC
Cj0814_AS_comp	GGGGAAGCTTTCTAGACAGGTTGTCCACCTTGAGC
Cj0814_AS_inverse	GAACACCGCCGAGCATCTTGCTAGAGTTTGTGAATTTGC
Cj0814_SE	CGGTACCCGGGGATCCAAGGGCATTTAGGCATTTACGC
Cj0814_SE_comp	GATTTAGATGTCTAGCAACAAGCATGGGGATTGAT
Cj0814_SE_inverse	GAACTAAAGGGCGCAGAACGCAATGGATGGACTTT
Cj0818_AS	CGACTCTAGAGGATCCATGGTTGTAAGCTCAGTTTTAATGG
Cj0818_AS_inverse	GAACACCGCCGAGCAAACCCCAGCACCTACTACCC
Cj0818_SE	CGGTACCCGGGGATCCTTGGAAGTGATTCAAGGCAAG
Cj0818_SE_inverse	GAACTAAAGGGCGCAAATTGACATGATGGCTGCAA
Cj0819_AS	CGACTCTAGAGGATCCAGCTATGGGGACGCAAAGTA
Cj0819_AS_inverse	GAACACCGCCGAGCATTTTCTAGGGTCTTGATAGAATAAAAA
Cj0819_SE	CGGTACCCGGGGATCCCCATTTTAGCGCCTTTTCAA
Cj0819_SE_inverse	GAACTAAAGGGCGCAGTCTTTCTAGGGCGAACAGC

Cj0900c_AS	CGACTCTAGAGGATCCACAAGCAAACTCGCCCTCTA
Cj0900c_AS_inverse	GAACACCGCCGAGCACCAAAACAATCATTAAAAACACAAA
Cj0900c_SE	CGGTACCCGGGGATCCAAAATTACCGGTGTTCCTCGT
Cj0900c_SE_inverse	GAACTAAAGGGCGCATCAATCATCAAATGATGCAAAA
Cj0947c_AS	CGACTCTAGAGGATCCTTTTAAACCGCTTTGGGAAA
Cj0947c_AS_comp	GGGGAAGCTTTCTAGAAACGAACAAGAAAAAGAGCAAA
Cj0947c_AS_inverse	GAACACCGCCGAGCACCCCGCTTACATCTTTTTCA
Cj0947c_SE	CGGTACCCGGGGATCCGGAGCTGAGCTTGTTTGCTT
Cj0947c_SE_comp	GATTTAGATGTCTAGTGCAGAACAAGAAAGGCAAA
Cj0947c_SE_inverse	GAACTAAAGGGCGCATTTTGTTTTTGGCCCTCAAG
Cj0949c_AS	CGACTCTAGAGGATCCTCGCACTTGAAAGTACTGCAAC
Cj0949c_AS	CGACTCTAGAGGATCCTCGCACTTGAAAGTACTGCAAC
Cj0949c_AS_inverse	GAACACCGCCGAGCACCAAAATCGCGTATCCAAGT
Cj0949c_AS_inverse	GAACACCGCCGAGCACCAAAATCGCGTATCCAAGT
Cj0949c_SE	CGGTACCCGGGGATCCATGCTTTGTCACCCAATGGATG
Cj0949c_SE	CGGTACCCGGGGATCCATGCTTTGTCACCCAATGGATG
Cj0949c_SE_inverse	GAACTAAAGGGCGCATGAGCATTATTTGCCTTTGC
Cj0949c_SE_inverse	GAACTAAAGGGCGCATGAGCATTATTTGCCTTTGC
Cj0977_AS	CGACTCTAGAGGATCCAAGGCTATGCTTGGGCTGATAC
Cj0977_AS_inverse	GAACACCGCCGAGCATCGTCAAAAAGTGCATGAGC
Cj0977_SE	CGGTACCCGGGGATCCGGCTATGAAGCACCCAAAAGAG
Cj0977_SE_inverse	GAACTAAAGGGCGCAGTTGTTAGCACCGATGAGCA
Cj1036c_AS	CGACTCTAGAGGATCCAAGCTTAAATCATAACGCTTCCA
Cj1036c_AS_comp	GGGGAAGCTTTCTAGGACGCCAACCTCGTTTTATT
Cj1036c_AS_inverse	GAACACCGCCGAGCACTTGCACCACTCTTGCTTGA
Cj1036c_SE	CGGTACCCGGGGATCCTCCAAGTCCTGGAAAAATAGGA
Cj1036c_SE_comp	GATTTAGATGTCTAGTGCAATAGCTGCTACGCTTAAA
Cj1036c_SE_inverse	GAACTAAAGGGCGCACAGGATGAATTTTCCGAATTT
Cj1159c_AS	CGACTCTAGAGGATCCAATGTGCAAAAAGCACTAACAA
Cj1159c_AS_inverse	GAACACCGCCGAGCAGCCTATATGATAAATCACGGGAGA
Cj1159c_SE	CGGTACCCGGGGATCCTGTGCTTTGCATTCCTATCG
Cj1159c_SE_inverse	GAACTAAAGGGCGCATTTATTGCCTTAACAGCTCTAAAAA
Cj1167_AS	CGACTCTAGAGGATCCACCAGGGATTCGTCAGTACATC
Cj1167_AS_inverse	GAACACCGCCGAGCAGGTGTCATTTGGATTTGTTGC
Cj1167_SE	CGGTACCCGGGGATCCACCTCAGCTATTCTTCCTACGC
Cj1167_SE_inverse	GAACTAAAGGGCGCAAGAACTCGAAAAAGCCGTGA
Cj1207c_AS	CGACTCTAGAGGATCCTAATTGCTCAATCGCACCTG
Cj1207c_AS_inverse	GAACACCGCCGAGCATTATTTTCACCATTAGCGACTTT
Cj1207c_SE	CGGTACCCGGGGATCCTTTGCAATGCCCTAAAATCTG
Cj1207c_SE_inverse	GAACTAAAGGGCGCAGCTTTAGGTGGGGTAAATGGA
Cj1209_AS	CGACTCTAGAGGATCCGCGAATTTCTCTTCCGGCATTG
Cj1209_AS_inverse	GAACACCGCCGAGCACTGCAAATTCACCTGCAAAA
Cj1209_SE	CGGTACCCGGGGATCCAGAACAAGCCAAAGCTAAAGCC
Cj1209_SE_inverse	GAACTAAAGGGCGCATACCGAGCAAGCTATGGACA
Cj1211_AS	CGACTCTAGAGGATCCCCTTTGGGGCTTGGGCTTAG
Cj1211_AS_inverse	GAACACCGCCGAGCATGGGTGATAATTCTAAGGCTCAA
Cj1211_SE	CGGTACCCGGGGATCCGCTAGTTTGGCATGGGCTATTG
Cj1211_SE_inverse	GAACTAAAGGGCGCATTTGCTATGGTTTTACCTGTGC

Cj1241_AS	CGACTCTAGAGGATCCAGCACCAAGATCAATGTCTTCG
Cj1241_AS_inverse	GAACACCGCCGAGCATCCTGCTATAAAGCGTGCAA
Cj1241_SE	CGGTACCCGGGGATCCACTCGCCAAACTTAAACCAAGC
Cj1241_SE_inverse	GAACTAAAGGGCGCATTGCCTTTTCAACCATACCTG
Cj1242_AS	CGACTCTAGAGGATCCTTCCTGCTTGACGCATCATCC
Cj1242_AS_inverse	GAACACCGCCGAGCATTGAAATTCATCTGCCGAAGT
Cj1242_SE	CGGTACCCGGGGATCCGCCTTTTCAACCATACCTGCAC
Cj1242_SE_inverse	GAACTAAAGGGCGCATCAAGCAAATTTACTAACGAAGACA
Cj1255_AS	CGACTCTAGAGGATCCTTTTTGAATTTGAGATCACTTTCTTG
Cj1255_AS_inverse	GAACACCGCCGAGCACCGTTACTCCTGCGATAAGC
Cj1255_SE	CGGTACCCGGGGATCCGAAACACTTTTTAATGCAAAATTAGA
Cj1255_SE_inverse	GAACTAAAGGGCGCACGGACTAGGTGGAAAAAGCA
Cj1335_AS	CGACTCTAGAGGATCCTGCCTTGAAGAGCATCTTTTG
Cj1335_AS_inverse	GAACACCGCCGAGCATTTTGGGTAGGGGTGAAGGT
Cj1335_SE	CGGTACCCGGGGATCCACCTACAACTGCACCGAAGG
Cj1335_SE_inverse	GAACTAAAGGGCGCACAAAAACATTGAGGCTTTAAACAA
Cj1340c_AS	CGACTCTAGAGGATCCGAGCCGCTTGAGTTGCCTTAG
Cj1340c_AS_inverse	GAACACCGCCGAGCATTGCTCCACCTTCAGTAGCA
Cj1340c_SE	CGGTACCCGGGGATCCATTGCTCTTGAGTGTGCTACGC
Cj1340c_SE_inverse	GAACTAAAGGGCGCAAGCCTTTGCTTATCGTGGAA
Cj1341c_AS	CGACTCTAGAGGATCCAGTCCTCGCTCATACATCACTG
Cj1341c_AS_inverse	GAACACCGCCGAGCATCATTAAGATTGAAGCGTTGG
Cj1341c_SE	CGGTACCCGGGGATCCGAGGATGTCTGGCATAAAGCAG
Cj1341c_SE_inverse	GAACTAAAGGGCGCAATGCAGGCAAAGGTGAAGTT
Cj1342c_AS	CGACTCTAGAGGATCCCTAACCAAGGCGCAATCTTAGC
Cj1342c_AS_inverse	GAACACCGCCGAGCAACCACAAACACCAAGGCTTC
Cj1342c_SE	CGGTACCCGGGGATCCAGCGGGGTTGAAAATGTTGATC
Cj1342c_SE_inverse	GAACTAAAGGGCGCATGTATTGGCAATCGTCCTCA
Cj1356c_AS	CGACTCTAGAGGATCCAGAACGTGCTCAAGGCATACTC
Cj1356c_AS_inverse	GAACACCGCCGAGCACCCGTTAAAGCAAAAAGCAA
Cj1356c_SE	CGGTACCCGGGGATCCGCAGCGGCAAATGGAATTAAAG
Cj1356c_SE_inverse	GAACTAAAGGGCGCATGTGCTTAGCGTAGGTTTTGG
Cj1377c_AS	CGACTCTAGAGGATCCACGCAACCATTCGCCACTTTC
Cj1377c_AS_comp	GGGGAAGCTTTCTAGCATCGGATTAGGTTCATTGGA
Cj1377c_AS_inverse	GAACACCGCCGAGCACAAGCCCCAAATCATAAACG
Cj1377c_SE	CGGTACCCGGGGATCCTGTGTATAACCACTCCGCTTGC
Cj1377c_SE_comp	GATTTAGATGTCTAGTGGAAAAGTTCTAAATTTGTTCATC
Cj1377c_SE_inverse	GAACTAAAGGGCGCATTGTTTGGGTTGTGGAGGAT
Cj1383c_AS	CGACTCTAGAGGATCCCACCACTTCCCCAAGTTGAA
Cj1383c_AS_comp	GGGGAAGCTTTCTAGGCCGCTCCTTCTGTATTTCC
Cj1383c_AS_inverse	GAACACCGCCGAGCATGAAAGTAAAAAGCGTATGTATTAAGC
Cj1383c_SE	CGGTACCCGGGGATCCGCCGATTCCTTGTGATACAGA
Cj1383c_SE_comp	GATTTAGATGTCTAGGAAGCTAAAAAGCGTAAAATTCCA
Cj1383c_SE_inverse	GAACTAAAGGGCGCATGTTTTGATGCGCAAATTTTA
Cj1388_AS	CGACTCTAGAGGATCCGTCATAAGTGTAAGTCCAAGCC
Cj1388_AS_inverse	GAACACCGCCGAGCATCTCCTGAAGCAGGGTTGAT
Cj1388_SE	CGGTACCCGGGGATCCGCAGTCAAGGGAGAATCTAAAC
Cj1388_SE_inverse	GAACTAAAGGGCGCACGGTGCTATCTTAGAAGAAAATGG

Cj1406c_AS	CGACTCTAGAGGATCCATTGACATGAGCGAGCAAGA
Cj1406c_AS_inverse	GAACACCGCCGAGCACACTTGCACCAAAAGCAAAA
Cj1406c_SE	CGGTACCCGGGGATCCAGAGCCTTGGAGCTTGTTTAT
Cj1406c_SE_inverse	GAACTAAAGGGCGCAAAAAATCGAAAAAGAACTTGATGC
mdaB_AS	CGACTCTAGAGGATCCCTCCTCCTTTGCCTGCCAAG
mdaB_AS_inverse	GAACACCGCCGAGCACACCAAGCTGGCATTTGATA
mdaB_SE	CGGTACCCGGGGATCCTGGGTGGAATTTGAGCGTATTC
mdaB_SE_inverse	GAACTAAAGGGCGCATGGTGTATTGGCATTTGCAT
Cj1613c_AS	CGACTCTAGAGGATCCTCACTCATCATCAAGCCCAAGC
Cj1613c_AS_inverse	GAACACCGCCGAGCACGTGTTTTCATCGGCTTTTT
Cj1613c_SE	CGGTACCCGGGGATCCTCCGCATCTTGTTCAAAACCTG
Cj1613c_SE_inverse	GAACTAAAGGGCGCATTGCTCGTATGCACCTTTTG
Cj1658_AS	ATGC**AGATCT**GAGGGATTAAAGTTTCATAGTAAGGA
Cj1658_AS_inverse	ATGC**GGATCC**ACCGCTTTTGGAGTTTCTTG
Cj1658_SE	ATGC**AGATCT**GCTCAGCTTTTGCTAGGGTAGA
Cj1658_SE_inverse	ATGC**GGATCC**GTTTGGCATTGGCTTCTAGG
Cj1661_AS	CGACTCTAGAGGATCCTGCCTAAAACCACCCCGCTTG
Cj1661_AS_inverse	GAACACCGCCGAGCATAATTTTTCTTCGCCCATGC
Cj1661_SE	CGGTACCCGGGGATCCAACAACATCACCGCACTTGCTC
Cj1661_SE_inverse	GAACTAAAGGGCGCATGGCACAGCACTTTCTCAAA
Cj1663_AS	CGACTCTAGAGGATCCAACACAGCGTAACGATCATTGG
Cj1663_AS_inverse	GAACACCGCCGAGCATGCTCTTCATCCATTTGCTCT
Cj1663_SE	CGGTACCCGGGGATCCGCACTGCGTTTAGCCTTGGG
Cj1663_SE_inverse	GAACTAAAGGGCGCATCGCAGATCGAACCCTTATC
cmeA_AS	CGACTCTAGAGGATCCGGCTTGATCAGGATCTGTACCG
cmeA_AS_inverse	GAACACCGCCGAGCACATCAAAAGGAGCTTTTATTTCG
cmeA_SE	CGGTACCCGGGGATCCAATGCCGCCTCAACCTGTAAC
cmeA_SE_inverse	GAACTAAAGGGCGCATGGCTTTAAAGTGCCTCAAAT
exbB1_AS	CGACTCTAGAGGATCCCTCTGCTTGCTGCGAACTCTTG
exbB1_AS_comp	GGGGAAGCTTTCTAGGCTGCGAACTCTTGGGTAAT
exbB1_AS_inverse	GAACACCGCCGAGCATGGTATTTTGCAAACGCAAT
exbB1_SE	CGGTACCCGGGGATCCCAATTCTGCTCGCGGTCGTAC
exbB1_SE_comp	GATTTAGATGTCTAGGCTCGCGGTCGTACTTTTAT
exbB1_SE_inverse	GAACTAAAGGGCGCAGCAAATCACAGCAAGCAAAA
exbB2_AS	CGACTCTAGAGGATCCAAATTTTCATGTTCTTTGGCTTTT
exbB2_AS_comp	GGGGAAGCTTTCTAGCATGCGCAATAAAGGTTGAA
exbB2_AS_inverse	GAACACCGCCGAGCATCGCATCATCAAATTGCTCT
exbB2_SE	CGGTACCCGGGGATCCAATCACGCCCTCTTTGGTAA
exbB2_SE_comp	GATTTAGATGTCTAGGAAGAACAAAAGAGGTAAAATTGTGA
exbB2_SE_inverse	GAACTAAAGGGCGCATTGGCGGGCAATATAGATGT
exbD1_AS	CGACTCTAGAGGATCCTAGCGGAGCACTGAGCGATTC
exbD1_AS_inverse	GAACACCGCCGAGCAGCTGCGAACTCTTGGGTAAT
exbD1_SE	CGGTACCCGGGGATCCAAATGGCTTGAGTTTGCTTGCG
exbD1_SE_inverse	GAACTAAAGGGCGCAAAACCAAAGGCAATAAAGAAGAAA
exbD2_AS	CGACTCTAGAGGATCCTTGGTATTGGGTGTGGAGGT
exbD2_AS_inverse	GAACACCGCCGAGCACATGCGCAATAAAGGTTGAA
exbD2_SE	CGGTACCCGGGGATCCTGGCATTTATAGCTTTTTGGTG
exbD2_SE_inverse	GAACTAAAGGGCGCACACTTCCTTCAAGTGAAAATGC

flaG_AS	CGACTCTAGAGGATCCAGACTTGCTGGAGGATTATCGC
flaG_AS_inverse	GAACACCGCCGAGCATCGCCTTCTTGACCTTGACT
flaG_SE	CGGTACCCGGGGATCCTATATGCTTGTTTGGCGTGTGG
flaG_SE_inverse	GAACTAAAGGGCGCAACAGCAACGAGGTGTGAGTG
flgD_AS	CGACTCTAGAGGATCCCCGCTACCATAACCACCTTGAG
flgD_AS_comp	GGGGAAGCTTTCTAGAAAGCCCGTGGTATTGACAT
flgD_AS_inverse	GAACACCGCCGAGCAGGTAGCATTTGGATTGCTCA
flgD_SE	CGGTACCCGGGGATCCCAACTCCAATGCCAATGCAATG
flgD_SE_comp	GATTTAGATGTCTAGGAGCAAAATCAAAATCAAGGAAA
flgD_SE_inverse	GAACTAAAGGGCGCACTATGGAGTGGCCAGGAAGA
flgE_AS	CGACTCTAGAGGATCCATCACCGCTATTTGCCGTTGC
flgE_AS_comp	GGGGAAGCTTTCTAGGCGAAAGCGACATAGAAGAAA
flgE_AS_inverse	GAACACCGCCGAGCACCCATAAGCCCAGCAACTCT
flgE_SE	CGGTACCCGGGGATCCCAAGTGGTGGTTCAAGCGATGG
flgE_SE_comp	GATTTAGATGTCTAGTATGCAAAAATGGCTGGACA
flgE_SE_inverse	GAACTAAAGGGCGCAACCGCAAGAAGGCGATAATA
flgE2_AS	CGACTCTAGAGGATCCTGCAGGTTCAGGTACACGGATG
flgE2_AS_inverse	GAACACCGCCGAGCAGGATATGCATACCTGGATCG
flgE2_SE	CGGTACCCGGGGATCCTCTGGCGTAAGCGGACTACAAG
flgE2_SE_inverse	GAACTAAAGGGCGCAGCAGCTTATTGGGATGCTGT
flgG_AS	CGACTCTAGAGGATCCAACCATTCCTGTGGGTCCTATG
flgG_AS_inverse	GAACACCGCCGAGCAACCCATTACCTGCAATAGCC
flgG_SE	CGGTACCCGGGGATCCACTCCAATGCTATTCGCCAAGG
flgG_SE_inverse	GAACTAAAGGGCGCACAAGATGGGCTTGGAACAAT
flgG2_AS	CGACTCTAGAGGATCCCGCTGTTGGACGCACACC
flgG2_AS_inverse	GAACACCGCCGAGCAGTCATTGCCAAATCCAAAGG
flgG2_SE	CGGTACCCGGGGATCCAAGGTAAGCGGTGGTTACGATG
flgG2_SE_inverse	GAACTAAAGGGCGCACAATGCTATTCGCCAAGGTT
flgH_AS	CGACTCTAGAGGATCCTCATGTCCAACTTGCGGTAGG
flgH_AS_comp	GGGGAAGCTTTCTAGTGCTTTAGGCGAAGCTAAGG
flgH_AS_inverse	GAACACCGCCGAGCATTGCTTTGTTTTGGTGCAAG
flgH_SE	CGGTACCCGGGGATCCTCCTCCATTGCCTCTCTAAAGG
flgH_SE_comp	GATTTAGATGTCTAGTGCCATCATTTTCTCCTTGA
flgH_SE_inverse	GAACTAAAGGGCGCACAACGGAGAGAAGCAAATCA
flgI_AS	CGACTCTAGAGGATCCTTTCATCGCTGGCATCTTTTCC
flgI_AS_comp	GGGGAAGCTTTCTAGTGGCTGCACGATCAAGTAAA
flgI_AS_inverse	GAACACCGCCGAGCATACTGTGCGAGAGTCGATGG
flgI_SE	CGGTACCCGGGGATCCCAGCCAAACTTCCAGCCTTTG
flgI_SE_comp	GATTTAGATGTCTAGCAACCATAAAAACTCCCGAAA
flgI_SE_inverse	GAACTAAAGGGCGCACAGGAACAGTGATTGCTGGA
flgK_AS	CGACTCTAGAGGATCCAGGGCGGCTAATTCTTCATTTG
flgK_AS_comp	GGGGAAGCTTTCTAGGCAATTTGCAAAGGATCTGG
flgK_AS_inverse	GAACACCGCCGAGCATGCGTGTTCTGTTGGTAAGG
flgK_SE	CGGTACCCGGGGATCCAACAGGTGGAGTTCAAGTAGGC
flgK_SE_comp	GATTTAGATGTCTAGTGATGGAACAAATAATGCTTATGG
flgK_SE_inverse	GAACTAAAGGGCGCATATCATGCGCCAAATCAATG
flgL_AS	CGACTCTAGAGGATCCCCCATTCTCCCATGCCAGGTG
flgL_AS_comp	GGGGAAGCTTTCTAGAAGCGTGGAGCTGGTAAAAA

flgL_AS_inverse	GAACACCGCCGAGCAACCCCACTATTTCCAGTTGC
flgL_SE	CGGTACCCGGGGATCCTCCAAGCAGCACAGGATGAAGG
flgL_SE_comp	GATTTAGATGTCTAGTTTTTGGAACAGTTATTGCTTTTG
flgL_SE_inverse	GAACTAAAGGGCGCAGAGAGCAGACTCCGAAAGTGA
flgM_AS	CGACTCTAGAGGATCCGCCATCAAGAAAATCTTTGACA
flgM_AS_comp	GGGGAAGCTTTCTAGTTCCGCGATAAGTTTGTTTTT
flgM_AS_inverse	GAACACCGCCGAGCATTTTTGAGTATCGTTTGTTTTAGTTTC
flgM_SE	CGGTACCCGGGGATCCGCAGCCAAAGCAAGAAGTTT
flgM_SE_comp	GATTTAGATGTCTAGAAAAGATGCCAGCGATGAAA
flgM_SE_inverse	GAACTAAAGGGCGCAAGCGAGTAAAATCGCAGAGC
flgP_AS	CGACTCTAGAGGATCCATTCTACGGTAAAACGCAAGGG
flgP_AS_comp	GGGGAAGCTTTCTAGACATTTTCGCTTTGCGTCAT
flgP_AS_inverse	GAACACCGCCGAGCAAGCATCTGGAGCCAACATTT
flgP_SE	CGGTACCCGGGGATCCGCAAAGCAGAGGTGGTAAGGG
flgP_SE_comp	GATTTAGATGTCTAGAGGGCGTAATACGAGTGGTG
flgP_SE_inverse	GAACTAAAGGGCGCATGCGCAAGTAAATGGTTTGA
flgR_AS	CGACTCTAGAGGATCCGCACCAGTAGCACCCACAATG
flgR_AS_comp	GGGGAAGCTTTCTAGCACCAGTAGCACCCACAATG
flgR_AS_inverse	GAACACCGCCGAGCAGCCATCAATTCCTGGCATA
flgR_SE	CGGTACCCGGGGATCCATCCTTAGCAATGACGCAAAGC
flgR_SE_comp	GATTTAGATGTCTAGTTTACCCTTGCGTTTTACCG
flgR_SE_inverse	GAACTAAAGGGCGCAAAATGGCGAATTTCGTTCAG
flhB_AS	CGACTCTAGAGGATCCGCCTACCAAAGAGCGGAAAATG
flhB_AS_comp	GGGGAAGCTTTCTAGAAGGTGGAGCAAATTTGAAAAA
flhB_AS_inverse	GAACACCGCCGAGCAAATAGCTGCCGCATCTTGAG
flhB_SE	CGGTACCCGGGGATCCCGTTCTTGCTTGATGCTGATGG
flhB_SE_comp	GATTTAGATGTCTAGCCTAAAGGCGTGGCTGAATA
flhB_SE_inverse	GAACTAAAGGGCGCAGTGGATTTTCTCGCTCTTCG
folP_AS	CGACTCTAGAGGATCCCTTCGCCATCGCCCCTAGTG
folP_AS_inverse	GAACACCGCCGAGCACTCACTCCCAGGTCTTGAGC
folP_SE	CGGTACCCGGGGATCCAGCGGGGTGCTTTTAGCTACTC
folP_SE_inverse	GAACTAAAGGGCGCATGCGTATTTTCAAAGCGAGA
hypC_AS	CGACTCTAGAGGATCCTCCAAAACCTCAAGTGGAGAA
hypC_AS_inverse	GAACACCGCCGAGCATCGCCTTGTTTTAAAGGTTCA
hypC_SE	CGGTACCCGGGGATCCAGCTGTCATTTGGACGCTTT
hypC_SE_inverse	GAACTAAAGGGCGCACATGTAGGCGTTGCTATGGA
P19_AS	ATGC**AGATCT**AAACAAGCAAGGCTAAAGCAA
P19_AS_inverse	ATGC**GGATCC**GACGCCATGTTGATGAAGAA
P19_SE	ATGC**AGATCT**GGCTACTTTCAAACGCACAA
P19_SE_inverse	ATGC**GGATCC**ACCTCTTGGCTCCATTTCAA
pseB_AS	CGACTCTAGAGGATCCGCATTAGCTGTAGCGGCAAAGG
pseB_AS_comp	GGGGAAGCTTTCTAGTCGCTTTGATCGATGTTTTG
pseB_AS_inverse	GAACACCGCCGAGCATAACACCAAAGCGTGTTTGC
pseB_SE	CGGTACCCGGGGATCCTCAAGCCCAAACTGGCATAACC
pseB_SE_comp	GATTTAGATGTCTAGAGGCAAGTATCAAGCCCAAA
pseB_SE_inverse	GAACTAAAGGGCGCAGCCCATGCTCTAGCTCCTAA
pstC_AS	CGACTCTAGAGGATCCAGAAGCTGCCATCACCACTATC
pstC_AS_comp	GGGGAAGCTTTCTAGTGCTTAAAAGCAGGAAATCCA

pstC_AS_inverse	GAACACCGCCGAGCAGCTGCCCACTGACTTGAGA
pstC_SE	CGGTACCCGGGGATCCGTGTTACGCCAAGCGAAGAAAG
pstC_SE_comp	GATTTAGATGTCTAGTGATTTGGCAAAAAGTGGTG
pstC_SE_inverse	GAACTAAAGGGCGCAGCAGATGGCACGAGTAAACA
trpF_AS	CGACTCTAGAGGATCCGCAAGCCCGTGTTGACCTG
trpF_AS_comp	GGGGAAGCTTTCTAGCATTGCACTTTCAGGCAAAA
trpF_AS_inverse	GAACACCGCCGAGCATCCATTACCGCCCTTTAAAAT
trpF_SE	CGGTACCCGGGGATCCACAGCCAATAAAGCAAGTTCGC
trpF_SE_comp	GATTTAGATGTCTAGGTAGAATGCAAGGGGCAAAA
trpF_SE_inverse	GAACTAAAGGGCGCAATTAGCCGGAGGCATAGGTT
truB_AS	CGACTCTAGAGGATCCTGTCAACAAGCTCAAGCTCATC
truB_AS_inverse	GAACACCGCCGAGCATTGGCGAAAGGATCAAGAGT
truB_SE	CGGTACCCGGGGATCCCCGTCTTGCTTATGTTGCCATC
truB_SE_inverse	GAACTAAAGGGCGCAAGCGCATTAAAGAAGGCAAA
ak233-SE	GCAAGAGTTTTGCTTATGTTAGCAG
ak234-SE	GAAATGGGCAGAGTGTATTCTCCG
ak235-SE	GTGCGGATAATGTTGTTTCTG
AR56-AS	CATCCTCTTCGTCTTGGTAGC
Cat-AS	TGCGCCCTTTAGTTCCTAAAGGGT
Cat-SE	TGCTCGGCGGTGTTCCTTTCCAAG

[a-] Restriction sites in bold.

TABLE S3. Genes selected for isogenic deletion mutant construction. Significantly differentially expressed genes from microarray analysis upon oxidant exposure or in a Δ*perR* background were targeted for deletion in *C. jejuni*. Genes successfully deleted are presented. Genes were attempted to be deleted at least 3 times.

	Microarray analysis[a] (condition assayed[b])				
Gene name	H_2O_2	CHP	MND	Δ*perR*	Mutant constructed?
cj0416	+[c]	+	+	+	Yes
mdaB	+	+	+	+	Yes
rpmF	+	+	+	+	No
cj1485c	+	+	+	+	No
cj0672	+	+	+	+	Yes
cj0148c	+	+	+	+	Yes
cj0202c	+	+	+	+	Yes
cj0344	+	+	+	+	Yes
maf4	+	+	+	+	Yes
cj0176c	+	+	+	+	No
cj0819	+	+	+	+	Yes
cj0253	+	+	+	+	Yes
folP	+	+	+	+	Yes
cj0877c	+	+		+	No
cj0295	+	+		+	Yes
cj0524	+	+		+	Yes
ald	+		+	+	Yes
cj1534c	+		+	+	No
cj0988c	+		+	+	No
cj1241	+			+	Yes
flaG	+			+	Yes
cj0878	+			+	No
cj1388	+			+	Yes
cj1383c	-[d]	-	-	+	Yes
chuC	-	-	-	+	Yes
chuD	-	-		+	Yes
aroC	-	-		+	No
chuB	-	-		+	Yes
flhB	-		-	+	Yes
cfbpB	-			+	Yes
chaN	-			+	Yes
exbB1	-			+	Yes
cj1386	-			+	Yes
cj1710c	-			+	No

cj0135	+	+	+	No
cj0260c	+	+	+	Yes
cj1667c	+	+	+	No
cj1159c	+		+	Yes
cj0554	+		+	Yes
cj1714	+		+	No
grpE	+		+	No
chuA	-		+	Yes
cj0786		+	+	Yes
rpmJ		+	+	No
cj1558		+	+	No
tonB2		-	+	Yes
fliK		-	+	Yes
exbD2		-	+	Yes
exbD1			+	Yes
cj1658			+	Yes
chuZ			+	Yes
cj1661			+	Yes
tonB3			+	Yes
exbB2			+	Yes
p19			+	Yes
cfbpA			+	Yes
ceuC			+	No
cj1384c			+	No
trxB			+	No
cfrA			+	Yes
cj0818			+	Yes
cj0040			+	Yes
cj0045c			+	Yes
flgD			+	Yes
flgK			+	Yes
cj0587			+	Yes
cj1664			+	No
pstC			+	Yes
cj1295			+	No
flgE			+	Yes
flgL			+	Yes
pstS			+	No
cj1663			+	Yes
cj0062c			+	Yes
cj0814			+	Yes
flgC			+	No
cj0428			+	No

flgP				+	Yes
pseB				+	Yes
flgI				+	Yes
asd				+	No
flgB				+	No
flgH				+	Yes
cj1294				+	No
flgG				+	Yes
flgG2				+	Yes
flgE2				+	Yes
flgR				+	Yes
cj0073c	+			-	Yes
spoT	-			-	Yes
cj1340c		-		-	Yes
maf7				-	Yes
maf6				-	Yes
fdxA				-	No
cj1345c				-	No
trpF	+	+	+		Yes
cj0309c	+	+	+		Yes
hypC	+	+			Yes
cj1677	+		+		No
cj1623	+		+		Yes
ccoQ	+		+		Yes
cft	+				No
cj0034c	+				No
cj1484c	+				Yes
cj1406c	+				Yes
cj1255	+				Yes
cj1036c	+				Yes
ktrB	-	-	-		No
tonB1	-				Yes
cfbpC	-				Yes
cj1356c		+	+		Yes
cj0011c		+	+		No
cj0900c		+	+		Yes
cj1211		+	-		No
cj0171		+			Yes
hrcA		+			No
dnaK		+			No
cj0561c		+			Yes
flgM		+			Yes
cj0367c		+			No

cj1207c	+		Yes
uvrC	-	-	No
rrc		+	Yes
cj1167		+	Yes
cj0741		+	Yes
acnB		+	Yes
truB		-	Yes
cj1343c[e]			No
dprA			Yes
cj0949c			Yes
acs			Yes
ceuB			Yes
murE			No
cj1377c			Yes
cj1375			No
cj0947c			Yes
cj0494			Yes
cj0977			Yes
cj0044c			Yes
cj1242			Yes
cj1209			Yes
cj0385c			Yes
cj0020c			Yes
cj0178			Yes
cj0358			Yes

[a] Genes considered significantly differentially expressed with fold changes of at least 1.5 fold, $p<10^{-4}$.

[b] microarray conditions: H_2O_2, hydrogen peroxide; CHP, cumene hydroperoxide; MND, menadione sodium bisulphite.

[c] '+' denotes gene is significantly upregulated.

[d] '-' denotes gene is significantly downregulated.

[e] Genes included in the mutant construction which were slightly below the cutoff threshold or of functional interest.

TABLE S4. Sensitivity of wild-type *C. jejuni*, isogenic deletion mutants and corresponding complemented strains to H_2O_2, cumene hydroperoxide or menadione bisulphite**.** The diameter of the zone of inhibition is represented as the mean clear zone ± standard error for each strain (in mm) after exposure to 10 µl of 3% H_2O_2, 3% cumene hydroperoxide, or 90 mM menadione bisulphite. Each experiment was repeated in quadruplicate. Values were considered significant (*) at $P < 0.001$ using Bayesian statistical analysis.

	Oxidant[a]		
Strain	H_2O_2	CHP	MND
C. jejuni NCTC11168	19.08 ± 0.19	24.50 ± 0.22	31.63 ± 0.36
Detoxification			
ΔCj0358	16.44 ± 0.72*	23.50 ± 0.53	29.63 ± 0.80
ΔCj0358+Cj0358	17.40 ± 0.40	22.50 ± 0.52	31.93 ± 1.13
Δrrc	21.08 ± 1.08	23.92 ± 1.08	34.50 ± 1.83
Δrrc+rrc	18.55 ± 0.38	20.94 ± 0.67	32.27 ± 1.60
Cation Transport/Binding Proteins			
Δ*chaN*	17.37 ± 0.30	21.47 ± 0.17*	29.83 ± 0.61
Δ*chaN*+c*haN*	17.26 ± 0.75	22.82 ± 0.66	34.08 ± 1.97
Δ*exbB1*	16.90 ± 0.31*	23.13 ± 0.64	28.30 ± 0.58
Δ*exbB1+exbB1*	17.33 ± 0.60	22.63 ± 0.37	32.90 ± 1.16
Δ*cfbpB*	19.30 ± 0.25	25.33 ± 0.83	29.98 ± 1.52
Δ*exbB2*	18.20 ± 0.31	24.37 ± 0.87	28.20 ± 0.50
Δ*exbB2+exbB2*	18.17 ± 0.17	23.53 ± 0.44	30.90 ± 0.90
Δ*tonB3*	18.16 ± 0.76	22.33 ± 0.58	28.83 ± 0.76
Δ*tonB1*	20.53 ± 0.17	24.37 ± 0.07	31.07 ± 0.32
Δ*tonB1+ΔtonB2*	21.10 ± 0.44	23.77 ± 0.67	33.27 ± 1.46
Δ*tonB2*	21.10 ± 0.46*	26.47 ± 0.67	33.07 ± 1.39
Δ*tonB2+ΔtonB3*	19.83 ± 0.49	24.20 ± 0.56	32.10 ± 1.33
Δ*ceuB*	19.15 ± 0.17	23.95 ± 0.45	31.60 ± 1.51
Δ*ceuE*	18.77 ± 0.29	22.90 ± 0.15	31.83 ± 0.61
Δ*cfrA*	19.40 ± 0.49	23.57 ± 0.35	32.37 ± 0.30
Δ*cfbpC*	19.08 ± 0.27	25.18 ± 0.64	30.50 ± 1.53
Δ*cfbpA*	19.13 ± 0.23	24.33 ± 0.57	30.27 ± 0.54
Δ*chuA*	17.70 ± 0.67	23.27 ± 0.43	31.47 ± 1.22
Δ*chuB*	20.13 ± 0.54	23.58 ± 0.48	35.08 ± 1.20
Δ*chuC*	19.33 ± 1.42	24.83 ± 0.85	34.29 ± 2.01
Δ*chuD*	18.88 ± 0.28	22.68 ± 0.50	34.30 ± 1.50
ΔCj0045c	19.15 ± 0.09	24.25 ± 0.88	30.38 ± 1.43
ΔCj0178	20.00 ± 0.25	25.17 ± 0.69	33.40 ± 0.83
Δ*exbD1*	18.23 ± 0.29	24.07 ± 0.79	28.57 ± 0.83
Δ*exbD2*	19.61 ± 0.97	22.33 ± 0.59	31.50 ± 0.66

Δ*chuZ*	20.30 ± 0.38	23.50 ± 0.17	34.90 ± 0.20
ΔCj1658	19.10 ± 0.15	22.90 ± 0.20	32.17 ± 0.44
ΔCj1661	19.10 ± 0.17	23.64 ± 0.76	33.00 ± 1.15
ΔCj1663	17.83 ± 0.52	23.67 ± 0.74	28.67 ± 0.38
Δ*p19*	19.67 ± 0.20	23.87 ± 0.47	32.67 ± 0.88
Δ*p19 +Δ*Cj1658	20.43 ± 0.54	25.38 ± 0.95	33.93 ± 0.07
Energy Metabolism			
Δ*ald*	17.70 ± 0.95	22.57 ± 0.23	32.07 ± 1.55
ΔCj0073c	17.43 ± 0.23	22.33 ± 0.68	29.67 ± 1.67
ΔCj0073c+Cj0073c	17.95 ± 0.65	23.43 ± 0.77	34.33 ± 1.92
ΔCj1377c	20.70 ± 1.07	25.30 ± 0.56	35.57 ± 2.50
ΔCj1377c+Cj1377c	17.93 ± 0.32	23.17 ± 0.42	32.83 ± 0.24
Δ*hypC*	19.40 ± 0.53	26.03 ± 0.92	33.03 ± 2.40
Δ*acnB*	21.22 ± 0.45*	23.28 ± 0.24	36.28 ± 0.72
*Δ*a*cnB+acnB*	20.27 ± 0.25	21.33 ± 0.44	33.44 ± 1.49
Δ*ccoQ*	17.83 ± 0.33	24.10 ± 0.91	28.97 ± 0.73
ΔCj1207c	18.27 ± 0.27	24.73 ± 0.79	29.43 ± 0.47
Surface Structures			
Δ*flaG*	19.17 ± 0.53	26.08 ± 1.06	35.50 ± 1.53
Δ*flgDik*	20.47 ± 0.47	26.27 ± 0.36	36.50 ± 0.31*
Δ*flgD+flgD*	18.40 ± 0.31	23.60 ± 0.80	31.70 ± 0.58
Δ*flgE*	20.17 ± 1.29	24.93 ± 1.12	35.85 ± 1.35
Δ*flgE+flgE*	17.93 ± 0.37	22.53 ± 0.17	35.20 ± 1.05
Δ*flgE2*	19.64 ± 0.72	24.57 ± 0.62	33.75 ± 1.04
Δ*flgG*	20.28 ± 0.71	25.80 ± 0.40	34.50 ± 1.07
Δ*flgG2*	19.83 ± 1.07	25.63 ± 1.01	32.96 ± 1.31
Δ*flgH*	21.00 ± 0.42*	26.55 ± 0.55	37.00 ± 1.30*
Δ*flgH+flgH*	19.07 ± 0.37	23.37 ± 0.23	32.33 ± 1.19
Δ*flgI*	21.35 ± 0.43*	26.00 ± 0.30	35.38 ± 1.89
Δ*flgI+flgI*	18.95 ± 0.34	23.95 ± 0.21	31.70 ± 1.13
Δ*flgK*	21.53 ± 0.13*	26.13 ± 0.46	34.90 ± 2.04
Δ*flgK+flgK*	19.67 ± 0.17	24.73 ± 0.15	31.10 ± 0.49
Δ*flgL*	21.00 ± 0.23*	25.08 ± 0.32	34.67 ± 1.73
Δ*flgL+flgL*	18.33 ± 1.17	21.25 ± 0.12	30.67 ± 0.10
Δ*flgM*	20.27 ± 0.50	24.33 ± 0.33	36.43 ± 1.40
Δ*flgM+flgM*	19.27 ± 0.48	24.20 ± 0.67	32.93 ± 2.02
Δ*flgP*	21.63 ± 1.24*	26.25 ± 0.86	35.25 ± 2.21
Δ*flgP+flgP*	19.94 ± 0.59	25.74 ± 0.62	33.08 ± 1.26
Δ*flgR*	20.47 ± 0.75	25.63 ± 0.34	36.78 ± 1.35*
Δ*flgR+flgR*	17.90 ± 0.61	22.17 ± 0.35	32.83 ± 0.87
Δ*flhB*	19.80 ± 0.44	23.18 ± 0.32	36.53 ± 1.86*

Δ*flhB+flhB*	18.18 ± 0.76	20.86 ± 0.82	32.15 ± 0.99
Δ*fliK*	20.43 ± 0.11	26.20 ± 0.45	35.95 ± 1.86
Δ*fliK+fliK*	17.83 ± 0.17	22.73 ± 0.62	32.67 ± 0.52
Δ*maf4*	18.97 ± 0.33	22.63 ± 0.35	29.77 ± 0.91
Δ*maf6*	18.40 ± 0.15	22.87 ± 0.17	30.93 ± 0.41
Δ*maf7*	19.50 ± 0.50	23.03 ± 0.15	29.90 ± 1.17
ΔpseB	20.50 ± 0.32	25.92 ± 0.53	35.95 ± 1.40*
ΔpseB+pseB	18.95 ± 1.13	23.67 ± 1.20	26.94 ± 2.96
Drug Efflux			
ΔCj0309c	19.71 ± 0.95	25.05 ± 0.51	34.53 ± 1.41
Δ*cmeA*	20.79 ± 0.85	25.60 ± 1.26	34.58 ± 1.15
Membranes, Lipoproteins and Porins			
ΔCj0385c	19.07 ± 0.32	23.30 ± 0.21	30.67 ± 0.67
ΔCj0587	18.93 ± 0.13	23.73 ± 1.02	30.03 ± 0.15
ΔCj0818	19.40 ± 0.21	23.63 ± 0.81	29.73 ± 0.72
ΔCj1211	20.27 ± 0.26	22.93 ± 0.30	34.27 ± 1.43
ΔCj1356c	20.35 ± 0.96	23.55 ± 0.63	33.03 ± 1.44
ΔCj1484c	20.60 ± 0.50	25.67 ± 0.57	32.17 ± 1.66
Hypothetical Unknown Proteins			
ΔCj0040	18.98 ± 0.79	25.93 ± 0.64	34.55 ± 1.63
ΔCj0044c	19.17 ± 0.44	22.80 ± 0.38	32.53 ± 0.77
ΔCj0148c	18.90 ± 0.30	22.50 ± 0.40	33.57 ± 0.72
ΔCj0171	19.92 ± 1.28	25.17 ± 1.16	34.00 ± 1.75
ΔCj0202c	18.77 ± 0.37	22.27 ± 0.32	31.53 ± 0.62
ΔCj0202c+Cj0202c	17.77 ± 0.39	23.60 ± 0.55	31.10 ± 1.46
ΔCj0253	18.88 + 1.31	25.00 ± 0.85	36.04 ± 1.76
ΔCj0260c	17.42 ± 0.19	21.67 ± 0.44*	30.87 ± 0.75
ΔCj0260c+Cj0260c	17.50 ± 0.35	22.83 ± 0.57	30.85 ± 0.35
ΔCj0344	20.92 ± 0.14*	23.92 ± 0.45	33.33 ± 1.01
ΔCj0344+Cj0344	18.12 ± 0.73	21.25 ± 1.24	30.36 ± 1.33
ΔCj0416	18.30 ± 0.60	23.47 ± 1.30	32.00 ± 0.93
ΔCj0524	20.53 ± 0.48	24.03 ± 0.72	32.18 ± 0.76
ΔCj0554	18.57 ± 0.23	23.07 ± 0.75	34.07 ± 0.41
ΔCj0741	17.80 ± 0.27	22.40 ± 0.62	28.90 ± 0.59
ΔCj0786	18.27 ± 0.15	23.23 ± 0.65	31.30 ± 0.56
ΔCj0814	17.27 ± 0.54	23.90 ± 0.35	29.33 ± 1.07
ΔCj0814+Cj0814	17.64 ± 0.39	23.80 ± 0.34	33.38 ± 1.62
ΔCj0819	19.03 ± 0.10	23.50 ± 0.87	31.33 ± 0.46
ΔCj0900c	19.17 ± 0.40	22.08 ± 0.45	30.92 ± 0.99
ΔCj0977	19.77 ± 0.35	22.50 ± 0.28	34.00 ± 1.00

ΔCj1159c	19.71 ± 0.90	22.25 ± 0.40*	30.42 ± 0.72
ΔCj1209	20.60 ± 0.40	24.17 ± 0.19	36.00 ± 1.08
ΔCj1242	19.77 ± 0.33	22.73 ± 0.03	32.63 ± 0.67
ΔCj1383c	20.30 ± 0.40	23.30 ± 0.45	30.73 ± 0.66
ΔCj1383c+Cj1383c	18.44 ± 0.51	21.11 ± 0.19	31.61 ± 1.42
Δ*mdaB*	18.40 ± 1.02	26.43 ± 0.43	33.00 ± 1.62
Miscellaneous			
ΔCj0062c	21.73 ± 0.21*	26.00 ± 0.39	35.67 ± 0.33
ΔCj0062c+Cj0062c	19.44 ± 0.39	25.20 ± 0.50	33.63 ± 1.80
ΔCj0295	19.10 ± 0.31	23.80 ± 0.31	34.10 ± 0.76
ΔCj0947c	23.94 ± 1.20*	26.44 ± 0.80	43.00 ± 3.76*
ΔCj0947c+Cj0947c	20.66 ± 1.50	25.55 ± 0.50	32.33 ± 0.19
ΔCj1036c	19.17 ± 0.20	22.27 ± 0.26	30.53 ± 0.50
ΔCj1036c+Cj1036c	18.73 ± 0.48	23.83 ± 0.48	33.83 ± 1.91
ΔCj1388	21.17 ± 0.41*	25.38 ± 0.61	35.33 ± 2.20
ΔCj1623	18.33 ± 0.50	21.95 ± 0.19*	34.78 ± 2.50
ΔCj1623+Cj1623	17.44 ± 0.49	22.70 ± 0.39	32.63 ± 1.44
Δ*folP*	19.06 ± 0.36	22.11 ± 0.39	33.39 ± 0.25
Δ*pstC*	20.75 ± 0.31*	27.25 ± 1.00*	32.33 ± 1.24
Δ*pstC+pstC*	20.60 ± 0.25*	25.30 ± 0.41	36.84 ± 1.79
Δ*spoT*	20.07 ± 0.41	25.00 ± 0.17	33.83 ± 1.04
Δ*trpF*	20.04 ± 0.68	25.67 ± 0.96	34.94 ± 2.24
Δ*trpF+trpF*	18.77 ± 0.45	23.85 ± 0.34	32.72 ± 1.07
Δ*truB*	19.43 ± 0.49	25.37 ± 0.36	34.00 ± 1.31
Δ*acs*	19.12 ± 0.24	23.89 ± 0.27	33.74 ± 1.12
ΔCj0494	20.47 ± 0.15	24.83 ± 0.71	31.47 ± 1.36
ΔCj0561c	18.63 ± 0.23	22.65 ± 0.60	30.08 ± 0.43
ΔCj0672	18.60 ± 0.29	22.93 ± 0.63	30.33 ± 1.02
ΔCj0949c	20.57 ± 0.41	23.57 ± 0.19	33.90 ± 0.90
ΔCj1167	18.40 ± 0.70	23.10 ± 0.40	33.07 ± 1.18
ΔCj1241	19.30 ± 0.38	24.65 ± 0.65	30.08 ± 0.82
ΔCj1255	19.33 ± 0.84	25.35 ± 1.30	33.38 ± 1.81
ΔCj1340c	18.80 ± 0.67	22.77 ± 0.32	29.43 ± 0.81
ΔCj1406c	19.60 ± 0.20	22.43 ± 0.30	35.33 ± 1.70
Δ*dprA*	18.70 ± 0.49	24.77 ± 0.82	28.83 ± 0.49

[d-] H_2O_2, hydrogen peroxide; CHP, cumene hydroperoxide; MND, menadione

Table S5. Sensitivity of wild-type *C. jejuni*, isogenic single and double deletion mutants to H_2O_2, cumene hydroperoxide or menadione bisulphite in the presence of 20 mM sodium fumarate. The diameter of the zone of inhibition is represented as the mean clear zone ± standard error for each strain (in mm) after exposure to 10 µl of 3% H_2O_2, 3% cumene hydroperoxide, or 90 mM menadione bisulphite. Each experiment was repeated in at least quadruplicate. Values were considered significant (*) at $P < 0.05$ using one way ANOVA.

	Fumarate	Oxidant[a]		
Strain	(+/-)	H_2O_2	CHP	MND
C. jejuni NCTC11168	-	18.34 ± 0.32	23.33 ± 0.20	26.59 ± 0.41
C. jejuni NCTC11168	+	19.00 ± 0.26	23.25 ± 0.24	25.99 ± 0.61
Detoxification				
Δ*sodB*	-	22.24 ± 0.29*	nd	34.00 ± 0.70*
Δ*sodB*	+	22.41 ± 0.11*	nd	33.38 ± 0.55*
Surface Structures				
Δ*flgD*	-	20.54 ± 0.40*	24.99 ± 0.82*	33.27 ± 1.56*
Δ*flgD*	+	nd	nd	28.83 ± 1.26
Δ*flgD*Δ*ccoQ*	-	19.30 ± 0.35	23.43 ± 0.35	26.23 ± 0.63
Δ*flgH*	-	20.50 ± 0.25*	25.57 ± 0.19*	29.81 ± 0.41*
Δ*flgH*	+	20.30 ± 0.22*	25.23 ± 0.24*	26.43 ± 0.77
Δ*flgH*Δ*ccoQ*	-	21.30 ± 0.52*	25.00 ± 0.34*	24.00 ± 0.52
Δ*flgP*	-	21.50 ± 0.97*	25.21 ± 0.23*	28.88 ± 0.66
Δ*flgP*	+	21.08 ± 1.25*	25.50 ± 0.83*	26.89 ± 0.31
Δ*flhB*	-	20.63 ± 0.23*	23.30 ± 0.14	28.94 ± 0.45*
Δ*flhB*	+	20.47 ± 0.22*	23.33 ± 0.17	26.21 ± 0.66
Δ*flhB*Δ*ccoQ*	-	20.60 ± 0.27*	22.33 ± 0.20	23.36 ± 1.05*
Δ*maf7*	-	21.91 ± 0.75*	24.16 ± 0.83	28.46 ± 0.53
Δ*maf7*	+	21.25 ± 0.92*	23.92 ± 0.58	27.79 ± 0.56
Δ*motAB*	-	20.80 ± 0.12*	24.76 ± 0.09*	30.02 ± 0.92*
Δ*motAB*	+	20.54 ± 0.18*	24.50 ± 0.10	24.17 ± 0.67
Δ*motAB*Δ*ccoQ*	-	19.92 ± 0.17	24.58 ± 0.28	24.04 ± 0.22
Δ*motAB+motAB*	-	17.87 ± 0.27	22.55 ± 0.21	29.12 ± 0.30*
Energy Metabolism				
Δ*ccoQ::kan*	-	19.22 ± 0.34	23.44 ± 0.38	25.38 ± 0.59

[a] H_2O_2, hydrogen peroxide; CHP, cumene hydroperoxide; MND, menadione

Nd, not determined

CHAPTER 6. RIGHTS AND PERMISSIONS

For Horizon Scientific Press (See General Introduction 1.5, 1.6):

"Caister Academic Press, Horizon Scientific Press, and Horizon Bioscience do not charge for and grant use without requiring your copyright permission request for:

- Original authors wanting to reproduce figures and tables of their own work in journal articles, book chapters, theses or dissertations.
- Authors wanting to reproduce or republish their own work in theses or dissertations.

For ASM publications (see Chapters 2.1, 2.2, 2.3):

"ASM authors also retain the right to reuse the full article in his/her dissertation or thesis. For a full list of author rights, please see: http://journals.asm.org/site/misc/ASM_Author_Statement.xhtml"

CHAPTER 7. CURRICULUM VITAE

Education

PhD in Biochemistry (In progress)

University of Ottawa, Ontario
May 2008 – present

Bachelor of Science with Honours

University of Ottawa, Ontario
Sept 2003- April 2008
Obtained undergraduate degree in Biopharmaceutical Science (genomics option)

Laboratory Experience

PhD project in Dr. Alain Stintzi's Lab

Department of Biochemistry, Microbiology, Immunology – Ottawa University, 451 Smyth Road, Ottawa, Canada
May 2008- present

Characterizing the role of the heme-trafficking protein Cj1386 in *Campylobacter jejuni*.

Honours project in Dr. Alain Stintzi's Lab

Department of Biochemistry, Microbiology, Immunology – Ottawa University, 451 Smyth Road, Ottawa, Canada
May 2007- April 2008

Conducting research into the identification and characterization of oxidative stress defense genes in *Campylobacter jejuni*.

Refereed Publications

Annika Flint and Alain Stintzi (2014). Cj1386, an atypical hemin-binding protein, mediates hemin trafficking to KatA in *Campylobacter jejuni*. Journal of Bacteriology. In press.

Annika Flint, Yi-Qian Sun, James Butcher, Martin Stahl, Hongsheng Huang, and Alain Stintzi (2014). Phenotypic screening of a targeted mutant library reveals *Campylobacter jejuni* defenses against oxidative stress. Infection and Immunity, 82(6), 2266-75.

Annika Flint, James Butcher, and Alain Stintzi (2013). Chapter 7: *Campylobacter* strategies for colonizing the host gastrointestinal tract. *Campylobacter* Evolution and Ecology (Horizon Press), 75-88.

Hemant Naikare, James Butcher, Annika Flint, Jide Xu, Kenneth Raymond, and Alain Stintzi (2013). *Campylobacter jejuni* ferric-enterobactin receptor CfrA is TonB dependent and mediates iron acquisition from structurally different catechol siderophores. Metallomics 5, 988-996.

Virginie Dufour, Jennifer Li, Annika Flint, Eric Rosenfeld E, Katell Rivoal, Sylvie Georgeault, Bachar Alazzam, Gwennola Ermel, Alain Stintzi, Martine Bonnaure-Mallet, and Christine Baysse (2013). Inactivation of LysR regulator Cj1000 of *Campylobacter jejuni* affects host colonization and respiration. Microbiology 159(6), 1165-1178.

Annika Flint, Yi-Qian Sun, and Alain Stintzi (2012). Cj1386 is an ankyrin-containing protein involved in heme trafficking to catalase in *Campylobacter jejuni.* Journal of Bacteriology 194(2), 334-345.

Annika Flint, James Butcher, Cyril Clarke, Denver Marlow and Alain Stintzi (2010). Use of a rabbit soft tissue chamber model to investigate *Campylobacter* – host interactions. Frontiers in Cellular and Infection Microbiology 1, 126.

James Butcher, Annika Flint, Martin Stahl and Alain Stintzi (2010). Chapter 10: *Campylobacter* Fur and PerR regulons. Iron Uptake in Microorganisms (Pierre Cornelis and Simon Andrews[eds]), 167-202.

Kiran Palyada, Yi-Qian Sun, Annika Flint, James Butcher, Hemant Naikare and Alain Stintzi (2009). Characterization of the oxidative stress stimulon and PerR regulon of *Campylobacter jejuni.* BMC Genomics *10*, 481-500.

Annika Flint and Alain Stintzi (2008). Oxidative stress defences and the acetate switch in *Campylobacter jejuni*. University of Ottawa, Honours thesis.

Conference Presentations

Annika Flint and Alain Stintzi. Cj1386 is a heme trafficking protein involved in hydrogen peroxide defence in *Campylobacter jejuni*. 2014 9th International Biometals Symposium, Durham, USA. Poster presentation.

Annika Flint and Alain Stintzi. Cj1386 is a heme trafficking protein involved in hydrogen peroxide defence in *Campylobacter jejuni*. 2013 Canadian Society of Microbiologists Conference, Ottawa, Canada. Poster presentation.

Annika Flint and Alain Stintzi. Cj1386 is a heme trafficking protein involved in hydrogen peroxide defence in *Campylobacter jejuni*. 2013 Ottawa Institute of Systems Biology Symposium, Mont Tremblant, Canada. Oral presentation.

Nitin Bhardwaj, Annika Flint, Hoang-Thanh Le, Nelson F. Eng, Rebecca Mulligan, Alain Stintzi and Francisco Diaz-Mitoma. Pre-clinical evaluation of KatA as a vaccine candidate against *Campylobacter jejuni* in mice. 2013 *Campylobacter, Helicobacter* and Related Organisms (CHRO) conference, Aberdeen, Scotland. Contributed experimental data used in a poster presentation by Nitin Bhardwaj.

Annika Flint and Alain Stintzi. A major role for Cj1386 in hydrogen peroxide defence in *Campylobacter jejuni*. 2012 Canadian *Campylobacter* Workshop, Ottawa, Canada. Oral presentation.

Annika Flint, Yi-Qian Sun, Hongsheng Huang and Alain Stintzi. Global characterization of oxidative stress defences in *Campylobacter jejuni*. 2012 China Canada Systems Biology Symposium and the 19th Methods in Protein Structure Analysis, Ottawa, Canada. Poster presentation.

Annika Flint and Alain Stintzi. A major role for Cj1386 in hydrogen peroxide defence in *Campylobacter jejuni*. 2012 Canadian Student Health Research Forum (CSHRF), Winnipeg, Canada. Poster presentation.

Alain Stintzi, James Butcher, Sabina Sarvan, Annika Flint, and Jean-Francois Couture. The regulation of iron homeostasis in *Campylobacter jejuni*: a structural and genome-wide analysis. 2012 8th International Biometals Symposium, Brussels, Belgium. Contributed experimental data used in an oral presentation by Alain Stintzi.

Annika Flint and Alain Stintzi. Oxidative stress defences in *Campylobacter jejuni*. 2011, *Campylobacter, Helicobacter* and Related Organisms (CHRO) conference, Vancouver, Canada. Poster presentation.

Annika Flint, Yi-Qian Sun and Alain Stintzi. Hydrogen peroxide defences in *Campylobacter jejuni.* 2009, FEMS Microbiology Congress, Gothenburg, Sweden. Poster presentation.

Annika Flint, Yi-Qian Sun and Alain Stintzi. Global characterization of oxidative stress defences in *Campylobacter jejuni*. 2009 Progress in Systems Biology Symposium, Ottawa, Canada. Poster presentation.

Annika Flint, Yi-Qian Sun and Alain Stintzi. Hydrogen peroxide defences in *Campylobacter jejuni.* 2008 Canadian *Campylobacter* Conference, Montreal, Canada. Poster presentation.

James Butcher, Annika Flint, Yi-Qian Sun and Alain Stintzi. Characterization of the regulatory networks controlling iron metabolism in *Campylobacter jejuni.* 2008 Canadian *Campylobacter* Conference, Montreal, Canada. Contributed experimental data used in an oral presentation given by James Butcher.

James Butcher, Yi-Qian Sun, Annika Flint, Kiran Palyada, Hemant Naikare and Alain Stintzi. The regulatory networks controlling the iron metabolism of *Campylobacter jejuni.* 6th International Biometals Symposium 2008, Santiago de Compostela, Spain. Contributed experimental data used in an oral presentation given by James Butcher.

Teaching Experience

Winter 2013, 2014 – Lab demonstrator for BCH3346 biochemistry laboratory course at the University of Ottawa.

Winter 2011, 2012 – Lab demonstrator for BCH2333 biochemistry laboratory course at the University of Ottawa.

Fall 2010, 2011, 2012, 2013, 2014 – Lab demonstrator for BCH3356 molecular biology laboratory course at the University of Ottawa.

Skills

Laboratory

Experience performing molecular and biochemical techniques including PCR, qRT-PCR, cloning, SDS PAGE, Western blotting, immunoprecipitation, immunofluorescence microscopy.

Construction of isogenic deletion mutants in bacteria.

Phenotypic characterization of mutants (disc-inhibition assays, bioscreens, catalase activity assays).

Experience working with *in vivo* chick and piglet models (handling, feeding, inoculating, necropsy, processing intestinal contents, CFU counts of contents).

Protein expression (His, GST, strep tagged proteins and tag cleavage) and HPLC purification.

Enzyme kinetics and ligand binding.

Experience performing microarrays.

Analytical

Experience using Adobe Illustrator, Photoshop, ImageJ.

Statistical analysis of results (Mann-Whitney rank sum test, ANOVA, t-tests).

Experience using MS Word, MS Excel, Graphpad Prism software, Minitab software.

Writing and editing papers for peer reviewed publications, book chapters, reviews and grants.

Awards

Jorge Crosa Poster Award at 9th International Biometals Symposium (2014).

Placed 3rd in the graduate seminar symposium for the PhD biochemistry discipline, University of Ottawa (2014).

QEII-GSST worth $15000 per year ($5000 per semester of graduate study – September 2012 to August 2013).

QEII-GSST worth $15000 per year ($5000 per semester of graduate study – September 2011 to August 2012).

OGSST worth $12000 per year ($4000 per semester of graduate study – September 2009 to August 2011).

Excellence scholarship for graduate studies (September 2009 to August 2013).

Terry Beveridge Poster Award at Canadian Society of Microbiologists Conference (2013).

University of Ottawa Faculty of Medicine Award of Excellence (2012).

Silver Award at CIHR Canadian Student Health Research Forum (2012).

Placed 1st in the graduate seminar symposium for the PhD biochemistry discipline, University of Ottawa (2012).

Placed 3rd in the graduate seminar symposium for the Master's biochemistry discipline, University of Ottawa (2010).

Entrance scholarship worth $2000 and bursary worth $500 for first year of undergraduate study.